

What lies beneath riparian black poplar (*Populus nigra* L.): Root distributions, associations and structures.

Holloway, James Vincent

The copyright of this thesis rests with the author and no quotation from it or information derived from it may be published without the prior written consent of the author

For additional information about this publication click this link.

<http://qmro.qmul.ac.uk/xmlui/handle/123456789/12867>

Information about this research object was correct at the time of download; we occasionally make corrections to records, please therefore check the published record when citing. For more information contact scholarlycommunications@qmul.ac.uk

**What lies beneath riparian black poplar
(*Populus nigra* L.):
Root distributions, associations
and structures**

James Vincent Holloway

Submitted in partial fulfilment of the requirements
of the Degree of Doctor of Philosophy

STATEMENT OF ORIGINALITY

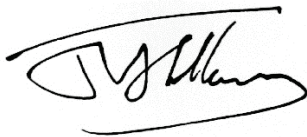
I, James Vincent Holloway, confirm that the research included within this thesis is my own work or that where it has been carried out in collaboration with, or supported by others, that this is duly acknowledged below and my contribution indicated. Previously published material is also acknowledged below.

I attest that I have exercised reasonable care to ensure that the work is original, and does not to the best of my knowledge break any UK law, infringe any third party's copyright or other Intellectual Property Right, or contain any confidential material.

I accept that the College has the right to use plagiarism detection software to check the electronic version of the thesis.

I confirm that this thesis has not been previously submitted for the award of a degree by this or any other university.

The copyright of this thesis rests with the author and no quotation from it or information derived from it may be published without the prior written consent of the author.

A handwritten signature in black ink, appearing to read 'J.V. Holloway', enclosed within a large, sweeping, horizontal loop that underlines the signature.

Date: 30/09/2015

Details of collaboration and publications: (N/A)



Erasmus Mundus
Joint Doctorate Programme

SMART - Science for Management of Rivers and their Tidal systems

PHD IN RIVER SCIENCE

Research for this thesis was funded with the support of the Erasmus Mundus programme of the European Union and was conducted within the framework of SMART (Science for Management of Rivers and their Tidal systems), which is an Erasmus Mundus Joint Doctoral Programme (EMJD).

EMJDs aim to foster cooperation between higher education institutions and academic staff in Europe and third countries with a view to creating centres of excellence and providing a highly skilled 21st century workforce enabled to lead social, cultural and economic developments. All EMJDs involve mandatory mobility between the universities in the consortia and lead to the award of recognised joint, double or multiple degrees.

The SMART programme represents a collaboration among The University of Trento, Queen Mary University of London, and the Free University of Berlin. Each doctoral student within the SMART programme has conformed to the following during their 3 years of study:

- Supervision by a minimum of two supervisors in two institutions (their primary and secondary institutions).
- Study for a minimum period of 6 months at their secondary institution.
- Successful completion of a minimum of 30 ECUs of taught courses.
- Collaboration with an associate partner to develop a particular component / application of their research that is of mutual interest.
- Submission of a thesis within 3 years of commencing the programme.

ABSTRACT

Vegetation plays a central role in river dynamics and riparian forest is itself a rare and valuable habitat. Tree roots stabilise riparian sediments and are key to regeneration after disturbance. However, despite mechanistic understanding of these effects, poor knowledge of spatial variability and its controls limits its practical application. With findings from field investigations undertaken within a dynamic and near-natural riparian forest system dominated by black poplar (*Populus nigra* L.), this thesis describes observed root distributions and investigates dimensions of their variability and potential controls that can contribute to both scientific understanding of river dynamics and river management at individual tree to landscape scales.

Following an introduction to the thesis (Chapter 1), critical literature review (Chapter 2), and descriptions of study sites and methods (Chapter 3), Chapter 4 presents observed root depth distributions, revealing a more complex picture than a simple decline with depth, with differences dependent on environmental variables that vary between and within study sites.

Chapter 5 tests the hypothesis that root distributions are significantly associated with the complex sediment profiles found in active riparian systems. It emerges that commonly-used aggregate root metrics are less well-predicted by sediment variables than parameters describing the local root diameter composition.

Further light is shed on the variability of root distributions in Chapter 6 by considering the development of gross subterranean tree structures, from which finer roots emanate. Analysis of root and buried stem system exposures demonstrates how these complex, often very massive structures are dependent on both local contemporary environmental conditions and the disturbance history of an individual tree.

Finally, the significance of the research findings for a whole-system understanding of river dynamics, management, conservation and restoration, is explored. What can be reasonably assumed, and its limitations, is distinguished from what may be more dependent on local context, and why. Investigations pursuant of additional questions emerging from the research are also suggested, alongside preliminary results from supplementary further studies.

TABLE OF CONTENTS

Chapter 1	Introduction	13
1.1	The value of riparian systems	13
1.1.1	Geodiversity	13
1.1.2	Biodiversity.....	15
1.1.3	Ecosystem services.....	15
1.2	Human impacts.....	16
1.2.1	Conservation and restoration	17
1.2.2	Management of riparian trees and vegetation	18
1.3	Structure of the thesis	18
1.4	References.....	19
Chapter 2	Review of Literature	22
2.1	Physical generation and maintenance of complexity.....	22
2.1.1	Catchment coupling.....	23
2.1.2	Inundation.....	23
2.1.3	Substrate	25
2.1.4	Summary.....	28
2.2	Plants in the riparian zone.....	29
2.2.1	Evolutionary consequences of dynamic physical conditions.....	29
2.2.2	Influences on physical dynamics: Ecosystem engineering.....	33
2.2.3	Summary.....	38
2.3	The realm of roots.....	39
2.3.1	Root physiology and development	39
2.3.2	Root reinforcement.....	44
2.3.3	Existing studies of riparian root structures	47
2.3.4	Summary.....	49
2.4	Identified knowledge gaps.....	50
2.4.1	Root system architecture of mature trees	50
2.4.2	Effective representation of root distributions within bank stability models	50
2.4.3	Persistence of root structures under fluvial disturbance	50
2.5	References.....	51
Chapter 3	Model Systems, Study Sites and Methods.....	61
3.1	Introduction	61
3.2	Primary Research Questions.....	61
3.3	Research design.....	62
3.3.1	Investigative approach.....	62
3.3.2	Model Systems	63
3.4	Methods	74

3.4.1	Field Campaign.....	74
3.4.2	Laboratory Protocols.....	77
3.5	References.....	79
Chapter 4	Distribution of Root Area and Density with Depth.....	83
4.1	Introduction	83
4.1.1	Research questions.....	86
4.2	Study sites	86
4.3	Methods	87
4.3.1	Field sampling.....	87
4.3.2	Data analysis.....	88
4.4	Results	92
4.4.1	Regression analysis of root properties with sediment profile depth	92
4.4.2	Analysis of cumulative root profiles and median rooting depths	101
4.4.3	Variability in root characteristics within bank profiles	103
4.4.4	Distribution of root diameters by frequency and area.....	107
4.5	Discussion.....	112
4.6	Conclusions	116
4.7	References.....	116
Chapter 5	Associations of Root Properties with the Local Rooting Environment.....	119
5.1	Introduction	119
5.1.1	Research questions.....	122
5.2	Methods	123
5.2.1	Field campaign.....	123
5.2.2	Data analysis.....	123
5.3	Results	127
5.3.1	Correlations between measured variables.....	127
5.3.2	Principal Components Analysis	140
5.3.3	Hierarchical Cluster Analysis.....	148
5.3.4	Distribution of root and abiotic variables within the five sediment classes and PC space.....	151
5.4	Discussion.....	158
5.4.1	Single variable correlates of root density and total area	158
5.4.2	Multivariate associations between roots and sediments	159
5.4.3	Implications and further work.....	161
5.5	Conclusions	162
5.6	References.....	164
Chapter 6	Buried Livewood and Coarse Root Systems of Riparian Black Poplar.....	166
6.1	Introduction	166
6.1.1	Research questions.....	169

6.2	Methods	169
6.2.1	Field methods	169
6.2.2	Data analysis.....	170
6.2.3	Qualitative and secondary observations.....	173
6.3	Results	173
6.3.1	Recent formative flood events	173
6.3.2	Case studies from excavations.....	176
6.3.3	Compiled observations from this and other studies.....	226
6.4	Discussion.....	236
6.4.1	Features common to most or all case studies	236
6.4.2	Differences between case studies and uncommon features.....	237
6.4.3	Implications.....	239
6.5	Conclusions	240
6.6	References.....	242
Chapter 7	Synthesis, Conclusions and Outlook.....	244
7.1	Summary of key findings.....	244
7.1.1	Root depth distributions	244
7.1.2	Associations with sediment and tree variables.....	245
7.1.3	Coarse structures	246
7.2	This study within the wider scientific context.....	246
7.2.1	Riparian plant growth and bank stability	247
7.2.2	Vegetation and landform dynamics.....	249
7.2.3	Applicability beyond the Tagliamento / black poplar system	250
7.3	Implications for river management.....	251
7.4	Further research possibilities: Completing the model of riparian root functions at all scales.....	253
7.4.1	Fine root associations with soil hydraulic properties, nutrients and mycorrhizae.....	254
7.4.2	Additional influences on root strength	257
7.4.3	Adventitious roots and poplar clonal patch dynamics.....	259
7.4.4	Extending whole root system investigations.....	262
7.5	References.....	263
Appendix A	Laser Particle Sizer Settings	266
Appendix B	Complete Correlation Tables.....	267
Appendix C	Aerial Image Sequences.....	271
Appendix D	Structure from Motion Photogrammetry	284
Appendix E	Site Information and Methods for Preliminary Further Data Collection	290

TABLE OF FIGURES

Figure 1.1	Idealised model of floodplain discontinuities and longitudinal gradients.....	14
Figure 1.2	Geodiversity and classification of surface waterbodies	14
Figure 1.3	Morphological modification of rivers and lakes in the European Union.	16
Figure 1.4	Urban encroachment and elimination of the riparian zone through revetment.	17
Figure 1.5	Bioengineered bank stabilisation incorporating mature tree roots.	17
Figure 2.1	Schematic longitudinal trends in fluvial geomorphic drivers and sediment.	26
Figure 2.2	Sediment heterogeneity within a floodplain due to past alluviation.	27
Figure 2.3	Recruitment Box Model for riparian cottonwoods.....	33
Figure 2.4	Typical topography and layout of isolated wood accumulations.	35
Figure 2.5	Four phases of the biogeomorphological life cycle of riparian black poplar	37
Figure 2.6	Shoot apical meristem of <i>Arabidopsis thaliana</i> L.....	40
Figure 2.7	Schematic structure of the root apical meristem.	41
Figure 2.8	Secondary growth progression in roots	42
Figure 2.9	Schematic representation of some different forms of mycorrhizae	44
Figure 2.10	Relationship between breaking strength and diameter of roots.....	45
Figure 3.1	Climatic setting of the Tagliamento.....	64
Figure 3.2	Map of the Tagliamento catchment.....	65
Figure 3.3	River corridor elements on the middle Tagliamento.	67
Figure 3.4	Distribution of <i>Populus nigra</i> L.	70
Figure 3.5	<i>P. grandidentata</i> (bigtooth aspen) sucker root system.	72
Figure 3.6	Locations of field sites for profile sampling.....	74
Figure 3.7	Typical pair of bank profile exposures during excavation.	75
Figure 3.8	Case study tree RA, illustrating the extent of sediment removal.	77
Figure 4.1	Study locations on the River Tagliamento.....	87
Figure 4.2	Distribution of field moisture content of all 2013 samples	89
Figure 4.3	Sampling structure as planned and as revised following moisture analysis	90
Figure 4.4	Site 5 showing aggradation of the bed between 2013 and 2014.....	90
Figure 4.5	Scatter plots of root density and root area ratio with depth.....	94
Figure 4.6	Best-fitting model for the global root density dataset.	96
Figure 4.7	Best-fitting root density model incorporating moisture zone.....	98
Figure 4.8	Best-fitting root area ratio model incorporating moisture zone.....	99
Figure 4.9	Regression models for root density against depth at individual sites.	100
Figure 4.10	Regression models for root area ratio against depth at individual sites.	101
Figure 4.11	Average profiles of cumulative root density and area	102
Figure 4.12	Comparative distributions of normalized median rooting depths	103
Figure 4.13	Distribution of all root data variability with depth.....	104
Figure 4.14	Distribution of root density data variability with depth	105
Figure 4.15	Distribution of root area data variability with depth	106
Figure 4.16	Histogram of relative diameter class frequencies for the full dataset.....	107
Figure 4.17	Proportional contribution of diameter classes to total root area	108
Figure 4.18	Mean proportional contribution of diameter classes to depth intervals	109
Figure 4.19	Proportional contribution of diameter classes to total root area with depth.	110
Figure 4.20	Mean proportional contribution of diameter classes to depth intervals with depth	111

Figure 5.1	An example of the diverse sediment types found in Tagliamento soils.....	121
Figure 5.2	Scatters of relationships between tree and root variables	130
Figure 5.3	Scatters of relationships between tree and fine and coarse root variables.....	131
Figure 5.4	Potential non-linear relationship between skewness of diameter distribution and mean radial growth rate of poplars at the site.....	132
Figure 5.5	Scatters of strongest sediment correlates of root density.....	137
Figure 5.6	Scatters of strongest sediment correlates of root area ratio.....	138
Figure 5.7	Scatters of relationships between sediment and fine and coarse root data.	139
Figure 5.8	Potential non-linear relationship between sediment sand content and skewness of the root diameter and area distributions	140
Figure 5.9	Scores and loadings for PCA of root diameter distribution parameters	141
Figure 5.10	Scores and loadings for PCA of diameter parameters, density and RAR.....	143
Figure 5.11	Scores and loadings for PCA of root area distribution parameters.....	144
Figure 5.12	Scores and loadings for PCA of sediment variables.	146
Figure 5.13	Distribution of sediment variables with respect to PC1 and PC2.	147
Figure 5.14	AHC dendrogram locating the five main sediment classes	149
Figure 5.15	AHC dendrogram from Figure 5.14 with a logarithmic axis.....	149
Figure 5.16	Scatter of sediment PCA scores by AHC class, with PCA loadings.....	150
Figure 5.17	Radar chart of sediment variable centroids in each sediment class.	150
Figure 5.18	Distribution of abiotic variables in relation to sediment PC1 and PC2.....	153
Figure 5.19	Distribution of key root variables in relation to sediment PC1 and PC2.	154
Figure 5.20	Root distribution parameters with respect to sediment PC1 and PC2.	155
Figure 5.21	Root PCA factor classes plotted with respect to sediment PC1 and PC2.....	156
Figure 6.1	Spatiotemporal sequence of the fluvial biogeomorphic succession	167
Figure 6.2	Locations of case study poplar trees.	169
Figure 6.3	Daily average stage record from January 1982 to October 2014.....	174
Figure 6.4	Hydrographs of the eight most recent large floods (> 3 m at Villuzza).	175
Figure 6.5	Case study trees R1-3 and RA	177
Figure 6.6	Case study trees RB-RE	178
Figure 6.7	R1 model with key features and main sedimentary strata identified.....	179
Figure 6.8	Key aerial images of the R1 neighbourhood, 1986-1991.	180
Figure 6.9	Key aerial images of the R1 neighbourhood, 2005-2012.	181
Figure 6.10	Estimates of dates of origin of different parts of the R1 root system	182
Figure 6.11	Summary of the proposed potential development trajectory R1	184
Figure 6.12	R2 root system with key features and main sedimentary strata identified.....	185
Figure 6.13	Detail of the upper part of the R2 root system.	186
Figure 6.14	Key aerial images of the R2 neighbourhood, 1986-1993.....	187
Figure 6.15	Key aerial images of the R2 neighbourhood, 1996-2012.	188
Figure 6.16	Estimates of dates of origin of different parts of the R2 root system.	189
Figure 6.17	Summary of the proposed potential development trajectory R2.....	191
Figure 6.18	R3 model with key features and main sedimentary strata identified.	192
Figure 6.19	Side view of R3 model, showing deflection into the bank.....	193
Figure 6.20	Key aerial images of the R3 and RC neighbourhood, 1988-1993.....	194
Figure 6.21	Key aerial images of the R3 and RC neighbourhood, 1997-2011.....	195
Figure 6.22	Estimates of dates of origin of different parts of the R3 root system	196
Figure 6.23	Proposed development trajectory of the lower part of the R3.....	197
Figure 6.24	Summary of the proposed potential development trajectory of R3.....	198

Figure 6.25	RA model with key features and main sedimentary strata identified.	199
Figure 6.26	Key aerial images of the RA neighbourhood, 1986-1991.	200
Figure 6.27	Key aerial images of the RA neighbourhood, 2005-2012.	201
Figure 6.28	Estimates of dates of origin of different parts of the RA root system	202
Figure 6.29	Summary of the proposed potential development trajectory of RA.	204
Figure 6.30	RB model with key features and main sedimentary strata identified.....	205
Figure 6.31	Key aerial images of the RB neighbourhood, 1986-1991.....	206
Figure 6.32	Key aerial images of the RB neighbourhood, 1996-2012.....	207
Figure 6.33	Estimates of dates of origin of different parts of the RB root system.....	208
Figure 6.34	Summary of the proposed potential development trajectory of RB.	210
Figure 6.35	RC model with key features and main sedimentary strata identified.....	211
Figure 6.36	Estimates of dates of origin of different parts of the RC root system.....	212
Figure 6.37	Detail of the RC model, showing node E	213
Figure 6.38	Summary of the proposed potential development trajectory of RC.	214
Figure 6.39	RD model with key features and main sedimentary strata identified.	215
Figure 6.40	Details of grafting observed between roots of RD and other stems.....	216
Figure 6.41	Key aerial images of the RD and RE neighbourhood, 1988-1993.	217
Figure 6.42	Key aerial images of the RD and RE neighbourhood, 1997-2012.	218
Figure 6.43	Estimates of dates of origin of different parts of the RD root system.....	219
Figure 6.44	Summary of the proposed potential development trajectory of RD.....	221
Figure 6.45	RE model with key features and main sedimentary strata identified.....	222
Figure 6.46	Detail of RE model showing the connecting axis ending downwards.....	223
Figure 6.47	Estimates of dates of origin of different parts of the RE root system.....	223
Figure 6.48	Summary of the proposed potential development trajectory of RE	225
Figure 6.49	Adventitious root structures and properties.	226
Figure 6.50	Basic representation of the commonly encountered 'J-shaped' form	227
Figure 6.51	Adventitious root distributions.	228
Figure 6.52	Deeply buried stems in fine sediments.	230
Figure 6.53	Features resulting from deposition of wood.	232
Figure 6.54	Interactions between bank dynamics and roots.	234
Figure 6.55	Typical examples of root systems evident on fluvially transported wood.....	239
Figure 7.1	Soil hyphal length depth profiles on the Tagliamento and Noce.....	256
Figure 7.2	Relationships between hyphal length density and root length density	257
Figure 7.3	Poplar root breaking stress as a function of diameter and alive/dead status..	258
Figure 7.4	Use of rigging thimbles for applying load to roots more evenly.....	259
Figure 7.5	Depth distribution of the areas of individual coarse roots	260
Figure 7.6	Distribution of coarse roots in 5 m bank exposures on the Tagliamento.	261

TABLE OF TABLES

Table 2.1	Functional trait associations with environmental and ecological stressors	31
Table 3.1	Catchment statistics of the River Tagliamento.	66
Table 4.1	Summary statistics for root density and root area ratio observations.....	93
Table 4.2	Components and goodness-of-fit for linear regression models	95
Table 4.3	Components and goodness-of-fit for quadratic regression models.....	95
Table 4.4	Components and goodness-of-fit for linear regression models incorporating a moisture dummy variable	97
Table 4.5	Components and goodness-of-fit for quadratic regression models incorporating a moisture dummy variable.....	97
Table 5.1	Some examples of threshold values used to define ‘fine roots’	124
Table 5.2	Descriptive statistics for tree variables.	128
Table 5.3	Descriptive statistics for tree variables as distributed among the 366 root sampling intervals.....	128
Table 5.4	Strongest correlations between root density and area and tree variables.	129
Table 5.5	Other informative significant correlations between tree and root variables.....	129
Table 5.6	Descriptive statistics for sediment samples	133
Table 5.7	Descriptive statistics for weighted average sediment data as distributed among the 350 coincident root sampling intervals.....	134
Table 5.8	Correlations between the eight sediment variables and root variables.....	135
Table 5.9	Other informative correlations between root and sediment variables.....	136
Table 5.10	Eigenvalues, percent variability explained and loadings of PCA of the root diameter distribution parameters.	141
Table 5.11	Eigenvalues, percent variability explained and loadings of PCA of root diameter distribution parameters, root density and root area ratio.	142
Table 5.12	Eigenvalues, percent variability explained and loadings of PCA of the root area distribution parameters.....	144
Table 5.13	Eigenvalues, percent variability explained and loadings of PCA of the eight main sediment variables, as distributed among the root sampling intervals.	145
Table 5.14	Centroid values of sediment variables within the five sediment classes.....	148
Table 5.15	Significant differences in abiotic and root variables across sediment classes ..	152
Table 5.16	Summary of key features of the five sediment classes	157
Table 6.1	Sources and dates (where known) of aerial and satellite imagery analysed.	172
Table 6.2	Key features of aerial stems of the case study trees.	176

ACKNOWLEDGEMENTS

First and foremost, I am deeply indebted to Prof. Angela Gurnell for her supervision of this research. Angela has provided the perfect blend of guidance, freedom, inspiration, rapid and comprehensive review, perspective, encouragement and also manual labour in the field! Sincere thanks also go to Prof. Matthias Rillig and colleagues at Freie Universität Berlin and Dr. Maria Cristina Bruno and colleagues at Fondazione Edmund Mach for going out of their way to facilitate this work, and for making me so welcome in their research groups.

Help in the field from Peter Richter, Peter Stam, Teresa Stuart, Sam Nicholass, Rachel Anderson, Alex Lumsdon, Giuditta Trinci, Howard Holloway and Elsa Barthram was also immeasurably important, and I thank all my assistants for their hard work. My other field companions in Mannazzons, including teams led by Dr. Alex Sukhodolov, Prof. Yasuhiro Takemon, Prof. Kozo Watanabe and Prof. Jana Petermann, will be fondly remembered.

Many ‘fixers’ have also helped with innumerable small matters, and particular thanks is due to Dr. Ulfah Mardhiah, Claudio Cruciat and family, Dr. Walter Bertoldi, Luca Ziliani and my fellow SMART doctorands and alumni.

Most importantly, I must acknowledge Pizzeria Leone di Damasco and ‘Blues’ brand budget iced tea for providing the vast amounts of fuel required for all the digging!

Chapter 1

INTRODUCTION

Dynamic transitional areas between the fluvial and terrestrial realms, riparian zones simultaneously comprise gradients and discontinuities in many physical variables, and constitute globally important geo- and bio-diversity capital. However, they also represent the main site of human interaction with rivers, and it is the characteristic feature of their dynamism which has led them to be stabilised and engineered by humans for millennia, across the developed world. Stabilisation of riparian land also occurs naturally, mediated by the roots of vegetation, and this thesis advances knowledge fundamental to the understanding of this sediment reinforcement phenomenon by describing and attempting to explain the distributions of roots in a natural riparian forest system. Depth distributions of roots are examined first, followed by an investigation into root associations with sediment variables. Coarse tree root structures are explored in the final results chapter. It is hoped that insights from this research will inform future river management such that the objectives of human development may be met through more sustainable practices which work as far as possible *with* the natural processes of riparian vegetation dynamics, rather than seeking to restrict or eliminate them, as has historically been the case. This first chapter presents the case for the research in a little more detail and then introduces the structure of the thesis.

1.1 THE VALUE OF RIPARIAN SYSTEMS

1.1.1 Geodiversity

At the catchment scale, river systems inherently represent a longitudinal gradient in altitude, with associated gradients in the physical characteristics of discharge, slope, stream power, sediment transport and grain size, and often climate as well. These changes, coupled with the tendency for threshold behaviour in fluvial morphogenesis (Church, 2002) and natural valley discontinuities (Figure 1.1) generate *longitudinal* diversity of forms and processes in all parts of the river corridor. The riparian zone constitutes that particular range of *transverse* valley topographic, hydrological and disturbance gradients closest to the flowing channel, and which similarly contributes to geodiversity. Within this range, dependent on the degree of floodplain confinement, such gradients may naturally be heterogeneously distributed in space (around features such as illustrated in Figure 1.2) and also in time, with variations in discharge, groundwater levels, evaporative demand and sediment delivery-dynamics.

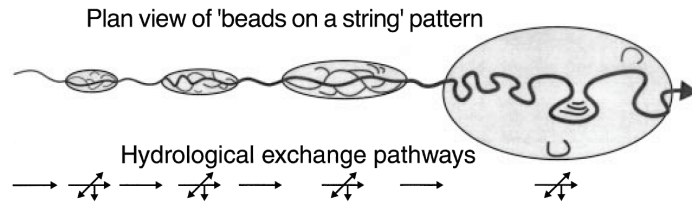


Figure 1.1 Idealised model of floodplain discontinuities and longitudinal gradients in river corridor form. Ward et al. (2002)

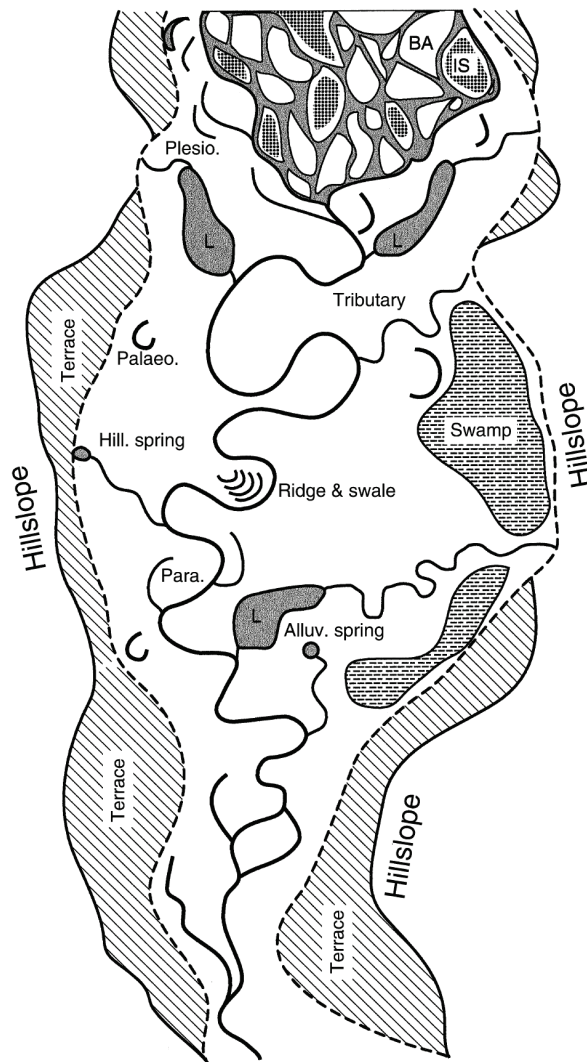


Figure 1.2 Geodiversity and classification of surface waterbodies and basic geomorphic features of an idealised river corridor in a braided-to-meandering transition zone. L: lateral or riparian lake; BA: bar; IS: island; Plesio: plesiotamal/-rhithral (abandoned braids); Palaeo: palaeopotamal/-rhithral (abandoned meanders); Para: parapotamal/-rhithral (dead arms). Ward et al. (2002)

1.1.2 Biodiversity

The diversity of physical habitat in naturally-functioning riparian zones supports a diversity of species and communities. Most taxonomic studies of these systems have been focused on vascular plants, and have recorded high species richness (see, e.g., Gregory et al., 1991, Burkart, 2001), but similarly high α -diversity has been observed in other groups: for example, beetles (French and Elliott, 2001, Michels Jr et al., 2010), birds (Berges et al., 2010), spiders (Ricetti and Bonaldo, 2008) and fungi (Laitung and Chauvet, 2005). Perhaps more importantly, though, the biological communities associated with riparian zones are distinct from those within adjacent exclusively aquatic or terrestrial habitats, and so, when intact, these ecotones contribute greatly to wider, landscape-scale biodiversity (Sabo et al., 2005). Hypothesised drivers of local diversity include the inherent longitudinal and lateral connectivity with colonisation sources (Ward et al., 1999, Sheldon et al., 2002, Moggridge et al., 2009) and the existence of habitats with intermediate levels of disturbance and stress (see, e.g., Lite et al., 2005), as well as 'landscape filtering' at hierarchical and spatially discrete habitat scales (Poff, 1997). While the mechanisms remain the subject of debate, there is little question that the biological diversity is dependent on the diversity of physical features and landforms found in functioning riparian corridors (Ward et al., 2002).

1.1.3 Ecosystem services

The same beneficial functions as support the diversity of species mentioned above (process regulation and habitat- and resource-provisioning) are also conferred by riparian systems to human society. Such ecosystem services as the interception of agriculturally-derived nutrients, sediment and pathogens are well-documented (see Polyakov et al., 2005 for an overview), but a diverse range of other benefits continue to be identified, including recruitment to fisheries (Growth et al., 2003, Sukhodolov et al., 2009), carbon storage (Giese et al., 2000, Giese et al., 2003), recreation (House and Sangster, 1991, Ehrenfeld, 2000), erosion control (Dwyer et al., 1997, Sotir, 1998), firewood provision (Girel and Manneville, 1998), water and sediment storage and flood wave attenuation (Hughes et al., 2003). There is an urgent need for both complete system-level and detailed mechanistic understanding of riparian zone behaviour in order to maintain the flow of these services by managing our influence upon freshwater ecosystems (Tabacchi et al., 2009, Capon et al., 2013).

1.2 HUMAN IMPACTS

Given that a reliable water source is a prerequisite for human settlement, developments of many kinds frequently come into direct contact with rivers – usually in the riparian zone. As demonstrated in the course of status assessments for the Water Framework Directive in the European Union, the majority of river systems in the developed world are affected in some way by morphological alterations (Figure 1.3 A) and, particularly in lowland, low energy water bodies, many acutely so (Figure 1.3 B). Such modifications are generally a result of severe urban, agricultural, silvicultural or transport-related encroachment or modification of river banks and floodplains (Poff et al., 2011), often with the complete elimination of riparian habitats through canalisation and/or revetment (Figure 1.4).

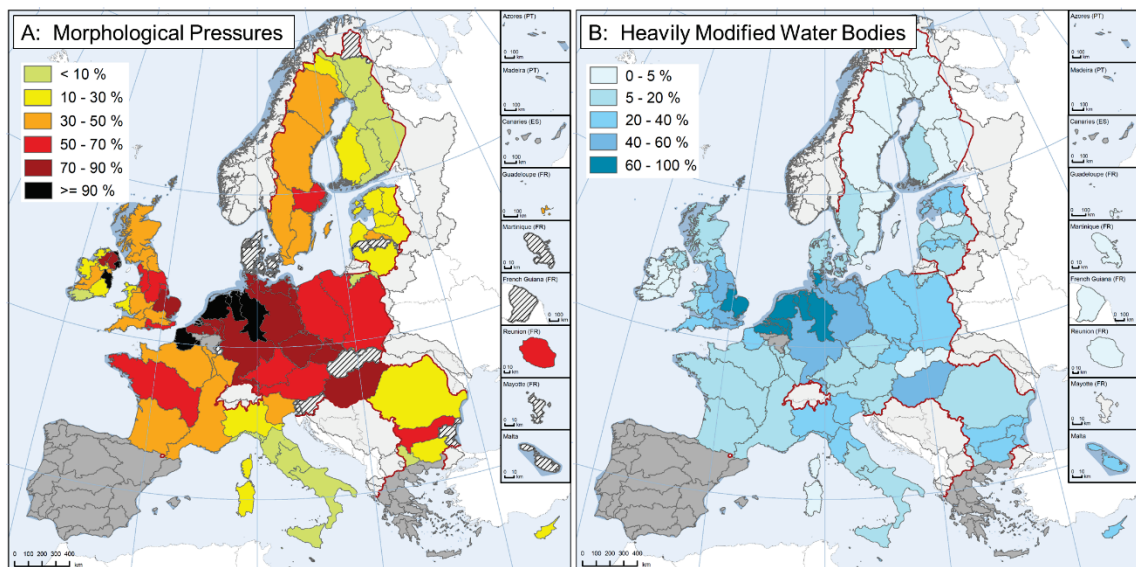


Figure 1.3 Morphological modification of rivers and lakes in the European Union. A: Percentage of river and lake water bodies affected by morphological alterations and water flow regulations; river management or other morphological alterations and pollution pressures. B: Map of percentage of heavily modified and artificial water bodies in EU River Basin Districts. WRC plc on behalf of the European Commission © DG Environment, 2012

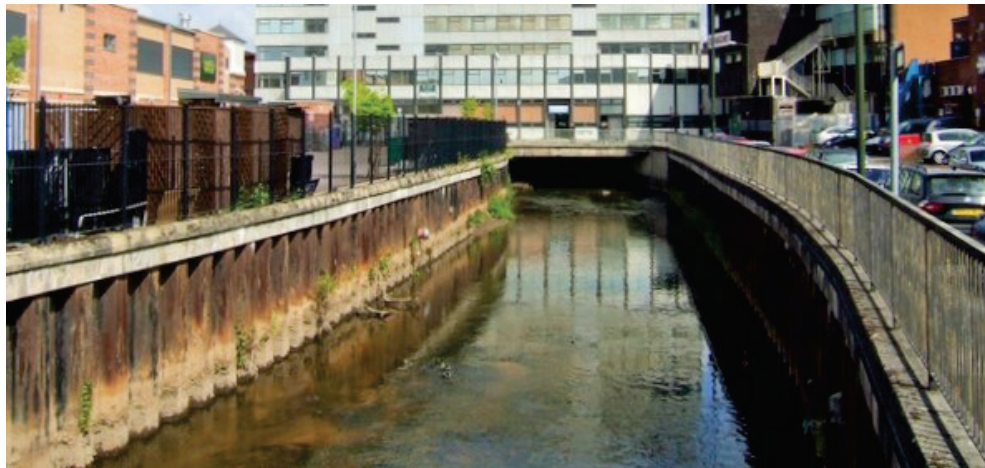


Figure 1.4 Urban encroachment and elimination of the riparian zone through revetment.

© John M: Geograph.org.uk creative commons licence

1.2.1 Conservation and restoration

With increasing appreciation of the value of intact river corridors with functioning riparian ecosystems, there are increasing efforts both to conserve (Dudgeon et al., 2006) and restore them (Bernhardt et al., 2005). However, there is still a very large number of situations in which human retreat from the riparian zone is not possible, and a bioengineering approach to channel bank stabilisation is often applied (e.g., Figure 1.5). There is still much uncertainty over the long-term performance of such techniques (which usually include woody riparian plants) due to their novelty and insufficient monitoring. Predicting the outcomes and longevity of such interventions is extremely difficult (Langendoen et al., 2009), and much of the reason for this is that it depends on the unseen and poorly-understood growth of roots.

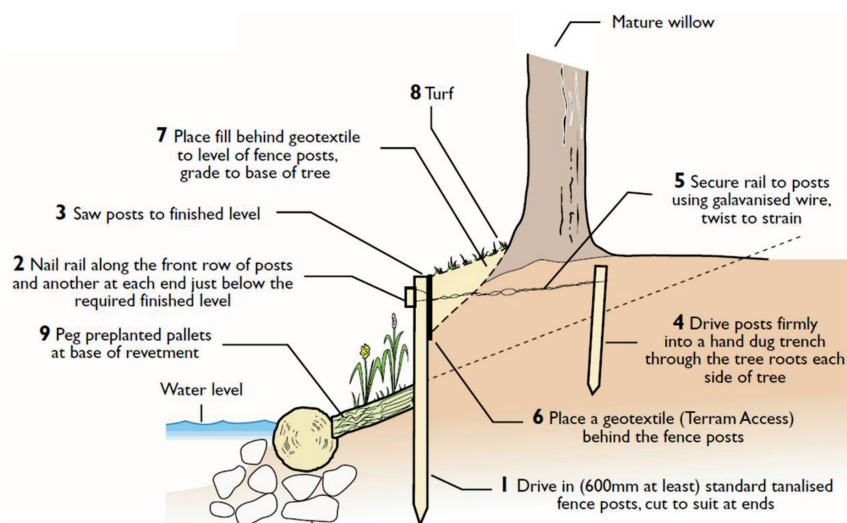


Figure 1.5 Bioengineered bank stabilisation incorporating mature tree roots. River Restoration Centre Manual of Techniques

1.2.2 Management of riparian trees and vegetation

Whether riverside trees are seen as a benefit or a problem by river managers depends on many factors. Trees are undoubtedly a natural feature of riparian corridors with sufficient water availability, but are one of the most intensively regulated features of riparian zones (Meleason et al., 2003). Perceptions of riparian trees vary widely: from appreciation of the benefits for erosion control (Evette et al., 2009, Stromberg et al., 2009) and cover for fish (Lyons et al., 2000, Growns et al., 2003); to concern over bank collapse from windthrow (Steil et al., 2009); but also recognition of benefits of windthrow for restoring in-channel wood (Phillips and Park, 2009); preference of recreational users for wooded corridors (House and Sangster, 1991); and concern over flooding due to in-channel debris (Le Lay et al., 2008). This variation reflects both the complicated effects of riverside trees and their dependence on the context and scale of evaluation, as well as our incomplete understanding of their behaviour.

The inevitable truth is that trees will continue to grow in riparian environments and we will continue to manage them. Gurnell and Petts (2006) present secondary and extensive primary evidence that riparian trees both modify large-scale channel dynamics and the retention and distribution of sediments within the riparian zone, thereby modulating the availability of resources to many other species and acting as ecosystem engineers (*sensu* Jones et al. (1994)). We need to understand the mechanisms underlying these effects in more detail if we wish to be able to modulate effectively the many influences of riparian vegetation on river processes, and root-mediated mechanisms are crucial to sediment and vegetation dynamics and hydrogeomorphology.

1.3 STRUCTURE OF THE THESIS

While a more targeted literature review is presented at the beginning of each of the three results chapters (4, 5 & 6), Chapter 2 provides an overview of current understanding of how physical forces and vegetation generate and maintain complexity in riparian zones, as well as an introduction to the relevant ecological, biological and geotechnical aspects of roots. Knowledge gaps are identified at the end of this review, and the main research questions are presented at the beginning of Chapter 3. As the different aspects of the research were all carried out on a model riparian tree system – black poplar (*Populus nigra* L.) on the Italian Tagliamento river – a detailed description of this system, the specific study sites and methods employed is presented in the third chapter.

Chapter 4 reports on root depth distributions observed at black poplar-dominated bank sites, investigates the influence of local water availability and assesses the validity of using simple depth functions to represent roots in bank erosion and stability modelling. Chapter 5 then analyses the extent to which the root profile is influenced by the sedimentology and characteristics of the nearest dominant trees. The final investigation identifies conserved features and the variability of form in the coarse root architecture and buried stems of black poplar via whole root system excavations of trees. These results are reported in Chapter 6, along with an interpretation of how the buried structures have been influenced by fluvial processes. Results and their implications are summarised, synthesised and interpreted in the context of river management in the final chapter. To aid consultation during reading, reference lists are presented at the end of each chapter. A number of appendices are attached with additional results and methodological detail.

1.4 REFERENCES

- BERGES, S. A., MOORE, L. A. S., ISENHART, T. M. & SCHULTZ, R. C. 2010. Bird species diversity in riparian buffers, row crop fields, and grazed pastures within agriculturally dominated watersheds. *Agroforestry Systems*, 79, 97-110.
- BERNHARDT, E. S., PALMER, M. A., ALLAN, J. D., ALEXANDER, G., BARNAS, K., BROOKS, S., CARR, J., CLAYTON, S., DAHM, C., FOLLSTAD-SHAH, J., GALAT, D., GLOSS, S., GOODWIN, P., HART, D., HASSETT, B., JENKINSON, R., KATZ, S., KONDOLF, G. M., LAKE, P. S., LAVE, R., MEYER, J. L., O'DONNELL, T. K., PAGANO, L., POWELL, B. & SUDDUTH, O. 2005. Synthesizing U.S. river restoration efforts. *Science*, 308, 636-637.
- BURKART, M. 2001. River corridor plants (Stromtalpflanzen) in Central European lowland: a review of a poorly understood plant distribution pattern. *Global Ecology and Biogeography*, 10, 449-468.
- CAPON, S. J., CHAMBERS, L. E., MAC NALLY, R., NAIMAN, R. J., DAVIES, P., MARSHALL, N., PITTOCK, J., REID, M., CAPON, T., DOUGLAS, M., CATFORD, J., BALDWIN, D. S., STEWARDSON, M., ROBERTS, J., PARSONS, M. & WILLIAMS, S. E. 2013. Riparian Ecosystems in the 21st Century: Hotspots for Climate Change Adaptation? *Ecosystems*, 16, 359-381.
- CHURCH, M. 2002. Geomorphic thresholds in riverine landscapes. *Freshwater Biology*, 47, 541-557.
- DUDGEON, D., ARTHINGTON, A. H., GESSNER, M. O., KAWABATA, Z. I., KNOWLER, D. J., LÉVÉQUE, C., NAIMAN, R. J., PRIEUR-RICHARD, A. H., SOTO, D., STIASSNY, M. L. J. & SULLIVAN, C. A. 2006. Freshwater biodiversity: Importance, threats, status and conservation challenges. *Biological Reviews of the Cambridge Philosophical Society*, 81, 163-182.
- DWYER, J. P., WALLACE, D. & LARSEN, D. R. 1997. Value of woody river corridors in levee protection along the Missouri River in 1993. *Journal of the American Water Resources Association*, 33, 481-489.
- EHRENFELD, J. G. 2000. Evaluating wetlands within an urban context. *Ecological Engineering*, 15, 253-265.
- EVETTE, A., LABONNE, S., REY, F., LIEBAULT, F., JANCKE, O. & GIREL, J. 2009. History of bioengineering techniques for erosion control in rivers in western europe. *Environmental Management*, 43, 972-984.
- FRENCH, B. W. & ELLIOTT, N. C. 2001. Species diversity, richness, and evenness of ground beetles in wheat fields and adjacent grasslands and riparian zones. *Southwestern Entomologist*, 26, 315-324.
- GIESE, L. A., AUST, W. M., TRETIN, C. C. & KOLKA, R. K. 2000. Spatial and temporal patterns of carbon storage and species richness in three South Carolina coastal plain riparian forests. *Ecological Engineering*, 15, S157-S170.
- GIESE, L. A. B., AUST, W. M., KOLKA, R. K. & TRETIN, C. C. 2003. Biomass and carbon pools of disturbed riparian forests. *Forest Ecology and Management*, 180, 493-508.
- GIREL, J. & MANNEVILLE, O. 1998. Present species richness of plant communities in alpine stream corridors in relation to historical river management. *Biological Conservation*, 85, 21-33.

- GREGORY, S. V., SWANSON, F. J., MCKEE, W. A. & CUMMINS, K. W. 1991. An ecosystem perspective of riparian zones. *Bioscience*, 41, 540-551.
- GROWNS, I., GEHRKE, P. C., ASTLES, K. L. & POLLARD, D. A. 2003. A comparison of fish assemblages associated with different riparian vegetation types in the Hawkesbury-Nepean River system. *Fisheries Management and Ecology*, 10, 209-220.
- GURNELL, A. & PETTS, G. 2006. Trees as riparian engineers: The Tagliamento River, Italy. *Earth Surface Processes and Landforms*, 31, 1558-1574.
- HOUSE, M. A. & SANGSTER, E. K. 1991. Public perception of river-corridor management. *Journal of the Institution of Water and Environmental Management*, 5, 312-317.
- HUGHES, F. M. R., RICHARDS, K., GIREL, J., MOSS, T., MULLER, E., NILSSON, C. & ROOD, S. B. (eds.) 2003. *The Flooded Forest: Guidance for policy makers and river managers in Europe on the restoration of floodplain forests.*, Department of Geography, University of Cambridge, UK: FLOBAR2.
- JONES, C. G., LAWTON, J. H. & SHACHAK, M. 1994. Organisms as ecosystem engineers. *Oikos*, 69, 373-386.
- LAITUNG, B. & CHAUVET, E. 2005. Vegetation diversity increases species richness of leaf-decaying fungal communities in woodland streams. *Archiv fur Hydrobiologie*, 164, 217-235.
- LANGENDOEN, E. J., LOWRANCE, R. R. & SIMON, A. 2009. Assessing the impact of riparian processes on streambank stability. *Ecohydrology*, 2, 360-369.
- LE LAY, Y. F., PIÉGAY, H., GREGORY, K., CHIN, A., DOLÉDEC, S., ELOSEGI, A., MUTZ, M., WYZGA, B. & ZAWIEJSKA, J. 2008. Variations in cross-cultural perception of riverscapes in relation to in-channel wood. *Transactions of the Institute of British Geographers*, 33, 268-287.
- LITE, S. J., BAGSTAD, K. J. & STROMBERG, J. C. 2005. Riparian plant species richness along lateral and longitudinal gradients of water stress and flood disturbance, San Pedro River, Arizona, USA. *Journal of Arid Environments*, 63, 785-813.
- LYONS, J., TRIMBLE, S. W. & PAINE, L. K. 2000. Grass versus trees: Managing riparian areas to benefit streams of central North America. *Journal of the American Water Resources Association*, 36, 919-930.
- MELEASON, M. A., GREGORY, S. V. & BOLTE, J. P. 2003. Implications of riparian management strategies on wood in streams of the Pacific Northwest. *Ecological Applications*, 13, 1212-1221.
- MICHELIS JR, G. J., CARNEY, V. A., JONES, E. N. & POLLOCK, D. A. 2010. Species diversity and qualitative assessment of ground beetles (Coleoptera: Carabidae) in three riparian habitats. *Environmental Entomology*, 39, 738-752.
- MOGGRIDGE, H. L., GURNELL, A. M. & MOUNTFORD, J. O. 2009. Propagule input, transport and deposition in riparian environments: the importance of connectivity for diversity. *Journal of Vegetation Science*, 20, 465-474.
- PHILLIPS, J. D. & PARK, L. 2009. Forest blowdown impacts of Hurricane Rita on fluvial systems. *Earth Surface Processes and Landforms*, 34, 1069-1081.
- POFF, B., KOESTNER, K. A., NEARY, D. G. & HENDERSON, V. 2011. Threats to riparian ecosystems in Western North America: An analysis of existing literature. *Journal of the American Water Resources Association*, 47, 1241-1254.
- POFF, N. L. 1997. Landscape filters and species traits: Towards mechanistic understanding and prediction in stream ecology. *Journal of the North American Benthological Society*, 16, 391-409.
- POLYAKOV, V., FARES, A. & RYDER, M. H. 2005. Precision riparian buffers for the control of nonpoint source pollutant loading into surface water: A review. *Environmental Reviews*, 13, 129-144.
- RICETTI, J. & BONALDO, A. B. 2008. Spiders diversity and richness estimates in four vegetations types of Serra do Cachimbo, Pará, Brazil. *Diversidade e estimativas de riqueza de aranhas em quatro fitofisionomias na Serra do Cachimbo, Pará, Brasil*, 98, 88-99.
- SABO, J. L., SPONSELLER, R., DIXON, M., GADE, K., HARMS, T., HEFFERNAN, J., JANI, A., KATZ, G., SOYKAN, C., WATTS, J. & WELTER, J. 2005. Riparian zones increase regional species richness by harboring different, not more, species. *Ecology*, 86, 56-62.
- SHELDON, F., BOULTON, A. J. & PUCKRIDGE, J. T. 2002. Conservation value of variable connectivity: aquatic invertebrate assemblages of channel and floodplain habitats of a central Australian arid-zone river, Cooper Creek. *Biological Conservation*, 103, 13-31.
- SOTIR, R. B. 1998. Watershed management for streambank protection and riverine restoration. *Proceedings of Conference 29 - International Erosion Control Association*, 29, 451-462.

- STEIL, J. C., BLINN, C. R. & KOLKA, R. 2009. Foresters' perceptions of windthrow dynamics in northern minnesota riparian management zones. *Northern Journal of Applied Forestry*, 26, 76-82.
- STROMBERG, J. C., CHEW, M. K., NAGLER, P. L. & GLENN, E. P. 2009. Changing perceptions of change: The role of scientists in Tamarix and river management. *Restoration Ecology*, 17, 177-186.
- SUKHODOLOV, A., BERTOLDI, W., WOLTER, C., SURIAN, N. & TUBINO, M. 2009. Implications of channel processes for juvenile fish habitats in Alpine rivers. *Aquatic Sciences*, 71, 338-349.
- TABACCHI, E., STEIGER, J., CORENBLIT, D., MONAGHAN, M. T. & PLANTY-TABACCHI, A. M. 2009. Implications of biological and physical diversity for resilience and resistance patterns within Highly Dynamic River Systems. *Aquatic Sciences*, 71, 279-289.
- WARD, J. V., TOCKNER, K., ARSCOTT, D. B. & CLARET, C. 2002. Riverine landscape diversity. *Freshwater Biology*, 47, 517-539.
- WARD, J. V., TOCKNER, K. & SCHIEMER, F. 1999. Biodiversity of floodplain river ecosystems: Ecotones and connectivity. *River Research and Applications*, 15, 125-139.

Chapter 2

REVIEW OF LITERATURE

This chapter summarises the findings of research to date on the dynamics of riparian zones, from the classical view of absolute control by physical, abiotic forces to the more nuanced contemporary view of ancient and complex systems which have co-evolved with the lifeforms they support. Of the riparian biota and second only to the effects of humans, the direct and indirect effects of plants predominantly constitute the main ecosystem engineering forces. This review begins by explaining riparian diversity through the action of physical forces (Section 2.1), moves on to discuss the effects on and of vegetation (Section 2.2), before focusing in on the root zone (Section 2.3). Finally, major knowledge gaps are identified and summarised in Section 2.4.

2.1 PHYSICAL GENERATION AND MAINTENANCE OF COMPLEXITY

Physical habitat within river corridors may extend the full length of the topographic and hydrologic gradient from the bed of the low flow channel to the break in slope at the edge of the floodplain. There are multiple definitions of the ‘riparian zone’, with the more restrictive confined to the area within the bankfull channel, and wider spatial definitions encompassing adjacent river-dependent ecosystems up to the entire active floodplain (Steiger et al., 2005). The spatial range of definitions can partly be explained by the fact that the position of this ecotone varies with the flow stage at any given time. In the present review, the riparian zone is considered to range from the channel banks to the outer edge of the more frequently inundated floodplain (*sensu* Gregory et al. (1991)).

Important physical limitations on plants are dependent on the interplay between river morphology and hydrology. The variables described here all have implications for the critical factors of water, nutrient and light availability, as well as the efficiency of gas exchange (particularly for roots) and thermal conditions (Bornette and Puijalon, 2011), and all are inter-dependent. Kyle and Leishman (2009), however, determined inundation frequency and substrate texture to be the two most powerful explanatory variables for observed differences in plant adaptations, and so these form the main components of the conceptual grouping of conditions below.

2.1.1 Catchment coupling

As well as being an area of mixing with flowing water, the riparian ecotone is a zone of concentration of subsurface flows accumulating from upslope areas as they enter the hyporheos (Naiman and Decamps, 1997). Consequently, a high loading of solutes of all kinds may be experienced, depending on the valley setting (Dahm et al., 1998). Nitrogen and phosphorus species and their transformation have received particular attention owing to their relevance for water quality management in agricultural settings (Cirimo and McDonnell, 1997, Drewry et al., 2006, Hoffmann et al., 2009), but inputs of dissolved organic carbon (Mulholland and Hill, 1997), agrochemicals and their degradation products (Puckett and Hughes, 2005) and other mobile, active contaminants such as methylmercury (Bishop et al., 1995, Heyes et al., 2000) can also be imported into the riparian zone in significant quantities. This loading varies greatly through time, depends both on precipitation and flow stage, and is therefore usually encountered in ‘hot moments’ (Gu et al., 2012, Vidon, 2012). Spatial variability in subsurface water quality (hot spots) is considered below in the context of substrate conditions.

2.1.2 Inundation

Flooding is characterised by its frequency, depth, velocity and duration, all of which tend to increase at the lower elevations of river valleys, particularly close to the flowing channel. These components of the inundation regime are intrinsically interrelated and responsible for the conditions which constitute both constraints and opportunities for riparian vegetation.

a Erosion and turnover

Flood frequency and flow velocity together characterize conditions in the riparian zone where parts of plants may be damaged or broken off, or indeed whole plants may be uprooted entirely as landforms are eroded (e.g., Bendix and Hupp, 2000, Johnson, 2000). The latter mechanism is a particularly important influence on young plants and can lead to patchy recruitment of trees to form distinct cohorts (Polzin and Rood, 2006). More established stands of trees, however, may be eroded progressively with the substrate, as channel banks migrate laterally (Bertoldi et al., 2013). Debris carried within overbank flows (e.g. sediment and wood) can also be a major cause of plant damage (Gurnell et al., 1995, Ruiz-Villanueva et al., 2010, Stoffel and Wilford, 2012).

While high flows present a destructive force, they also maintain a constant turnover of the substrate in the riparian zone, ensuring availability of freshly exposed sediments for colonisation (Ward et al., 2002, Beechie et al., 2006, Collins et al., 2012). Concurrently,

however, fine particulate organic matter and nutrients may be retained only in sheltered 'hotspots', such that nutrient availability is often very low in exposed sites (Mahoney and Rood, 1998).

b Accretion of sediment

Although there is complex spatial variability dependent on topography and the presence of flow obstructions (Piegay et al., 2000), at broad scales water velocities in floods are lower further from the main channel and net deposition, rather than net removal of sediment tends to occur. Finer silts and clays represent a significant adsorbed nutrient input, particularly of phosphorus (Antheunisse et al., 2006), which is often limiting in more stable terrestrial systems. Aside from fine mineral sediment, inundation often brings with it organic debris (including viable plant propagules), providing a pulsed source of organic carbon and nitrogen (Steiger and Gurnell, 2003) and, potentially, plant recruitment.

Though plants can beneficially promote deposition, passive burial is a potential hazard in the riparian zone, and is a major cause of mortality for seedlings (e.g., Polzin and Rood, 2006). The magnitude and frequency of burial events influences the extent of physical stresses imposed (Kent et al., 2001), which primarily comprise limitation of photosynthesis and gas exchange. Though there are undoubtedly significant differences between river systems, and local conditions, Steiger et al. (2001) report greatest deposition during intermediate scale flood events, illustrating a trade-off between sediment delivery and erosive power. Further discussion of the sediment environment appears in subsequent sections of this review.

c Water table dynamics

The water table in the riparian zone is under the influence of local and hillslope precipitation and transpiration, as well as river stage (through bank seepage/capillary action and over-bank inundation) (Vidon, 2012). The relative extent of influences at any point depends particularly on the proximity of the break of the valley side slope and the river channel, and structural characteristics of the substrate (discussed in more detail later). In all situations, however, the water table level in the riparian zone varies through time at least seasonally (Burt et al., 2002), and can fluctuate significantly over short time periods, even on a daily or more frequent basis (Schilling, 2007, Guilloy et al., 2011). As a consequence, riparian plants may experience extremes from complete inundation and waterlogging to severe drought (Rood et al., 2011, Gurnell et al., 2012) and extremes may occur over quite short periods. Oxygen availability and knock-on effects on the redox conditions can also be extreme (Carlyle and Hill, 2001).

d Temperature

The local and regional physical environment (particularly aspect and position in the catchment) exert primary controls over daily and seasonal air and water temperature regimes, which are further moderated by the plant canopy (Arscott et al., 2001). However, when compared to strictly terrestrial environments, the patchy surface and sub-surface sediment structure of riparian zones created by frequent fluvial disturbances lead to significant variations in sub-surface permeability, water retention and transmission characteristics, the mixing of surface and subsurface waters and as a result, high heterogeneity in surface and subsurface water temperatures (Tonolla et al., 2010), which may also influence local, near-surface air temperature and humidity. Thermal exchange between subsurface and surface waters is a major component of the flood pulse concept (Junk and Wantzen, 2004), and hyporheic flow paths may produce areas where diel fluctuations in water temperature are buffered near the substrate surface (Acuña and Tockner, 2009). Of course, the source of surface water (e.g. snowmelt or a warmer, slower-flowing tributary) and groundwater (e.g. shallow or deep) entering the riparian zone also has a major effect on the surface and subsurface thermal environment. Air, water and solid substrate temperatures are particularly important from the plant perspective owing to their powerful influence on chemical reaction rates and thus processes such as growth and respiration.

2.1.3 Substrate

Natural riparian zones function as a temporary store of alluvial sediments in which, over the long term, deposition is more-or-less matched by erosion. The mineral basis of riparian soils, therefore, depends on current and historic sediment supply, which varies through the catchment; and sediment delivery to the channel and its riparian zone, which varies locally according to the fluvial process regime and thus the balance between erosion and deposition processes. Longitudinal trends in bed grain size and extent of stored sediment in fluvial systems are linked to stream power (a product of gradient and discharge) and catchment coupling (Figure 2.1), such that there tends to be downstream fining in the dominant river channel and riparian substrate texture (Petts et al., 2000).

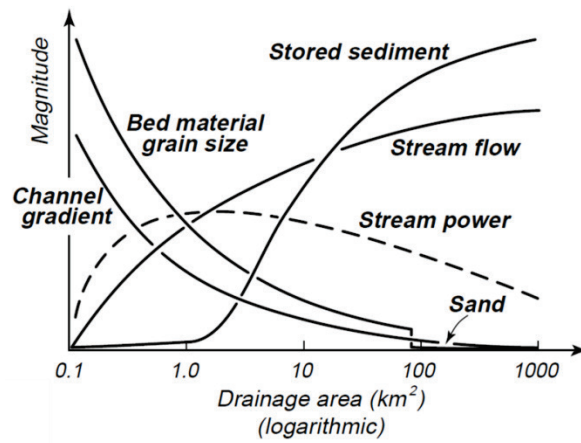


Figure 2.1 Schematic longitudinal trends in key fluvial geomorphic drivers and sediment. Church (2002)

However, local variability (longitudinally, laterally, and with depth – see Figure 2.2) in grain size distributions can be exceedingly high, reflecting multiple deposition and erosion events associated with mobilisation, transfer and deposition of sediments of varying grain size. The resulting sediment patchwork is a product of the cumulative history of alluvial ‘fill’ created by overbank vertical accretion of floodplain surfaces, including infill of abandoned channels, and predominantly lateral erosion and lateral/oblique accretion of river banks as channels and bars are formed and migrate (Nanson and Croke, 1992, Huggenberger et al., 1998). These erosion and accretion processes vary spatially in response to local variations in flow velocity and shear stresses which govern the mobilisation, transport, deposition and sorting of different sediment grain sizes.

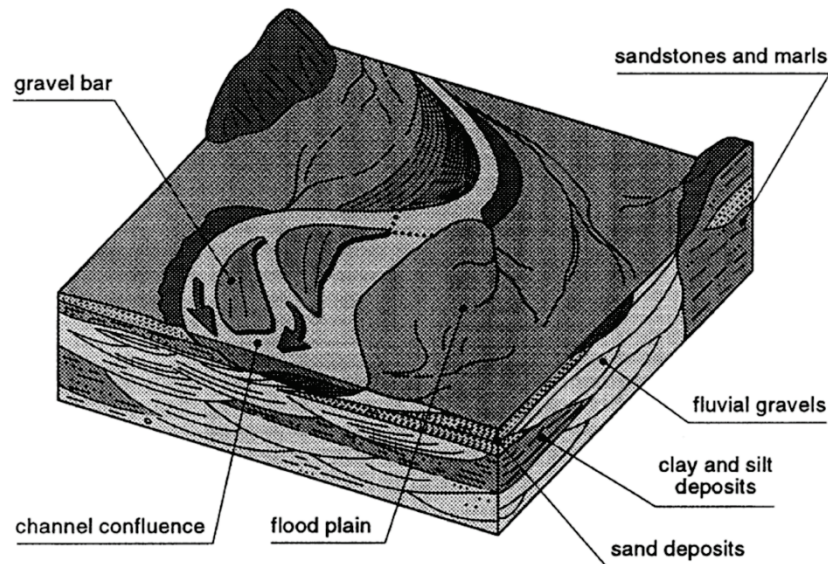


Figure 2.2 Sediment heterogeneity within a floodplain due to past alluviation. Huggenberger et al. (1998)

a Hydrological implications

The juxtaposition of sediment patches of widely varying grain size (cobbles, gravels, sands, silts and clays) representing former channel beds, bars and banks; active and cut-off channel and pond fill deposits, including very fine sediment lenses deposited in stillwaters; and more general floodplain vertical accretion leads to highly spatially variable hydraulic conductivity within river corridor alluvial sediments (Fuchs et al., 2009). As a result of spatially and temporally varying gradients in hydraulic head among surface (rivers and ponds) and subsurface waters, coupled with the complex pattern of hydraulic conductivity described above, the riparian zone experiences complex subsurface flow patterns and moisture gradients. Surface-subsurface water exchanges and flow patterns through riffles (e.g., Kasahara and Wondzell, 2003) and in-channel bars are well-characterised; but similar complex flow patterns are also recognised through old point bar (Revelli et al., 2008) and other alluvial deposits within the riparian zone. Furthermore, bed incision not only lowers water levels within the active channel but creates a major change in hydraulic gradients between the riparian zone and the channel. This can lead to the abandonment of secondary channels (both surface and sub-surface flow paths) and lowering of the water table more generally within the riparian zone (Wondzell and Swanson, 1999), but the precise spatial effects across the riparian zone are moderated by the lateral extent and depth of the alluvial aquifer; its sedimentary structure at multiple scales; and their joint impacts on alluvial aquifer capacity, hydraulic connectivity and conductivity (Stanford and Ward, 1993, Kasahara and

Wondzell, 2003). From the plant perspective, this leads to an environment in which water supply may be localised and temporary in the short-to-medium term.

b Geochemical implications

The soluble nutrient transport consequences of such heterogeneous shallow groundwater flow have been investigated in the context of riparian diffuse pollution buffers, and nitrogen (Cirimo and McDonnell, 1997, Devito et al., 2000), phosphorus (Carlyle and Hill, 2001, Fuchs et al., 2009) and other contaminant species (Heeren et al., 2010), and these have been observed to exhibit hotspot phenomena. Additionally, water and solute transport are further complicated by the existence of large diameter macropores in riparian wetlands, attributed particularly to dead roots and stems (Parsons et al., 2004, Casey and Klaine, 2001). Again, from the plant perspective, this constitutes a rooting substrate where the inputs, retention and availability of macronutrients may be widely and variably distributed.

2.1.4 Summary

The particular combination of conditions of hydrological connectivity, disturbance, resource availability and riparian substrate composition is unique to each river system and reach. However, within such physiographic boundary conditions, the riparian ecotone represents a suite of habitats in a zone of extreme spatial and temporal variability, in which physical disturbance dominates (in natural systems) and present conditions are a product of past as well as present events.

Though water is never too far away (whether in time or space), the often coarse-structured riparian soils can become drier than those of the surrounding catchment, and this can represent a challenging environment for plants. There are potentially great fitness advantages resulting from large resource inflows, *if* they can be retained for exploitation and not lost downstream. Capitalising on such opportunities requires a particular suite of adaptations which are discussed in the following section.

2.2 PLANTS IN THE RIPARIAN ZONE

Plants in the riparian zone are both passively influenced by the dynamic physical environment, and actively interact with and modify it. In this section, the role of vegetation is presented first in relation to adaptations to allogenic pressures and constraints, and then ecosystem engineering and autogenic conditions.

2.2.1 Evolutionary consequences of dynamic physical conditions

Variability in the physical environment of the riparian zone leads to a diversity of habitats and ecological niches (Ward et al., 1999, Viers et al., 2012), and so making generalisations about plant strategies and characteristics can be problematic. In light of this, the following discussion is limited to perennial woody species.

In attempting to relate adaptations to environmental conditions at the community level, a traditional taxonomic approach is of limited value. Instead, there has been a move to synthesize understanding of common features at species-level by classifying ‘functional traits’ (Lavorel et al., 1997). Though there are several approaches, Cornelissen et al. (2003) attempted a unifying framework of 28 such characteristics (Table 2.1), which has been widely adopted. Note that clonality, form, physical strength attributes, nutrient strategy, root architecture and regenerative traits are all considered to be important associations with disturbance, and that many of these are also recognized to be involved with reciprocal influences upon the disturbance regime. Traits below are structured within the context of the plant life cycle.

a Shoot growth

Growth rates of riparian trees can be extremely high (Stromberg, 2001, Francis et al., 2006) by comparison to their strictly terrestrial counterparts. This is particularly the case for early successional species, mirroring the behaviour of terrestrial species (e.g., Baker et al., 2003). This trait is contradictory to early assertions that ‘stress-tolerators’ may have limited ability to exploit favourable conditions when they become suddenly available (Grime, 1979, Chapin, 1980), and suggests instead either that plants inhabiting disturbance-prone riparian areas have more of a ‘sit and wait’, responsive strategy or (perhaps more likely – see below) have sufficient root systems to secure continued access to widely dispersed resources. Fast shoot growth rates are of course crucial for survival where burial is a common hazard (Kent et al., 2001).

Rapid growth in pioneer species requires characteristics (such as low-density, low-cost stems and high concentrations of nutrients in leaves associated with the proteins involved in photosynthesis) which usually come at the cost of factors enhancing survival (e.g., dense-wooded, damage-resistant stems and unpalatable leaves with low nutrient concentrations and more fibre and tannins) (King et al., 2006). Certainly, members of the Salicaceae (willows, poplars and their allies) are usually characterised by fast growth and low density wood with large xylem vessels and sieve tube elements, and this imparts a low breaking strength and poor drought resistance.

Woody riparian plants often readily reproduce vegetatively, by re-sprouting either from root systems, stem fragments or entire downed trees. This is a common trait in disturbed environments (Rood et al., 2007, Bendix and Cowell, 2010), and describes a strategy in which standing stems are somewhat expendable, and so material strength is less crucial for survival. The ‘persistence niche’ imparts fitness advantage over seedling recruitment in such cases, as greater resource stores are available to the shoot post-disturbance (Bond and Midgley, 2001). Indeed the mass of the sprouting fragment appears to be one of the best predictors of shoot growth rate (Stenvall et al., 2006, Chong et al., 2007, Francis, 2007).

Stem growth rate does depend on geomorphic context, however, and the elevation and substrate texture of stem fragment deposition sites have been found to be strongly influential (Francis, 2007). Local competition is also a determining factor which interacts with position in relation to specific landforms (Willms et al., 2006).

b Root growth

Much study in this area has been focused on the rapid initial water-table tracking growth of roots of cuttings or seedlings, in order to link patterns of recruitment with hydrological characteristics, partly motivated by concerns over riparian forest decline in the USA (Rood et al., 2005). These studies show rapid growth of up to nearly 5 cm day⁻¹, which is actually promoted by declining water table depth (Kranjcec et al., 1998). Abrupt drops are rarely tolerated, however, but can lead to preferential recruitment of only the most resistant genotypes and species (Guilloy et al., 2011). Fine root growth preferentially exploits the capillary fringe and is inhibited in the saturated zone (Imada et al., 2008), reflecting the relatively high oxygen demand of such rapid growth.

Table 2.1 Functional trait associations with environmental and ecological stressors, and feedbacks. Cornelissen et al. (2003)

Traits		Stressors / feedbacks	Climate response	CO ₂ response	Response to soil resources	Response to disturbance	Competitive strength	Plant defence / protection	Effects on biogeochemical cycles	Effects on disturbance regime
Whole-plant traits	Growth form		x	x	x	X	x	x	x	x
	Life form		x	x	x	X	x		x	x
	Height		x	x	x	X	x	x	x	x
	Clonality		x	?	x	X	x			?
	Spinescence		x	?			x	x		?
	Flammability			?			x	?	x	x
Leaf traits	Specific leaf area		x	x	x		x	x	x	
	Leaf size		x	?	x		x	x	x	
	Dry matter content		x	?	x			x	x	x
	N and P concentration		x	x	x	X	x	x	x	
	Physical strength		x	?	x	X		x	x	
	Leaf lifespan		x	x	x	X	x	x	x	x
	Leaf phenology		x		x		x		x	x
	Frost resistance		x				x	x		
Stem and belowground traits	Stem specific density		x	?	?	X		x	x	x
	Twig dry matter content		x	?	?	?		x	x	x
	Twig drying time		x	?	?				?	x
	Bark thickness				x	X		x		?
	Specific root length		x	?	x		x	x		?
	Fine root diameter		x	?	x					
	Root depth distribution		x	x	x	X	x		x	x
	95 % rooting depth		x	?	x		x			x
	Nutrient uptake strategy		x	x	x	X	x		x	
Regenerative traits	Dispersal mode					X				
	Dispersule shape and size					X				
	Seed mass				x	X	x	x		
	Resprouting capacity			x	x	X			x	

Bioengineering has been an alternative motivation behind studies of more established riparian root systems, and further discussion of these is presented in Section 2.3.3, below. Edmaier et al. (2011) present a good overview of literature describing the diversity of root architecture, noting that, overall, primary roots tend to be positively geotropic, secondary ones tend to be diageotropic and further branches are more likely to be ageotropic, responding to water and nutrient demand and availability. Notable differences in taproot-

dominated (e.g., *Salix* spp.) and more extensive suckering horizontal root systems have been interpreted as alternative adaptations for better anchorage on the bank face versus bank top and floodplain (Mallik and Rasid, 1993). Though there is great diversity of rooting patterns, reflecting the heterogeneity of water and nutrient sources in the riparian substrate, perennial woody species generally all have extensive laterals (Stromberg, 2013), presumably in order to secure continuing resource supply. There is also significant plasticity in the development of perennial root systems, with facultative phreatophyty observed in response to longer-term changes in the water table (Naumburg et al., 2005, Rood et al., 2011).

c Sexual reproduction

Though vegetative reproduction is a valuable adaptation to continuous disturbance, genetic recombination is also essential for ensuring developmental plasticity and the ability to exploit evolving niches, and to effectively compete in environmentally and ecologically changing conditions. Riparian flowering strategies are highly variable (Barrat-Segretain, 1996), but among the majority of trees in the temperate zone, wind pollination dominates.

Interestingly, Nielsen et al. (2010) report the unusually high occurrence of dioecy in riparian shrubs and trees, and their observations of geomorphic segregation of the sexes in *Populus* spp. illustrates the extent of variability in genetically-determined physiology even within species. Hybridisation is also a common feature which increases the sympatric diversity of genotypes and potential adaptability (Rieseberg et al., 1996) in long-lived riparian plants.

d Dispersal and recruitment

As mentioned above, re-sprouting vegetative fragments are a much more reliable mode of regeneration than seedling recruitment for many riparian species, representing *dependence* (cf. tolerance) on physical disturbance. Rood et al. (2003) concluded that damage, rather than cladoptosis, was the primary source of successfully establishing fragments.

Seed production by woody riparian species around the globe predominantly follows the ruderal strategy (many seeds with small nutrient investment in each) (Pettit and Froend, 2001), which is consistent with unpredictable physical conditions (Grime, 1979). Wind dispersal is associated with this strategy, and riparian trees are no exception, though in such close proximity to flowing water, hydrochory is also a dominant process, imparting a directionality in seed dispersal (Bertuzzo et al., 2007, Gurnell, 2007) which can be countered almost solely by air movement.

The tendency toward small seeds reduces the period of viability, however, and so the temporal variation in seedling recruitment can be very large indeed, relying upon the ideal

superposition of seed release and optimal hydrological events for dispersal to suitable (and limited) germination sites (Greet et al., 2011). These concepts are incorporated into the ‘recruitment box’ model of Mahoney and Rood (1998) (Figure 2.3), which takes into account the rate of tolerable water table decline. Successful establishment requires a sufficient period without disturbance, post-germination (Polzin and Rood, 2006).

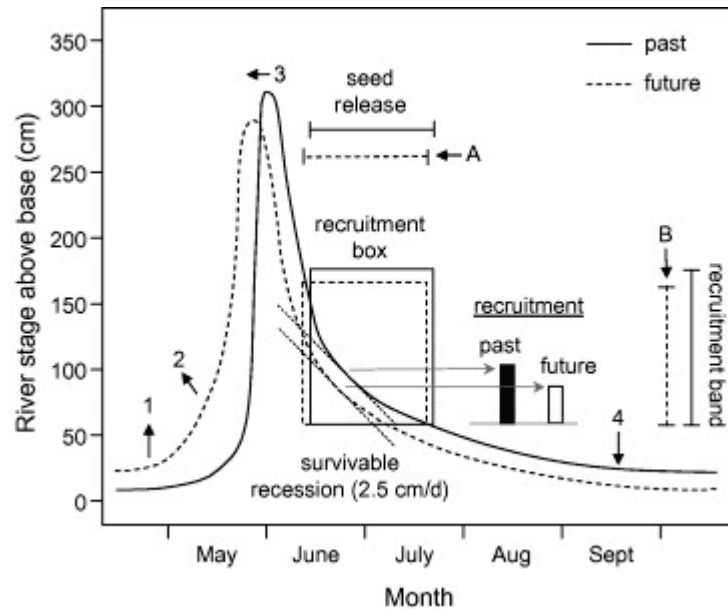


Figure 2.3 Recruitment Box Model for riparian cottonwoods, showing predicted response to changes in seasonal hydrology. Under this model, recruitment occurs only when stage decline is below a critical rate, within a certain elevational band and during the period of seed dispersal and viability. Rood et al. (2008), after Mahoney and Rood (1998)

Owing to the variability of substrate types in the riparian zone, spatial variability in recruitment is high. Particular areas of more successful establishment include abandoned channels (Stella et al., 2011) and zones on channel margins (Gurnell et al., 2008), fine-textured bars (Dixon et al., 2002) and areas within braidplains of a particular elevational range (Francis, 2004).

2.2.2 Influences on physical dynamics: Ecosystem engineering

By altering the spatial distribution of flow velocities not only within the channel but also the riparian zone during floods, vegetation alters the spatial distribution of sediment deposition and erosion. This section first describes small-scale, direct influences on physical dynamics, and then discusses their emergent implications for landform dynamics and channel styles, as well as circular feedbacks to the development of vegetation itself.

a Short term plant- and patch-scale aerial processes

For the duration of their inundation (from near continuous at low-flow river margins, to perhaps infrequent hours on the floodplain), above-ground riparian plant structures represent discrete yet complex drag elements. This has the overall effect of increasing hydraulic roughness and reducing flow velocities in the vicinity of vegetation, and thus reducing sediment transport. However, numerical and physical modelling in flumes has demonstrated that effects on the flow field are complex, and depend on many factors.

The fundamental features of submerged vegetation affecting flow velocity are its frontal area (i.e. the reduction in the cross-sectional area available to accommodate flow) and its complexity in terms of the surface area of the solid-liquid boundary. Numerical and physical models frequently simply represent vegetation as an array of rigid upright cylinders, and this can replicate the *broad* flow patterns observed in real-world channels (e.g., McBride et al., 2007, Larsen et al., 2009), although field validation is often lacking. However, the vegetation profile is dependent on the flexibility of stems, and so yielding plants such as *Vallisneria spiralis* tend to be of lower morphological impact than rigid macrophytes such as *Sparganium angustifolium* (O'Hare et al., 2012) or woody stems (Yagci and Kabdasli, 2008, Hopkinson and Wynn, 2009). The situation is furthermore complicated in reality by the variety of growth forms (Puijalon et al., 2011) and leaf morphologies (Albayrak et al., 2012). Even with a simple rigid cylindrical canopy model, drag and turbulence is variable within the water column (Garcia et al., 2004).

Such fluid dynamic effects are highly dependent on discharge and the absolute size of the plant, owing to scale-related variability in the dominance of viscous forces (Reynolds number). Therefore, while a field of vegetation elements of the order of a few millimetres can produce rapid aggradation (e.g., Wu and Wang, 2004), a comparable patch of centimetre-scale 'simulated trees' may result in wider propagation of turbulence and potential erosion (McBride et al., 2007, Sanjou and Nezu, 2011). This also explains why the canopy branching architecture and fractal properties of the plant are important, as different hydraulic effects may be observed in different parts of the organism (consider the form of an isolated riparian tree, for example, with a large, single trunk and dense canopy).

Mature woody riparian vegetation also presents a source of in-channel wood, which can have very significant hydrogeomorphological effects. In steep, narrow headwaters, wood jams are likely to span the channel and retain a large volume of sediment, resulting in a stepped river bed long-profile (Bunn and Montgomery, 2004, Cadol and Wohl, 2013). Where wood only partly blocks the channel section in small but lower-gradient streams, dead wood is usually

highly important for maintaining a diversity of hydraulic environments and thus variability in the cross-section (Piégay and Gurnell, 1997, Daniels and Rhoads, 2004, Cadol and Wohl, 2013). In large rivers, wood accumulates at channel margins (Gurnell et al., 2002), but also in isolated patches on bars, typically formed around large pieces or ‘key members’. Whether these key members are dead trunks (Abbe and Montgomery, 1996) or remain alive on deposition (Gurnell et al., 2005), the pattern of flow modification and thus erosion and deposition around these isolated features can be remarkably similar (Figure 2.4). Such wood deposits are particularly important as new colonisation sites for vegetation (Francis et al., 2008), in the harsher, exposed areas of large rivers, and have important follow-on effects, as discussed in the next subsection. Unlike living in-channel vegetation, large wood is often rather transient, being subject to re-mobilisation (e.g., Van der Nat et al. (2003) observed 95 % turnover in a single flood event) and decay (Pettit et al., 2006, Bataineh and Daniels, 2014). Wood jams may also have much lower porosity and thus greater hydraulic effects than living vegetation (Manners et al., 2007).

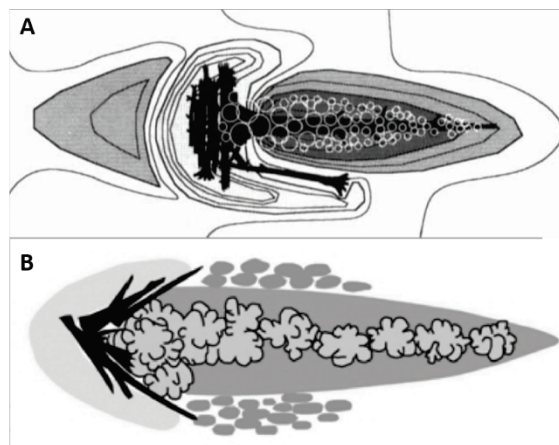


Figure 2.4 Typical topography and layout of isolated wood accumulations where the key member is a dead (A (Abbe and Montgomery, 1996)) or living and resprouts (B (Gurnell et al., 2005)). Smaller wood pieces accumulate on upstream-facing root plate, causing development of upstream arcuate pool. Slow or still water causes peak elevation around root plate of key member, tailing off in raised depositional ridge in lee, which has steep sides caused by flow concentration along its margins. Flow direction is left to right.

b Long term, channel scale

Boundary layer effects are experienced across the full range of spatial scales in interactions between vegetation and flowing water. In a similar way to which plant stems, if in sufficient density, start to behave as a hydraulic unit or patch, at greater temporal and spatial scales, patches may coalesce to produce increasingly terrestrial landforms (Gurnell et al., 2005).

Early research identified simple associations between channel forms and vegetation, but now it is increasingly appreciated that vegetation, energy dissipation, sediment, nutrient and biomass dynamics and channel form all act in a complex and tightly linked system (Gurnell, 2014).

Early investigators observed that, by reducing bank erosion, the plant community influences channel width, with forested reaches generally being wider than those with predominantly grassy riparian vegetation (Trimble, 1997, Hession et al., 2003, Sweeney et al., 2004). Gurnell et al. (2015) propose a conceptual model whereby the strongest interactions between vegetation and morphology occur in a critical elevation zone where inundation is frequent, but not continuous. In multi-thread rivers, where the length of channel margin is high, this critical zone occupies a large area, and vegetation has the greatest potential to influence morphodynamics.

The density of plants has been observed (Kondolf and Curry, 1986) and shown experimentally (Crosato and Saleh, 2011) to influence the actual transition between single- and multi-thread planforms. The gradual coalescence of pioneer patches of vegetation as they grow is a feature common in anabranching (e.g., Tooth and Nanson, 2000) and braided rivers (e.g., Bertoldi et al., 2011a), and leads to flow concentration around increasingly large stabilised landforms (Welber et al., 2012). The resulting increase in the topographic range within the active width of vegetation-stabilised rivers is very apparent in elevation surveys (Bertoldi et al., 2011b). Erosion of vegetation and re-setting of the plant community succession occurs frequently, however, and physical disturbance helps maintain an ever-changing system. In cases of extremely rapid vegetation growth or extensive cover, the vegetation itself may cause catastrophic changes, such as channel blockages leading to avulsion in anastomosing rivers (Tal et al., 2004). At the largest scales, riparian vegetation influences river-scale hydrology by dissipating flood waves (Anderson et al., 2006) and having a significant influence on the magnitude of losses due to evapotranspiration (Nagler et al., 2008, Jarvis, 2011, García-Arias and Francés, 2015).

Geological evidence of changes in alluvial river forms at the time of the evolution of land plants suggests that their influence over river morphology is indeed profound and ancient (Davies and Gibling, 2010). Greater understanding of coupled vegetation and fluvial landform dynamics is therefore achieved through consideration of the evolutionary processes (Steiger and Corenblit, 2012) which have led to the development of the systems observed today, integrating several million generations of bi-directional influences. This is a concept explored by Corenblit et al. (2008), and further developed for the Salicaceae in northern temperate zones (Corenblit et al., 2010, Corenblit et al., 2014). The fluvial

biogeomorphologic succession (FBS) model of these authors is a cyclical progression of four phases of contrasting dominance of biotic and abiotic forces (Figure 2.5).

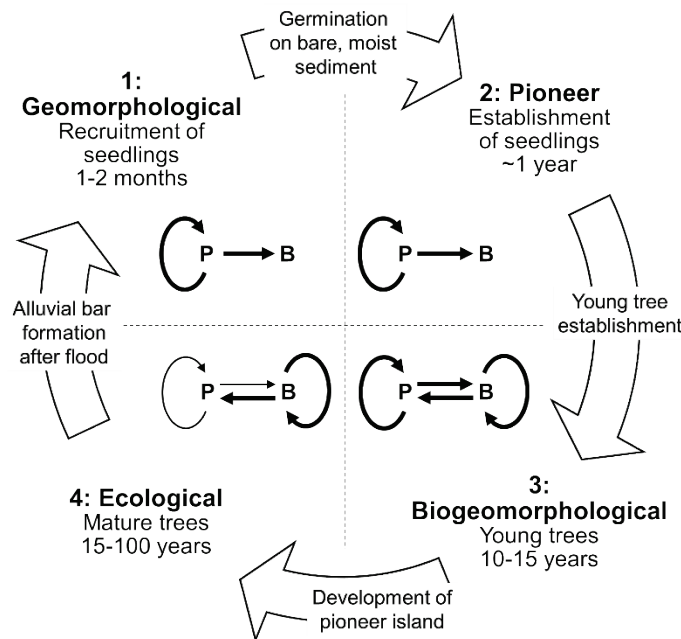


Figure 2.5 Four phases of the biogeomorphological life cycle of riparian black poplar and their approximate durations. The strength of interactions between and physical (P) and biosocial (B) components are indicated in the central portion by the thickness of the arrows. The schematic form of the plants and associated landforms are presented later in Figure 6.1. After Corenblit et al. (2014)

The initial recruitment of seedlings or vegetative fragments in the first phase is dependent on the production of suitable substrate sites and transport of propagules to these, and is therefore virtually entirely under the influence of the physical forces of the river and its microclimate. The pioneer phase is one of survival, where seedlings or initial shoots are vulnerable to physical disturbance and must secure a foothold. It is not until the biogeomorphological phase, where young trees have properly established, that the vegetation begins significantly to influence the physical environment. Vegetation at this point is much more resistant to disturbance and begins to cause the deposition of fine sediment and the development of pioneer landforms which enhance its own growth and survival. This is the phase of true ecosystem engineering which, in this conceptual model, leads then to the development of a much more terrestrial ecosystem, dominated by internal, ecological processes such as resource competition and cycling, increasingly independent of the physical fluvial effects.

The cycle above may be reset at any stage by erosion of vegetation, but the probability of this decreases not only with progression in the cycle but with longitudinal variation in, e.g., gradient or the degree of floodplain confinement (Gurnell et al., 2015). Collins et al. (2012) argue that a similar, self-reinforcing cycle occurs in association with very large pieces of slow-decaying wood delivered from mature forests to river systems. Acting as nuclei for accumulating transported organic and fine sedimentary material and consequent sediment accretion, very large deposited wood may trigger landform development by providing safe recruitment sites for vegetation. As a result of the size and slow decay of the wood, many of these sites remain highly resistant to river erosion and persist until the trees therein mature and eventually become a source of further very large wood pieces. Thus the initially small effects of riparian vegetation (living or dead) accrue over time to promote a physically complex, biodiverse and self-reinforcing state.

2.2.3 Summary

Unpredictability, disturbance and extreme variability of the physical environment leads to a wide variety of viable plant life history and functional trait strategies, but for those persistent, woody riparian plant species, a particular suite of adaptations proves successful. Such species are able to tolerate unfavourable conditions by securing access to multiple water and nutrient resources, and possess the ability to exploit the unique but sporadic benefits of living in the riparian zone.

Further to this, however, flexibility of form, dispersal and physiology is a particularly advantageous adaptation in such an environment. This is exhibited through highly responsive growth both above and below the ground surface, the ability to reproduce vegetatively in multiple ways, and the ability to fine-tune the genotype through hybridisation and wind-pollinated sexual reproduction.

The successful colonisation of the riparian zone by plants has led to the latter becoming a major factor in the way the zone physically evolves and responds to fluctuating flows of water and resources. Vegetation generally increases the retention of sediment within the fluvial system, but creates structure and form at all scales by differentially altering patterns of erosion, deposition and sediment sorting. The complexity of such patterns is due in large part to the diversity of life history and ecosystem engineering strategies of plants, and the fact that their influences are mediated through multiple feedbacks and complex process pathways within the plant community and wider ecosystem.

2.3 THE REALM OF ROOTS

Whilst a strong case has been made for the crucial role of above-ground plant biomass in the natural functioning and formation and maintenance of physical complexity of the riparian zone, it is clear that this vegetation must be able to maintain a strong foothold in order to perform this role. Furthermore, the associated root systems and below-ground biomass directly influence erosion and aggradation-degradation processes and are critically important to the vitality of above-ground ecosystems.

We will ascertain from the following section exactly what we know of the physical mechanisms at work in the riparian rhizosphere, and discover that the field is somewhat undersupplied with information and interpretation relating to the key biological and ecological parameters which frame the system. In answer to this, advances in understanding the way root systems develop are explored, as well as knowledge on the means of sediment reinforcement by roots.

2.3.1 Root physiology and development

Preceding sections have revealed multiple ways in which subaerial plant biomass can influence the physical dynamics of river banks and the functioning of the wider riparian ecosystem. It is apparent, however, that most advances in this field have resulted from a growing appreciation of the importance of such influences for fluvial geomorphology or wider riparian ecology, as opposed to much direct interest in the riparian context from the particular perspective of plant science. There is, therefore, a need for interpretation of current knowledge on root systems in order to tease out pertinent issues for riparian zone dynamics. A review of the factors determining the structure of root systems, and a reading of this from the riparian perspective, is presented below. This is followed by brief consideration of the physical make-up of roots, with consideration given to their mechanical properties.

a Root system architecture and its control

A significant problem encountered in the modelling of root reinforcement is predicting root system architecture; i.e., at what depth, density and orientation roots will be encountered in the sediment or soil mass. This is due to the inherently indeterminate nature of plant development, which is the most fundamental way in which plant physiology is regulated. Geotechnical models which include a root component almost always assume a simple deterministic structure or require large amounts of input data regarding root distributions.

If the situation is to be improved, we must gain a better handle on the factors influencing root architecture.

Plant form develops in a linear process driven by clusters of stem cells limited to the tips of extending axes, known as apical meristems. These localised regions of cell division lay down a growing root or shoot behind them and, in the shoot, define the particular conserved arrangement of organs such as leaves and flowers by producing regular cell clusters called ‘primordia’ (Figure 2.6), which may then continue to follow a path of differentiation to form lateral structures. The initial shoot and root axes are pre-formed in the embryo of seed plants and the original ‘seminal’ root often forms the basis of the root system structure and can penetrate and persist in the substrate to significant depth (Johnson, 1994). From this primary root branch lateral roots which, in turn, may also form their own second order laterals, and so on. The extent and direction of apical growth and the positioning and frequency of lateral roots form the basic determinants of root system architecture (Jones and Ljung, 2012).

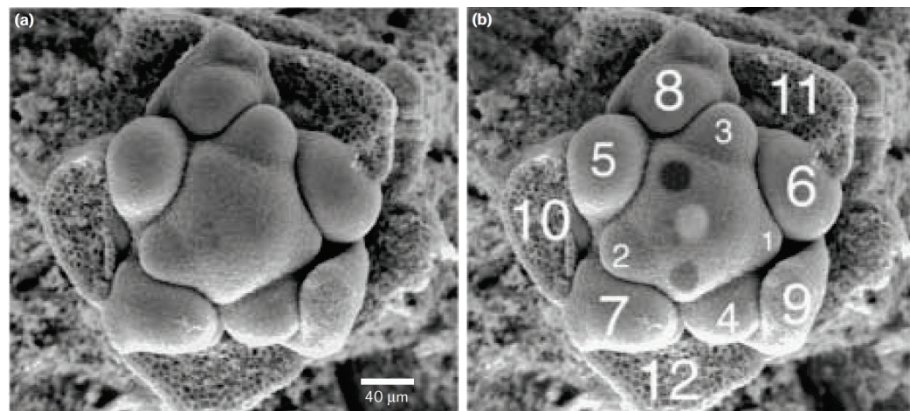


Figure 2.6 Shoot apical meristem of *Arabidopsis thaliana* L., showing spirally-arranged primordia just prior to flowering. Organs are labelled from youngest to oldest in (b), where the meristem is also marked with a light dot, and the positions of the next two primordia with dark dots. Clark (2001)

The root apical meristem (RAM) is less studied than that of the shoot (SAM) but is markedly different in structure and function Figure 2.7. As it forces its way through the rooting medium, the RAM is protected by a layer of sacrificial cells – the root cap – which are constantly eroded and replaced by the most distal cells of the meristem. Root cap cells secrete mucilage to lubricate the passage of the root apex through the soil, and also sense the gravity vector via sedimentation of starch-filled statoliths (Boonsirichai et al., 2002). Unlike the SAM, the RAM also possesses a ‘quiescent centre’ of cells which do not actively divide (Dolan et al., 1993), and there is no clear pattern of organ primordia. Instead, in the zone of cell elongation behind the advancing meristem, lateral root primordia develop in the pericycle

– the tissue surrounding the vascular core of the root. The mechanisms regulating the formation of these lateral root progenitors is incompletely understood, but there is evidence that they are produced regularly under the control of an oscillating ‘molecular clock’ (Moreno-Risueno et al., 2010). The extent of influence of external factors on this initial priming phase is unclear, but Jones and Ljung (2012) cite studies which suggest it can be influenced by changes in the gravity vector and the density of primordia can be altered by varying soil nitrogen and phosphorus levels. Subsequent ‘activation’ of later development of lateral roots is certainly influenced by many external factors, as described below. Lateral roots, once initiated, develop their own apical meristems and their growth becomes increasingly less influenced by the parent RAM as the new root apex becomes more distant from it.

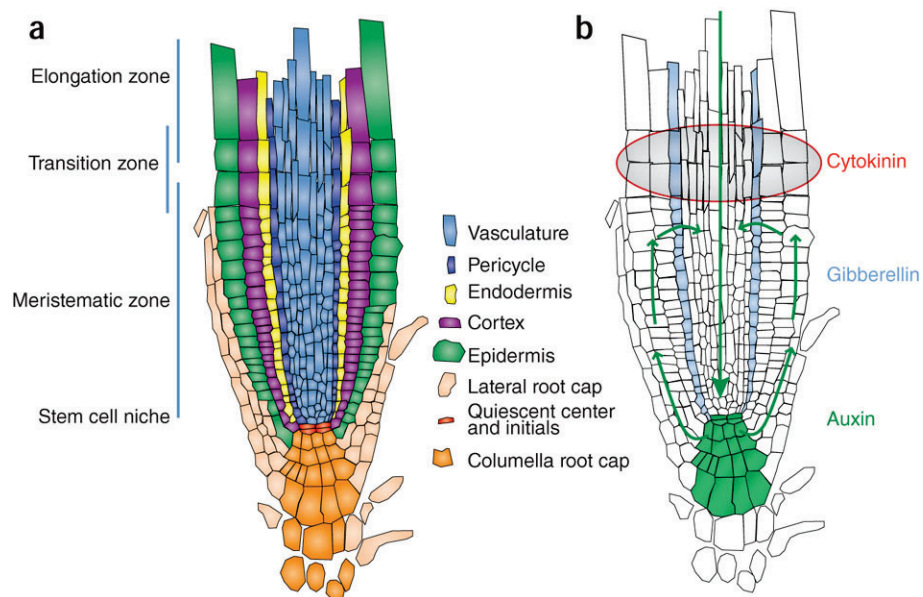


Figure 2.7 Schematic structure (a) and primary hormone concentration maxima and transport dynamics (b) of the root apical meristem. Jaillais and Chory (2010)

Root structure is complicated in woody plants by secondary (radial, as opposed to simply apical) growth. Secondary vasculature (wood) is produced by a cylindrical meristem termed the vascular cambium. This lays down xylem (conducting tissue for water for transpiration) adaxially and phloem (conducting tissue for photosynthate and other organic compounds) abaxially (Figure 2.8). A second lateral meristem, the cork cambium in the periderm, produces protective bark, replacing the primary root epidermis. Meristems are both internally organised Figure 2.7(b) and also coordinated across the whole plant by movement and resulting concentration gradients of hormones. However, the complexities of these signal transduction systems, though receiving the lion’s share of attention within plant developmental research (see, e.g., Jung and McCouch, 2013, for a review), are beyond the

scope of this review. Instead, we will focus on the stimuli and responses critical to the development of root system architecture.

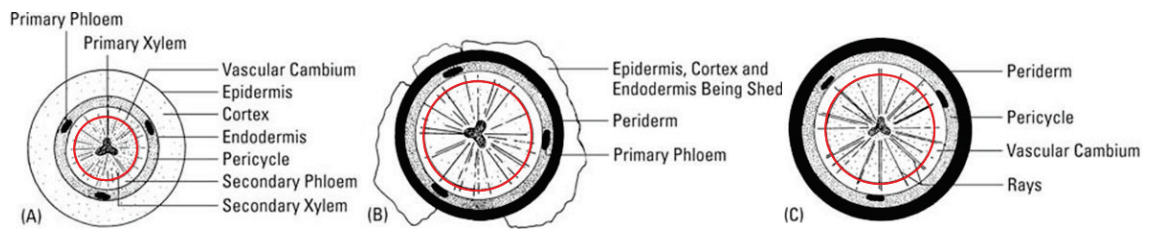


Figure 2.8 Secondary growth progression in roots, showing position of vascular cambium in red. Schematic transverse sections. A: Early secondary growth. B: New secondary tissues crush and shed primary tissues. C: Periderm replaces outer primary protective tissues.

b Exogenous influences on root system architecture

While inherited and conserved root architecture traits can confer fitness in particular environments, it is often the ability to modify the root system to exploit the soil, varying as it usually does in both time and space, which confers a selective advantage. Firstly, physical factors of the rooting medium affect growth in diverse ways. The sensing of gravity in the root cap was mentioned above, and this information can be modulated via hormones to change the direction of growth depending on the specific plant needs (Boonsirichai et al., 2002). All cells have advanced mechanisms to maintain a favourable water balance, and this cellular machinery is also believed to be recruited into the sensation of hydrological gradients in the soil (Monshausen and Gilroy, 2009). However, reactions to moisture gradients in the soil are often masked by positive gravitropism (Eapen et al., 2015), which of course is likely to be associated with water discovery. Water stress tends to suppress lateral root emergence, promoting deeper primary axes (Deak and Malamy, 2005). Excess water in the soil can lead to hypoxia, which inhibits all root growth, but may be alleviated in many species by the formation of tissue with gas spaces (aerenchyma), improving diffusion (Jackson and Armstrong, 1999). Plants growing on high water tables are typified by shallow root systems, and extended flooding may lead to the production of near-surface adventitious roots where flood water is well-oxygenated (Kozlowski, 1997). Physical obstacles also elicit specific responses (thigmotropism), modulating the gravitropic response and causing the root to track along the surface of an impenetrable obstacle (Massa and Gilroy, 2003), and also altering the pattern of lateral root initiation at the point of bending (De Smet et al., 2007). In woody plants, the wood density and secondary growth is more often altered in response mechanical stimuli, rather than the root architecture *sensu stricto* (Danjon et al., 2013, Trupiano

et al., 2012), but it is also possible for physical stresses to induce, for example, the proliferation of lateral roots (Scippa et al., 2008).

Plants do not just require mineral nutrients for survival and growth, but require them in the correct proportions. Therefore, it is often difficult to unravel root system responses to particular chemical species, as these are modulated and coordinated by hormones and other signalling pathways across the plant as a whole. Experimental manipulations of two of the most typically growth-limiting nutrients, nitrogen (N) and phosphorus (P), provide much insight, however. In general, when global N availability is high, both lateral and primary root elongation are inhibited (Linkohr et al., 2002), however, local patches of high N concentrations promote lateral root growth (Drew, 1975), such that the nutrient source may be better exploited. High global P availability stimulates primary root growth and restricts lateral root density and elongation (Linkohr et al., 2002), whereas more P-starved plants show the reverse (López-Bucio et al., 2002). P exists in much less mobile forms in the soil than N, and so this adaptation can be explained by a need for much greater root length per unit soil volume in order to access P. Another growth-limiting macronutrient which has received some attention is sulphur. Here, there appear to be differential responses for chronic (reduced growth of the whole root system (Dan et al., 2007)) and acute deficiency (increased lateral branching (Kutz et al., 2002)) (Lewandowska and Sirko, 2008). Besides macro- and micronutrients, toxic chemical species in the soil can have profound effects on root systems. Aluminium and chloride salts are two particularly common harmful substances and root responses can be variable – particularly to salinity – depending on the level of adaptation to these stresses. Al^{3+} tends to inhibit all root growth (Matsumoto et al., 1996), whereas salt stress may reduce cell elongation rates owing to osmotic effects, and increased lateral root production has been observed in *Arabidopsis* (He et al., 2005).

The rhizosphere is an incredibly complex ecosystem, with many more attributes than just physical and chemical properties which may affect root development. Pathogenic microorganisms may cause diverse effects such as the proliferation of short lateral roots (Simonetta et al., 2007), the formation of abnormal lateral root structures (Zolobowska and Van Gijsegem, 2006) or an increase in root diameter (Ma et al., 2014). Symbiotic microorganisms cause the roots to undergo particular structural alterations such as the formation of root nodules to accommodate rhizobia bacteria (Sprent, 2007), or the development of coralloid roots in cycads (Ahern and Staff, 1994). Of particular significance are mycorrhizal symbioses with fungi, from which most plant species benefit (Brundrett, 2002) via improved access to soil nutrient and water resources, by supplying the fungus with photosynthate. These types of cross-kingdom interactions are now considered to occur

across a continuum from parasitism to mutualism (Karst et al., 2008), and cause different changes in root structure depending on the particular type of species-pairing Figure 2.9. For example, arbuscular mycorrhizal colonisation has been observed to cause dramatic increases in root length and proliferation of laterals in poplar (Hooker et al., 1992), but reduced root length in leek (Berta et al., 1990), and altered branching topology in plane trees (Tisserant et al., 1996). Ectomycorrhizal root tips usually have a distinct thick, stunted form and are generally totally encased in a sheath of fungal hyphae (Figure 2.9, top left). The root apices actually cease growth completely in this case (Clowes, 1981).

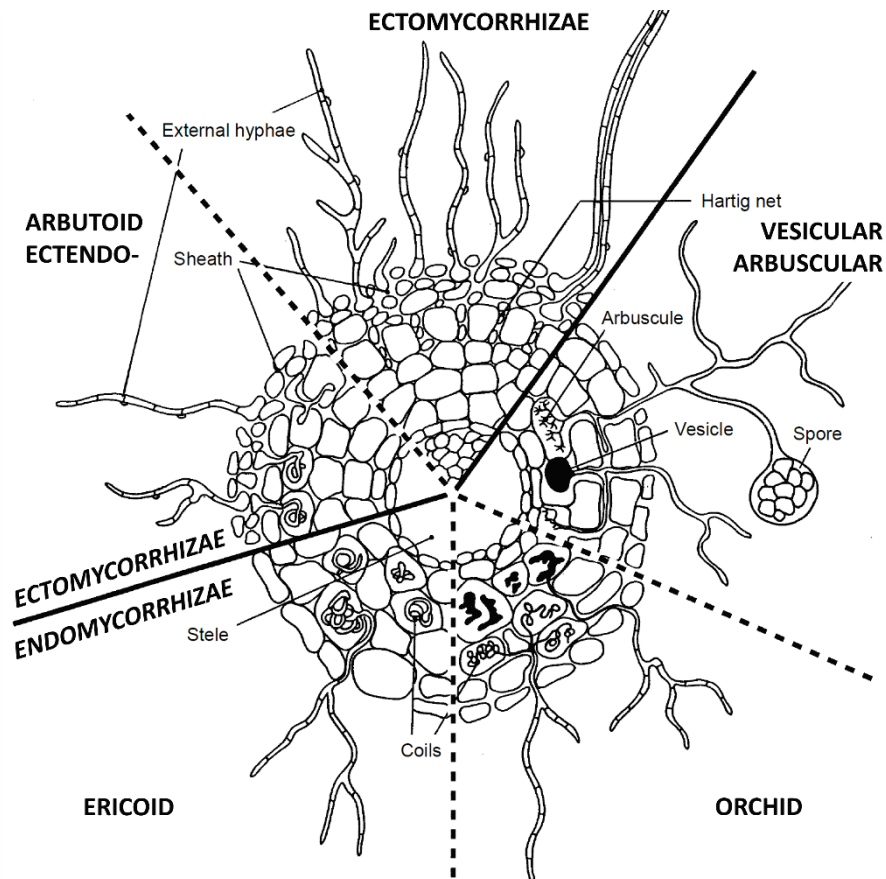


Figure 2.9 Schematic representation of some of the different forms of mycorrhizal-root interfaces. Root transverse section. Selosse and Le Tacon (1998)

2.3.2 Root reinforcement

Notwithstanding the protective boundary layer due to above-ground biomass, vegetated sediments are more able to resist physical deformation and disintegration, both above and below water, as compared to a purely mineral matrix. Mechanisms of reinforcement could be considered as either direct (dependent on strength of the biomass), or indirect (dependent on extraradical factors which are in turn dependent on roots). Research reported by Abernethy and Rutherford (1998) suggested a scale dependence of the dominant bank

erosion mechanism (from indirect processes, through direct erosion resistance to direct mass failure resistance in small, through medium to large catchments, respectively), though in reality all types of process are likely to be active simultaneously to some degree. Integrating all processes into models is only in its early stages, however (Rinaldi and Darby, 2007, Rinaldi and Nardi, 2013). An introduction to the three main and conceptually different root reinforcement effects is presented below.

a Mechanical mechanisms: Mass failure resistance

Analogous to the steel bars in reinforced concrete, plant roots increase the stresses required to cause blocks of sediment to ‘calve off’ river banks, by traversing potential failure planes and tying sediment masses to each other (Abernethy and Rutherford, 2000). Given the complex geometry of root systems, approaches to quantifying this effect have modelled it as a distributed, isotropic additional cohesion applied to traditional geotechnical calculations, based on assumptions of failure of roots perpendicularly crossing a shear plane at a critical tension threshold (Wu et al., 1979). There was consequently some degree of effort put into experimentally determining these critical breaking stresses for roots of different diameters and species (Hathaway and Penny, 1975, Stokes and Mattheck, 1996, Watson and Marden, 2004, Bischetti et al., 2005, Tosi, 2007, De Baets et al., 2008), with the clear result that the finest roots are disproportionately strong, with some notable differences between species (Figure 2.10).

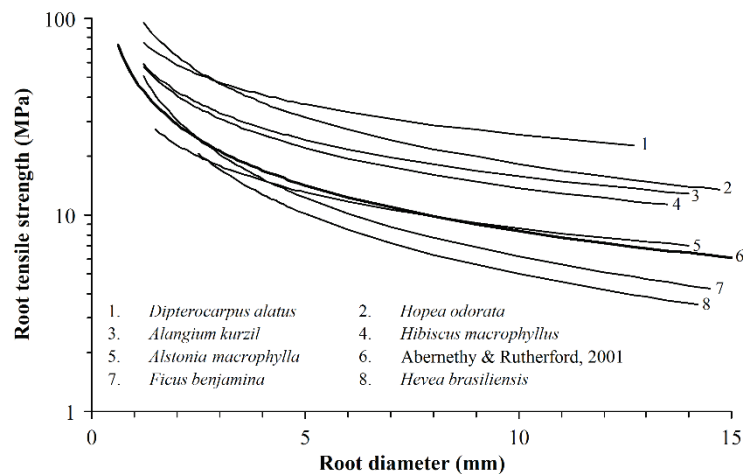


Figure 2.10 Relationship between breaking strength and diameter of roots of a number of different plant species. Abernethy and Rutherford (2001)

However, in reality, roots in soil break progressively, and the ‘maximum strength’ approach has been found to over-predict the reinforcement effect (Waldron and Dakessian, 1981). In recognition of this, Pollen and Simon (2005) developed an elaborated iterative ‘fibre bundle’

root model, where the load on n roots is redistributed among the remaining $(n - 1)$ roots after the weakest one fails. Later investigations have looked at the phenomena of root ‘pullout’ and soil friction interactions more closely, with finds highlighting the importance of root branching (Docker and Hubble, 2008), root orientation and density in relation to the angle of the failure surface (Thomas and Pollen-Bankhead, 2010, Giadrossich et al., 2013), and the moisture status of the soil (Pollen, 2007). Modelling studies have also identified that root mass failure resistance is maximised when vegetation is positioned near the ends of the failure plane (Van de Wiel and Darby, 2007).

b Mechanical mechanisms: Hydraulic erosion resistance

At smaller scales and below the waterline, hydraulic erosion is considered a relatively continuous process once a critical flow rate and boundary shear stress is exceeded (*cf.* mass failure) (Rinaldi and Darby, 2007). Early water jet experiments reported that plant roots could reduce erosion by up to 20,000 times (Smith, 1976), but it is clear that the effect can vary by several orders of magnitude (Hooke, 1980), and Gyssels et al. (2005) argue that the erosion rate is exponentially related to root parameters. Comparative experiments have demonstrated that it is primarily fine roots (with the highest surface area and tensile strength (Burylo et al., 2012)) which enmesh sediment particles and aggregates and increase the shear stress threshold required to detach them from the river bank or bed surface.

As well as the physical binding effect, roots also increase surface hydraulic roughness, reducing boundary shear stress (Kean and Smith, 2004). *In extremis*, protection may constitute an almost continuous bank cover of tightly interwoven roots, effectively preventing any movement of water over the sediment surface beneath. This effect is rather like the use of geotextiles to reduce soil erosion, though there appears to be little investigation of this phenomenon in the scientific literature. While roughness parameter estimates for the aerial parts of vegetation have been constantly investigated and improved, such variables are understandably more difficult to interpret for exposed roots.

The reliability of all erosion models – with or without root-related effects – is highly sensitive to parameters which must be estimated or determined empirically. Rinaldi and Darby (2007) consequently argue that great care must be invested in the sampling strategies employed to make such parameter estimates for model applications.

c Indirect mechanisms

From a geotechnical perspective, sediment or soil strength is conceptualised as resistance to failure, which is due solely to friction and cohesion between particles in a root-free soil. Pore

water affects both these properties, but is constantly removed by vegetation to supply the transpiration stream, usually at a rate close to theoretical potential evapotranspiration in actively growing riparian forest (Tabacchi et al., 2000). The resulting reduction of pore water pressure and development of matric suction can reduce the risk of bank failure by a much greater degree than mechanical reinforcement (Simon and Collison, 2002, Pollen-Bankhead and Simon, 2010), but the effect is seasonal and at its minimum in periods of vegetation dormancy, when bank failure risk is usually greatest. Furthermore, rapid deep infiltration and locally high water content due to preferential flow paths induced by vegetation may be detrimental to bank stability. However, over the longer term, roots often redistribute significant quantities of soil water to dissipate such intense local gradients (Neumann and Cardon, 2012) and maintain lower pore water pressure than would be expected without vegetation.

Root-secreted mucilage probably affords the plant much finer control of rhizosphere moisture than previously appreciated (Carminati and Vetterlein, 2013), and such substances can dramatically affect soil cohesion. Plant- and microbe-derived polysaccharides, proteins and other complex organic molecules bridge and bind the smallest soil particles (Bronick and Lal, 2005), and increase shear strength of the matrix in concert with the physical binding of soil particles and aggregates by fungal hyphae (Beare et al., 1997, Ritz and Young, 2004). By supporting mycorrhizal fungi, plant roots increase the length density of soil hyphae and the concomitant reinforcement effect (Rillig and Mummey, 2006).

2.3.3 Existing studies of riparian root structures

The understanding (and indeed modelling) of river bank reinforcement by roots requires information on root distribution, and this has been the main motivation for studies of root system structure in riparian zones to date. Parameters required for such enterprises include the distributions of root area ratio (sectional area of roots per unit sectional area of bank), root diameters (since breaking stress is dependent on size) and root density (frequency per unit area of bank section) or occasionally root length density (length per unit volume of sediment). Another route for insight into these systems has been via ecohydrological studies, although the focus here has been more on emergent hydrological function as opposed to structures (e.g., Singer et al., 2014). With the exception of one study in which large roots were observed in eroding banks from a boat (Rood et al., 2011), and another in which whole tree root systems were removed from man-made canal, dam and flood protection dikes (Venetier et al., 2015, Zanetti et al., 2015), it appears all riparian root investigations to date have been conducted using the wall-profile or 'trenching' method (Maeght et al., 2013).

Some early excavations by Abernethy and Rutherford (2001) and Simon and Collison (2002) found a steep (near exponential) decline in root numbers with depth, though this only approached a steady curve at distances of several metres from the trunk, at which point numbers and area of roots became extremely low. Depth distributions of root area ratio varied dramatically with species and site, and were particularly erratic close to the main stems of trees. Interestingly, the willow species investigated by Simon and Collison (2002) were found to be quite shallow-rooted. However, all tree species investigated had much deeper root systems than the grasses excavated.

The variability of soil moisture retention and water sources appears to be an over-riding determinant of riparian root system structure. Root systems extending down tens of metres (and even into water-holding caves) have been reported for drought-prone Australian systems (Hubble et al., 2010), and more typical values of maximum rooting depths were reported between 35 and 45 % of tree height by Docker and Hubble (2008). Pollen et al. (2004) found large diameter roots to be more closely associated with particular areas of moisture availability than the fine root system, and asymmetries in large roots of the whole systems removed from man-made dikes mentioned above (Zanetti et al., 2015) reflect asymmetries in soil moisture.

It appears that riparian species are particularly well-adapted to reaching and utilising deep phreatophytic water sources. The extensive meta-analysis of Stromberg (2013) highlights this fact, and also that maximum rooting depth is highly variable and dependent both on the climate to which riparian species are adapted and their growth form (shrubs being most deeply rooted). In their observations of river cut-banks, Rood et al. (2011) note that non-riparian species such as *Picea glauca* do not develop the deep roots observed in *Populus* spp. which allow permanent access to the capillary fringe. These authors also identify associations with this deep phreatophytic root distribution and climatic moisture availability in the growth season, suggesting that when shallow (precipitation-related) water sources are reliable during critical seasons, there is less investment in these deep systems. Stable isotope studies suggest, however, that riparian trees (at least poplars) are able to switch between deep and shallow water sources within and between years (Singer et al., 2014), implying that they maintain a well-developed system of roots both within surface layers and deeper deposits. Glasshouse experiments on riparian species confirm that fine root investment is highly plastic and driven by both water availability and shoot photosynthetic demand (Snyder and Williams, 2007).

As studies of the roots of any mature trees in their natural context are sparse, and this dearth is particularly acute for the riparian context, a few further piecemeal observations are worthy of reporting here. In their large riparian study, Pollen et al. (2004) note that fine root density

is much greater in the vicinity of older trees, and that taproot systems are more common on free-draining ex-sand bar deposits. None of the trees species removed from dikes by Zanetti et al. (2015) penetrated the water table, with the exception of *Alnus* spp. With respect to *Populus* spp., the same authors noted the occurrence of vertical ‘sinker’ roots exploiting pre-existing cracks in the soil matrix, but only within three metres of the trunk. Finally, in a comparative study of riparian buffer zone vegetation, Fortier et al. (2013) noted the consistently high root biomass and proliferation of fine roots in poplar stands.

2.3.4 Summary

The current model of root development is incomplete, and nearly all findings have been from one small annual plant: *Arabidopsis thaliana*. Even if we did have an exhaustive model of plant physiology and development, to predict root system structure would require a complete assessment of the current and past condition of the whole plant and a comprehensive map of the complex states and processes in the soil. The latter is particularly far from being achieved.

There is a great deal of simplification and many assumptions about root system structure in the modelling of sediment reinforcement, but without a strong evidence base. Research is highlighting the great importance of access to water in structuring riparian root systems, but there is clearly a very large amount of variability in the forms occurring in natural systems. Given the dramatic effects of parameter uncertainties in models of bank stability and the effect of roots, there is still a requirement for further, carefully planned field sampling strategies to evaluate such parameters and their availability.

2.4 IDENTIFIED KNOWLEDGE GAPS

The above review attempts to provide an overview of the current state of knowledge of vegetation dynamics, particularly of woody species, in riparian zones, and the role of tree root systems in biogeomorphological processes. This appraisal also highlights some key areas where our understanding of these processes is lacking. These are introduced below and provide the justification for the research presented in this thesis. Research questions to frame testable hypotheses leading to improved understanding within these knowledge gaps are presented in the next chapter.

2.4.1 Root system architecture of mature trees

Owing mainly to the difficulties involved with their observation, very little is actually known about the root architecture of mature trees in natural environments, particularly in the riparian setting. Most studies have been conducted on lab-grown annual plants, or in the case of woody species, seedlings or the early growth of cuttings. While great new insights are emerging from an increasingly complex molecular model of root growth and its controlling variables, there is a need to integrate growth responses and patterns over spatio-temporal scales relevant to riparian zone dynamics.

2.4.2 Effective representation of root distributions within bank stability models

Though it is of course necessary to simplify, it is clear that the assumed geometry of root systems included in many geotechnical models is not particularly realistic. There is a tendency to adopt deterministic, continuous depth decline models, independent of many of the factors which are known to induce variability in roots system structure. There is a need, therefore, to investigate and explain the variability of root systems around the basic models currently employed.

2.4.3 Persistence of root structures under fluvial disturbance

Studies have shown the impressive tolerance of dramatic physical disturbance in many riparian species – even to the point of complete uprooting, transport over large distances, and deposition on bare alluvial sediments. Current models of the sub-aerial components of fluvial vegetation dynamics extend only to progressive burial of pioneer vegetation, but what becomes of the buried structures is unknown. Whether they persist or decompose, and to what extent, has significant hydrogeomorphological, as well as ecological implications, and may prove to be an important unaccounted process in riparian vegetation dynamics.

2.5 REFERENCES

- ABBE, T. B. & MONTGOMERY, D. R. 1996. Large woody debris jams, channel hydraulics and habitat formation in large rivers. *Regulated Rivers: Research and Management*, 12, 201-221.
- ABERNETHY, B. & RUTHERFURD, I. D. 1998. Where along a river's length will vegetation most effectively stabilise stream banks? *Geomorphology*, 23, 55-75.
- ABERNETHY, B. & RUTHERFURD, I. D. 2000. The effect of riparian tree roots on the mass-stability of riverbanks. *Earth Surface Processes and Landforms*, 25, 921-937.
- ABERNETHY, B. & RUTHERFURD, I. D. 2001. The distribution and strength of riparian tree roots in relation to riverbank reinforcement. *Hydrological Processes*, 15, 63-79.
- ACUÑA, V. & TOCKNER, K. 2009. Surface-subsurface water exchange rates along alluvial river reaches control the thermal patterns in an Alpine river network. *Freshwater Biology*, 54, 306-320.
- AHERN, C. P. & STAFF, I. A. 1994. Symbiosis in cycads: The origin and development of coralloid roots in *Macrozamia communis* (Cycadaceae). *American Journal of Botany*, 81, 1559-1570.
- ALBAYRAK, I., NIKORA, V., MILER, O. & O'HARE, M. 2012. Flow-plant interactions at a leaf scale: Effects of leaf shape, serration, roughness and flexural rigidity. *Aquatic Sciences*, 74, 267-286.
- ANDERSON, B. G., RUTHERFURD, I. D. & WESTERN, A. W. 2006. An analysis of the influence of riparian vegetation on the propagation of flood waves. *Environmental Modelling & Software*, 21, 1290-1296.
- ANTHEUNISSE, A. M., LOEB, R., LAMERS, L. P. M. & VERHOEVEN, J. T. A. 2006. Regional differences in nutrient limitation in floodplains of selected European rivers: Implications for rehabilitation of characteristic floodplain vegetation. *River Research and Applications*, 22, 1039-1055.
- ARSCOTT, D. B., TOCKNER, K. & WARD, J. V. 2001. Thermal heterogeneity along a braided floodplain river (Tagliamento River, northeastern Italy). *Canadian Journal of Fisheries and Aquatic Sciences*, 58, 2359-2373.
- BAKER, T. R., SWAINE, M. D. & BURSLEM, D. F. R. P. 2003. Variation in tropical forest growth rates: Combined effects of functional group composition and resource availability. *Perspectives in Plant Ecology, Evolution and Systematics*, 6, 21-36.
- BARRAT-SEGRETAIN, M. H. 1996. Strategies of reproduction, dispersion, and competition in river plants: A review. *Vegetatio*, 123, 13-37.
- BATAINEH, M. M. & DANIELS, L. D. 2014. An objective classification of largewood in streams. *Forest Ecology and Management*, 313, 1-9.
- BEARE, M. H., HU, S., COLEMAN, D. C. & HENDRIX, P. F. 1997. Influences of mycelial fungi on soil aggregation and organic matter storage in conventional and no-tillage soils. *Applied Soil Ecology*, 5, 211-219.
- BEECHIE, T. J., LIERMANN, M., POLLOCK, M. M., BAKER, S. & DAVIES, J. 2006. Channel pattern and river-floodplain dynamics in forested mountain river systems. *Geomorphology*, 78, 124-141.
- BENDIX, J. & COWELL, C. M. 2010. Fire, floods and woody debris: Interactions between biotic and geomorphic processes. *Geomorphology*, 116, 297-304.
- BENDIX, J. & HUPP, C. R. 2000. Hydrological and geomorphological impacts on riparian plant communities. *Hydrological Processes*, 14, 2977-2990.
- BERTA, G., FUSCONI, A., TROTTA, A. & SCANNERINI, S. 1990. Morphogenetic modifications induced by the mycorrhizal fungus *Glomus* strain E3 in the root system of *Allium porrum* L. *New Phytologist*, 114, 207-215.
- BERTOLDI, W., DRAKE, N. A. & GURNELL, A. M. 2011a. Interactions between river flows and colonizing vegetation on a braided river: Exploring spatial and temporal dynamics in riparian vegetation cover using satellite data. *Earth Surface Processes and Landforms*, 36, 1474-1486.
- BERTOLDI, W., GURNELL, A. M. & DRAKE, N. A. 2011b. The topographic signature of vegetation development along a braided river: Results of a combined analysis of airborne lidar, color air photographs, and ground measurements. *Water Resources Research*, 47.
- BERTOLDI, W., GURNELL, A. M. & WELBER, M. 2013. Wood recruitment and retention: The fate of eroded trees on a braided river explored using a combination of field and remotely-sensed data sources. *Geomorphology*, 180-181, 146-155.
- BERTUZZO, E., MARITAN, A., GATTO, M., RODRIGUEZ-ITURBE, I. & RINALDO, A. 2007. River networks and ecological corridors: Reactive transport on fractals, migration fronts, hydrochory. *Water Resources Research*, 43.

- BISCHETTI, G. B., CHIARADIA, E. A., SIMONATO, T., SPEZIALI, B., VITALI, B., VULLO, P. & ZOCCO, A. 2005. Root strength and root area ratio of forest species in lombardy (Northern Italy). *Plant and Soil*, 278, 11-22.
- BISHOP, K., LEE, Y. H., PETTERSSON, C. & ALLARD, B. 1995. Terrestrial sources of methylmercury in surface waters: The importance of the riparian zone on the Svartberget catchment. *Water, Air, and Soil Pollution*, 80, 435-444.
- BOND, W. J. & MIDGLEY, J. J. 2001. Ecology of sprouting in woody plants: The persistence niche. *Trends in Ecology and Evolution*, 16, 45-51.
- BOONSIRICHAI, K., GUAN, C., CHEN, R. & MASSON, P. H. 2002. Root gravitropism: An experimental tool to investigate basic cellular and molecular processes underlying mechanosensing and signal transmission in plants. *Annual Review of Plant Biology*.
- BORNETTE, G. & PUIJALON, S. 2011. Response of aquatic plants to abiotic factors: A review. *Aquatic Sciences*, 73, 1-14.
- BRONICK, C. J. & LAL, R. 2005. Soil structure and management: A review. *Geoderma*, 124, 3-22.
- BRUNDRETT, M. C. 2002. Coevolution of roots and mycorrhizas of land plants. *New Phytologist*, 154, 275-304.
- BUNN, J. T. & MONTGOMERY, D. R. 2004. Patterns of wood and sediment storage along debris-flow impacted headwater channels in old-growth and industrial forests of the western Olympic Mountains, Washington. *Riparian Vegetation and Fluvial Geomorphology*. Washington, DC: AGU.
- BURT, T. P., PINAY, G., MATHESON, F. E., HAYCOCK, N. E., BUTTURINI, A., CLEMENT, J. C., DANIELESCU, S., DOWRICK, D. J., HEFTING, M. M., HILLBRICHT-ILKOWSKA, A. & MAITRE, V. 2002. Water table fluctuations in the riparian zone: Comparative results from a pan-European experiment. *Journal of Hydrology*, 265, 129-148.
- BURYLO, M., REY, F., MATHYS, N. & DUTOIT, T. 2012. Plant root traits affecting the resistance of soils to concentrated flow erosion. *Earth Surface Processes and Landforms*, 37, 1463-1470.
- CADOL, D. & WOHL, E. 2013. Variable contribution of wood to the hydraulic resistance of headwater tropical streams. *Water Resources Research*, 49, 4711-4723.
- CARLYLE, G. C. & HILL, A. R. 2001. Groundwater phosphate dynamics in a river riparian zone: Effects of hydrologic flowpaths, lithology and redox chemistry. *Journal of Hydrology*, 247, 151-168.
- CARMINATI, A. & VETTERLEIN, D. 2013. Plasticity of rhizosphere hydraulic properties as a key for efficient utilization of scarce resources. *Annals of Botany*, 112, 277-290.
- CASEY, R. E. & KLAINE, S. J. 2001. Nutrient attenuation by a riparian wetland during natural and artificial runoff events. *Journal of Environmental Quality*, 30, 1720-1731.
- CHAPIN, F. S., III 1980. Mineral nutrition of wild plants. *Johnston, R. F.*
- CHONG, C., EDWARDS, W. & WAYCOTT, M. 2007. Differences in resprouting ability are not related to seed size or seedling growth in four riparian woody species. *Journal of Ecology*, 95, 840-850.
- CHURCH, M. 2002. Geomorphic thresholds in riverine landscapes. *Freshwater Biology*, 47, 541-557.
- CIRMO, C. P. & MCDONNELL, J. J. 1997. Linking the hydrologic and biogeochemical controls of nitrogen transport in near-stream zones of temperate-forested catchments: A review. *Journal of Hydrology*, 199, 88-120.
- CLARK, S. E. 2001. Meristems: Start your signaling. *Current Opinion in Plant Biology*, 4, 28-32.
- CLOWES, F. A. L. 1981. Cell proliferation in ectotrophic mycorrhizas of *Fagus sylvatica* L. *New Phytologist*, 87, 547-555.
- COLLINS, B. D., MONTGOMERY, D. R., FETHERSTON, K. L. & ABBE, T. B. 2012. The floodplain large-wood cycle hypothesis: A mechanism for the physical and biotic structuring of temperate forested alluvial valleys in the North Pacific coastal ecoregion. *Geomorphology*, 139, 460-470.
- CORENBLIT, D., GURNELL, A. M., STEIGER, J. & TABACCHI, E. 2008. Reciprocal adjustments between landforms and living organisms: Extended geomorphic evolutionary insights. *Catena*, 73, 261-273.
- CORENBLIT, D., STEIGER, J., GONZÁLEZ, E., GURNELL, A. M., CHARRIER, G., DARROZES, J., DOUSSEAU, J., JULIEN, F., LAMBS, L., LARRUE, S., ROUSSEL, E., VAUTIER, F. & VOLDOIRE, O. 2014. The biogeomorphological life cycle of poplars during the fluvial biogeomorphological succession: a special focus on *Populus nigra* L. *Earth Surface Processes and Landforms*, 39, 546-563.
- CORENBLIT, D., STEIGER, J. & TABACCHI, E. 2010. Biogeomorphologic succession dynamics in a Mediterranean river system. *Ecography*, 33, 1136-1148.

- CORNELISSEN, J. H. C., LAVOREL, S., GARNIER, E., DÍAZ, S., BUCHMANN, N., GURVICH, D. E., REICH, P. B., TER STEEGE, H., MORGAN, H. D., VAN DER HEIJDEN, M. G. A., PAUSAS, J. G. & POORTER, H. 2003. A handbook of protocols for standardised and easy measurement of plant functional traits worldwide. *Australian Journal of Botany*, 51, 335-380.
- CROSATO, A. & SALEH, M. S. 2011. Numerical study on the effects of floodplain vegetation on river planform style. *Earth Surface Processes and Landforms*, 36, 711-720.
- DAHM, C. N., GRIMM, N. B., MARMONIER, P., VALETT, H. M. & VERVIER, P. 1998. Nutrient dynamics at the interface between surface waters and groundwaters. *Freshwater Biology*, 40, 427-451.
- DAN, H., YANG, G. & ZHENG, Z. L. 2007. A negative regulatory role for auxin in sulphate deficiency response in *Arabidopsis thaliana*. *Plant Molecular Biology*, 63, 221-235.
- DANIELS, M. D. & RHOADS, B. L. 2004. Spatial pattern of turbulence kinetic energy and shear stress in a meander bend with large woody debris. *Riparian Vegetation and Fluvial Geomorphology*. Washington, DC: AGU.
- DANJON, F., KHUDER, H. & STOKES, A. 2013. Deep phenotyping of coarse root architecture in *R. Pseudoacacia* reveals that tree root system plasticity is confined within its architectural model. *PLoS ONE*, 8.
- DAVIES, N. S. & GIBLING, M. R. 2010. Cambrian to Devonian evolution of alluvial systems: The sedimentological impact of the earliest land plants. *Earth-Science Reviews*, 98, 171-200.
- DE BAETS, S., POESEN, J., REUBENS, B., WEMANS, K., DE BAERDEMAEKER, J. & MUYS, B. 2008. Root tensile strength and root distribution of typical Mediterranean plant species and their contribution to soil shear strength. *Plant and Soil*, 305, 207-226.
- DE SMET, I., TETSUMURA, T., DE RYBEL, B., DIT FREY, N. F., LAPLAZE, L., CASIMIRO, I., SWARUP, R., NAUDTS, M., VANNESTE, S., AUDENAERT, D., INZÉ, D., BENNETT, M. J. & BEECKMAN, T. 2007. Auxin-dependent regulation of lateral root positioning in the basal meristem of *Arabidopsis*. *Development*, 134, 681-690.
- DEAK, K. I. & MALAMY, J. 2005. Osmotic regulation of root system architecture. *Plant Journal*, 43, 17-28.
- DEVITO, K. J., FITZGERALD, D., HILL, A. R. & ARAVENA, R. 2000. Nitrate dynamics in relation to lithology and hydrologic flow path in a river riparian zone. *Journal of Environmental Quality*, 29, 1075-1084.
- DIXON, M. D., TURNER, M. G. & JIN, C. F. 2002. Riparian tree seedling distribution on Wisconsin River sandbars: Controls at different spatial scales. *Ecological Monographs*, 72, 465-485.
- DOCKER, B. B. & HUBBLE, T. C. T. 2008. Quantifying root-reinforcement of river bank soils by four Australian tree species. *Geomorphology*, 100, 401-418.
- DOLAN, L., JANMAAT, K., WILLEMSSEN, V., LINSTREAD, P., POETHIG, S., ROBERTS, K. & SCHERES, B. 1993. Cellular organisation of the *Arabidopsis thaliana* root. *Development*, 119, 71-84.
- DREW, M. C. 1975. Comparison of the effects of a localised supply of phosphate, nitrate, ammonium and potassium on the growth of the seminal root system, and the shoot, in barley. *New Phytologist*, 75, 479-490.
- DREWRY, J. J., NEWHAM, L. T. H., GREENE, R. S. B., JAKEMAN, A. J. & CROKE, B. F. W. 2006. A review of nitrogen and phosphorus export to waterways: Context for catchment modelling. *Marine and Freshwater Research*, 57, 757-774.
- EAPEN, D., MARTÍNEZ, J. J. & CASSAB, G. I. 2015. Assays for root hydrotropism and response to water stress. *Methods in Molecular Biology*. Humana Press Inc.
- EDMAIER, K., BURLANDO, P. & PERONA, P. 2011. Mechanisms of vegetation uprooting by flow in alluvial non-cohesive sediment. *Hydrology and Earth System Sciences*, 15, 1615-1627.
- FORTIER, J., TRUAX, B., GAGNON, D. & LAMBERT, F. 2013. Root biomass and soil carbon distribution in hybrid poplar riparian buffers, herbaceous riparian buffers and natural riparian woodlots on farmland. *SpringerPlus*, 2, 1-19.
- FRANCIS, R. A. 2004. *Riparian tree establishment and river island formation within the active zone of the River Tagliamento, northeast Italy*. PhD, University of Birmingham.
- FRANCIS, R. A. 2007. Size and position matter: riparian plant establishment from fluvially deposited trees. *Earth Surface Processes and Landforms*, 32, 1239-1243.
- FRANCIS, R. A., GURNELL, A. M., PETTS, G. E. & EDWARDS, P. J. 2006. Riparian tree establishment on gravel bars: interactions between plant growth strategy and the physical environment. In: SAMBROOK SMITH, G. H., BEST, J. L., BRISTOW, C. S. & PETTS, G. E. (eds.) *Braided Rivers: Process, Deposits, Ecology and Management*. Blackwell.

- FRANCIS, R. A., TIBALDESCHI, P. & MCDUGALL, L. 2008. Fluvially-deposited large wood and riparian plant diversity. *Wetlands Ecology and Management*, 16, 371–382.
- FUCHS, J. W., FOX, G. A., STORM, D. E., PENN, C. J. & BROWN, G. O. 2009. Subsurface transport of phosphorus in riparian floodplains: Influence of preferential flow paths. *Journal of Environmental Quality*, 38, 473-484.
- GARCÍA-ARIAS, A. & FRANCÉS, F. 2015. The RVDM: Modelling impacts, evolution and competition processes to determine riparian vegetation dynamics. *Ecobydrology*.
- GARCIA, M. H., LOPEZ, F., DUNN, C. & ALONSO, C. V. 2004. Flow, turbulence, and resistance in a flume with simulated vegetation. *Riparian Vegetation and Fluvial Geomorphology*. Washington, DC: AGU.
- GIADROSSICH, F., SCHWARZ, M., COHEN, D., PRETI, F. & OR, D. 2013. Mechanical interactions between neighbouring roots during pullout tests. *Plant and Soil*, 367, 391-406.
- GREET, J. O. E., ANGUS WEBB, J. & COUSENS, R. D. 2011. The importance of seasonal flow timing for riparian vegetation dynamics: a systematic review using causal criteria analysis. *Freshwater Biology*, available on-line, no-no.
- GREGORY, S. V., SWANSON, F. J., MCKEE, W. A. & CUMMINS, K. W. 1991. An ecosystem perspective of riparian zones. *Bioscience*, 41, 540-551.
- GRIME, J. P. 1979. *Plant strategies and vegetation processes*, Chichester ; New York, Wiley.
- GU, C., ANDERSON, W. & MAGGI, F. 2012. Riparian biogeochemical hot moments induced by stream fluctuations. *Water Resources Research*, 48.
- GUILLOY, H., GONZÁLEZ, E., MULLER, E., HUGHES, F. R. & BARSOUM, N. 2011. Abrupt drops in water table level influence the development of populus nigra and salix alba seedlings of different ages. *Wetlands*, 31, 1249-1261.
- GURNELL, A. 2014. Plants as river system engineers. *Earth Surface Processes and Landforms*, 39, 4-25.
- GURNELL, A., THOMPSON, K., GOODSON, J. & MOGGRIDGE, H. 2008. Propagule deposition along river margins: Linking hydrology and ecology. *Journal of Ecology*, 96, 553-565.
- GURNELL, A., TOCKNER, K., EDWARDS, P. J. & PETTS, G. E. 2005. Effects of deposited wood on biocomplexity of river corridors. *Frontiers in Ecology and Environment*, 3, 377–382.
- GURNELL, A. M. 2007. Analogies between mineral sediment and vegetative particle dynamics in fluvial systems. *Geomorphology*, 89, 9–22.
- GURNELL, A. M., BERTOLDI, W. & CORENBLIT, D. 2012. Changing river channels: The roles of hydrological processes, plants and pioneer fluvial landforms in humid temperate, mixed load, gravel bed rivers. *Earth-Science Reviews*, 111, 129-141.
- GURNELL, A. M., CORENBLIT, D., GARCÍA DE JALÓN, D., GONZÁLEZ DEL TÁNAGO, M., GRABOWSKI, R. C., O'HARE, M. T. & SZEWCZYK, M. 2015. A Conceptual Model of Vegetation-hydrogeomorphology Interactions Within River Corridors. *River Research and Applications*.
- GURNELL, A. M., GREGORY, K. J. & PETTS, G. E. 1995. The role of a coarse woody debris in forest aquatic habitats: Implications for management. *Aquatic Conservation: Marine and Freshwater Ecosystems*, 5, 143-166.
- GURNELL, A. M., PIÉGAY, H., SWANSON, F. J. & GREGORY, S. V. 2002. Large wood and fluvial processes. *Freshwater Biology*, 47, 601-619.
- GYSSSELS, G., POESEN, J., BOCHET, E. & LI, Y. 2005. Impact of plant roots on the resistance of soils to erosion by water: A review. *Progress in Physical Geography*, 29, 189-217.
- HATHAWAY, R. L. & PENNY, D. 1975. Root Strength in Some Populus and Salix Clones. *New Zealand Journal of Botany*, 13, 333-344.
- HE, X. J., MU, R. L., CAO, W. H., ZHANG, Z. G., ZHANG, J. S. & CHEN, S. Y. 2005. AtNAC2, a transcription factor downstream of ethylene and auxin signaling pathways, is involved in salt stress response and lateral root development. *Plant Journal*, 44, 903-916.
- HEEREN, D. M., MILLER, R. B., FOX, G. A., STORM, D. E., HALIHAN, T. & PENN, C. J. 2010. Preferential flow effects on subsurface contaminant transport in alluvial floodplains. *Transactions of the American Society of Agricultural and Biological Engineers*, 53, 127-136.
- HESSION, W. C., PIZZUTO, J. E., JOHNSON, T. E. & HORWITZ, R. J. 2003. Influence of bank vegetation on channel morphology in rural and urban watersheds *Geology*, 31, 147-150.
- HEYES, A., MOORE, T. R., RUDD, J. W. M. & DUGOUA, J. J. 2000. Methyl mercury in pristine and impounded boreal peatlands, Experimental Lakes Area, Ontario. *Canadian Journal of Fisheries and Aquatic Sciences*, 57, 2211-2222.

- HOFFMANN, C. C., KJAERGAARD, C., UUSI-KÄMPPIÄ, J., BRUUN HANSEN, H. C. & KRONVANG, B. 2009. Phosphorus retention in riparian buffers: Review of their efficiency. *Journal of Environmental Quality*, 38, 1942-1955.
- HOOKE, J. M. 1980. Magnitude and distribution of rates of river bank erosion. *Earth Surface Processes*, 5, 143-157.
- HOOKER, J. E., MUNRO, M. & ATKINSON, D. 1992. Vesicular-arbuscular mycorrhizal fungi induced alteration in poplar root system morphology. *Plant and Soil*, 145, 207-214.
- HOPKINSON, L. & WYNN, T. 2009. Vegetation impacts on near bank flow. *Ecobydrology*, 2, 404-418.
- HUBBLE, T. C. T., DOCKER, B. B. & RUTHERFURD, I. D. 2010. The role of riparian trees in maintaining riverbank stability: A review of Australian experience and practice. *Ecological Engineering*, 36, 292-304.
- HUGGENBERGER, P., HOEHN, E., BESCHTA, R. & WOESSNER, W. 1998. Abiotic aspects of channels and floodplains in riparian ecology. *Freshwater Biology*, 40, 407-425.
- IMADA, S., YAMANAKA, N. & TAMAI, S. 2008. Water table depth affects *Populus alba* fine root growth and whole plant biomass. *Functional Ecology*, 22, 1018-1026.
- JACKSON, M. B. & ARMSTRONG, W. 1999. Formation of aerenchyma and the processes of plant ventilation in relation to soil flooding and submergence. *Plant Biology*, 1, 274-287.
- JAILLAIS, Y. & CHORY, J. 2010. Unraveling the paradoxes of plant hormone signaling integration. *Nature Structural and Molecular Biology*, 17, 642-645.
- JARVIS, N. J. 2011. Simple physics-based models of compensatory plant water uptake: Concepts and eco-hydrological consequences. *Hydrology and Earth System Sciences*, 15, 3431-3446.
- JOHNSON, W. C. 1994. Woodland expansion in the platte river, Nebraska: Patterns and causes. *Ecological Monographs*, 64, 45-84.
- JOHNSON, W. C. 2000. Tree recruitment and survival in rivers: Influence of hydrological processes. *Hydrological Processes*, 14, 3051-3074.
- JONES, B. & LJUNG, K. 2012. Subterranean space exploration: The development of root system architecture. *Current Opinion in Plant Biology*, 15, 97-102.
- JUNG, J. K. H. & MCCOUCH, S. 2013. Getting to the roots of it: Genetic and hormonal control of root architecture. *Frontiers in Plant Science*, 4.
- JUNK, W. J. & WANTZEN, K. M. 2004. The flood pulse concept: new aspects, approaches, and applications—an update. In: WELCOMME, R. L. & PETR, T. (eds.) *Proceedings of the Second International Symposium on the Management of Large Rivers for Fisheries*. Food and Agriculture Organization & Mekong River Commission. FAO Regional Office for Asia and the Pacific, Bangkok.
- KARST, J., MARCZAK, L., JONES, M. D. & TURKINGTON, R. 2008. The mutualism-parasitism continuum in ectomycorrhizas: A quantitative assessment using meta-analysis. *Ecology*, 89, 1032-1042.
- KASAHARA, T. & WONDZELL, S. M. 2003. Geomorphic controls on hyporheic exchange flow in mountain streams. *Water Resources Research*, 39, SBH31-SBH314.
- KEAN, J. W. & SMITH, J. D. 2004. Flow and boundary shear stress in channels with woody bank vegetation. *Riparian Vegetation and Fluvial Geomorphology*. Washington, DC: AGU.
- KENT, M., OWEN, N. W., DALE, P., NEWNHAM, R. M. & GILES, T. M. 2001. Studies of vegetation burial: A focus for biogeography and biogeomorphology. *Progress in Physical Geography*, 25, 455-482.
- KING, D. A., DAVIES, S. J., TAN, S. & NOOR, N. S. M. 2006. The role of wood density and stem support costs in the growth and mortality of tropical trees. *Journal of Ecology*, 94, 670-680.
- KONDOLF, G. M. & CURRY, R. R. 1986. Channel erosion along the Carmel River, Monterey County, California (USA). *Earth Surface Processes & Landforms*, 11, 307-319.
- KOZLOWSKI, T. T. 1997. Responses of woody plants to flooding and salinity. *Tree Physiology*, 17, 490-490.
- KRANJCEC, J., MAHONEY, J. M. & ROOD, S. B. 1998. The responses of three riparian cottonwood species to water table decline. *Forest Ecology and Management*, 110, 77-87.
- KUTZ, A., MÜLLER, A., HENNIG, P., KAISER, W. M., PIOTROWSKI, M. & WEILER, E. W. 2002. A role for nitrilase 3 in the regulation of root morphology in sulphur-starving *Arabidopsis thaliana*. *Plant Journal*, 30, 95-106.
- KYLE, G. & LEISHMAN, M. R. 2009. Plant functional trait variation in relation to riparian geomorphology: The importance of disturbance. *Austral Ecology*, 34, 793-804.
- LARSEN, L. G., HARVEY, J. W. & CRIMALDI, J. P. 2009. Predicting bed shear stress and its role in sediment dynamics and restoration potential of the Everglades and other vegetated flow systems. *Ecological Engineering*, 35, 1773-1785.

- LAVOREL, S., MCINTYRE, S., LANDSBERG, J. & FORBES, T. D. A. 1997. Plant functional classifications: From general groups to specific groups based on response to disturbance. *Trends in Ecology and Evolution*, 12, 474-478.
- LEWANDOWSKA, M. & SIRKO, A. 2008. Recent advances in understanding plant response to sulfur-deficiency stress. *Acta Biochimica Polonica*, 55, 457-471.
- LINKOHR, B. I., WILLIAMSON, L. C., FITTER, A. H. & LEYSER, H. M. O. 2002. Nitrate and phosphate availability and distribution have different effects on root system architecture of *Arabidopsis*. *Plant Journal*, 29, 751-760.
- LÓPEZ-BUCIO, J., HERNÁNDEZ-ABREU, E., SÁNCHEZ-CALDERÓN, L., NIETO-JACOBO, M. F., SIMPSON, J. & HERRERA-ESTRELLA, L. 2002. Phosphate availability alters architecture and causes changes in hormone sensitivity in the *Arabidopsis* root system. *Plant Physiology*, 129, 244-256.
- MA, J., JARABA, J., KIRKPATRICK, T. L. & ROTHROCK, C. S. 2014. Effects of *Meloidogyne incognita* and *Thielaviopsis basicola* on cotton growth and root morphology. *Phytopathology*, 104, 507-512.
- MAEGHT, J. L., REWALD, B. & PIERRET, A. 2013. How to study deep roots-and why it matters. *Frontiers in Plant Science*, 4.
- MAHONEY, J. M. & ROOD, S. B. 1998. Streamflow requirements for cottonwood seedling recruitment - An integrative model. *Wetlands*, 18, 634-645.
- MALLIK, A. U. & RASID, H. 1993. Root-shoot characteristics of riparian plants in a flood control channel: implications for bank stabilization. *Ecological Engineering*, 2, 149-158.
- MANNERS, R. B., DOYLE, M. W. & SMALL, M. J. 2007. Structure and hydraulics of natural woody debris jams. *Water Resources Research*, 43.
- MASSA, G. D. & GILROY, S. 2003. Touch modulates gravity sensing to regulate the growth of primary roots of *Arabidopsis thaliana*. *Plant Journal*, 33, 435-445.
- MATSUMOTO, H., SENOO, Y., KASAI, M. & MAESHIMA, M. 1996. Response of the plant root to aluminum stress: Analysis of the inhibition of the root elongation and changes in membrane function. *Journal of Plant Research*, 109, 99-105.
- MCBRIDE, M., HESSION, W. C., RIZZO, D. M. & THOMPSON, D. M. 2007. The influence of riparian vegetation on near-bank turbulence: a flume experiment. *Earth Surface Processes and Landforms*, 32, 2019-2037.
- MONSHAUSEN, G. B. & GILROY, S. 2009. The exploring root - root growth responses to local environmental conditions. *Current Opinion in Plant Biology*, 12, 766-772.
- MORENO-RISUENO, M. A., VAN NORMAN, J. M., MORENO, A., ZHANG, J., AHNERT, S. E. & BENFEY, P. N. 2010. Oscillating gene expression determines competence for periodic *Arabidopsis* root branching. *Science*, 329, 1306-1311.
- MULHOLLAND, P. J. & HILL, W. R. 1997. Seasonal patterns in streamwater nutrient and dissolved organic carbon concentrations: Separating catchment flow path and in-stream effects. *Water Resources Research*, 33, 1297-1306.
- NAGLER, P. L., GLENN, E. P., HINOJOSA-HUERTA, O., ZAMORA, F. & HOWARD, K. 2008. Riparian vegetation dynamics and evapotranspiration in the riparian corridor in the delta of the Colorado River, Mexico. *Journal of Environmental Management*, 88, 864-874.
- NAIMAN, R. J. & DECAMPS, H. 1997. The Ecology of Interfaces: Riparian Zones. *Annual Review of Ecology and Systematics*, 28, 621-658.
- NANSON, G. C. & CROKE, J. C. 1992. A genetic classification of floodplains. *Geomorphology*, 4, 459-486.
- NAUMBURG, E., MATA-GONZALEZ, R., HUNTER, R. G., MCLENDON, T. & MARTIN, D. W. 2005. Phreatophytic vegetation and groundwater fluctuations: A review of current research and application of ecosystem response modeling with an emphasis on great basin vegetation. *Environmental Management*, 35, 726-740.
- NEUMANN, R. B. & CARDON, Z. G. 2012. The magnitude of hydraulic redistribution by plant roots: a review and synthesis of empirical and modeling studies. *New Phytologist*, 194, 337-352.
- NIELSEN, J. L., ROOD, S. B., PEARCE, D. W., LETTS, M. G. & JISKOOT, H. 2010. Streamside trees: Responses of male, female and hybrid cottonwoods to flooding. *Tree Physiology*, 30, 1479-1488.
- O'HARE, J. M., O'HARE, M. T., GURNELL, A. M., SCARLETT, P. M., LIFFEN, T. & MCDONALD, C. 2012. Influence of an ecosystem engineer, the emergent macrophyte *Sparganium erectum*, on seed trapping in lowland rivers and consequences for landform colonisation. *Freshwater Biology*, 57, 104-115.

- PARSONS, D. F., HAYASHI, M. & VAN DER KAMP, G. 2004. Infiltration and solute transport under a seasonal wetland: Bromide tracer experiments in Saskatoon, Canada. *Hydrological Processes*, 18, 2011-2027.
- PETTTT, N. E. & FROEND, R. H. 2001. Availability of seed for recruitment of riparian vegetation: A comparison of a tropical and a temperate river ecosystem in Australia. *Australian Journal of Botany*, 49, 515-528.
- PETTTT, N. E., LATTERELL, J. J. & NAIMAN, R. J. 2006. Formation, distribution and ecological consequences of flood-related wood debris piles in a bedrock confined river in semi-arid South Africa. *River Research and Applications*, 22, 1097-1110.
- PETTS, G. E., GURNELL, A. M., GERRARD, A. J., HANNAH, D. M., HANSFORD, B., MORRISSEY, I., EDWARDS, P. J., KOLLMANN, J., WARD, J. V., TOCKNER, K. & SMITH, B. P. G. 2000. Longitudinal variations in exposed riverine sediments: A context for the ecology of the Fiume Tagliamento, Italy. *Aquatic Conservation: Marine and Freshwater Ecosystems*, 10, 249-266.
- PIEGAY, H., BORNETTE, G., CITTERIO, A., HEROUIN, E., MOULIN, B. & STATIOTIS, C. 2000. Channel instability as a control on silting dynamics and vegetation patterns within perfluvial aquatic zones. *Hydrological Processes*, 14, 3011-3029.
- PIÉGAY, H. & GURNELL, A. M. 1997. Large woody debris and river geomorphological pattern: Examples from S.E. France and S. England. *Geomorphology*, 19, 99-116.
- POLLEN-BANKHEAD, N. & SIMON, A. 2010. Hydrologic and hydraulic effects of riparian root networks on streambank stability: Is mechanical root-reinforcement the whole story? *Geomorphology*, 116, 353-362.
- POLLEN, N. 2007. Temporal and spatial variability in root reinforcement of streambanks: Accounting for soil shear strength and moisture. *Catena*, 69, 197-205.
- POLLEN, N. & SIMON, A. 2005. Estimating the mechanical effects of riparian vegetation on stream bank stability using a fiber bundle model. *Water Resources Research*, 41, 1-11.
- POLLEN, N., SIMON, A. & COLLISON, A. 2004. *Advances in assessing the mechanical and hydrologic effects of riparian vegetation on streambank stability*.
- POLZIN, M. L. & ROOD, S. B. 2006. Effective disturbance: Seedling safe sites and patch recruitment of riparian cottonwoods after a major flood of a mountain river. *Wetlands*, 26, 965-980.
- PUCKETT, L. J. & HUGHES, W. B. 2005. Transport and fate of nitrate and pesticides: Hydrogeology and riparian zone processes. *Journal of Environmental Quality*, 34, 2278-2292.
- PUIJALON, S., BOUMA, T. J., DOUADY, C. J., VAN GROENENDAEL, J., ANTEN, N. P. R., MARTEL, E. & BORNETTE, G. 2011. Plant resistance to mechanical stress: Evidence of an avoidance-tolerance trade-off. *New Phytologist*, 191, 1141-1149.
- REVELLI, R., BOANO, F., CAMPOREALE, C. & RIDOLFI, L. 2008. Intra-meander hyporheic flow in alluvial rivers. *Water Resources Research*, 44.
- RIESEBERG, L. H., SINERVO, B., LINDER, C. R., UNGERER, M. C. & ARIAS, D. M. 1996. Role of gene interactions in hybrid speciation: Evidence from ancient and experimental hybrids. *Science*, 272, 741-745.
- RILLIG, M. C. & MUMMEY, D. L. 2006. Mycorrhizas and soil structure. *New Phytologist*, 171, 41-53.
- RINALDI, M. & DARBY, S. E. 2007. Modelling river-bank-erosion processes and mass failure mechanisms: progress towards fully coupled simulations. In: HABERSACK, H., PIEGAY, H. & RINALDI, M. (eds.) *Developments in Earth Surface Processes*.
- RINALDI, M. & NARDI, L. 2013. Modeling Interactions between Riverbank Hydrology and Mass Failures. *Journal of Hydrologic Engineering*, 18, 1231-1240.
- RITZ, K. & YOUNG, I. M. 2004. Interactions between soil structure and fungi. *Mycologist*, 18, 52-59.
- ROOD, S. B., BIGELOW, S. G. & HALL, A. A. 2011. Root architecture of riparian trees: river cut-banks provide natural hydraulic excavation, revealing that cottonwoods are facultative phreatophytes. *Trees-Structure and Function*, 25, 907-917.
- ROOD, S. B., GOATER, L. A., MAHONEY, J. M., PEARCE, C. M. & SMITH, D. G. 2007. Floods, fire, and ice: disturbance ecology of riparian cottonwoods. *Canadian Journal of Botany-Revue Canadienne De Botanique*, 85, 1019-1032.
- ROOD, S. B., KALISCHUK, A. R., POLZIN, M. L. & BRAATNE, J. H. 2003. Branch propagation, not cladogenesis, permits dispersive, clonal reproduction of riparian cottonwoods. *Forest Ecology and Management*, 186, 227-242.

- ROOD, S. B., PAN, J., GILL, K. M., FRANKS, C. G., SAMUELSON, G. M. & SHEPHERD, A. 2008. Declining summer flows of Rocky Mountain rivers: Changing seasonal hydrology and probable impacts on floodplain forests. *Journal of Hydrology*, 349, 397-410.
- ROOD, S. B., SAMUELSON, G. M., BRAATNE, J. H., GOURLEY, C. R., HUGHES, F. M. R. & MAHONEY, J. M. 2005. Managing river flows to restore floodplain forests. *Frontiers in Ecology and the Environment*, 3, 193-201.
- RUIZ-VILLANUEVA, V., DÍEZ-HERRERO, A., STOFFEL, M., BOLLSCHWEILER, M., BODOQUE, J. M. & BALLESTEROS, J. A. 2010. Dendrogeomorphic analysis of flash floods in a small ungauged mountain catchment (Central Spain). *Geomorphology*, 118, 383-392.
- SANJOU, M. & NEZU, I. 2011. Turbulence structure and concentration exchange property in compound open-channel flows with emergent trees on the floodplain edge. *International Journal of River Basin Management*, 9, 181-193.
- SCHILLING, K. E. 2007. Water table fluctuations under three riparian land covers, Iowa (USA). *Hydrological Processes*, 21, 2415-2424.
- SCIPPA, G. S., TRUPIANO, D., ROCCO, M., DI IORIO, A. & CHIATANTE, D. 2008. Unravelling the response of poplar (*Populus nigra*) roots to mechanical stress imposed by bending. *Plant Biosystems*, 142, 401-413.
- SELOSSE, M. A. & LE TACON, F. 1998. The land flora: A phototroph-fungus partnership? *Trends in Ecology and Evolution*, 13, 15-25.
- SIMON, A. & COLLISON, A. J. C. 2002. Quantifying the mechanical and hydrologic effects of riparian vegetation on streambank stability. *Earth Surface Processes and Landforms*, 27, 527-546.
- SIMONETTA, S., AVIDANO, L. & BERTA, G. 2007. Morphogenetic effects induced by pathogenic and non pathogenic *Rhizoctonia solani* Kühn strains on tomato roots. *Caryologia*, 60, 141-145.
- SINGER, M. B., SARGEANT, C. I., PIÉGAY, H., RIQUIER, J., WILSON, R. J. S. & EVANS, C. M. 2014. Floodplain ecohydrology: Climatic, anthropogenic, and local physical controls on partitioning of water sources to riparian trees. *Water Resources Research*, 50.
- SMITH, D. G. 1976. Effect of vegetation on lateral migration of anastomosed channels of a glacier meltwater river. *Bulletin of the Geological Society of America*, 87, 857-860.
- SNYDER, K. A. & WILLIAMS, D. G. 2007. Root allocation and water uptake patterns in riparian tree saplings: Responses to irrigation and defoliation. *Forest Ecology and Management*, 246, 222-231.
- SPRENT, J. I. 2007. Evolving ideas of legume evolution and diversity: A taxonomic perspective on the occurrence of nodulation: Tansley review. *New Phytologist*, 174, 11-25.
- STANFORD, J. A. & WARD, J. V. 1993. An Ecosystem Perspective of Alluvial Rivers: Connectivity and the Hyporheic Corridor. *Journal of the North American Benthological Society*, 12, 48-60.
- STEIGER, J. & CORENBLIT, D. 2012. The emergence of an 'evolutionary geomorphology'? *Central European Journal of Geosciences*, 4, 376-382.
- STEIGER, J. & GURNELL, A. M. 2003. Spatial hydrogeomorphological influences on sediment and nutrient deposition in riparian zones: observations from the Garonne River, France. *Geomorphology*, 49, 1-23.
- STEIGER, J., GURNELL, A. M. & PETTS, G. E. 2001. Sediment deposition along the channel margins of a reach of the middle river Severn, UK. *River Research and Applications*, 17, 443-460.
- STEIGER, J., TABACCHI, E., DUFOUR, S., CORENBLIT, D. & PEIRY, J. L. 2005. Hydrogeomorphic processes affecting riparian habitat within alluvial channel-floodplain river systems: a review for the temperate zone. *River Research and Applications*, 21, 719-737.
- STELLA, J. C., HAYDEN, M. K., BATTLES, J. J., PIÉGAY, H., DUFOUR, S. & FREMIER, A. K. 2011. The Role of Abandoned Channels as Refugia for Sustaining Pioneer Riparian Forest Ecosystems. *Ecosystems*, 14, 776-790.
- STENVALL, N., HAAPALA, T. & PULKKINEN, P. 2006. The role of a root cutting's diameter and location on the regeneration ability of hybrid aspen. *Forest Ecology and Management*, 237, 150-155.
- STOFFEL, M. & WILFORD, D. J. 2012. Hydrogeomorphic processes and vegetation: Disturbance, process histories, dependencies and interactions. *Earth Surface Processes and Landforms*, 37, 9-22.
- STOKES, A. & MATTHECK, C. 1996. Variation of wood strength in tree roots. *Journal of Experimental Botany*, 47, 693-699.
- STROMBERG, J. C. 2001. Influence of stream flow regime and temperature on growth rate of the riparian tree, *Platanus wrightii*, in Arizona. *Freshwater Biology*, 46, 227-239.
- STROMBERG, J. C. 2013. Root patterns and hydrogeomorphic niches of riparian plants in the American Southwest. *Journal of Arid Environments*, 94, 1-9.

- SWEENEY, B. W., BOTT, T. L., JACKSON, J. K., KAPLAN, L. A., NEWBOLD, J. D., STANDLEY, L. J., HESSION, W. C. & HORWITZ, R. J. 2004. Riparian deforestation, stream narrowing, and loss of stream ecosystem services. *Proceedings of the National Academy of Sciences of the United States of America*, 101, 14132-14137.
- TABACCHI, E., LAMBS, L., GUILLOY, H., PLANTY-TABACCHI, A. M., MULLER, E. & DÉCAMP, H. 2000. Impacts of riparian vegetation on hydrological processes. *Hydrological Processes*, 14, 2959-2976.
- TAL, M., GRAN, K., MURRAY, A. B., PAOLA, C. & HICKS, D. M. 2004. Riparian vegetation as a primary control on channel characteristics in multi-thread rivers. *Riparian Vegetation and Fluvial Geomorphology*. Washington, DC: AGU.
- THOMAS, R. E. & POLLEN-BANKHEAD, N. 2010. Modeling root-reinforcement with a fiber-bundle model and Monte Carlo simulation. *Ecological Engineering*, 36, 47-61.
- TISSERANT, B., GIANINAZZI, S. & GIANINAZZI-PEARSON, V. 1996. Relationships between lateral root order, arbuscular mycorrhiza development, and the physiological state of the symbiotic fungus in *Platanus acerifolia*. *Canadian Journal of Botany*, 74, 1947-1955.
- TONOLLA, D., ACUÑA, V., UEHLINGER, U., FRANK, T. & TOCKNER, K. 2010. Thermal heterogeneity in river floodplains. *Ecosystems*, 13, 727-740.
- TOOTH, S. & NANSON, G. C. 2000. The role of vegetation in the formation of anabranching channels in an ephemeral river, Northern plains, arid central Australia. *Hydrological Processes*, 14, 3099-3117.
- TOSI, M. 2007. Root tensile strength relationships and their slope stability implications of three shrub species in the Northern Apennines (Italy). *Geomorphology*, 87, 268-283.
- TRIMBLE, S. W. 1997. Stream channel erosion and change resulting from riparian forests. *Geology*, 25, 467-469.
- TRUPIANO, D., DI IORIO, A., MONTAGNOLI, A., LASSERRE, B., ROCCO, M., GROSSO, A., SCALONI, A., MARRA, M., CHIATANTE, D. & SCIPPA, G. S. 2012. Involvement of lignin and hormones in the response of woody poplar taproots to mechanical stress. *Physiologia Plantarum*, 146, 39-52.
- VAN DE WIEL, M. J. & DARBY, S. E. 2007. A new model to analyse the impact of woody riparian vegetation on the geotechnical stability of riverbanks. *Earth Surface Processes and Landforms*, 32, 2185-2198.
- VAN DER NAT, D., TOCKNER, K., EDWARDS, P. J. & WARD, J. V. 2003. Large wood dynamics of complex Alpine river floodplains. *Journal of the North American Benthological Society*, 22, 35-50.
- VENNETIER, M., ZANETTI, C., MERIAUX, P. & MARY, B. 2015. Tree root architecture: new insights from a comprehensive study on dikes. *Plant and Soil*, 387, 81-101.
- VIDON, P. 2012. Towards a better understanding of riparian zone water table response to precipitation: Surface water infiltration, hillslope contribution or pressure wave processes? *Hydrological Processes*, 26, 3207-3215.
- VIERS, J. H., FREMIER, A. K., HUTCHINSON, R. A., QUINN, J. F., THORNE, J. H. & VAGHTI, M. G. 2012. Multiscale Patterns of Riparian Plant Diversity and Implications for Restoration. *Restoration Ecology*, 20, 160-169.
- WALDRON, L. J. & DAKESSIAN, S. 1981. Soil reinforcement by roots: Calculation of increased soil shear resistance from root properties. *Soil Science*, 132, 427-435.
- WARD, J. V., TOCKNER, K., ARSCOTT, D. B. & CLARET, C. 2002. Riverine landscape diversity. *Freshwater Biology*, 47, 517-539.
- WARD, J. V., TOCKNER, K. & SCHIEMER, F. 1999. Biodiversity of floodplain river ecosystems: Ecotones and connectivity. *River Research and Applications*, 15, 125-139.
- WATSON, A. J. & MARDEN, M. 2004. Live root-wood tensile strengths of some common New Zealand indigenous and plantation tree species. *New Zealand Journal of Forestry Science*, 34, 344-353.
- WELBER, M., BERTOLDI, W. & TUBINO, M. 2012. The response of braided planform configuration to flow variations, bed reworking and vegetation: The case of the Tagliamento River, Italy. *Earth Surface Processes and Landforms*, 37, 572-582.
- WILLMS, C. R., PEARCE, D. W. & ROOD, S. B. 2006. Growth of riparian cottonwoods: A developmental pattern and the influence of geomorphic context. *Trees - Structure and Function*, 20, 210-218.
- WONDZELL, S. M. & SWANSON, F. J. 1999. Floods, channel change, and the hyporheic zone. *Water Resources Research*, 35, 555-567.
- WU, T. H., MCKINNELL III, W. P. & SWANSTON, D. N. 1979. Strength of tree roots and landslides on Prince of Wales Island, Alaska. *Canadian Geotechnical Journal*, 16, 19-33.

- WU, W. & WANG, S. S. Y. 2004. A depth-averaged two-dimensional numerical model of flow and sediment transport in open channels with vegetation. *Riparian Vegetation and Fluvial Geomorphology*. Washington, DC: AGU.
- YAGCI, O. & KABDASLI, M. S. 2008. The impact of single natural vegetation elements on flow characteristics. *Hydrological Processes*, 22, 4310-4321.
- ZANETTI, C., VENNETIER, M., MÉRIAUX, P. & PROVANSAL, M. 2015. Plasticity of tree root system structure in contrasting soil materials and environmental conditions. *Plant and Soil*, 387, 21-35.
- ZOLOBOWSKA, L. & VAN GIJSEGEM, F. 2006. Induction of lateral root structure formation on petunia roots: A novel effect of GMI1000 *Ralstonia solanacearum* infection impaired in Hrp mutants. *Molecular Plant-Microbe Interactions*, 19, 597-606.

Chapter 3

MODEL SYSTEMS, STUDY SITES AND METHODS

3.1 INTRODUCTION

This chapter provides three sets of background information to introduce and support the remainder of this thesis. Following a formal statement of the primary research questions investigated (Section 3.2), a section on research design (Section 3.3) first gives a broad outline of the field sites and types and timing of research undertaken, and then introduces the river (Tagliamento) and plant (*Populus nigra* L.) model systems that were investigated. Finally, some key field and laboratory methods are described in detail (Section 3.4) for clarity and to avoid repetition in the following chapters.

3.2 PRIMARY RESEARCH QUESTIONS

From the review of contemporary scientific understanding and the knowledge gaps identified in Chapter 2 have emerged the following four important questions, which form the foundations of this thesis:

A. What are the principal patterns and extent of variability in root depth distributions of riparian trees?

The way in which important characteristics such as root numbers, diameters and relative sectional area of roots are distributed on average within a riparian sediment profile is still unknown. Indeed, the overall descriptive power of the ‘depth’ variable relative to other environmental influences, such as moisture availability, remains to be properly evaluated. Are depth patterns conserved or highly variable?

B. What are the relationships between physical properties of riparian sediments and root distributions?

It is hypothesized that the riparian tree root distribution is likely to be strongly influenced by local factors such as sediment calibre and organic content, and the condition of the above-ground tree biomass. However, such relationships have not yet been investigated in a natural, dynamic river system, and the full extent to which root and physical properties may vary it is not yet known.

C. How does exposure to the fluvial disturbance regime shape root systems?

Riparian zones offer many differing niches to plants, with trees being able to survive in those habitats experiencing some of the greatest physical disturbance forces due to floods. What are the critical levels of disturbance for survival? What becomes of broken, deflected and buried parts of trees exposed to shifting channels, bars and other features? Do riparian trees have abnormal root architecture as a result of such events? The answers to these questions remain to be discovered.

D. What are the implications of variability in root distribution and root system structure for broader understanding of rivers and their management?

Contemporary understanding in river science is now allowing us both to appreciate and evaluate the many societal benefits of natural fluvial processes, and also the vast extent to which river forms and processes have been modified and compromised. Trees, roots and their combined effects at the interface between the river and terrestrial realms need to be better understood in order to develop sustainable management strategies to safeguard the benefits of riparian zones well into the future.

Each of these primary research questions is addressed in a separate chapter (Chapters 4 – 7, respectively, in the same order as the questions above), and broken down to more specific questions at the beginning of each chapter.

3.3 RESEARCH DESIGN

3.3.1 Investigative approach

The research presented in this thesis is the result of direct observational field studies supported by secondary data sources. The principal objective was to describe and explain features of the root systems of riparian trees in a fully functioning, natural system, such that phenomena observed may be used as a baseline model for the interpretation of other comparable riparian systems, perhaps impacted by stressors such as flow regulation or bank revetment. The model system selected for study was the middle-to-lower River Tagliamento in northeast Italy, and species-focused work was limited to *Populus nigra* L. (black poplar), which is the dominant riparian tree species. Characteristics of this system are described below. It was necessary to limit the investigations this way to minimise variability of the unmeasured and un-controlled variables inherent in such an observational study. The approach also allows for adding value by integration with other research on the same model river and tree species, which is already extensive.

Fieldwork was undertaken in three separate campaigns: Phase 1 in summer 2013, Phase 2 in summer 2014 and Phase 2A in spring 2015. The Phase 1 work involved excavation, measurement and sampling of bank profiles, producing data for the first and second primary research questions (Chapters 4 and 5). Phase 2 work focused on the excavation, measurement and sampling of whole root systems of individual trees near active banks (Primary Research Question C, Chapter 6). The field campaigns were timed to take advantage of low flow periods, allowing access to the deepest bank sediment profiles.

3.3.2 Model Systems

a River Tagliamento

This alluvial Alpine-to-Mediterranean, gravel-bed river constitutes an excellent model for the study of interactions between vegetation and hydrogeomorphology. Being relatively unmanaged and exhibiting rapid turnover of channel and floodplain features, the Tagliamento retains the dynamics and resulting spatial complexity that has been removed from most European rivers by engineering and other human interventions. Particularly in its island- and bar-braided middle reaches (circa Venzone to San Vito, Figure 3.2), the unconstrained channel morphology changes frequently and rapidly under exposure to a largely un-modified flooding regime (Tockner et al., 2003), and poplar, willow and alder species colonize and stabilise bar surfaces and channel margins (Gurnell et al., 2001).

The Tagliamento experiences a dramatic north-south climate gradient from cool, wet Alpine conditions to a warmer and drier Mediterranean environment in its lower reaches (Figure 3.1). Mean annual temperatures range from 5 to 14° C, and the southern Alpine fringe frequently experiences severe storms, particularly in autumn, resulting in high floods, erosion and sediment supply from the mountainous parts of the catchment (Tockner et al., 2003). Snowmelt is the other major driver of the Tagliamento's flashy, pluvio-nival flow regime, typically causing flow peaks in May, whereas more acute rainfall-related peaks tend to occur in November.

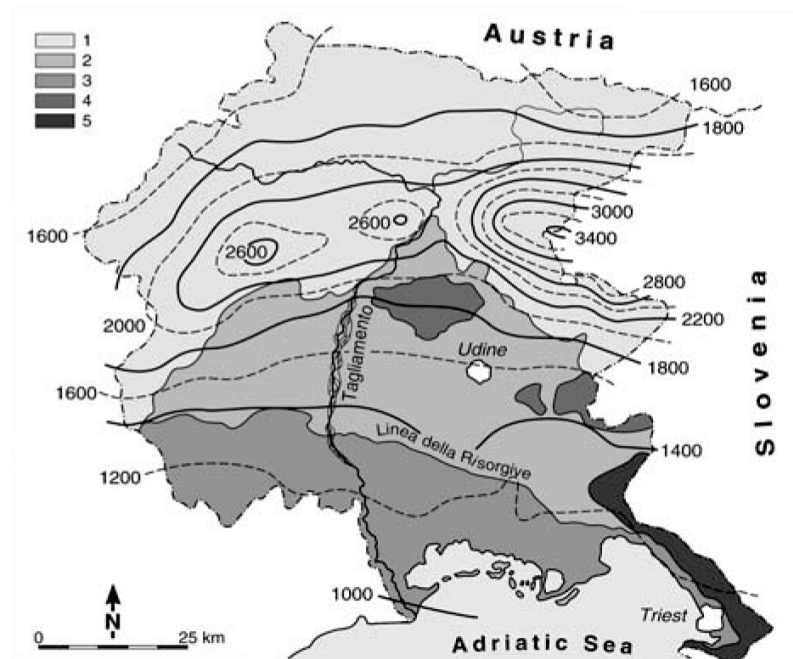


Figure 3.1 Climatic setting of the Tagliamento within the region of Friuli Venezia Giulia. Annual precipitation (1951-1970) isohyets are in mm. Catchment regions: 1. Alps and prealps; 2. Upper Friulian Plain; 3. Glacial moraines; 4. Lower Friulian Plain; 5. Karstic area. Tockner et al. (2003)

Discharge estimations are problematic owing to the lack of stable cross-sections and the river's sheer scale (active channel width sometimes exceeding a kilometre), however, some estimated values are presented along with other catchment statistics in Table 3.1. Two, five and ten year floods were estimated by Maione and Machne (1982) to be 1100, 1600 and 2150 $\text{m}^3 \text{s}^{-1}$ at Venzone. Floods in excess of around 4000 $\text{m}^3 \text{s}^{-1}$ have been recorded (Ward et al., 1999). The flow regime is relatively unmodified by human activities, though there is a low barrage on the main stem, and abstractions from tributaries, which divert water, mainly to Lake Cavazzo, west of Venzone, from where it is released for hydropower generation. Baseflow is also affected by abstractions for agriculture and aquaculture, but the pattern and magnitude of medium to large floods is essentially unaffected by these human activities.

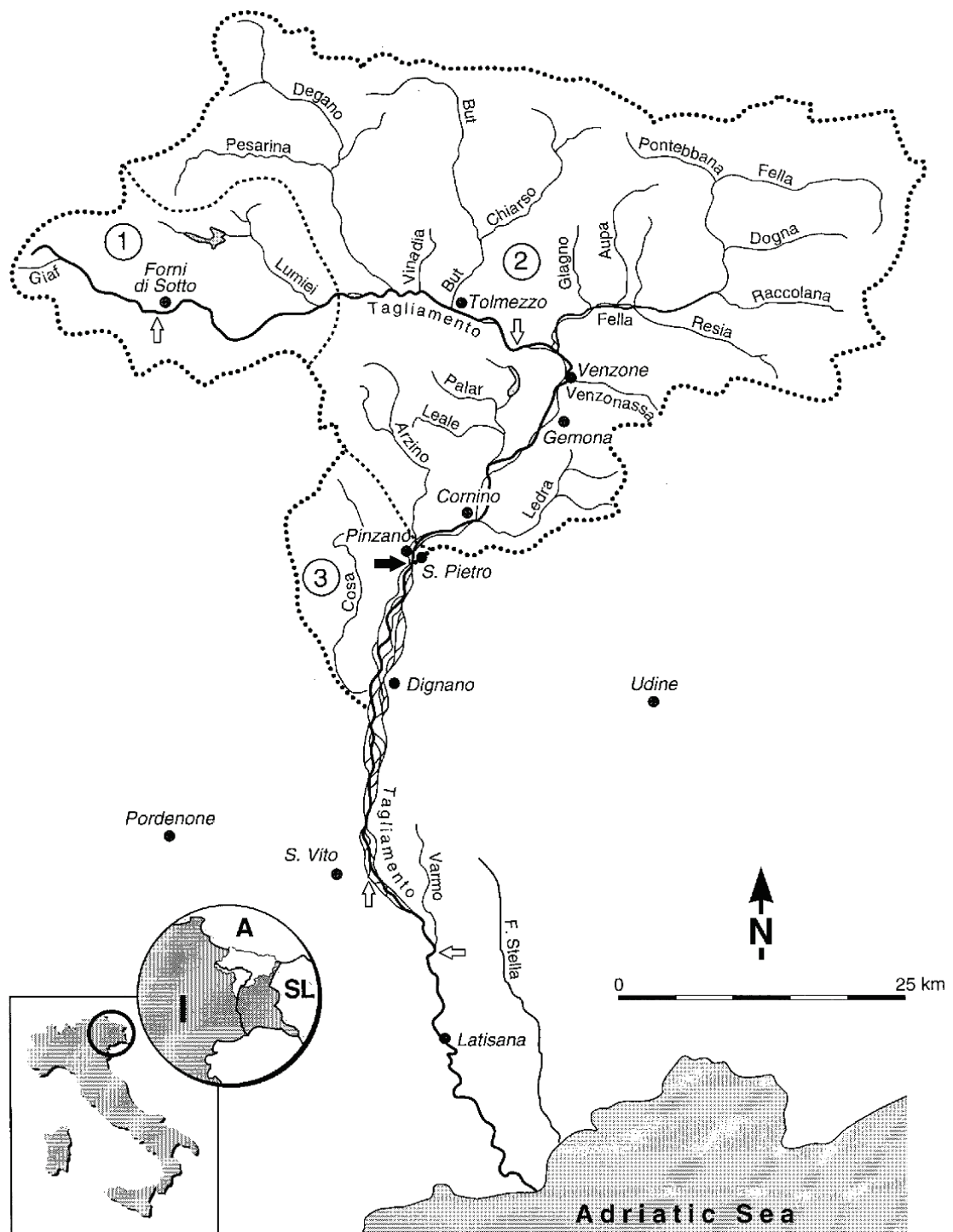


Figure 3.2 Map of the Tagliamento catchment, with location in Italy ('I', bordering Austria 'A' and Slovenia 'SL', inset). Towns, major tributaries and sub-basins (1–3) are also marked. Arrows indicate locations of discharge estimations quoted in Table 3.1. After Ward et al. (1999).

Table 3.1 Catchment statistics of the River Tagliamento. After Ward et al. (1999)

Stream order	7
Catchment area (km ²)	2580
Maximum altitude (m a.s.l.)	2781
Mean altitude (m a.s.l.)	1159
River length (km)	172
Slope (% approx.)	
Upper section (to Fella confluence)	10
Middle section (to Cosa confluence)	1
Lower section	0.1
Estimated Q ₈₀ (i.e. low flow) discharge (upstream to downstream, m ³ s ⁻¹)	
Forni di Sotto	3
Amaro	31
Ragogna	78
Camino al Tagliamento	36
Varmo	32
Specific discharge (L km ² s ⁻¹)	45.6
Average precipitation (mm a ⁻¹)	2150

Flow data used in the present study are from the Villuzza station, which is an ultrasonic water surface level gauge located at UTM 33T 342409 5116230, immediately downstream of the Pinzano gorge (indicated by the black arrow in Figure 3.2). The river cross-section is confined laterally by bedrock at this site, although the bed is alluvial and so is mobile, affecting the stability of the channel cross section. Despite some gaps, the Villuzza river stage record dates back to 1982 and provides hourly estimates (recently increased to 15 minutes). It provides the longest, high resolution river stage record for the Tagliamento, and because of the river's lateral confinement at this site, it also provides the most reliable estimates of high (flood) flows (Bertoldi et al., 2009). Furthermore, it is conveniently located in the middle of the field locations selected for the investigations reported here.

Downstream of the gorge at Pinzano, the Tagliamento loses a large proportion of its surface flow to the extensive alluvial aquifer, identified as the Upper Friulian Plain in Figure 3.1. This frequently results in totally dry reaches in summer, a condition that is exacerbated by abstraction. This deep and highly porous aquifer facilitates significant cross-catchment transfers to neighbouring watercourses such as the River Stella (Ward et al., 1999). Further downstream, perennial flows return where water rises again at the ‘linea della resorgive’ marked in Figure 3.1. In addition to this regional scale downwelling and upwelling within the alluvial aquifer, thermal and other tracer studies have also highlighted complex, local, shallower exchanges of large volumes of water between the surface and subsurface through the coarse river bed sediments (Arscott et al., 2001, Acuña and Tockner, 2009).

Except for local revetment and groyne fields around key infrastructure, and some flood embankments set well back from the active channel, the Tagliamento’s riparian corridor is intact and unconstrained by engineering works until its downstream-most meandering sections. The river in the upper basin is characterized by a sequence of braided and naturally confined, single-thread segments, whereas for most of its length (between the Lumiei and Varmo confluences), the Tagliamento comprises a mosaic of open gravel bars, islands, floodplain forest and braided channels (Gurnell et al., 2000b, Figure 3.3). There is one further strongly confined section at the Pinzano gorge, and the transition to a meandering (via wandering) planform begins at the Varmo confluence. The active channel width, the number of channels, islands and bars in the river cross section and the associated length of the riparian ecotone all peak in the middle reaches of the river (Tockner et al., 2003).



Figure 3.3 River corridor elements on the middle Tagliamento. Multiple channels, bars with vegetation of varying maturity, and established, forested islands are visible.

Longitudinal variability in dominant sediment calibre (Petts et al., 2000), climate and groundwater exchange enabled the selection of sites covering a significant range of both whole plant and root growth conditions. The continuous and rapid turnover of sediments by fluvial and aeolian processes on the Tagliamento (Gurnell et al., 2008) has resulted in complex sediment profiles within the floodplain and active channel (Bertoldi et al., 2009, Surian et al., 2009, Welber et al., 2012) which also provided a wide range of conditions for the investigation of relationships between root systems and sediment characteristics. Furthermore, the regular but variable natural flooding regime allows exploration of temporal associations between major fluvial disturbances, sediments and vegetation.

Previous studies of vegetation

As previously mentioned, selection of the Tagliamento as a study site allows findings to be integrated with the large body of existing research on this system. Indeed, many of the fundamental processes of tree-mediated fluvial landform development were first studied on this river.

Earlier investigations focused on quantities, patterns and storage of transported large wood, identifying pioneer islands as being particularly important wood stores (Gurnell et al., 2000a, Gurnell et al., 2000b), and detecting almost complete turnover of large wood deposited within the active channel in single flood events (Van der Nat et al., 2003). Researchers subsequently directed their attention to the plants producing this wood. Karrenberg et al. (2003b) identified longitudinal patterns such as a decreasing downstream dominance of *Alnus incana* (L.) Moench and *Salix* spp. and the extreme dominance of *Populus nigra* L. where total basal area of trees peaked, in the middle-lower reaches. Exposure, moisture and sediment factors influencing the establishment of key species have been investigated (Francis and Gurnell, 2006, Francis, 2007), as well as dependencies on wood deposits (Francis et al., 2008) and the features of the roots of young plants which confer tolerance of the disturbances associated with the environments in which they begin their lives (Karrenberg et al., 2003a).

Such primary studies on the Tagliamento have influenced the progression of conceptual models of the ecosystem engineering role of vegetation in fluvial environments. Edwards et al. (1999) noted the progressive growth of pioneer islands from deposited wood, which underpinned concepts of wood and island dynamics (Gurnell et al., 2001) and the full cycle through to eventual erosion was observed in aerial imagery by Kollmann et al. (1999). The river's mosaic of varying levels of plant colonisation has inspired the concepts of a self-organising (Francis et al., 2009) and long co-evolved system (Corenblit et al., 2009) and physical ecosystem engineering by plants (Gurnell et al., 2012, Gurnell, 2014) whereby

physical and biotic elements are inextricably linked. Phenomena of vegetation establishment, development and destruction have later been confirmed by more in-depth studies of aerial imagery (e.g., Zanoni et al., 2008, Mardhiah et al., 2015) and the gradual accretion of sediment by vegetated patches and islands has been observed through the analysis of airborne LiDAR data (Bertoldi et al., 2011b, Picco et al., 2015).

Within this conceptual framework of vegetation-mediated landform dynamics, the Tagliamento has constituted a living laboratory for the investigation of key processes and mechanisms. There have been many studies of the wider ecology of the habitat mosaic, and one particular tree-focused area of investigation has been into poplar leaf litter as a nutrient source, and the control of nutrient release by inundation (Langhans and Tockner, 2006, Ostojic et al., 2013). Bertoldi et al. (2011a) have begun to elucidate the controls and effects of tree growth rates, while flow thresholds for erosion and landform turnover (e.g., Bertoldi et al., 2009, Surian et al., 2015) as well as patterns of deposition after erosion of trees (Bertoldi et al., 2013) have been other areas of enquiry. The study of mature root systems will undoubtedly contribute much to this rapidly advancing mechanistic understanding of vegetation and landform dynamics on the Tagliamento and comparable rivers.

b Populus nigra L.

Black poplar is a fast-growing member of the family Salicaceae which is found extensively throughout the middle and lower reaches of the Tagliamento (Karrenberg et al., 2003b). *Populus* is now widely adopted as *the* model woody plant genus in biological disciplines (Taylor, 2002, Jansson and Douglas, 2007) owing to several characteristics which are convenient for experimentation:

- High genetic diversity and ease of hybridisation within the genus.
- Relatively small genome which has now been sequenced.
- Convenience of sexual propagation in the greenhouse and the abundance of seed that can be obtained in 4-8 weeks.
- Wide range of traits in morphology, anatomy, physiology, and pest susceptibility.
- Ability to resprout and to be propagated vegetatively, which allows replication in time and space very much as with inbred lines of *Drosophila* or *Arabidopsis*.
- Amenability to cell and tissue culture, and genetic transformation (Stettler et al., 1996).

Moreover, black poplar is by far the most important plant ecosystem engineer in those parts of the Tagliamento where vegetation and geomorphology interact most strongly. Though there is not a comprehensive literature specifically relating to *Populus nigra*, most of the features described below are believed to be shared across the genus.

Evolution and biogeography

The *Populus* genus includes poplars, cottonwoods and aspens, and is currently classified in six morphologically and ecologically distinct ‘sections’, the most speciose of which are the Tacamahaca (balsam poplars) and Populus (the aspens and white poplar). Black poplar is included in the section Aigeiros, alongside *P. deltoides* Marshall and *P. fremontii* s.l. Though some species are found in more upland habitats, all have a high soil moisture requirement and most have riparian populations, thus it is believed that the genus has evolved in association with river and lake margins since its tropical origins in the Paleocene (Eckenwalder, 1996).

The *Populus* genus is presently naturally distributed widely across the northern hemisphere, and across the globe as a commercial crop. The range of *Populus nigra* L., strictly known as the ‘European black poplar’, extends across Europe to around 55° latitude, and into the wetter parts of western Asia between 35° and 60° latitude (Figure 3.4). This distribution has fluctuated throughout the Quaternary, and genetic studies reveal that the present situation is a result of recolonisation from ice age refugia in southern Italy, the Balkans and (to a lesser extent due to the barrier of the Pyrenees) Spain (Cottrell et al., 2005).

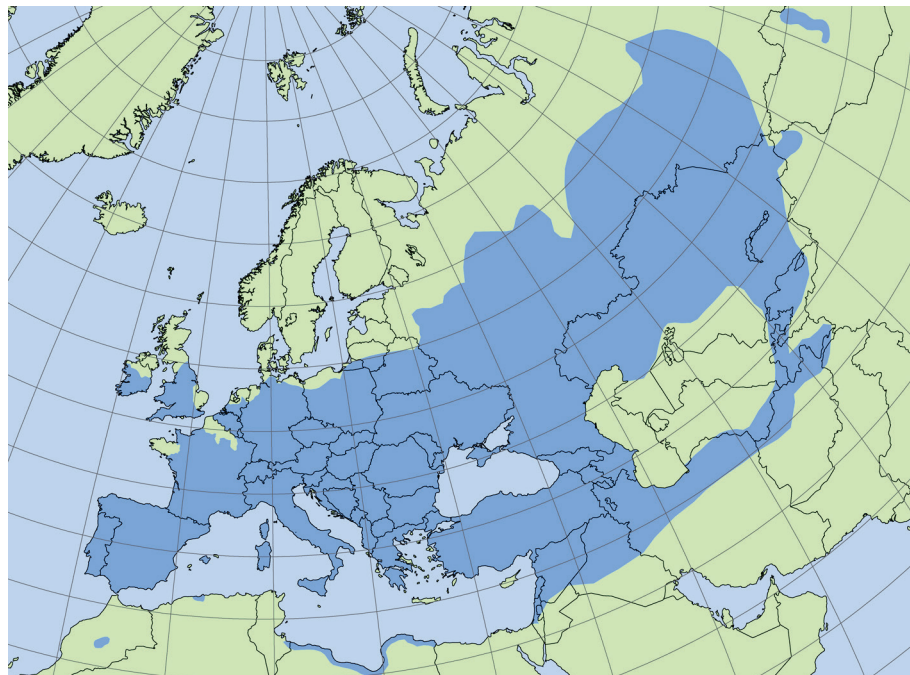


Figure 3.4 Distribution of *Populus nigra* L. © EUFORGEN 2015

Though currently classified under ‘least concern’ on the IUCN Red List, there is widespread concern in the literature over habitat loss of black poplar and other riparian *Populus* species (particularly cottonwoods in North America, due to flow regulation – see, e.g., Rood et al., 2005) resulting from river management. Low levels of recruitment are attributed to

constrained morphological dynamics and the resulting lack of exposed sediments for seedling establishment (Polzin and Rood, 2006), restriction of the natural flood regime (Hughes and Rood, 2003), and more intensive management of river banks in recent centuries (Lefèvre et al., 1998). The conservation movement for black poplar is particularly strong in countries at the edge of its range, such as the UK, where local extinction risks are greater. In this case, the recruitment problem is also exacerbated by historic human selection of only male trees, due to the perceived nuisance of the vast quantities airborne seed produced by females (Cottrell, 2004). A further concern is the limited genetic diversity of many wild *P. nigra* populations and the potential dilution of the gene pool by intercrossing with the many widely planted cultivars and hybrids (Storme et al., 2004).

Reproduction, ecophysiology and growth

Black poplars are a dioecious species, with individuals producing only male or female flowers (catkins) in March to April. The flowers are wind-pollinated and release many millions of small seeds per tree between May and July, possibly triggered by rainfall events (Herbison et al., 2015). Seeds weigh only a few hundred micrograms and possess a coma of fine hairs which allow them to be dispersed long distances by wind and water. In light of the increasing scarcity of sites for their establishment, the initial growth of seedlings has been an area of particularly strong investment in terms of research. The miniscule seeds of black poplar represent minimal investment in stored energy reserves, and so their viability period is only a few weeks and they require full sun to fuel sufficiently rapid root growth to track declining water tables in the riparian environment (Lefevre et al., 2001, Guillois et al., 2011). Upon germination, a ring of ‘root fibres’ emerge from the base of the hypocotyl. Anatomically distinct from root hairs, these features are believed to be an adaptation to enhance initial anchorage and water uptake of the seedling while the cotyledons emerge and begin to produce sufficient photosynthate to drive extension of the radicle (Lefevre et al., 2001). The ideal substrate for seedling establishment must balance moisture retention and aeration, as seedlings require moist soil for several weeks after germination but are also susceptible to death from waterlogging (Barsoum and Hughes, 1998). Roots are capable of reaching depths of 1.5 m or more after the first growing season (Johnson, 1994).

Poplars are pioneer species, exhibiting ‘r strategy’ (Grime, 1979) traits of rapid growth and colonisation of disturbed habitats in their early life. Their anatomy permits high transpiration rates to maintain photosynthesis to fuel this growth, which allows them, for example, to survive stem burial. However, associated adaptations such as large and numerous wood vessels, and long petioles to induce leaf ‘trembling’ thereby disrupting boundary layer formation, also make them particularly exposed to risk of drought-related mortality (Tyree

et al., 1994, Rood et al., 2000). Corenblit et al. (2014) have promoted the idea that black poplars change to a competitive ‘K strategy’ as they mature, and since fundamental wood element anatomy cannot change, it is supposed that the increased resilience of mature trees is mostly supported by a well-developed root system.

Root growth of *Populus* species beyond the first few growing seasons is still a poorly understood aspect, however, the knowledge base is improving with the increased adoption of the genus as a model tree. Some conserved gross features of mature root systems can be identified, though these are largely findings from studies conducted many decades ago. They are summarised by Pregitzer and Friend (1996). The deep primary taproot is usually retained from germination, and there is also extensive proliferation of long horizontal lateral roots, often extending to distances far beyond the height of the tree. The production of vertical ‘sinker roots’ from these horizontal laterals is something which Pregitzer and Friend (1996) conclude to be common across the genus, and these horizontal roots also exhibit the somewhat peculiar feature of root suckering, as was introduced in the previous chapter. There do not appear to be any existing studies of sucker morphology in *P. nigra*, however, Figure 3.5 demonstrates the possible form, based on observations of *P. grandidentata*. Aspens such as this are known to have particularly long-lived root systems from which are borne clonal shoots (Romme et al., 2005). The figure shows diameter growth of the parent root preferentially on the distal side in aspen, while new roots emerge from the base of the sucker shoot. The potentially vast root biomass of mature poplars clearly represents an important store of resources such as non-structural carbohydrates. Indeed, the ability to fix and translocate carbon below-ground rapidly has sparked interest in the utility of poplar plantations for greenhouse gas reduction (Dewar and Cannell, 1992). These stored resources can, however, be quickly mobilised for shoot growth when required, whether simply for seasonal bud-burst or the regeneration of aerial parts of the plant after destruction or disturbance (Wachowski et al., 2014).

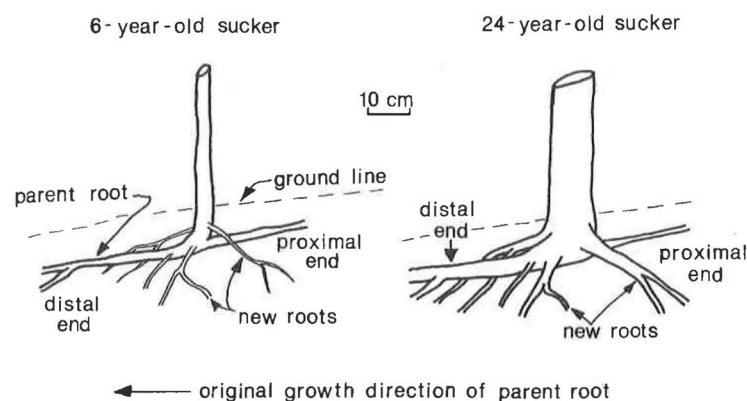


Figure 3.5 *P. grandidentata* (bigtooth aspen) sucker root system. Zahner and DeByle (1965)

Fine roots of poplars are, like all other trees, much more dynamic, and lend themselves more readily to in-situ study and experimentation. Furthermore, the carbon cycling implications of root turnover have made it a priority for research in this model tree (see, e.g., Dewar and Cannell, 1992, Block, 2004). Fine root lifespan is clearly highly plastic and dependent on a whole host of variables, including soil nutrient status (particularly nitrogen availability), temperature, moisture and shoot growth. Mean fine root longevity may vary (very approximately) from a few tens to a couple of hundred days (Block et al., 2006) and production and mortality often occur simultaneously, though production is usually greatest in summer, to match shoot growth demand (Kern et al., 2004).

Populus is also an interesting genus for the study of mycorrhizae, owing to its ability to form facultative associations with both arbuscular endo- and ectomycorrhizal fungi (Lodge, 1989). Distributions of the two types (Beauchamp et al., 2006, Gryta et al., 2006) suggest that generalist arbuscular mycorrhizae may be more important for the initial establishment on bare substrates, whereas more specialist ectomycorrhizae become dominant in supporting established stands (Corenblit et al., 2014). As well as almost certainly increasing resilience to water stress (Beniwal et al., 2010), these mycorrhizal associations and their modulation by the plant (Gryta et al., 2006) appear to be tailored to the different growth conditions experienced at the different successional stages of riparian black poplars. Indeed, the evidence that ectomycorrhizae confer access to nutrients otherwise locked up in dead plant material (Moore et al., 2015) (cf. mineral nutrition benefits associated with arbuscular fungi) and deliver increased root pathogen resistance, does indeed support the concept of a switch to a competitive life history strategy in the later stages of the biogeomorphic succession.

Finally, asexual (vegetative) reproduction is a significant means of propagation in black poplar. This can take the form of the production of suckers or new shoots from established root systems (in response to damage due to prolonged inundation (Barsoum and Hughes, 1998), burial or physical disturbance by floodwaters, transported ice or even fire (Rood et al., 2007)) or fragmented parts of stems or roots. The latter mechanism can be dominant in natural riparian systems (Barsoum, 2001). While resprouting from vegetative fragments appears to confer many survival advantages over recruitment from seed (Lefevre et al., 2001), as introduced in the previous chapter) and has great geomorphological significance, clones do not appear to dominate populations in natural, dynamic river systems (Legionnet et al., 1997, Barsoum, 1998). Instead, a positive relationship found between the degree of flow regulation and genetic duplication (Smulders et al., 2008) highlights the over-arching dominance of seedling recruitment site availability as a control over the size of natural *P. nigra* populations.

3.4 METHODS

As several of the subsequent chapters use data and sample information collected in the same field and laboratory operations, common methods are described below, in order to avoid repetition. Unique methods and further details (where relevant) are described within each of the following three ‘results’ chapters.

3.4.1 Field Campaign

a Phase 1: Root and sediment profile sampling (2013)

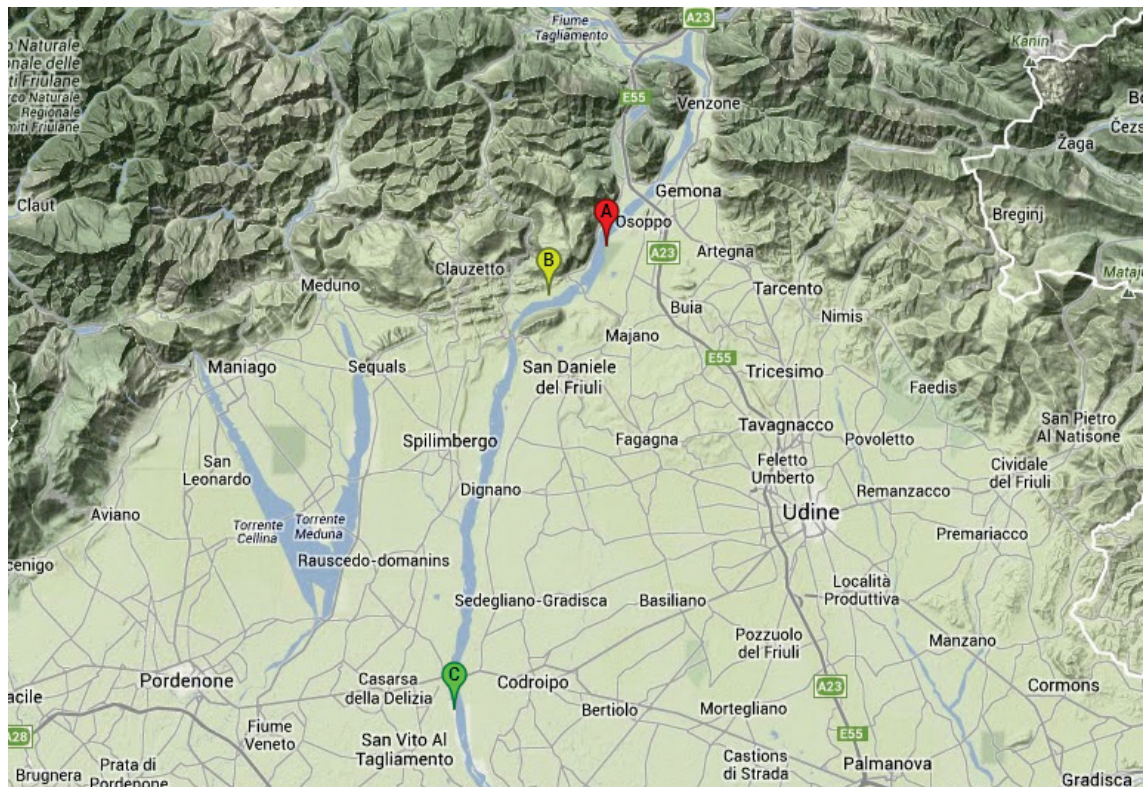


Figure 3.6 Locations of field sites for profile sampling. **A: Osoppo; B: Flagogna; C: San Vito.** Map data © 2013 Google

Three main locations with recently eroded banks dominated by *P. nigra* and covering a 140 m altitudinal and 0.3° latitudinal gradient were identified from preliminary fieldwork (April 2013) along 40 km of the pre-Alpine to piedmont reaches of the Tagliamento (Figure 3.6). These were also intended to cover a range of climatic and groundwater conditions. Each of these three locations yielded three sites where replicate bank profiles were excavated following the procedure below:

1. Site extensively photographed and accurately geolocated (UTM eastings and northings, ± 0.5 m, from averaged samples taken using Garmin GPSmap 62s).
2. Bank-top datum established for local measurements.
3. Largest *P. nigra* stems (> 50 mm diameter) within ten metres of the datum marked, cored for tree ring dating (5.15 mm increment borer (Haglöf, Sweden)) and measured:
 - a. Diameter at breast height (± 1 mm, at 1.2 m from ground surface).
 - b. Estimated height (± 0.25 m, using Suunto PM5-1520 clinometer).
 - c. Position (distance (± 25 mm) and bearing from datum ($\pm 1^\circ$, by magnetic compass)).
4. Excessively long roots trimmed and debris preventing access to profile removed.
5. In two locations separated by approx. 1 – 3 m, bank excavated back at least 0.2 m from natural face to create a flat vertical profile approx. 0.5 m in width (Figure 3.7).
6. At both profiles excavated, diameter of all roots > 0.1 mm diameter (\emptyset) intersecting bank face within a 0.2 m wide vertical transect were measured using digital calipers (DK Tools, Middlesex) and recorded. Measurements were aggregated by 0.1 m depth intervals.
7. Profile faces re-cleaned, photographed in detail (with measuring staff reference) and the position (± 2.5 mm) and following details noted of the major sedimentary strata visible:
 - a. Dominant grain size classes (assessed visually).
 - b. Colour (particularly regarding iron oxidation state, where obvious).
 - c. Presence of intact large (> 5 mm) pieces of organic material.
 - d. Cohesion class (strong/weak/not cohesive).
8. Sediment collected from each major stratum, from at least 0.1 m horizontal depth into the profile face to avoid drying. Samples sealed immediately in polyethylene bags and kept cool. Samples were of sufficient size that mass of the < 4 mm fraction was > 30 g.



Figure 3.7 Typical pair of bank profile exposures during excavation. Visible part of the measuring staff is approx. 2.2 m. Water table is at bottom of profiles.

Root diameters were used to calculate, for each profile interval, root density (numbers per unit area of bank face) and root area ratio (total sectional area of roots per unit area of bank face). Sediment samples were used to analyse particle size distribution and gravimetric water and organic matter content, which were assayed in the laboratory by methods described below.

b Phase 2: Tree root exposures (2014-15)

The tree selection protocol is described in Chapter 6. The procedure for each tree root exposure executed in the field was as follows:

1. Dimensions of the tree measured and recorded:
 - a. Stem length (± 0.25 m, using Suunto PM5-1520 clinometer).
 - b. Diameter at breast height (± 1 mm, at 1.2 m from ground surface).
 - c. Location (UTM eastings and northings, ± 0.5 m, from averaged samples taken using Garmin GPSmap 62s).
2. Tree secured by ropes to other nearby stems to prevent collapse.
3. Sediments excavated by hand back at least as far as the main stem axis, thereby exposing a minimum of half of the root system, as in Figure 3.8. During excavation, small roots (< 2 mm \varnothing) were entirely removed, and larger protruding roots were cut back to permit access to the main axis.
4. Excavated structures photographed from multiple angles for photogrammetric modelling (mean 217 JPEG images (16 MP) per tree, using Nikon D7000 with 18-200 mm Nikkor lens set at 18 mm; ISO-500; variable aperture and shutter).
5. Main stem(s) and larger diameter buried axes cored (5.15 mm increment borer (Haglöf, Sweden))
6. Sections of approx. 1 cm thickness cut from smaller roots of interest.
7. Visual assessment and recording of extent (to nearest 5 mm depth) of broad sediment calibre class (occurrence of silt, sand, gravel and pebbles), degree of consolidation (high or low) and presence of obvious oxidised iron compounds in the main exposed sediment strata.

Cores and sections were prepared according to the procedure outlined below and used to estimate age and timing of burial or disturbance. Photographic images were used to build photogrammetric models, as detailed in Chapter 6 and Appendix D.



Figure 3.8 Case study tree RA, illustrating the extent of sediment removal.

3.4.2 Laboratory Protocols

a Sediment water content

Within 6 hours of collection, the gross mass of the sealed samples (in polyethylene bags) was measured (Ohaus ARRV70 balance). Samples were then dried in foil trays of known mass in a ventilated oven at 105 °C to stable mass. The empty bags were left, open, to dry at room temperature for 2 days before re-weighing; this value being subtracted from the gross mass to obtain the sample net field fresh mass. Sediment water content is hereafter reported as the mass lost in this drying process as a proportion of net fresh mass, calculated according to the formula below. All measurements were taken to the nearest 10 mg.

$$\frac{(\text{Field gross}-\text{Bag dry})-(\text{Dry gross}-\text{Tray})}{(\text{Field gross}-\text{Bag dry})}$$

b Sediment organic matter content

The total proportion of organic material in dry sieved (< 1 mm) sediment was approximated by mass loss on ignition at 550 °C (for 4 hrs). Triplicate subsamples of 3 g each were oven-dried overnight at 105 °C (note that samples had already been dried to stable mass for moisture content analysis) in porcelain crucibles of known mass. Dry samples were weighed ($\pm 50 \mu\text{g}$, Sartorius MSE225S-100 balance) immediately before entering the muffle furnace and after having cooled to approx. 100 °C. Reported organic matter content hereafter is the mean proportional mass loss (as a fraction of original dry mass) for the 3 subsamples, accounting for crucible mass as in the formula below. All samples were kept at 105 °C or in desiccators between measurements.

$$\frac{\text{Dry gross}-\text{Ignited gross}}{\text{Dry gross}-\text{Crucible}}$$

c Sediment particle size distribution

The size distribution of > 1 mm calibre fractions of sediment samples was determined by dry sieving. Sub-mm fractions were analysed on a Beckman Coulter LS 13 320 Laser Diffraction Particle Size Analyzer.

The coarsest sieve grade used was 8 mm in all cases. Below 4 mm, meshes at half-phi intervals were used for samples collected in 2013 (Chapter 5, i.e., 8.0, 4.0, 2.8, 2.0, 1.4 and 1.0 mm), and whole-phi intervals for the fixed-volume samples collected in 2014 (Chapter 7, i.e., 8.0, 4.0, 2.0 and 1.0 mm). Aggregates, where encountered, were broken up manually on the mesh, large fragments of organic material were removed (and roots retained for 2014 samples), and sieves were brushed and wiped thoroughly clean between samples.

Remaining organic matter was removed from duplicate 3 g subsamples of the < 1 mm sediment fractions before laser diffraction analysis. Samples collected in 2013 (Chapter 5) were digested in 30 % hydrogen peroxide at 85 °C until the reaction ceased. For samples collected in 2014 (Chapter 7), the same subsamples were used following the loss-on-ignition assay for organic matter, assuming all organic material had been removed in this process. This is consistent with methods of Gurnell et al. (2008) who conducted comparable particle size analysis on Tagliamento sediments. All subsamples were then agitated overnight on a rotary shaker (350 rpm) in 30 ml of dispersal agent (50 g L⁻¹ sodium hexametaphosphate plus 7 g L⁻¹ anhydrous sodium carbonate). Approximately 10 ml of each of these treated subsamples was then extracted by pipette under agitation by a rotary stirrer (500 rpm, approx.) from the mid-depth of a 100 ml beaker and loaded into the laser sizer's auto-sampler. The settings and standard operating procedure of the instrument can be found in Appendix A. Final sample size class data are the means of 4 runs.

Laser diffraction analysis and sieving data were compiled into a single particle size distribution for each sample (with variable class widths) and parameters of this were measured using the GRADISTAT software of Blott and Pye (2001). As the laser analysis is performed on a proportional volume basis, whereas sieving is by proportional mass, equivalence of these variables was assumed (i.e., particle density was assumed consistent across size classes).

d Dendrochronology sample preparation

Upon extraction, tree cores were placed in paper straws for transport back to the laboratory. Here they were oven dried (105° C) overnight, and then fixed with PVA adhesive to wooden mounts for surface preparation. Sections were also dried overnight at 105° C and then both types of samples were sanded with increasingly fine sandpaper up to 400 grit. The final surface was finished with furniture polish and rings were inspected using a hand lens with 10x magnification.

3.5 REFERENCES

- ACUÑA, V. & TOCKNER, K. 2009. Surface-subsurface water exchange rates along alluvial river reaches control the thermal patterns in an Alpine river network. *Freshwater Biology*, 54, 306-320.
- ARSCOTT, D. B., TOCKNER, K. & WARD, J. V. 2001. Thermal heterogeneity along a braided floodplain river (Tagliamento River, northeastern Italy). *Canadian Journal of Fisheries and Aquatic Sciences*, 58, 2359-2373.
- BARSOUM, N. 1998. *Acomparision of vegetative and non-vegetative regeneration strategies in Populus nigra L. and Salix alba L.* PhD, University of Cambridge.
- BARSOUM, N. 2001. Relative contributions of sexual and asexual regeneration strategies in *Populus nigra* and *Salix alba* during the first years of establishment on a braided gravel bed river. *Evolutionary Ecology*, 15, 255-279.
- BARSOUM, N. & HUGHES, F. M. R. 1998. Regeneration response of Black poplar to changing river levels. In: WHEATER, H. & KIRBY, C. (eds.) *Hydrology in a Changing Environment*. John Wiley & Sons Ltd.
- BEAUCHAMP, V. B., STROMBERG, J. C. & STUTZ, J. C. 2006. Arbuscular mycorrhizal fungi associated with *Populus-Salix* stands in a semiarid riparian ecosystem. *New Phytologist*, 170, 369-380.
- BENIWAL, R. S., LANGENFELD-HEYSER, R. & POLLE, A. 2010. Ectomycorrhiza and hydrogel protect hybrid poplar from water deficit and unravel plastic responses of xylem anatomy. *Environmental and Experimental Botany*, 69, 189-197.
- BERTOLDI, W., DRAKE, N. A. & GURNELL, A. M. 2011a. Interactions between river flows and colonizing vegetation on a braided river: Exploring spatial and temporal dynamics in riparian vegetation cover using satellite data. *Earth Surface Processes and Landforms*, 36, 1474-1486.
- BERTOLDI, W., GURNELL, A., SURIAN, N., TOCKNER, K., ZANONI, L., ZILIANI, L. & ZOLEZZI, G. 2009. Understanding reference processes: Linkages between river flows, sediment dynamics and vegetated landforms along the Tagliamento River, Italy. *River Research and Applications*, 25, 501-516.
- BERTOLDI, W., GURNELL, A. M. & DRAKE, N. A. 2011b. The topographic signature of vegetation development along a braided river: Results of a combined analysis of airborne lidar, color air photographs, and ground measurements. *Water Resources Research*, 47.
- BERTOLDI, W., GURNELL, A. M. & WELBER, M. 2013. Wood recruitment and retention: The fate of eroded trees on a braided river explored using a combination of field and remotely-sensed data sources. *Geomorphology*, 180-181, 146-155.
- BLOCK, R. M. A. 2004. *Fine root dynamics and carbon sequestration in juvenile hybrid poplar plantations in Saskatchewan, Canada*. MSc, University of Saskatchewan.
- BLOCK, R. M. A., VAN REES, K. C. J. & KNIGHT, J. D. 2006. A review of fine root dynamics in *Populus* plantations. *Agroforestry Systems*, 67, 73-84.
- BLOTT, S. J. & PYE, K. 2001. Gradistat: A grain size distribution and statistics package for the analysis of unconsolidated sediments. *Earth Surface Processes and Landforms*, 26, 1237-1248.
- CORENBLIT, D., STEIGER, J., GONZÁLEZ, E., GURNELL, A. M., CHARRIER, G., DARROZES, J., DOUSSEAU, J., JULIEN, F., LAMBS, L., LARRUE, S., ROUSSEL, E., VAUTIER, F. & VOLDOIRE, O. 2014. The biogeomorphological life cycle of poplars during the fluvial

- biogeomorphological succession: a special focus on *Populus nigra* L. *Earth Surface Processes and Landforms*, 39, 546-563.
- CORENBLIT, D., STEIGER, J., GURNELL, A. M. & NAIMAN, R. J. 2009. Plants intertwine fluvial landform dynamics with ecological succession and natural selection: A niche construction perspective for riparian systems. *Global Ecology and Biogeography*, 18, 507-520.
- COTTRELL, J. 2004. Conservation of Black Poplar (*Populus nigra* L.). *Forestry Commission Information Note*. Edinburgh: Forestry Commission.
- COTTRELL, J. E., KRYSTUFEK, V., TABBENER, H. E., MILNER, A. D., CONNOLLY, T., SING, L., FLUCH, S., BURG, K., LEFÈVRE, F., ACHARD, P., BORDÁCS, S., GEBHARDT, K., VORNAM, B., SMULDERS, M. J. M., BROECK, A. H. V., SLYCKEN, J. V., STORME, V., BOERJAN, W., CASTIGLIONE, S., FOSSATI, T., ALBA, N., AGÚNDEZ, D., MAESTRO, C., NOTIVOL, E., BOVENSCHEN, J. & DAM, B. C. V. 2005. Postglacial migration of *Populus nigra* L.: Lessons learnt from chloroplast DNA. *Forest Ecology and Management*, 206, 71-90.
- DEWAR, R. C. & CANNELL, M. G. R. 1992. Carbon sequestration in the trees, products and soils of forest plantations: an analysis using UK examples. *Tree Physiology*, 11, 49-71.
- ECKENWALDER, J. E. 1996. Systematics and evolution of *Populus*. In: STETTLER, R. F., BRADSHAW, H. D., JR., HEILMAN, P. E. & HINCKLEY, T. M. (eds.) *Biology of Populus and its implications for management and conservation*. Ottawa, ON, Canada: NRC Research Press, National Research Council of Canada.
- EDWARDS, P. J., KOLLMANN, J., GURNELL, A. M., PETTS, G. E., TOCKNER, K. & WARD, J. V. 1999. A conceptual model of vegetation dynamics of gravel bars of a large Alpine river. *Wetlands Ecology and Management*, 7, 141-153.
- FRANCIS, R. A. 2007. Size and position matter: riparian plant establishment from fluvially deposited trees. *Earth Surface Processes and Landforms*, 32, 1239-1243.
- FRANCIS, R. A., CORENBLIT, D. & EDWARDS, P. J. 2009. Perspectives on biogeomorphology, ecosystem engineering and self-organisation in island-braided fluvial ecosystems. *Aquatic Sciences*, 71, 290-304.
- FRANCIS, R. A. & GURNELL, A. M. 2006. Initial establishment of vegetative fragments within the active zone of a braided gravel-bed River (River Tagliamento, NE Italy). *Wetlands*, 26, 641-648.
- FRANCIS, R. A., TIBALDESCHI, P. & MCDUGALL, L. 2008. Fluvially-deposited large wood and riparian plant diversity. *Wetlands Ecology and Management*, 16, 371-382.
- GRIME, J. P. 1979. *Plant strategies and vegetation processes*, Chichester ; New York, Wiley.
- GRYTA, H., CARRICONDE, F., CHARCOSSET, J. Y., JARGEAT, P. & GARDES, M. 2006. Population dynamics of the ectomycorrhizal fungal species *Tricholoma populinum* and *Tricholoma scalpturatum* associated with black poplar under differing environmental conditions. *Environmental Microbiology*, 8, 773-786.
- GUILLOY, H., GONZÁLEZ, E., MULLER, E., HUGHES, F. R. & BARSOUM, N. 2011. Abrupt drops in water table level influence the development of *populus nigra* and *salix alba* seedlings of different ages. *Wetlands*, 31, 1249-1261.
- GURNELL, A. 2014. Plants as river system engineers. *Earth Surface Processes and Landforms*, 39, 4-25.
- GURNELL, A. M., BERTOLDI, W. & CORENBLIT, D. 2012. Changing river channels: The roles of hydrological processes, plants and pioneer fluvial landforms in humid temperate, mixed load, gravel bed rivers. *Earth-Science Reviews*, 111, 129-141.
- GURNELL, A. M., BLACKALL, T. D. & PETTS, G. E. 2008. Characteristics of freshly deposited sand and finer sediments along an island-braided, gravel-bed river: The roles of water, wind and trees. *Geomorphology*, 99, 254-269.
- GURNELL, A. M., PETTS, G. E., HANNAH, D. M., SMITH, B. P. G., EDWARDS, P. J., KOLLMANN, J., WARD, J. V. & TOCKNER, K. 2000a. Wood storage within the active zone of a large European gravel-bed river. *Geomorphology*, 34, 55-72.
- GURNELL, A. M., PETTS, G. E., HANNAH, D. M., SMITH, B. P. G., EDWARDS, P. J., KOLLMANN, J., WARD, J. V. & TOCKNER, K. 2001. Riparian vegetation and island formation along the gravel-bed Fiume Tagliamento, Italy. *Earth Surface Processes and Landforms*, 26, 31-62.
- GURNELL, A. M., PETTS, G. E., HARRIS, N., WARD, J. V., TOCKNER, K., EDWARDS, P. J. & KOLLMANN, J. 2000b. Large wood retention in river channels: The case of the Fiume Tagliamento, Italy. *Earth Surface Processes and Landforms*, 25, 255-275.
- HERBISON, B., POLZIN, M. L. & ROOD, S. B. 2015. Hydration as a possible colonization cue: Rain may promote seed release from black cottonwood trees. *Forest Ecology and Management*, 350, 22-29.

- HUGHES, F. M. & ROOD, S. B. 2003. Allocation of River Flows for Restoration of Floodplain Forest Ecosystems: A Review of Approaches and Their Applicability in Europe. *Environmental Management*, 32, 12–33.
- JANSSON, S. & DOUGLAS, C. J. 2007. Populus: A model system for plant biology. *Annual Review of Plant Biology*.
- JOHNSON, W. C. 1994. Woodland expansion in the platte river, Nebraska: Patterns and causes. *Ecological Monographs*, 64, 45-84.
- KARRENBERG, S., BLASER, S., KOLLMANN, J., SPECK, T. & EDWARDS, P. J. 2003a. Root anchorage of saplings and cuttings of woody pioneer species in a riparian environment. *Functional Ecology*, 17, 170-177.
- KARRENBERG, S., KOLLMANN, J., EDWARDS, P. J., GURNELL, A. M. & PETTS, G. E. 2003b. Patterns in woody vegetation along the active zone of a near-natural Alpine river. *Basic and Applied Ecology*, 4, 157–166.
- KERN, C. C., FRIEND, A. L., JOHNSON, J. M. F. & COLEMAN, M. D. 2004. Fine root dynamics in a developing Populus deltoides plantation. *Tree Physiology*, 24, 651-660.
- KOLLMANN, J., VIELI, M., EDWARDS, P. J., TOCKNER, K. & WARD, J. V. 1999. Interactions between vegetation development and island formation in the Alpine river Tagliamento. *Applied Vegetation Science*, 2, 25-36.
- LANGHANS, S. D. & TOCKNER, K. 2006. The role of timing, duration, and frequency of inundation in controlling leaf litter decomposition in a river-floodplain ecosystem (Tagliamento, northeastern Italy). *Oecologia*, 147, 501-509.
- LEFEVRE, F., BARSOUM, N., HEINZE, B., KAJBA, D., ROTACH, P., DE VRIES, S. & TUROK, J. 2001. EUFORGEN Technical Bulletin: In situ conservation of Populus nigra. Rome, Italy: International Plant Genetic Resources Institute.
- LEFÈVRE, F., LÉGIONNET, A., DE VRIES, S. & TUROK, J. 1998. Strategies for the conservation of a pioneer tree species, Populus nigra L., in Europe. *Genet. Sel. Evol.*, 30, S181-S196.
- LEGIONNET, A., FAIVRE-RAMPANT, P., VILLAR, M. & LEFÈVRE, F. 1997. Sexual and asexual reproduction in natural stands of Populus nigra. *Botanica Acta*, 110, 257-263.
- LODGE, D. J. 1989. The influence of soil moisture and flooding on formation of VA-endo- and ectomycorrhizae in Populus and Salix. *Plant and Soil*, 117, 243-253.
- MAIONE, U. & MACHNE, G. 1982. Studio sulla formazione delle piene del Fiume Tagliamento. Milano: ECOCONSULT.
- MARDHIAH, U., RILLIG, M. C. & GURNELL, A. 2015. Reconstructing the development of sampled sites on fluvial island surfaces of the Tagliamento River, Italy, from historical sources. *Earth Surface Processes and Landforms*, 40, 629-641.
- MOORE, J. A. M., JIANG, J., POST, W. M. & CLASSEN, A. T. 2015. Decomposition by ectomycorrhizal fungi alters soil carbon storage in a simulation model. *Ecosphere*, 6.
- OSTOJIĆ, A., ROSADO, J., MILIŠA, M., MORAIS, M. & TOCKNER, K. 2013. Release of nutrients and organic matter from river floodplain habitats: Simulating seasonal inundation dynamics. *Wetlands*, 33, 847-859.
- PETTS, G. E., GURNELL, A. M., GERRARD, A. J., HANNAH, D. M., HANSFORD, B., MORRISSEY, I., EDWARDS, P. J., KOLLMANN, J., WARD, J. V., TOCKNER, K. & SMITH, B. P. G. 2000. Longitudinal variations in exposed riverine sediments: A context for the ecology of the Fiume Tagliamento, Italy. *Aquatic Conservation: Marine and Freshwater Ecosystems*, 10, 249-266.
- PICCO, L., TONON, A., RAVAZZOLO, D., RAINATO, R. & LENZI, M. A. 2015. Monitoring river island dynamics using aerial photographs and lidar data: the tagliamento river study case. *Applied Geomatics*, 7, 163-170.
- POLZIN, M. L. & ROOD, S. B. 2006. Effective disturbance: Seedling safe sites and patch recruitment of riparian cottonwoods after a major flood of a mountain river. *Wetlands*, 26, 965-980.
- PREGITZER, K. & FRIEND, A. L. 1996. The structure and function of Populus root systems. In: STETTLER, R. F., BRADSHAW, H. D., JR., HEILMAN, P. E. & HINCKLEY, T. M. (eds.) *Biology of Populus and its Implications for Management and Conservation*. Ottawa, Ontario, Canada: National Research Council of Canada Research Press.
- ROMME, W. H., TURNER, M. G., TUSKAN, G. A. & REED, R. A. 2005. Establishment, persistence, and growth of aspen (Populus tremuloides) seedlings in Yellowstone National Park. *Ecology*, 86, 404-418.

- ROOD, S. B., GOATER, L. A., MAHONEY, J. M., PEARCE, C. M. & SMITH, D. G. 2007. Floods, fire, and ice: disturbance ecology of riparian cottonwoods. *Canadian Journal of Botany-Revue Canadienne De Botanique*, 85, 1019-1032.
- ROOD, S. B., PATIÑO, S., COOMBS, K. & TYREE, M. T. 2000. Branch sacrifice: Cavitation-associated drought adaptation of riparian cottonwoods. *Trees - Structure and Function*, 14, 248-257.
- ROOD, S. B., SAMUELSON, G. M., BRAATNE, J. H., GOURLEY, C. R., HUGHES, F. M. R. & MAHONEY, J. M. 2005. Managing river flows to restore floodplain forests. *Frontiers in Ecology and the Environment*, 3, 193-201.
- SMULDERS, M. J. M., COTTRELL, J. E., LEFÈVRE, F., VAN DER SCHOOT, J., ARENS, P., VOSMAN, B., TABBENER, H. E., GRASSI, F., FOSSATI, T., CASTIGLIONE, S., KRYSUFEK, V., FLUCH, S., BURG, K., VORNAM, B., POHL, A., GEBHARDT, K., ALBA, N., AGÚNDEZ, D., MAESTRO, C., NOTIVOL, E., VOLOSANCHUK, R., POSPIŠKOVÁ, M., BORDÁCS, S., BOVENSCHEN, J., VAN DAM, B. C., KOELEWIJN, H. P., HALFMAERTEN, D., IVENS, B., VAN SLYCKEN, J., VANDEN BROECK, A., STORME, V. & BOERJAN, W. 2008. Structure of the genetic diversity in black poplar (*Populus nigra* L.) populations across European river systems: Consequences for conservation and restoration. *Forest Ecology and Management*, 255, 1388-1399.
- STETTLER, R. F., BRADSHAW, H. D., JR., HEILMAN, P. E. & HINCKLEY, T. M. (eds.) 1996. *Biology of Populus and its Implications for Management and Conservation*, Ottawa, Ontario, Canada: National Research Council of Canada Research Press.
- STORME, V., VANDEN BROECK, A., IVENS, B., HALFMAERTEN, D., VAN SLYCKEN, J., CASTIGLIONE, S., GRASSI, F., FOSSATI, T., COTTRELL, J. E., TABBENER, H. E., LEFÈVRE, F., SAINTAGNE, C., FLUCH, S., KRYSUFEK, V., BURG, K., BORDÁCS, S., BOROVICS, A., GEBHARDT, K., VORNAM, B., POHL, A., ALBA, N., AGÚNDEZ, D., MAESTRO, C., NOTIVOL, E., BOVENSCHEN, J., VAN DAM, B. C., VAN DER SCHOOT, J., VOSMAN, B., BOERJAN, W. & SMULDERS, M. J. M. 2004. Ex-situ conservation of Black poplar in Europe: Genetic diversity in nine gene bank collections and their value for nature development. *Theoretical and Applied Genetics*, 108, 969-981.
- SURIAN, N., BARBAN, M., ZILIANI, L., MONEGATO, G., BERTOLDI, W. & COMITI, F. 2015. Vegetation turnover in a braided river: Frequency and effectiveness of floods of different magnitude. *Earth Surface Processes and Landforms*, 40, 542-558.
- SURIAN, N., ZILIANI, L., COMITI, F., LENZI, M. A. & MAO, L. 2009. Channel adjustments and alteration of sediment fluxes in gravel-bed rivers of north-eastern Italy: Potentials and limitations for channel recovery. *River Research and Applications*, 25, 551-567.
- TAYLOR, G. 2002. *Populus*: Arabidopsis for forestry. Do we need a model tree? *Annals of Botany*, 90, 681-689.
- TOCKNER, K., WARD, J. V., ARSCOTT, D. B., EDWARDS, P. J., KOLLMANN, J., GURNELL, A. M., PETTS, G. E. & MAIOLINI, B. 2003. The Tagliamento River: a model ecosystem of European importance. *Aquatic Sciences*, 65, 239-253.
- TYREE, M. T., KOLB, K. J., ROOD, S. B. & PATINO, S. 1994. Vulnerability to drought-induced cavitation of riparian cottonwoods in Alberta: A possible factor in the decline of the ecosystem? *Tree Physiology*, 14, 455-466.
- VAN DER NAT, D., TOCKNER, K., EDWARDS, P. J. & WARD, J. V. 2003. Large wood dynamics of complex Alpine river floodplains. *Journal of the North American Benthological Society*, 22, 35-50.
- WACHOWSKI, J., LANDHÄUSSER, S. M. & LIEFFERS, V. J. 2014. Depth of root placement, root size and carbon reserves determine reproduction success of aspen root fragments. *Forest Ecology and Management*, 313, 83-90.
- WARD, J. V., TOCKNER, K., EDWARDS, P. J., KOLLMANN, J., BRETSCHKO, G., GURNELL, A. M., PETTS, G. E. & ROSSARO, B. 1999. A reference river system for the Alps: The 'Fiume Tagliamento'. *Regulated Rivers-Research & Management*, 15, 63-75.
- WELBER, M., BERTOLDI, W. & TUBINO, M. 2012. The response of braided planform configuration to flow variations, bed reworking and vegetation: The case of the Tagliamento River, Italy. *Earth Surface Processes and Landforms*, 37, 572-582.
- ZAHNER, R. & DEBYLE, N. V. 1965. Effect of Pruning the Parent Root on Growth of Aspen Suckers. *Ecology*, 46, 373-375.
- ZANONI, L., GURNELL, A., DRAKE, N. & SURIAN, N. 2008. Island dynamics in a braided river from analysis of historical maps and air photographs. *River Research and Applications*, 24, 1141-1159.

Chapter 4

DISTRIBUTION OF ROOT AREA AND DENSITY WITH DEPTH

4.1 INTRODUCTION

The distribution of roots within a soil profile is of great significance not only for an ecophysiological understanding of aboveground plant biomass, but for a wide range of sub-surface processes at many different spatial scales. At the molecular level, root exudates accelerate mineral weathering, chelate, mobilize and redistribute nutrients and are a fundamental input of organic carbon to the sub-surface environment (e.g., Gregory, 2006). These processes have effects at larger scales, as root-derived material forms the trophic foundation of almost all soil ecosystems, and regional and global biogeochemical cycling is thus regulated by vegetation (Metcalf et al., 2011). Hydrological processes are also highly dependent on the root distribution and its secondary effects on the structure of the sub-surface environment. Whether trees access shallow or deep groundwater, and how infiltration rates are influenced by the rhizosphere, for example, are both key factors in catchment responsiveness to rainfall as well as the catchment water balance (Jackson et al., 2000). The depth through which plant roots are distributed is one of the principal determinants of the strength of interactions between the biosphere and subsurface mineral materials.

Furthermore, the mechanical consequences of vegetation interactions with water or wind (and the material transported therein) can be geomorphologically significant in all parts of the landscape (Corenblit and Steiger, 2009, Marston, 2010, Osterkamp et al., 2012), but are particularly so in the fluvial context, where fluxes of water and sediment are concentrated (Curran and Hession, 2013). By slowing flows of surface water and thus promoting deposition of water-transported sediment, by reinforcing the deposited sediment with roots, and thus by altering the distribution and effectiveness of erosive forces across the aggrading land surface, many plant species ‘engineer’ more terrestrial niches for themselves (Gurnell, 2014). These local-scale processes combine across river margins, driving a ‘fluvial biogeomorphic succession’ of landform development (Corenblit et al., 2007, Corenblit et al., 2014). The present study aims to help elucidate one of the hitherto under-investigated components of this model – the distribution of roots and their potential sediment-reinforcing effect – but its findings will also be relevant for the many contingent fields mentioned above.

Root-related reinforcement of riparian sediments is conceptualised as occurring through several mechanisms. Most comprehensively explored is the tethering of soil masses by root penetration across shear planes, reducing the risk of mass failure. At the pore scale, removal of moisture by plants for transpiration reduces the occurrence of saturated conditions which exert pressure on soil particles, reducing sediment cohesion and internal friction (Pollen-Bankhead and Simon, 2010). Finally, roots exposed across bank surfaces interact with flows to produce a slow-flowing layer. The presence of this boundary layer reduces the shear stresses imposed on the bank surface and the detachment of sediment particles and soil aggregates, which is in turn further reduced by their enmeshment in fine roots within the bank sediments (Rinaldi and Darby, 2007). One of the main uncertainties in modelling root-related erosion resistance of bank surfaces is how these processes are spatially distributed, and this depends upon the horizontal and vertical distribution of roots (Pollen, 2007). There are starkly different implications for bank erosion resistance in the presence of, for example, a plate root or a deep taproot system with many laterals.

Attempts at modelling root distributions have tended to evolve either from a 'bottom-up', plant development and physiology perspective, or from a larger and 'top-down' biogeographic scale (e.g., for parameterisation of landscape-scale process models). The extent and form of the rhizosphere are products of both plant autogenic (genetic) factors and the cumulative history of allogenic (environmental) conditions in which the root system developed. Therefore, reconciliation of these bottom-up and top-down approaches is necessary for the prediction of root distributions in the real world (Dupuy et al., 2010). Furthermore, plant physiological studies usually use (for convenience and replicability) a limited number of model species which have small growth forms. Developmental studies of secondary root growth and the root system architecture of trees are very limited in number, despite woody species covering at least 52 % of the global vegetated land area (Latham et al., 2014). As forest is the natural climax community in most riparian systems, characterization of the tree root-permeated forest soil is important for predicting fluvial dynamics, as it constitutes the floodplain morphogenetic substrate. Various continuous-depth models or curves to describe vertical root density variations have been suggested and tested empirically, including inverse square (Monteith et al., 1989), exponential (Gerwitz and Page, 1974), proportional exponential (fraction of entire root system) (Jackson et al., 1996) and logistic (Schenk and Jackson, 2002), but such empirically-determined relationships are not always appropriate or transferable to the natural environment.

In the riparian context, there has been much research on the initial, extremely rapid, root growth of seedlings (Mahoney and Rood, 1998, Gonzalez et al., 2010, Guilloy et al., 2011, Edmaier et al., 2014) cuttings (Francis et al., 2005, Pasquale et al., 2012) and branch fragments (Rood et al., 2003, Francis and Gurnell, 2006) of *Salix* spp. and *Populus* spp., which must keep pace with a declining water table on the falling limb of a regenerative flood event. However, how the root system further develops and differentiates following successful establishment and interaction with subsequent flood and erosion events, is unclear. Corenblit et al. (2014) cite many reports of adventitious rooting and sucker shoots in flood-deposited fine sediments in their 'biogeomorphologic life cycle' model for *Populus nigra* L., but a simple depth distribution of these new laterals is implied, directly linked to deposition rates. There is a need to determine the validity of this assumption, which has major implications for boundary conditions in bank stability models (Pollen-Bankhead and Simon, 2009). In a study with some similarities to the present investigation, *Populus* coarse root (> 10 mm diameter) profiles in North America were found by Rood et al. (2011) to exhibit a wide range of rooting depths, with differences best explained by the humidity of the climate, demonstrating considerable developmental plasticity within species. The distribution, development and turnover of finer, absorptive roots (tolerating the greatest mechanical stresses) is particularly poorly understood in woody riparian genera (Pregitzer and Friend, 1996), though there is an increasing body of work on *Populus* spp., given that these are widely planted tree crops, and are adopted as a 'model trees' for research now that full genomes have been sequenced.

The aims of the present study were to describe the depth distribution and structure of root systems in sediments of an island-braided river system, where the dominant tree species is *Populus nigra* L. The study was designed to investigate both broad-scale patterns as well as local differences within and between sites. The research builds on the work of Rood et al. (2011) by including sub-centimetre roots and the explicit investigation of root diameters. It investigates the hypothesis that, in the highly heterogeneous and dynamic riparian sediment environment, in addition to the widely-recognised decline in root density with depth described above, significant differences in root density and diameter distributions exist within and between sites. It also investigates the hypothesis, that a significant component of such differences is attributable to the availability of soil moisture. The testing of these hypotheses provides a foundation for chapter 5, which investigates associations between root density and diameter and the properties of the sediments in which the roots have developed.

4.1.1 Research questions

Specific questions addressed in this chapter are as follows:

- i. To what extent does depth determine the number and total sectional area of roots in riparian sediments?
- ii. Do depth relationships differ between riparian areas of contrasting water availability (in terms of groundwater depth and average precipitation)?
- iii. Do relative (cumulative) root density and area depth structures differ between regions of contrasting water availability?
- iv. Does the predictability of root distributions vary with depth and depend on local water availability?
- v. What are the principal patterns in the distributions of root diameters?

4.2 STUDY SITES

Investigations were conducted on the River Tagliamento in northeast Italy, described in further detail in Chapter 3. The present study was conducted on the river's lower-middle reaches (Figure 4.1), where the 0.5 – 1 km wide active tract of the Tagliamento comprises a mosaic of open braided channel and bar surfaces, vegetated islands and floodplain forest. Over this part of the river's length there is an approximate 900 mm decrease in mean annual rainfall from upstream to downstream (Tockner et al., 2003) and a wide range of groundwater conditions relating to varying confinement of the river corridor, sedimentology of the alluvial aquifer (Acuña and Tockner, 2009) and also to widespread abstraction of floodplain groundwater in the lower reaches to support irrigated agriculture. These factors together provide wide spatial variability in the water table level and vadose moisture regime and thus the availability of water to riparian plants. The constant re-working of sediments by fluvial and aeolian processes also results in complex vertical sediment profiles comprised of layers with strongly varying sediment calibre, and thus water retention-drainage characteristics, which can vary enormously at the local scale (Gurnell et al., 2008, Bertoldi et al., 2009, Welber et al., 2012).

In order to investigate variability in root density and diameter profiles under different soil moisture conditions, three widely-spaced sampling locations were selected at Osoppo (location A), Flagogna (location B), and San Vito (location C) (Figure 4.1). In addition to being widely spaced along the river, these locations showed broad differences in valley confinement (A – partly confined, B – confined, C – unconfined) and river flow reliability, which is an indicator of alluvial groundwater conditions (A and B – perennial flow; C – the

river often dries up in summer). These contrasts suggest that location C is likely to have much drier moisture conditions than locations A and B, and that, given its valley confinement, location B is probably moister than A. Previous analyses of downstream variations in the growth performance of *P. nigra* also indicate that such differences in moisture availability exist (Bertoldi et al., 2011, Gurnell, 2015 (in press)). The actual characterization of sites with respect to soil moisture was explored in more detail and revised following sampling, as detailed below.

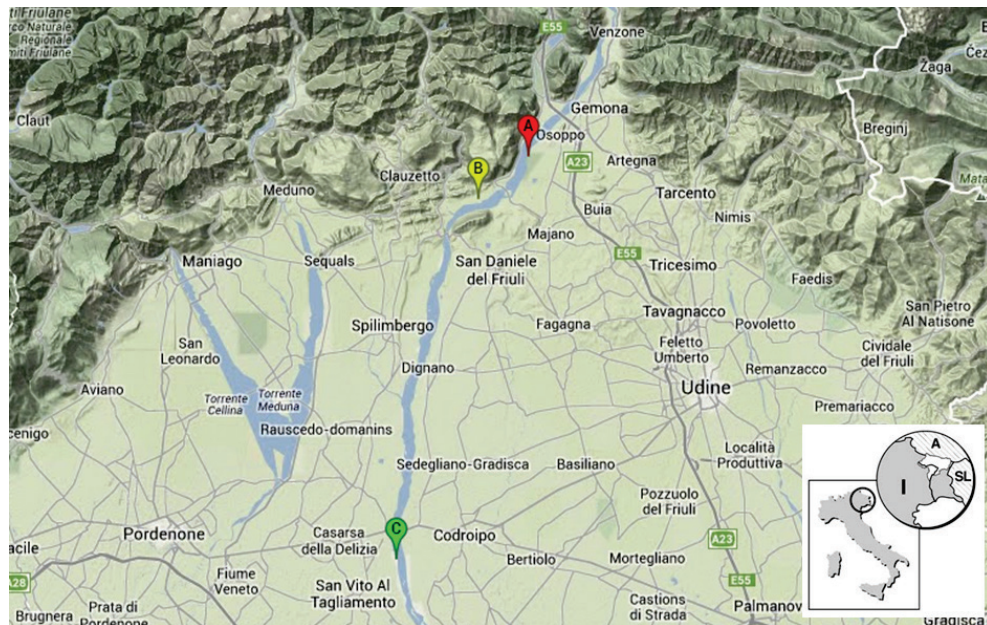


Figure 4.1 Study locations on the River Tagliamento. A: Osoppo; B: Flagogna; C: San Vito. Map data © 2014 Google Maps. Inset from Tockner et al. (2003)

4.3 METHODS

4.3.1 Field sampling

Root and sediment profiles within the riparian zone at locations A, B and C were sampled between July and August 2013. At each location, three sites were selected according to the following criteria:

- Steep unvegetated bank face (assumed eroded by floods in the same hydrological year)
- Bank-top vegetation dominated by *P. nigra*
- Safely accessible bank toe (i.e. no fast-flowing water or deep channel at the bank toe)

At Osoppo and San Vito there were continuous stretches of bank meeting these criteria, resulting in the availability of three similar sites within a relatively short distance (spanning 60 m and 100 m, respectively). At Flagogna, bank characteristics were variable and the

availability of suitable sites was patchy, and so the three sampled sites were spread widely along a 1.6 km length reach.

Profiles were excavated and recorded as per the procedure detailed in Chapter 3, described briefly here. The diameters of all roots > 0.1 mm diameter within each 0.2 m wide profile were measured either down to the level of the water table at the time of sampling or to the maximum depth to which it was feasible to dig (between 1.0 and 2.4 m from the bank top). The measurements were grouped in 0.1 m depth intervals. Owing to the difficulty of species identification of small roots, all apparently living roots were measured and recorded, although, given the criteria for site selection, the vast majority were probably roots of *P. nigra*. The position and extent of distinct sediment layers were recorded for each profile, distinguished by sediment calibre, colour and structure. Samples of each stratum were collected for later measurement of field moisture and organic matter content, as well as particle size analysis to be determined during laboratory analysis.

All of the above measurements were taken during summer 2013. However, additional, dedicated, fixed depth sampling of sediments was also undertaken at all sites on August 2nd 2014, when there had been no rainfall at any site in the previous 3 days. At each site, approximately 100 g sediment samples were taken from as close to the 2013 profiles as was possible, and at 0.5, 0.75 and 1.0 m depth from the surface. These samples were assayed gravimetrically in the same way as the 2013 samples.

4.3.2 Data analysis

a Classification of sites according to soil moisture

Water availability (represented by the mean gravimetric moisture content) in the sediment samples taken during July and August 2013 was found to be much more variable between the sampled sites at Flagogna (means between 1.9 and 16.2 %) than at the other two locations (6.8 - 13.0 % at Osoppo and 1.5 – 5.0 % at San Vito). Although sampling took place over a two month period, sites were visited on several occasions during this period and all were sampled at low flow conditions when the bank profiles were well-drained, providing confidence that soil moisture content was mainly representative of genuine contrasts in moisture availability between sites rather than ambient hydrological conditions at the time of sampling. These data were used to revise the pre-sampling site environmental moisture classifications (Figure 4.2) and then the between-site soil moisture contrasts were validated using the dedicated, fixed depth sampling on August 2nd 2014.

Analysis of both the 2013 and 2014 soil moisture data revealed that sites did not divide into three soil moisture groups as had originally been anticipated. Pairwise comparisons using the 2013 data and Steel-Dwass-Critchlow-Fligner procedure found that only San Vito sites formed a distinct group ($W_{Osoppo} = 8.07$, $W_{Flagogna} = 8.65$, both $P < 0.0001$). Instead, a two-category subdivision was adopted (Figure 4.3). Moisture contents of sediment samples from the new ‘drier’ and ‘wetter’ groups were found to be significantly different based on both the 2014 validation samples (Mann-Whitney $U = 114$, $P < 0.0001$, 1-tailed) and the soil moisture dataset obtained in 2013 ($U = 2549$, $P < 0.0001$, 1-tailed).

Note that between the 2013 and 2014 sampling, there had been several metres of channel bed aggradation at the bank toe at Site 5 (Figure 4.4), and approx. 60 m of bank retreat at the San Vito sites, but this did not appear to affect the moisture characterisation based on sampling the nearest accessible banks. This supports the assumption that precipitation, potential evapotranspiration, river flow and groundwater are primary controls on soil moisture at the site scale. At San Vito, dedicated soil moisture sampling was undertaken at the nearest points possible to the original profiles, which were similar in vegetation cover and stratigraphy to the original 2013 sites.

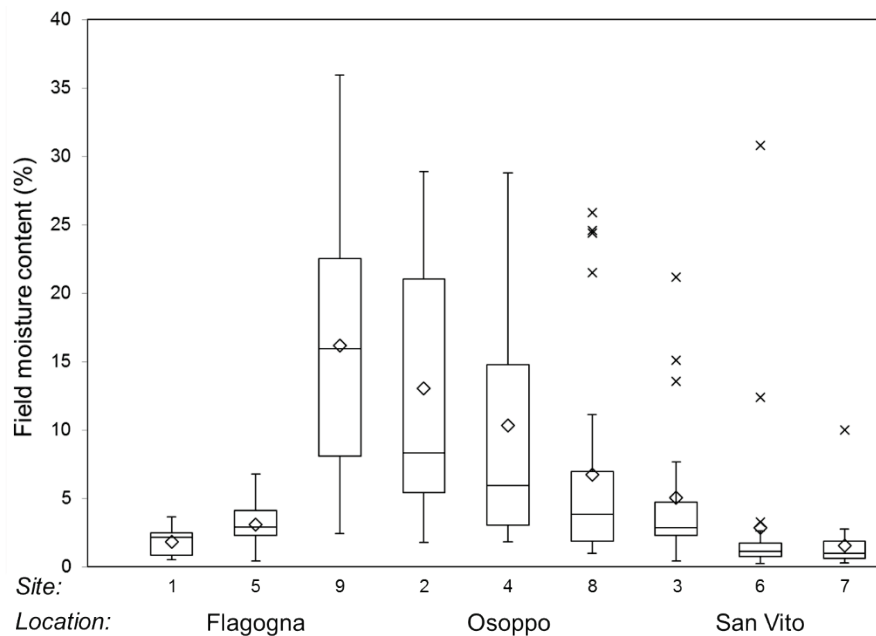


Figure 4.2 Distribution of field moisture content of all 2013 samples. Diamond symbols within interquartile range boxes represent means, whereas the horizontal lines represent medians; boxes enclose the upper and lower quartiles of the data, and crosses are outliers.

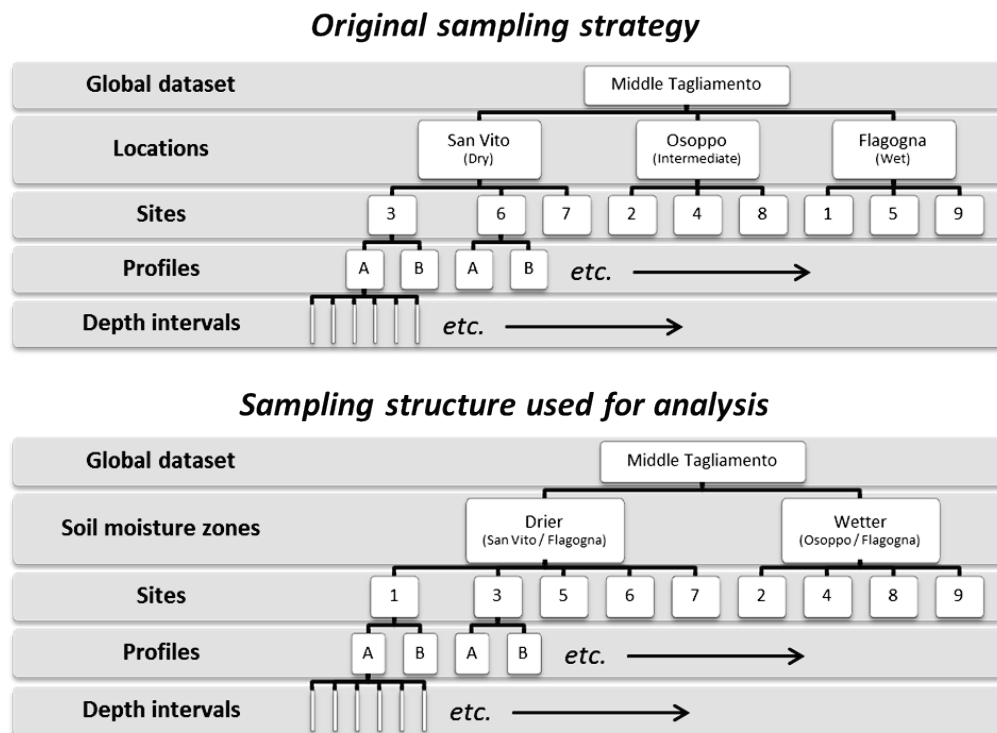


Figure 4.3 Sampling structure as planned (top, with dry, wet and intermediate locations), and as revised following sample moisture analysis (bottom).



Figure 4.4 Site 5 during root and sediment sampling in 2013 (top) and during validation sediment sampling in 2014 (bottom) showing aggradation of the side channel bed between 2013 and 2014. Measuring staff visible is 3 m.

b Analysis of root data

Having established differences in soil moisture by site, a range of analyses were applied to the root profile data in an attempt to investigate vertical trends in root characteristics across and between the sampled sites. Three specific root characteristics were investigated: root density (the number of roots per unit exposed bank face area), root area (the proportion of the exposed bank face area occupied by roots), and root diameter. The following sequence of analyses of the root data was applied:

Variations in root density with depth in the bank profile

In order to test the first hypothesis that there was significant variability within and between sites around any simple decline in root properties with depth, and so to support inter-site comparisons, root data from the different sites were summarised in 0.1 m bank profile depth increments. Following previous work on the idealised distribution of roots with depth, relationships between interval midpoint depth and root density (number of roots per unit area) and root area ratio (RAR: total root area per bank section area) were initially explored by applying linear regression analysis to raw and then square- and log-transformed data, using MiniTab 16 software. A quadratic polynomial model was also tested. However, as no significant increase in the top-most profile layers was detectable, and maximum rooting depth was not clear, the logistic dose-response curve used by Schenk and Jackson (2002) could not be tested.

Differences in root density or root area and depth relationships between wet and dry soil moisture sites were then investigated by expanding the linear and quadratic regression models to include dummy (dry = 0, wet = 1) and 'dummy x depth' interaction variables. Differences in the depth relationship between individual sites were then investigated by including dummy and depth interaction variables for each site, with Site 6, selected as the base site against which other sites were compared, owing to its wide depth coverage. Model selection was step-wise (forward and backward), using a threshold of $\alpha = 0.15$ for inclusion and exclusion of independent variables.

Variations in cumulative root profiles

Mean values of root area ratio and density for each depth interval were also examined cumulatively with increasing depth. Although roots continued to be found at the maximum depth interval at most profiles (16 out of 23), for the purposes of these analyses it was assumed that the full root system had been sampled. Cumulative profiles were used to estimate median (50 %) rooting depth in terms of both density and root area, by fitting curves most closely matching the 10 – 90 % range through the measured data. Linear, quadratic

and cubic regression models were tested across this range, and the model with the highest R^2 (adjusted for degrees of freedom) was selected. To account for differences in maximum depth sampled when comparing median depths, the 50 % estimates were normalized by dividing by the 90 % depth value, as estimated by a similar curve-fitting process using data in the range 80 – 100 %.

Root diameter distributions

Differences between root diameter frequency distributions in dry and wet soil moisture zones were investigated using the Chi-squared test on geometrically-binned diameter classes (with boundary values 0.1, 0.2, 0.4, 0.8 mm, etc.). The total root area due to these diameter classes was also plotted and compared between soil moisture zones (contribution to ‘global root area’ – Figure 4.16). Furthermore, as an indication of the variability of root diameter distributions with depth, the proportional contribution to root area within each depth interval was calculated for each root sampled. These proportions were summed for each diameter class and averaged across profiles (mean contribution to ‘local root area’ – Figure 4.18). In comparing local area distributions at different depths (Figure 4.19 and Figure 4.20), data were aggregated into larger diameter classes (boundaries at 0.2, 0.8, 3.2 and 12.8 mm) and depth intervals (of 0.5 m), in order to present more statistically robust mean proportions of local root area. The deepest class was excluded, as well as the largest diameter class for local area depth distributions, owing to their small sample sizes. All these area distributions are presented as proportions, as sampling effort differed between drier and wetter soil moisture zones.

4.4 RESULTS

The total number of 0.1 m depth intervals sampled was 366, of which 28 contained no roots. Across the investigated profiles, a total of 9717 roots was measured, with 9675 roots remaining when dead roots were excluded. The largest root recorded was 31.0 mm in diameter.

4.4.1 Regression analysis of root properties with sediment profile depth

a Full root dataset from all sites

Summary statistics for the entire dataset of root measurements are presented in Table 4.1 and scatter plots illustrating relationships between root density and root area ratio and depth are presented in Figure 4.5. In all cases the root data relates to 0.1 m profile depth increments.

Among the 366 depth intervals sampled, the scatter of root density and area across sampling depth was large (Figure 4.5).

When simple regression relationships were estimated between the two root variables (as dependent variable) and depth (independent variable), including a variety of transformations of the root variables (Table 4.2), the variance explained by these simple models was low (R^2 (adjusted for degrees of freedom) varied between 0 and 30 %). In all cases, a square transformation of the dependent variable did not improve model fit. Furthermore, regression models incorporating root density as the dependent variable had a consistently higher R^2 value than those for root area.

When more complex polynomial regression models were estimated (Table 4.3), the quadratic term was statistically significant for the analyses including root density as the dependent variable and explanatory power increased, but the quadratic term was not significant (at $\alpha = 0.05$) in the root area ratio regressions. In linear or quadratic models with depth as the only predictor, log-transforming the root data resulted in an increase in R^2 , particularly when root area ratio was the dependent variable.

All fitted models showed a decline in root density or area with depth. The model with the highest explanatory power was the quadratic log-transformed root density model (adj. $R^2 = 17.0$ %) (Figure 4.6). However, note that depth data below 2 m are disproportionately influenced by just 4 of the 23 profiles for which it was possible to sample to this depth.

Table 4.1 Summary statistics for root density and root area ratio observations at all sampled sites.

Statistic	Root density (hundreds m ⁻²)	Root area ratio (cm m ⁻²)
Count	366	366
Maximum	207	396
Mean	26.4	14.4
Standard error of mean	1.60	2.10
Standard deviation	30.7	40.1
Median	16.0	2.85
Variance	941	1610
Coefficient of variation	116	278
Skewness	2.35	6.62
Kurtosis	7.99	53.0

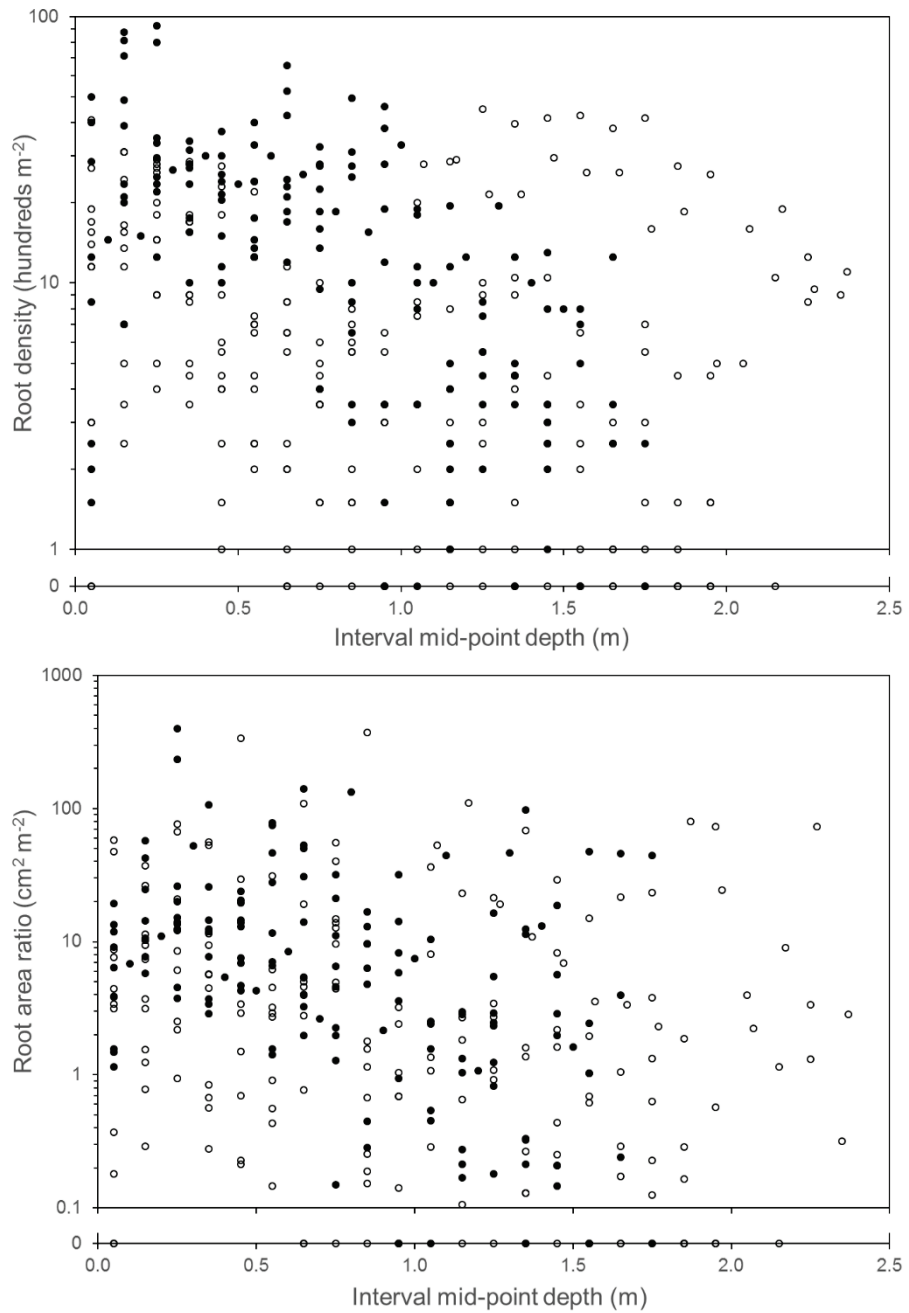


Figure 4.5 Scatter plots of root density (top) and root area ratio (bottom) with depth in the bank profile. Open symbols represent drier sites; filled symbols represent Wetter sites. Note logarithmic scales (zero values are plotted below the depth axis).

Table 4.2 Components and goodness-of-fit for linear regression models incorporating the root variable as the dependent variable and depth as the independent variable. * Denotes significance ($P < 0.05$).

Data transformation	Coefficients of model components		R^2 (adj.)
	Constant	Depth	
Root Density			
None	21.45 *	-9.178 *	11.5 %
Squared	823.3 *	-460.5 *	5.8 %
Log-transformed	2.793 *	-0.776 *	15.2 %
Root Area Ratio			
None	22.09 *	-8.524 *	1.2 %
Squared	3384 *	-1744	0.3 %
Log-transformed	2.193 *	-0.701 *	8.2 %

Table 4.3 Components and goodness-of-fit for quadratic regression models incorporating the root variable as the dependent variable and depth and depth² as the independent variables. * Denotes significance ($P < 0.05$).

Data transformation	Coefficients of model components			R^2 (adj.)
	Constant	Depth	Depth ²	
Root Density				
None	26.35 *	-23.76 *	7.230 *	14.0 %
Squared	1135 *	-1389 *	460.8 *	7.8 %
Log-transformed	3.105 *	-1.706 *	0.461 *	17.0 %
Root Area Ratio				
None	23.81 *	-13.64	2.535	1.0 %
Squared	3381	-1735	-4.32	0.1 %
Log-transformed	2.433 *	-1.416 *	0.355	8.7 %

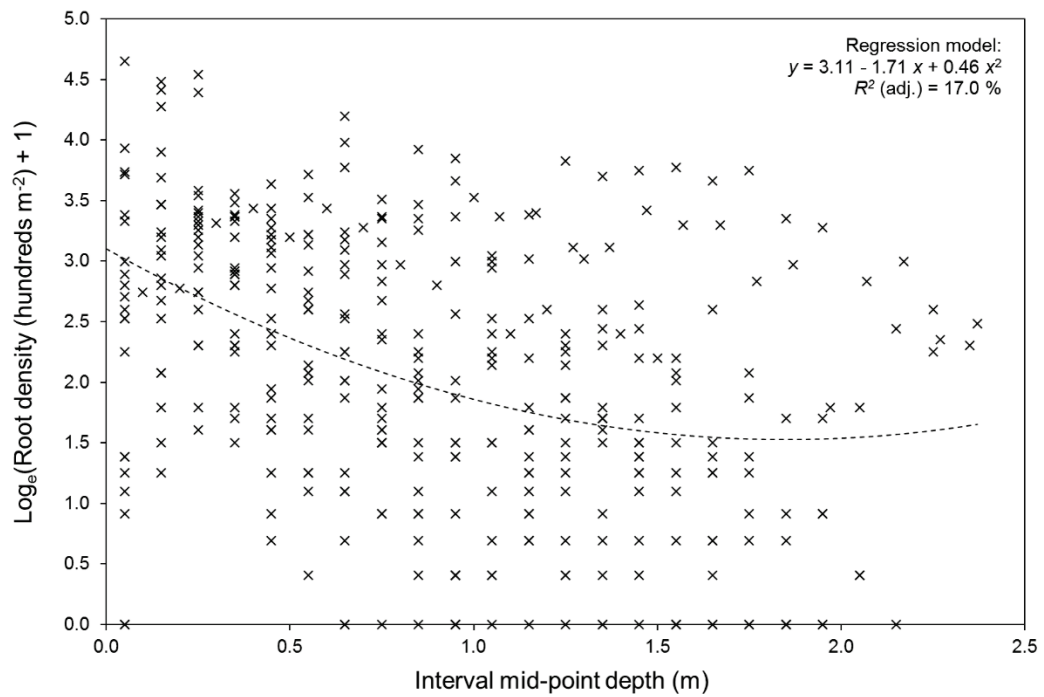


Figure 4.6 Best-fitting (quadratic, log-density) model for the global root density dataset.

b Comparison of wet and dry sites

To assess the degree to which root properties responded differently with depth in wetter and drier sites, a dummy variable was incorporated into the regression analyses. The dummy variable was included as an additional independent variable to bank profile depth and the interaction between these two variables was also incorporated as a third independent variable. By adopting these three independent variables into the regression analysis, it is possible to identify whether there are statistically different relationships between root variables and depth at drier and wetter sites, and also whether the differences are accounted for by a statistically significant difference in the slope or the intercept term of the regression model.

The inclusion of the dummy variable into the analyses resulted in a significant improvement in the explanatory power of both the untransformed and squared root density regression models, and the R^2 (adj.) of the log-transformed root area ratio model also increased. The explanatory power of the root area ratio models only increased when the dependent variable was log-transformed. The statistically significant coefficients for the dummy and interaction variables in the root density regression models demonstrates that wet and dry sites show different behaviour in root density in their surface layers and also in their rate of decline with depth.

Table 4.4 Components and goodness-of-fit for linear regression models incorporating a moisture dummy variable to represent wetter and drier sites. * Denotes significance (P < 0.05).

Data transformation	Coefficients of model components				R^2 (adj.)
	Constant	Moisture Indicator	Depth	Indicator x Depth	
Root Density					
None	11.22 *	25.26 *	-2.340	-19.67 *	29.5 %
Squared	214.6	1539 *	-31.0	-1280 *	19.0 %
Log-transformed	2.171 *	1.453 *	-0.411 *	-0.950 *	27.3 %
Root Area Ratio					
None	16.54 *	13.77	-4.771	-10.89	1.5 %
Squared	2549x10 ⁴	2412x10 ⁴	-9663x10 ³	-2658x10 ⁴	0.1 %
Log-transformed	5.510 *	2.047 *	-0.990 *	-1.014 *	15.9 %

Table 4.5 Components and goodness-of-fit for quadratic regression models incorporating a moisture dummy variable to represent wetter and drier sites. * Denotes significance (P < 0.05).

Data transformation	Coefficients of model components						R^2 (adj.)
	Constant	Moisture Indicator	Depth	Depth ²	Indicator x Depth	Indicator x Depth ²	
Root Density							
None	15.43 *	21.65 *	-14.42 *	5.643 *	-9.800	-4.290	30.3 %
Squared	293.4	1926 *	-257.0	105.6	-2751 *	933.6 *	20.3 %
Log-transform	2.702 *	0.572 *	-1.933 *	0.711 *	1.847 *	-1.492 *	31.0 %
Root Area Ratio							
None	16.29 *	16.87	-4.050	-0.338	-21.96	6.670	1.0 %
Squared	1.40x10 ⁷	4.64x10 ⁷	2.34x10 ⁷	-1.54x10 ⁷	-9.87x10 ⁷	3.94x10 ⁷	0.0 %
Log-transform	6.218 *	1.312 *	-3.020 *	0.948 *	1.109	-1.005	16.5 %

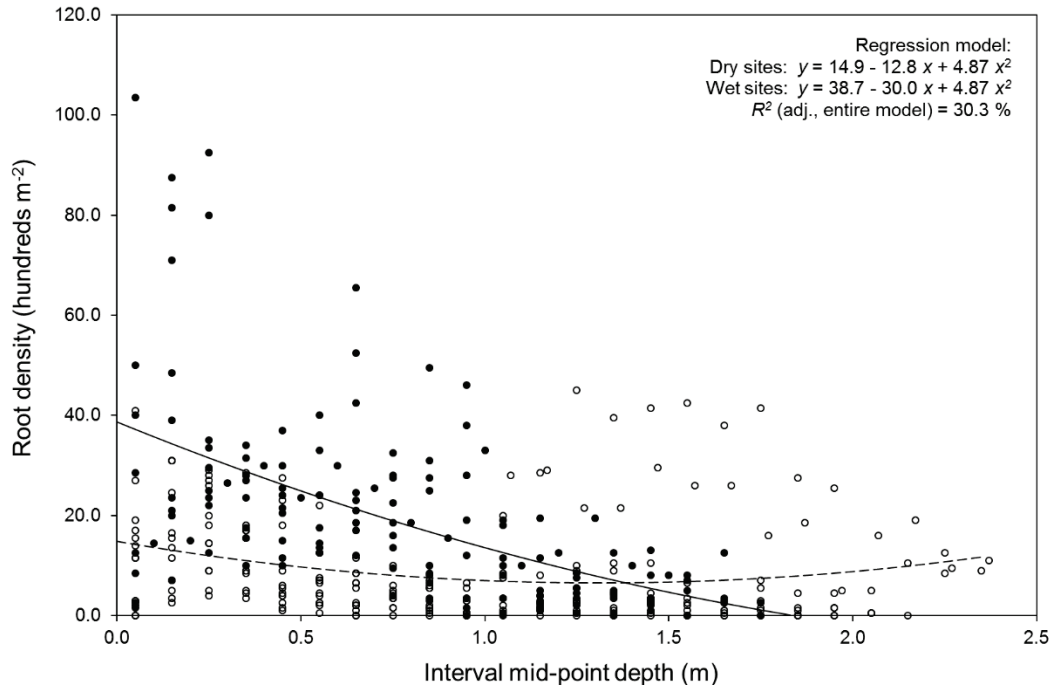


Figure 4.7 Best-fitting (quadratic) root density model incorporating moisture zone dummy variable. Open symbols and dashed line: drier sites; filled symbols and solid line: wetter sites.

Figure 4.7 shows that wetter sites have higher root density at low (shallower) depth, but a steeper decline in root density with depth. Note from Table 4.4 that the site moisture indicator is a more significant descriptor than depth in two of the three models tested. Root area distributions show a less distinct trend, but differences in both root area ratio at zero depth and its rate of decline are apparent in the linear (log-transformed) model. The quadratic (log-transformed) form suggests a significantly different value of root area ratio in the surface layers but no significant difference in the rate of decline with depth. Note, however, that the explanatory power remains low (R^2 (adj.) 16.5 % max.).

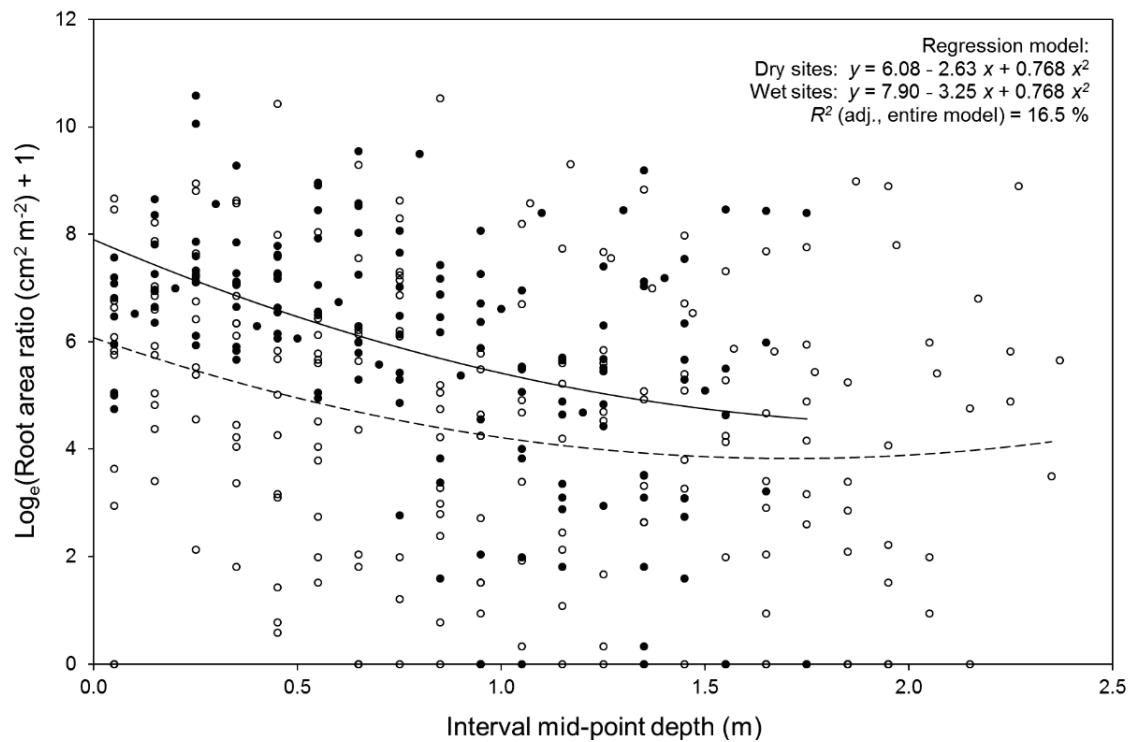


Figure 4.8 Best-fitting (quadratic, log-transformed) root area ratio model incorporating moisture zone dummy variable. Open symbols and dashed line: drier sites; filled symbols and solid line: wetter sites.

c Differences between individual sampling sites

In order to explore whether there were differences in the distribution of the root variables with depth between the individual sampling sites, site dummy variables, as well as a linear depth interaction term (dummy x depth), were generated for each site. Site 6 was incorporated as the base site from which deviations of the other sites were assessed. Linear regression models were then estimated using this new set of independent variables, with a criterion of $P < 0.05$ for each component to be included in the final model. By undertaking this site-based dummy variable analysis, it was possible to identify sites that showed a significant deviation from the base site (Site 6) in terms of their root properties at zero depth (the bank top) and the rate of decline (or increase) with depth. Log-transformed root variables were used in these analyses owing to their higher predictive power in the previous linear regression analyses of the entire dataset (see Table 4.2).

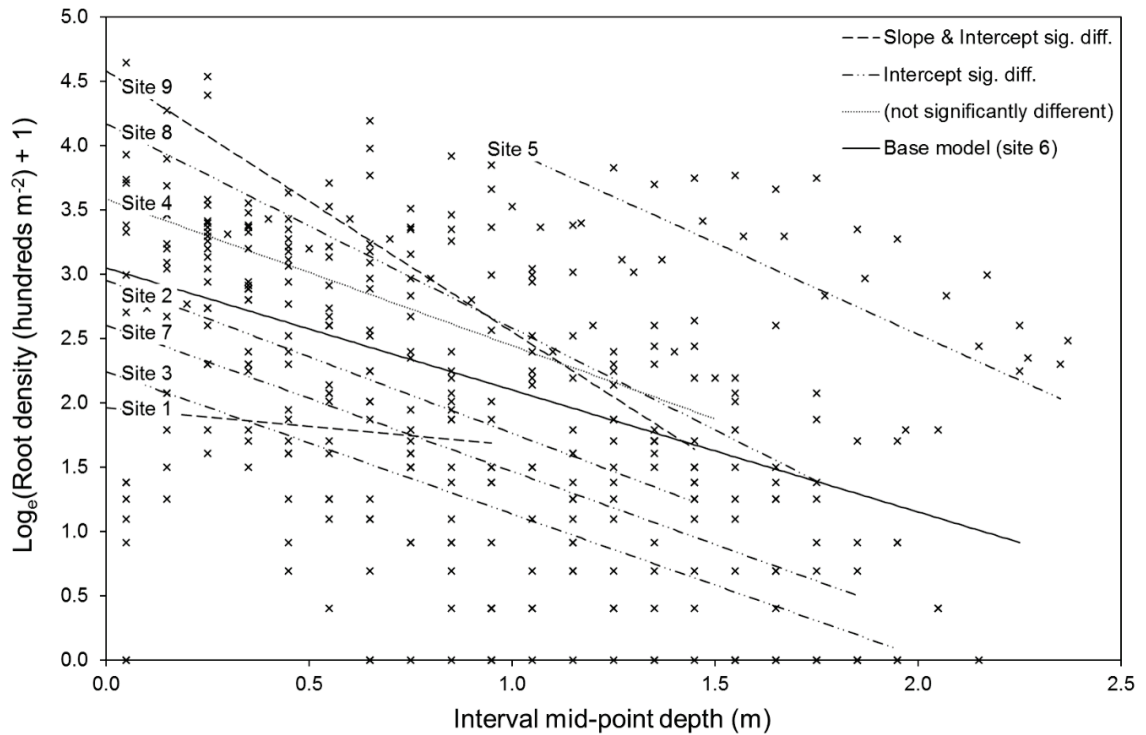


Figure 4.9 Regression models for (log-transformed) root density against depth at individual sites.

A final regression model describing variations in root density with depth (R^2 (adj.) = 56.1%) was based on 9 significant site predictors. Sites 5, 9, 8, 2, 7, 3 and 1 had significantly different zero depth intercept values to Site 6 (reported in decreasing order – i.e., Site 5 had greatest predicted root density at the soil surface (though this is an unreasonably large extrapolation for this site)). These sites are identifiable on Figure 4.9 as vertically displaced regression lines. Only two sites had significantly different rates of change with depth. Site 9 had a markedly steeper decline, whereas that of Site 1 was significantly more gradual than that at Site 6 (and therefore all other sites). Note that, except Site 5, those regressions plotting prominently above Site 6 are for wetter sites, whereas those falling distinctly below are from drier sites.

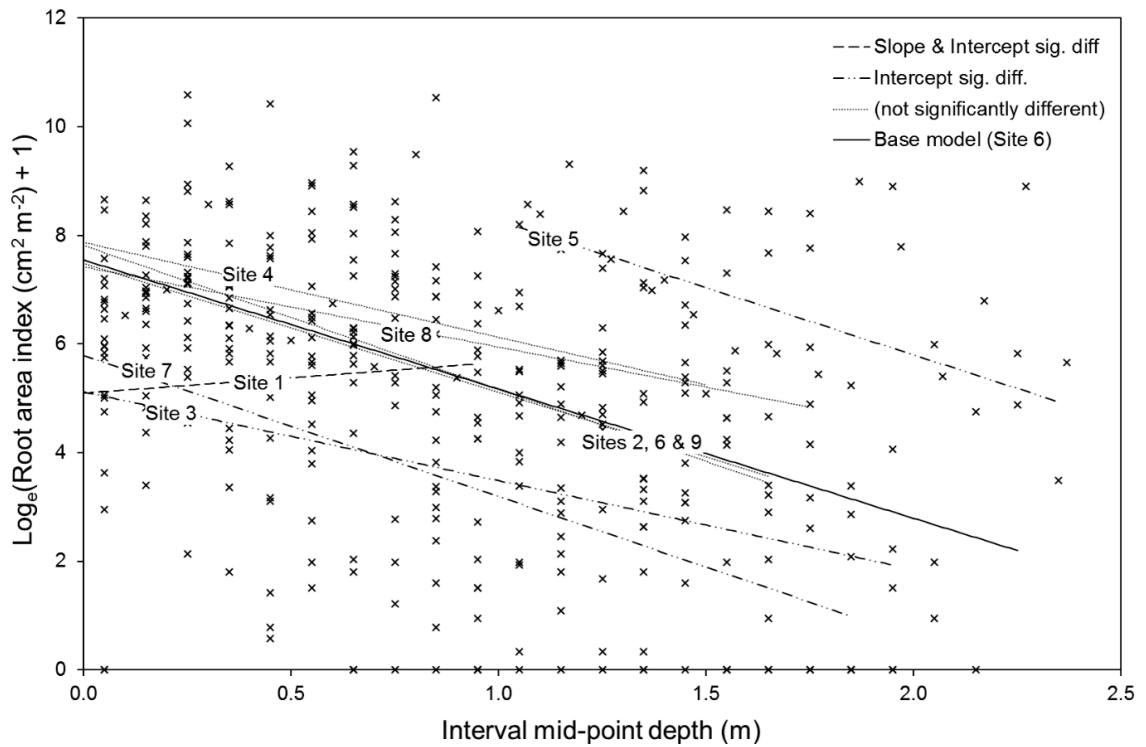


Figure 4.10 Regression models for (log-transformed) root area ratio against depth at individual sites.

The total explanatory power of the root area model was less than for root density (R^2 (adj.) = 31.8%), and identified fewer sites that were significantly different from the others ($P < 0.05$). Only Site 1 was found to have a different rate of change in root area ratio with depth, actually showing an increase in area with depth (Figure 4.10). Sites 5, 7, 3 and 1 had increasingly lower values at the bank top surface. Again, apart from Site 5, wetter sites generally plotted above the base model.

4.4.2 Analysis of cumulative root profiles and median rooting depths

As discussed above, the analysis of the cumulative root profiles is affected by the limited validity of the assumption of having sampled the complete root profile. Nevertheless, cumulative root density and root area ratio data exhibited a curved profile with depth, confirming the concentration of most roots – and indeed most root area – in the upper layers of the profile at all sites (Figure 4.11). At drier sites, the decline in cumulative root density occurred at shallower depths but then continued more steadily to deeper layers. In spite of deeper sampling, the depth above which 50% of root density occurred was significantly shallower at drier sites (0.32 m, vs. 0.43 m at wet sites; $T = 2.52$, $P = 0.014$, 11 d.f., 1-tailed), and normalized median depth was even more significantly shallower (0.31 m, vs. 0.44 m;

$T = 3.01$, $P = 0.004$, 17 d.f., 1-tailed). The depths to which 50 % root area occurred showed more variability and were not significantly different between drier and wetter sites (Figure 4.12).

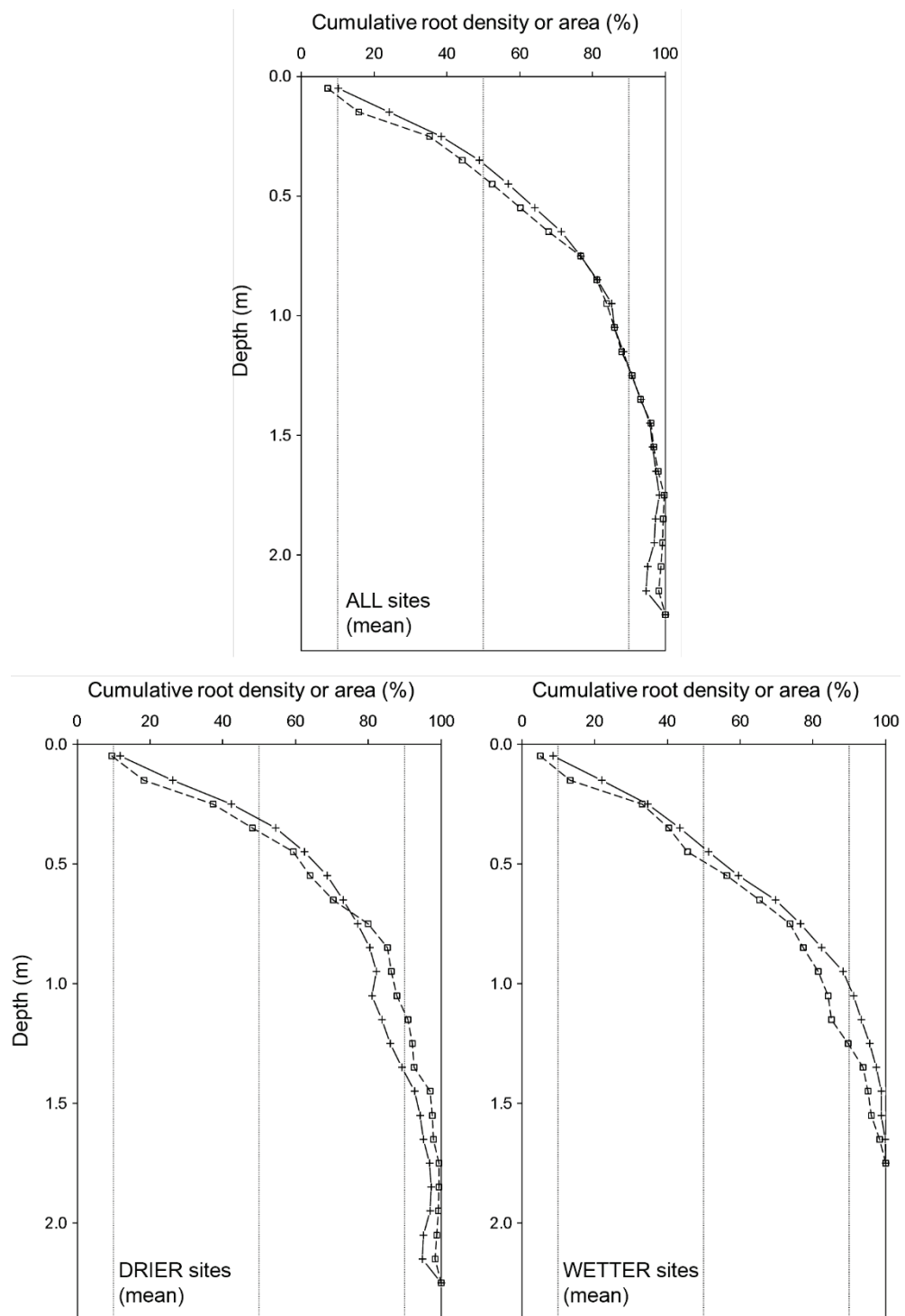


Figure 4.11 Average profiles of cumulative root density (crosses, solid line) and area (boxes, dashed line) for all (top), drier (lower left) and wetter (lower right) sites. Median, 10 and 90 % values are marked with vertical lines.

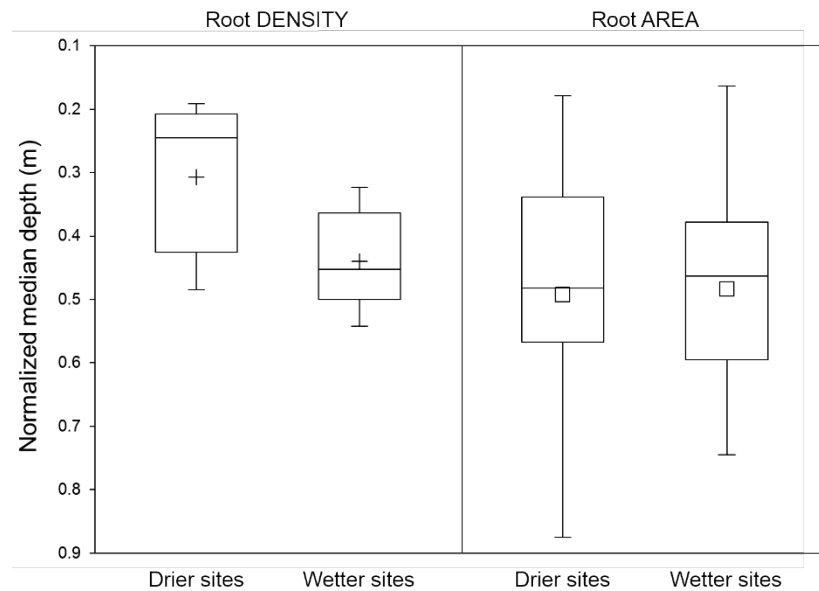


Figure 4.12 Comparative distributions of normalized median (50 % / 90 %) depths of profiles for root density (left) and area (right) at drier and wetter sites. Symbols (density: crosses; area; boxes) within interquartile range boxes represent means; bars, medians.

4.4.3 Variability in root characteristics within bank profiles

In addition to the general trends in root characteristics identified above, it is also important to emphasise how these properties vary. Across all sampled sites, variability (displayed in terms of inter-quartile range in Figures 4.13 – 4.15) of both root density and root area ratio was generally greater in the upper soil layers (Figure 4.13). Extreme outlier values also tended to occur in the upper metre of the bank profile, but were more evenly distributed in the root area ratio data than in the root density data. In comparing root density between wet and dry sites (Figure 4.14), while the former had both more and more variable numbers of roots in the upper metre of the profile, dry site density was more variable at depth. It is also apparent from Figure 4.14 and Figure 4.15 that the incidence of depth intervals without any roots at all was higher in drier sites. Root area ratios were also both greater and more variable at shallow depth at wet sites (Figure 4.15). However, there was a greater incidence of unusually high root area ratio values at drier sites (24, vs. 10).

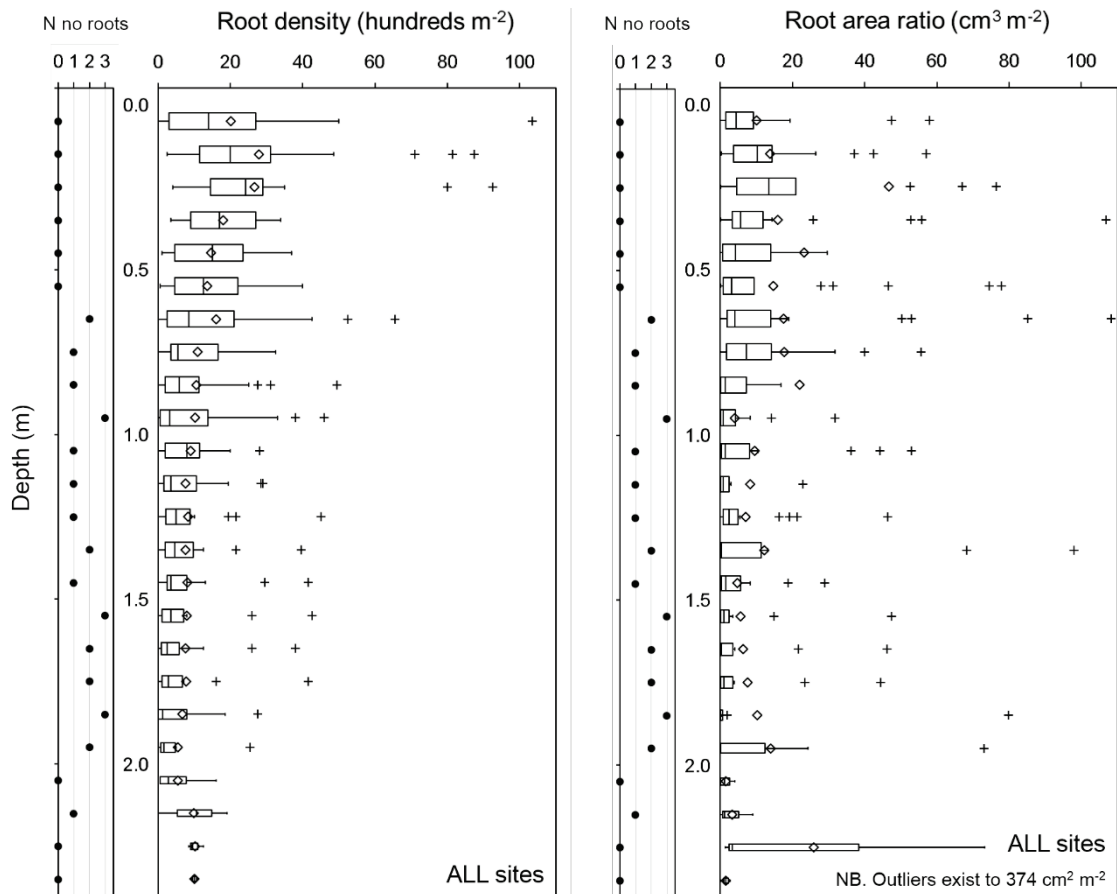


Figure 4.13 Distribution of all root density (left) and root area (right) data variability with depth. Boxes: interquartile range; diamonds: means; bars: medians; crosses: outliers. Width of boxes is representative of sample size. Side-panels show frequency of sampled depth intervals containing no roots.

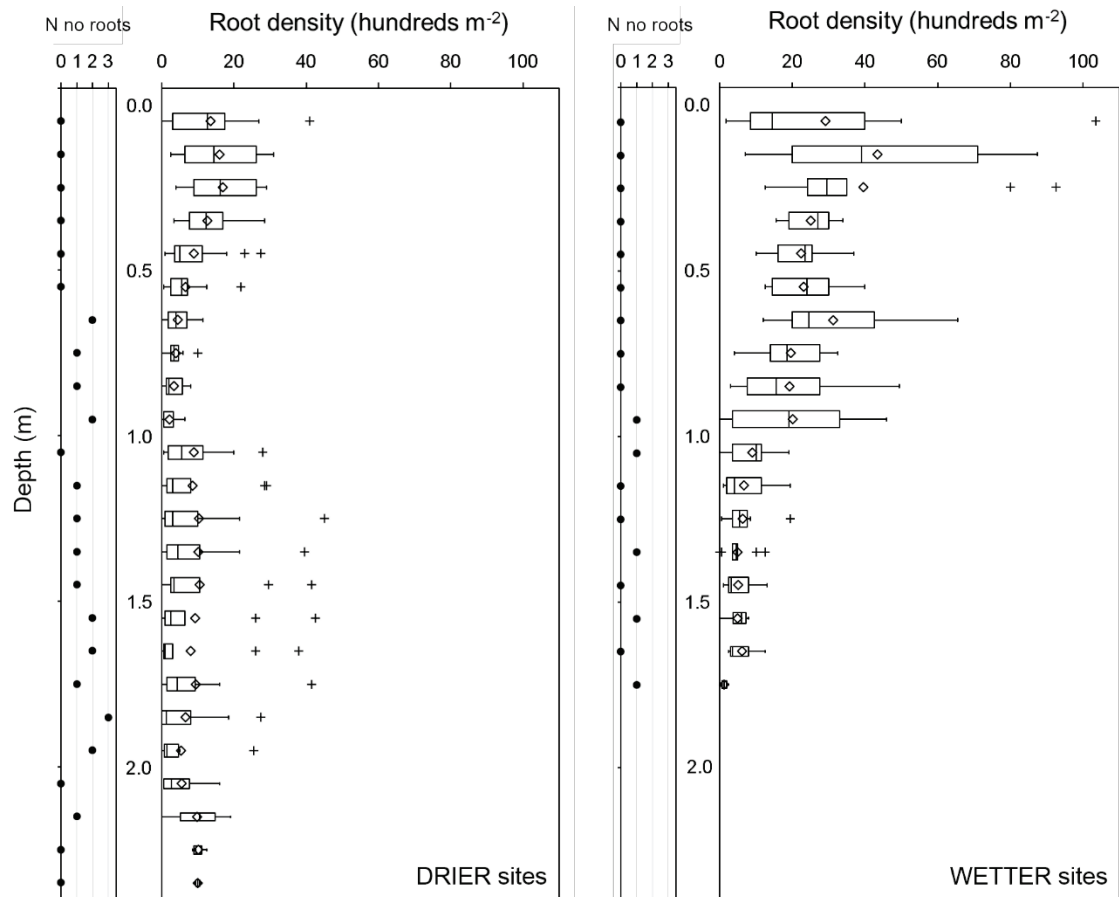


Figure 4.14 Distribution of root density data variability with depth at drier (left) and wetter (right) sites. Boxes: interquartile range; diamonds: means; bars: medians; crosses: outliers. Width of boxes is representative of sample size. Side-panels show frequency of sampled depth intervals containing no roots.

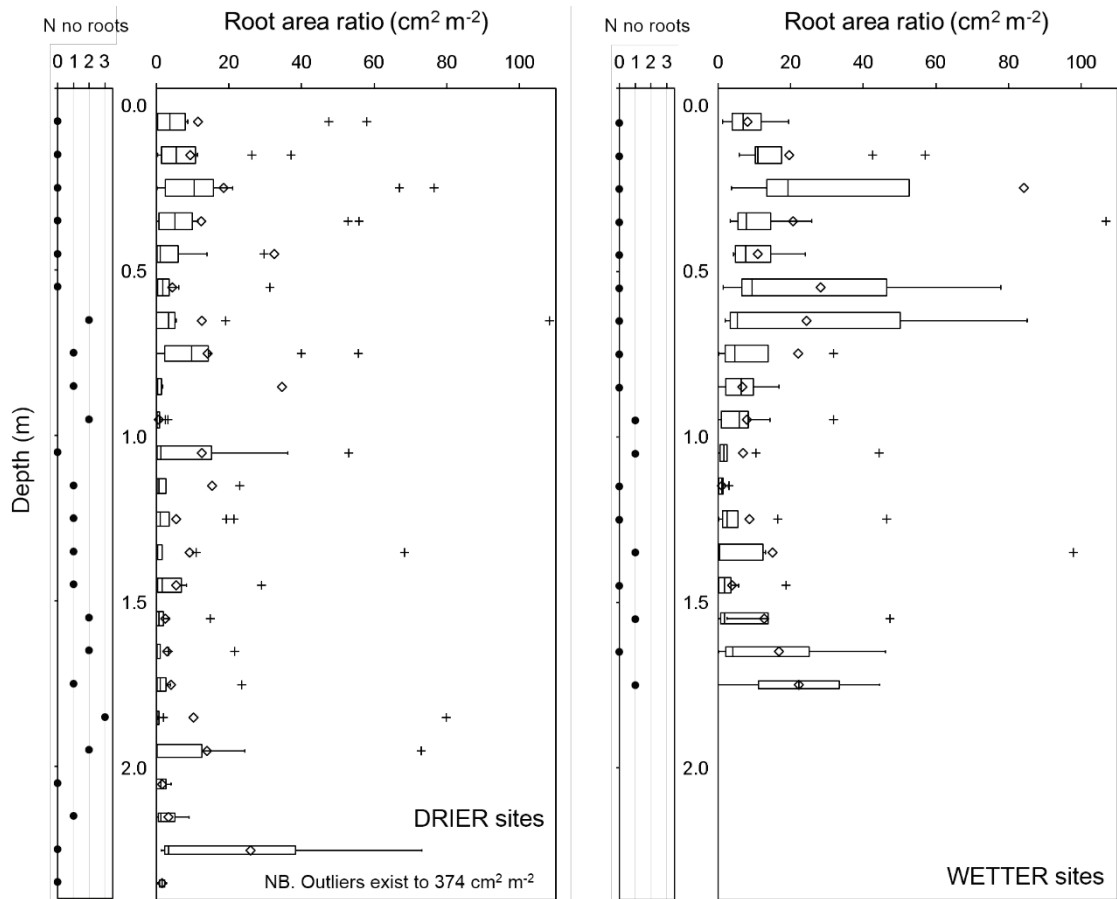


Figure 4.15 Distribution of root area data variability with depth at drier (left) and wetter (right) sites. Boxes: interquartile range; diamonds: means; bars: medians; crosses: outliers. Width of boxes is representative of sample size. Side-panels show frequency of sampled depth intervals containing no roots.

4.4.4 Distribution of root diameters by frequency and area

a Frequency distributions

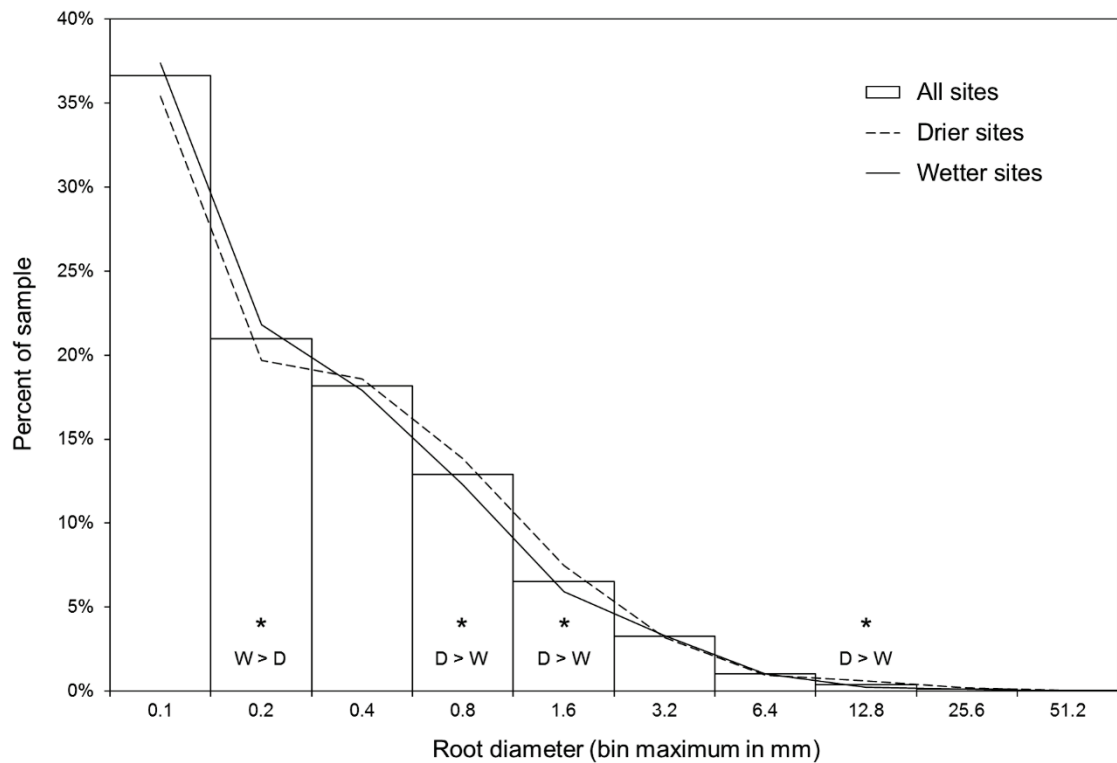


Figure 4.16 Histogram of relative diameter class frequencies for the full dataset and for drier and wetter sites. Significant differences between diameter classes at wetter and drier sites are marked ($P < 0.05$).

Root systems were dominated by the smallest roots when measured in terms of frequency (Figure 4.16). The diameter distribution was significantly different between dry and wet sites ($\chi^2 = 23.9$, 8 d.f., $P < 0.001$), with a greater proportion of very fine roots in wetter, and more fine-to-intermediate diameters in drier profiles (significant differences at $\alpha = 0.05$ marked on Figure 4.16; $\chi^2 = 4.83$, 4.38, 8.41 and 7.93 for 0.2, 0.8, 1.6 and 12.8 mm maximum diameter classes, respectively, all with 1 d.f.).

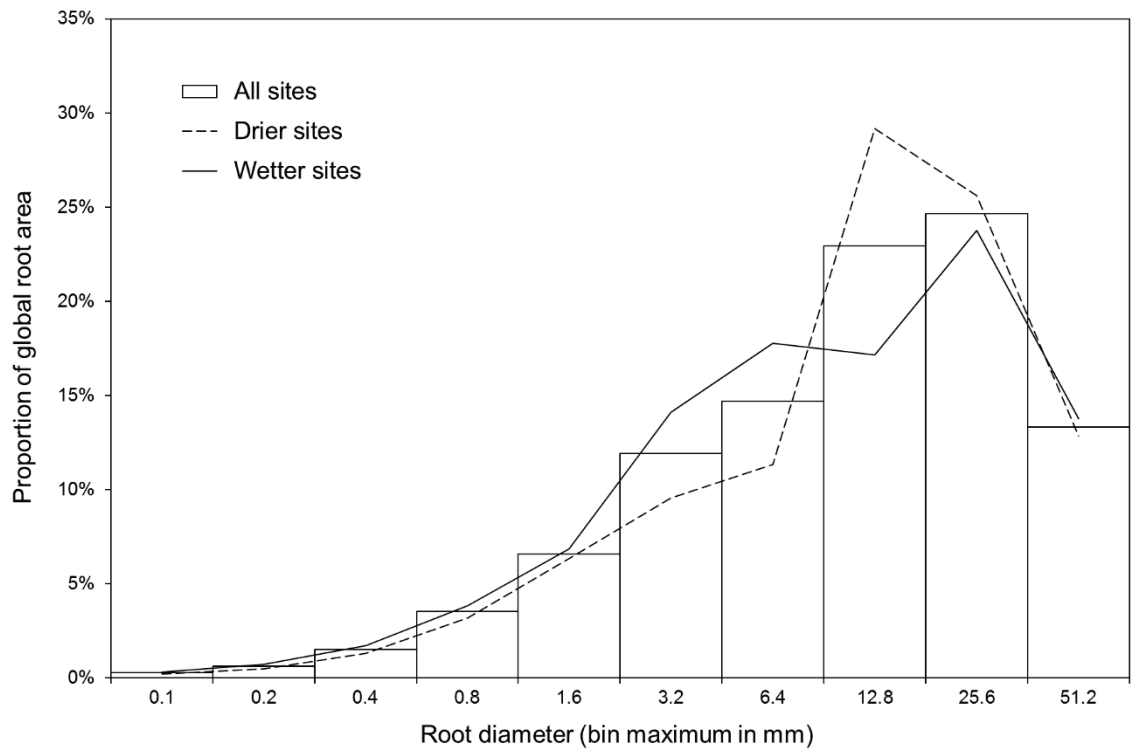


Figure 4.17 Proportional contribution of diameter classes to total root area for the entire, dry site and wet site datasets.

Examination of the diameter distributions by root area show that, across the whole dataset, the 12.8 to 25.6 mm diameter class contributed most root area (24.7 %), and nearly half of all root area was due to this and the next smaller class together (47.6 % of root area from roots between 6.4 and 25.6 mm) (Figure 4.17). Root area was more strongly dominated by these two classes in drier sites (54.8 % of area), though the smaller 6.4 to 12.8 mm class was responsible for a greater sectional area in this case. As was the situation for the full dataset, wetter site root area was greatest for the 12.8 to 25.6 mm diameter class (23.8 %), but there was an additional peak for medium-sized roots (1.6 to 6.4 mm, contributing 31.9 %).

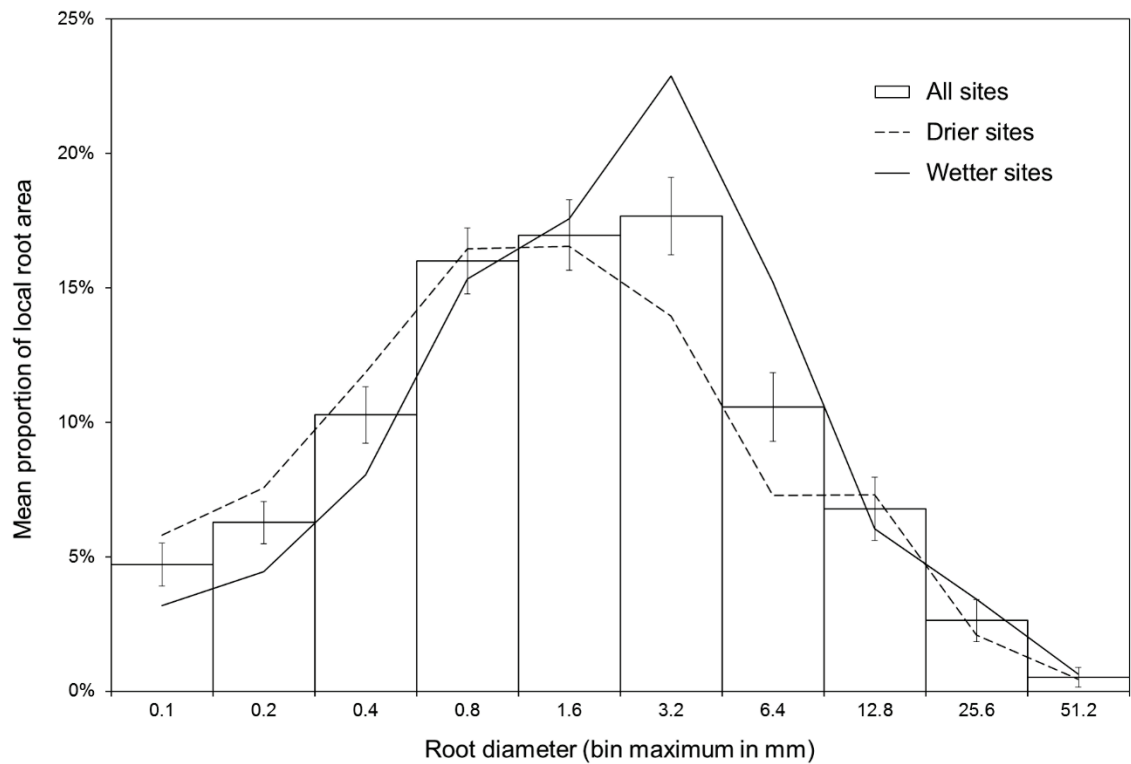


Figure 4.18 Mean proportional contribution of diameter classes to individual 0.1 m depth intervals for the entire, drier site and wetter site datasets. Bars represent standard error of the mean.

As a proportion of root area within each 0.1 m depth interval, the 1.6 to 3.2 mm diameter class was most dominant in the overall area distribution (mean 17.7 % \pm 1.44 % SE), and most of the local sectional area was due to roots between 0.4 and 3.2 mm diameter (54.8 % of the sum of all proportions) (Figure 4.18). In wetter sites, the 1.6 to 3.2 mm class contributed even more greatly (mean 22.9 % \pm 2.37 % SE) and slightly larger roots prevailed as compared to drier sites, where the distribution was less peaked and translated towards fine root dominance. Here, the 0.4 to 0.8 and 0.8 to 1.6 mm diameter classes predominated (16.5 \pm 1.74 and 16.5 \pm 1.81 % means \pm standard errors, respectively) and on average the finest roots (< 0.4 mm diameter) made up more of local root area.

c Root diameters and depth

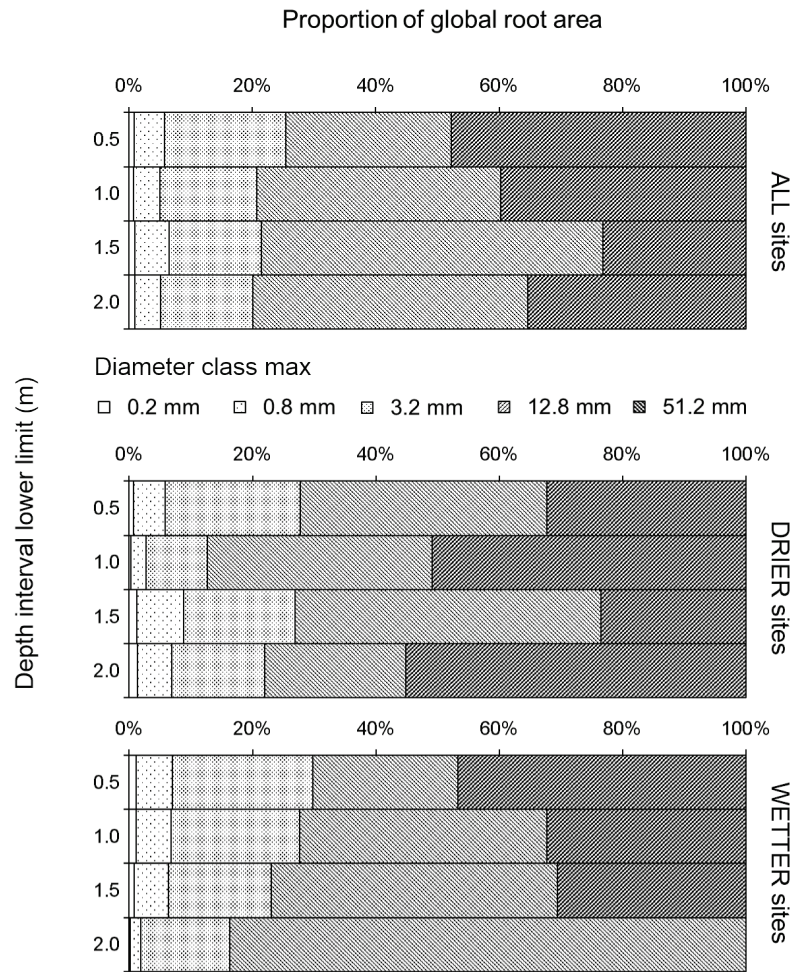


Figure 4.19 Proportional contribution at varying depth of root diameter classes to total root area for the entire (top), drier site (middle) and wetter site (bottom) datasets.

Examining the diameter structure of root area with depth (Figure 4.19), the dominance of whole profile (entire dataset) root area by the larger diameter classes is apparent throughout (roots > 3.2 mm, mean 78.1 % of total area across the depth classes). There does appear to be an increase in the proportion of area attributable to the 3.2 to 12.8 mm class with depth, however, and this is more apparent in the wetter profiles (increasing from 23.5 to 83.7 % of all root area). The relative contributions of the different diameter classes appear to be more variable with depth in drier sites.

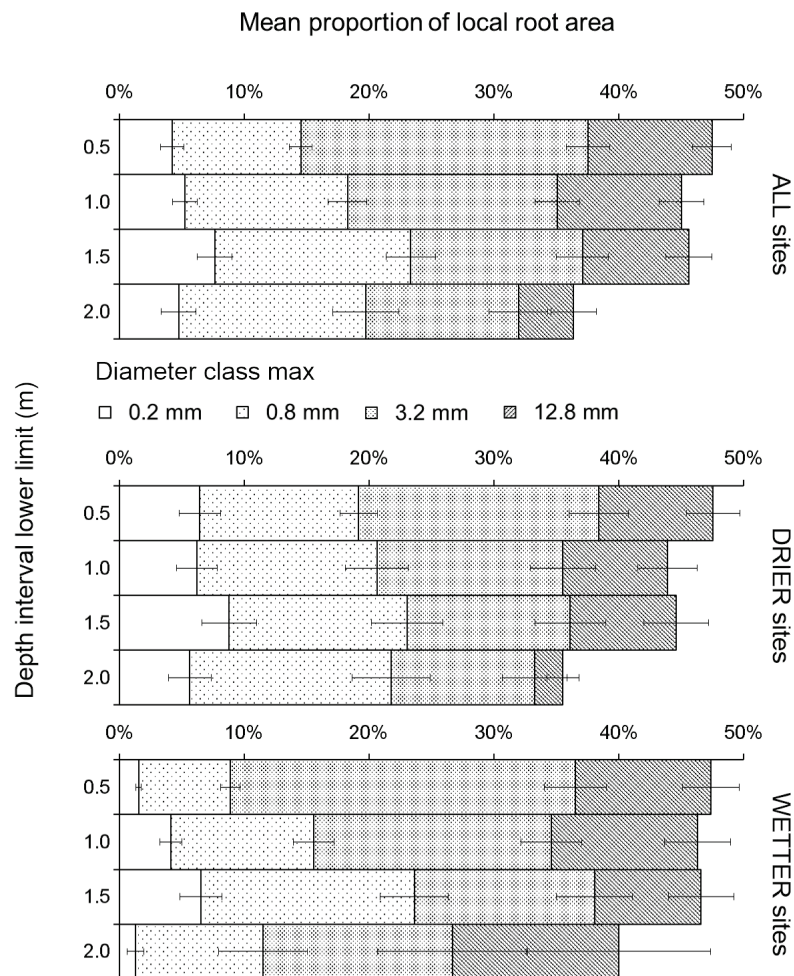


Figure 4.20 Mean proportional contribution at varying depth of diameter classes to individual 0.1 m depth intervals for the entire, drier site and wetter site datasets. Bars represent standard error of the mean. NB. Sample sizes of largest root diameter class in Figure 4.19 (51.2 mm max) were too small to calculate averages across depth and are not plotted.

At the level of the local 0.1 m depth interval, across all sites, the 0.8 to 3.2 mm class most frequently dominated root area near the surface (mean 23.0 % \pm 1.75 % SE at 0.0 to 0.5 m), but this influence declined with depth (12.2 % \pm 2.37 % at 2.0 m). A similar pattern was seen in the larger 3.2 to 12.8 mm class, with the smaller roots conversely increasing in their average contribution with depth. There appeared to be a distinct peak in mean fine root (< 0.2 mm) dominance between 1.0 and 1.5 m, and this was particularly marked in data from wetter sites, where it was also apparent in the adjacent 0.2 to 0.8 mm class. Overall, the diameter distribution of local root area in drier sites appeared to be less affected by depth than in wetter sites (mean variances across depth classes are 0.05 % and 0.13 % for dry and wet, respectively).

4.5 DISCUSSION

The research reported in this chapter has described the distribution, variability and size-class structure of deep root profiles in a dynamic riparian forest – a novel biome for such investigations which exhibits a peculiarly complex ‘high contrast’ stratigraphic environment as a result of flood-related deposition and erosion of sediment. The study focussed on roots from *Populus nigra* L., the locally dominant riparian tree species, although all roots within the bank sediment profile were assessed. Perhaps most importantly (and further supported by excavations of complete root systems, described elsewhere in this thesis), roots continued in significant numbers and cross-sectional area beyond the maximum sampling depth (2 m, in most cases) in 70 % of the profiles investigated, suggesting that the investigated systems are unusually deeply-rooted. The Tagliamento bank profiles compare favourably with desert and temperate coniferous forest biomes, which show the deepest profiles in the global analysis of Jackson et al. (1996), displaying median rooting depths greater than 0.3 m. None of the riparian species studied by Simon and Collison (2002) were found to root below 0.9 m, although their sites was presumably located in fine-grained and slower-draining loess sediments (more similar to the stratigraphy of the wetter profiles in the current study). Such deep root distributions may be due to water limitation in these counter-intuitively xeric, free-draining riverside soils – necessitating access to the alluvial aquifer throughout the growing season or possibly simply reflecting the rapid accretion of sediment and progressive burial of the roots.

Across the dataset as a whole, a curved profile in root characteristics, exhibiting an initially sharp decline, is observed in both root numbers and total root area per unit area of the bank profile, as expected and reported in most similar investigations (Jackson et al., 1996, Schenk and Jackson, 2002) and reasonably described by simple empirical continuous depth decline models. However, these model profiles are crude approximations to the real situation in the present case, with the best-fitting root property with depth regression models of those tested describing only 17.0 % and 8.7 % of the variability in root density and root area ratio, respectively. This being so, there seems little value in exhaustive testing of different or increasingly complex curved relationships. Such models as the ones tested here may be less informative for hydrological or geomorphological process modelling (dependent on cross-sectional area information for quantitative estimates of fluxes and forces) than for understanding underlying autogenic patterns in the development of root system architecture (more closely allied to data on numbers, presence or absence of roots when examining planar profiles) in these riparian systems. Furthermore, in light of the obvious violation of the assumption of sampling to maximum rooting depth, the application of widely used

cumulative proportional asymptotic decline models (as mentioned in the introduction) would be not be valid here. Clearly, in this riparian forest environment there are other strongly influential factors at play, presumably including the specific within-profile distribution of sediments and soil development, and between-profile differences in plant-available water relating to the broader environmental setting.

Evidence for dependence on within-profile variability in sediment characteristics is presented later in this thesis, but the influence of between-profile moisture availability is visible in the many differences between root distributions in drier and wetter soil moisture zones identified by the present analyses. Indeed, the predictive power of the various regression models is almost doubled when these drier and wetter datasets are treated separately. As in the profiles studied by Rood et al. (2011), who found a threefold variation, the range of median depths was large. In the present case, normalized (50 ÷ 90 %) root density varied approximately threefold, and more than fivefold for normalized area depths (values for non-normalized depths varied by a factor of approximately 4 for both). In spite of a significantly lower rate of decline with depth, however, the shallower median root density depth of drier sites suggests that more water-stressed vegetation tends to pack a greater *proportion* of its below-ground structures into the upper profile. The similar root area depths, though, may indicate that the apportionment of biomass across the profile is more conserved, and thus more independent of soil moisture.

Across the whole dataset, both root density and area are more variable in the upper ~ 0.75 m. Plastic root density structure is consistent with these upper horizons being a zone of reactive foraging, related to the heterogeneity of organic matter and thus nutrients. Variability of root *area* is likely to be linked to root density and foraging, but may also be due to the existence of large structural roots and clonal expansion via adventitious, large suckering roots in the more favourable, finer deposits normally found in these upper layers. This assumed near-surface foraging strategy is much more pronounced in wetter sites – visible in the wide interquartile range of both density and area measurements – though still apparent in dryer sites. By contrast, however, dry profile rooting covers a far greater range of densities beyond 1.0 m depth, suggesting perhaps a deeper zone of structural plasticity. The root area distributions do not strongly match those of the root numbers, but there is a much greater number of unusually large root area ratios in dry sites, due to isolated large-diameter roots (or clumps thereof) throughout the depth range sampled. It is hypothesized that these may represent a perennial coarse structure from which short-lived, absorptive roots emanate where and when sediment conditions are favourable. Higher root area ratio with depth may also be species-related, however. Simon et al. (2006) found area profiles

much like the drier sites presented here around *Salix lemmonii* Bebb, but much more similar to wetter Tagliamento sites around *Pinus contorta* Douglas. At wetter sites there is a perhaps an indication of an increase in mean width of distribution of root area ratio beyond 1.5 m, possibly due to the occasional sampling of large diameter, phreatophytic roots, though there is a high probability of this being an artefact of low sample sizes approaching these maximum depths (also seen at the lowest depths in drier profiles).

That so many significant differences were found between the root property - depth relationships at specific sites gives further support to the notion that an understanding of locally variable plant-relevant factors is important for upscale interpretation of vegetation effects such as root reinforcement or hydraulic redistribution from alluvial aquifers. Between-site differences in both root density and root area profiles mainly took the form of vertical displacements – i.e., the rate of decline was conserved, but the size of the root systems varied. This may relate to the root profiles' variable proximity to individual trees (see, e.g., Abernethy and Rutherford, 2001), but is also likely to be highly dependent on the density and type of forest stand on the bank top, which varied substantially within the scope of the site selection criteria (see analysis later in this thesis). The steep decline in root density at Site 9 (Figure 4.9) may be due to particularly large numbers of fine roots in the upper profile. The site had a well-developed, moist soil beneath a long-established mixed-species stand and was in an area sheltered from fluvial disturbance. Site 5, however, was much closer to the main, active channel and, as Figure 4.4 and the strongly layered sediment profile suggest, has probably been subjected to significant rates of organic debris trapping and burial, sustaining particularly dense and fast-developing root systems. Regression results for Site 1 are inconclusive as sampling was to a much more limited depth. It seems probable that higher root density and area in the lower part of the profile may have had an unduly strong influence on the fit of the regression model as compared to other sites. An ecological explanation is not immediately apparent.

Interestingly, whereas the cumulative profiles of Rood et al. (2011) (mapping solely coarse poplar roots) show an initial increase in numbers from the soil surface (as in the logistic depth function applied by Schenk and Jackson (2002)), over the complete size range mapped here, there was rarely such an increase detected. This is most likely due to abundant surface fine roots in a very shallow organic horizon within such young soils. It is not unexpected, particularly as sampling took place during the growing season, that fine roots made up the bulk of root numbers (Figure 4.16), and more so in the finer-grained, wetter profiles, where nutrient cycling is presumed to be more active. The apparent slight under-representation of the 0.2 mm maximum diameter class may be a sampling artefact due to compression of these

more delicate, finer roots during measurement with calipers. A greater proportion of fine-to-intermediate diameter roots in drier profiles may possibly represent anatomical (e.g., thicker epidermis and/or changes to xylem anatomy) or root system architectural adaptations (fewer, more transient absorptive fine roots emanating from a longer-lived larger-diameter network (Tibbett, 2000)) to stresses in this environment. Across complete profiles, root biomass (assumed closely matched to area) appears to be concentrated in the diameter range of laterally extensive adventitious (as opposed to structural) poplar roots (Figure 4.17), supporting assertions that they play an important role in whole plant resource partitioning, storage and transport, as suggested by Pregitzer and Friend (1996). Their function in water and carbohydrate storage, as well as clonal expansion and exploitation of patchy soil resources (Hutchings and de Kroon, 1994) appears to be more important in drier sites. Such large roots do not dominate root area across all depths, however (Figure 4.18). Though size resolution is more limited, Figure 4.19 and Figure 4.20 show that the largest roots generally contribute less to local root area totals with increasing depth.

The evidence presented here demonstrates that simple empirical models of root distribution are of only very limited value in a natural, dynamic riparian landscape. Rooting patterns are broadly deeper and more evenly distributed where soil moisture is low, and where it is high, there is far more investment in root biomass and architecture nearer the soil surface, in absolute terms. This has implications for the vertical distribution of bank erosion and failure susceptibility, which may vary with the water status of the riparian vegetation. There is, however, great variability in these rooting depth patterns between sites of similar moisture availability, presumably related to the diversity of sediment profiles which exists in such dynamic fluvial environments (the subject of further research reported in the next chapter). The variability in deep root structure is greatest at dry sites, where soil resources are likely to be more crucial to survival, whereas roots in better developed soils at wetter sites show distributions suggesting more active foraging and below-ground competition at shallower depths.

4.6 CONCLUSIONS

With respect to the specific questions outlined in Section 4.1.1, the following conclusions can be made from observations on the Tagliamento-black poplar system:

- i. Root numbers and root area both significantly decline with depth. However, there is an extremely large degree of variability around these inverse relationships, and root area ratio is much more difficult to predict. The best models explained 17 % of root density variability and 9 % of root area variability based on depth alone.
- ii. Drier sites show a more gradual decline in root density with depth, but start from lower densities near the soil surface. Root area ratio depth relationships are not so significantly different between drier and wetter sites, though drier sites tend to have lower root sectional area.
- iii. Though dry sites have lower root densities overall and a weaker depth decline, there appears to be greater proportional investment in the upper layers of sediment. Root area depth structure appears less dependent on water availability than root densities.
- iv. The erratic nature of the root area ratio distribution precludes strong conclusions with regards depth-dependent predictability. However, root density appears to show more variability in upper layers, interpreted as greater flexibility and ‘foraging’. In drier sites, there is evidence of a second, deeper region of such variability.
- v. While the finest, absorptive roots dominate with regard to density, larger roots corresponding in diameter to the specialist, horizontally-extending and often suckering adventitious roots of black poplar dominate the root area distribution. A general increasing dominance of larger roots is observed with depth, and the size class exhibiting this dominance is larger at drier sites.

The general depth relationships investigated in this chapter uncover some broad trends and conserved features, however, the extensive variability outside these relationships hints at much underlying complexity and highlights the risks associated with attempting to represent riparian rooting patterns using depth alone. Chapter 5 investigates one potential source of this superimposed variance: the complex spatial distributions of sediment resources in dynamic fluvial environments.

4.7 REFERENCES

- ABERNETHY, B. & RUTHERFURD, I. D. 2001. The distribution and strength of riparian tree roots in relation to riverbank reinforcement. *Hydrological Processes*, 15, 63-79.
- ACUÑA, V. & TOCKNER, K. 2009. Surface-subsurface water exchange rates along alluvial river reaches control the thermal patterns in an Alpine river network. *Freshwater Biology*, 54, 306-320.

- BERTOLDI, W., DRAKE, N. A. & GURNELL, A. M. 2011. Interactions between river flows and colonizing vegetation on a braided river: Exploring spatial and temporal dynamics in riparian vegetation cover using satellite data. *Earth Surface Processes and Landforms*, 36, 1474-1486.
- BERTOLDI, W., GURNELL, A., SURIAN, N., TOCKNER, K., ZANONI, L., ZILIANI, L. & ZOLEZZI, G. 2009. Understanding reference processes: Linkages between river flows, sediment dynamics and vegetated landforms along the Tagliamento River, Italy. *River Research and Applications*, 25, 501-516.
- CORENBLIT, D. & STEIGER, J. 2009. Vegetation as a major conductor of geomorphic changes on the Earth surface: Toward evolutionary geomorphology. *Earth Surface Processes and Landforms*, 34, 891-896.
- CORENBLIT, D., STEIGER, J., GONZÁLEZ, E., GURNELL, A. M., CHARRIER, G., DARROZES, J., DOUSSEAU, J., JULIEN, F., LAMBS, L., LARRUE, S., ROUSSEL, E., VAUTIER, F. & VOLDOIRE, O. 2014. The biogeomorphological life cycle of poplars during the fluvial biogeomorphological succession: a special focus on *Populus nigra* L. *Earth Surface Processes and Landforms*, 39, 546-563.
- CORENBLIT, D., TABACCHI, E., STEIGER, J. & GURNELL, A. M. 2007. Reciprocal interactions and adjustments between fluvial landforms and vegetation dynamics in river corridors: A review of complementary approaches. *Earth-Science Reviews*, 84, 56-86.
- CURRAN, J. C. & HESSION, W. C. 2013. Vegetative impacts on hydraulics and sediment processes across the fluvial system. *Journal of Hydrology*, 505, 364-376.
- DUPUY, L., GREGORY, P. J. & BENGOUGH, A. G. 2010. Root growth models: Towards a new generation of continuous approaches. *Journal of Experimental Botany*, 61, 2131-2143.
- EDMAIER, K., CROUZY, B., ENNOS, R., BURLANDO, P. & PERONA, P. 2014. Influence of root characteristics and soil variables on the uprooting mechanics of *Avena sativa* and *Medicago sativa* seedlings. *Earth Surface Processes and Landforms*, 39, 1354-1364.
- FRANCIS, R. A. & GURNELL, A. M. 2006. Initial establishment of vegetative fragments within the active zone of a braided gravel-bed River (River Tagliamento, NE Italy). *Wetlands*, 26, 641-648.
- FRANCIS, R. A., GURNELL, A. M., PETTS, G. E. & EDWARDS, P. J. 2005. Survival and growth responses of *Populus nigra*, *Salix elaeagnos* and *Alnus incana* cuttings to varying levels of hydric stress. *Forest Ecology and Management*, 210, 291-301.
- GERWITZ, A. & PAGE, E. R. 1974. An Empirical Mathematical Model to Describe Plant Root Systems. *Journal of Applied Ecology*, 11, 773-781.
- GONZALEZ, E., COMIN, F. A. & MULLER, E. 2010. Seed dispersal, germination and early seedling establishment of *Populus alba* L. under simulated water table declines in different substrates. *Trees-Structure and Function*, 24, 151-163.
- GREGORY, P. J. 2006. Roots, rhizosphere and soil: The route to a better understanding of soil science? *European Journal of Soil Science*, 57, 2-12.
- GUILLOY, H., GONZÁLEZ, E., MULLER, E., HUGHES, F. R. & BARSOUM, N. 2011. Abrupt drops in water table level influence the development of *populus nigra* and *salix alba* seedlings of different ages. *Wetlands*, 31, 1249-1261.
- GURNELL, A. 2014. Plants as river system engineers. *Earth Surface Processes and Landforms*, 39, 4-25.
- GURNELL, A. 2015 (in press). Trees, wood and river morphodynamics: results from 15 years research on the Tagliamento river, Italy. In: GILVEAR, D., GREENWOOD, M., THOMS, M. & WOOD, P. (eds.) *River Science: Research and Applications for the 21st Century*. Hoboken, NJ: John Wiley and Sons.
- GURNELL, A. M., BLACKALL, T. D. & PETTS, G. E. 2008. Characteristics of freshly deposited sand and finer sediments along an island-braided, gravel-bed river: The roles of water, wind and trees. *Geomorphology*, 99, 254-269.
- HUTCHINGS, M. J. & DE KROON, H. 1994. Foraging in plants: The role of morphological plasticity in resource acquisition. *Advances in Ecological Research*, 25, 159-238.
- JACKSON, R. B., CANADELL, J., EHLERINGER, J. R., MOONEY, H. A., SALA, O. E. & SCHULZE, E. D. 1996. A global analysis of root distributions for terrestrial biomes. *Oecologia*, 108, 389-411.
- JACKSON, R. B., SCHENK, H. J., JOBBÁGY, E. G., CANADELL, J., COLELLO, G. D., DICKINSON, R. E., FIELD, C. B., FRIEDLINGSTEIN, P., HEIMANN, M., HIBBARD, K., KICKLIGHTER, D. W., KLEIDON, A., NEILSON, R. P., PARTON, W. J., SALA, O. E. & SYKES, M. T. 2000. Belowground consequences of vegetation change and their treatment in models. *Ecological Applications*, 10, 470-483.

- LATHAM, J., CUMANI, R., ROSATI, I. & BLOISE, M. 2014. FAO Global Land Cover (GLC-SHARE) Beta-Release 1.0 Database. In: FOOD AND AGRICULTURE ORGANIZATION OF THE UNITED NATIONS, L. A. W. D. (ed.) Beta-Release 1.0 ed. Rome, Italy.
- MAHONEY, J. M. & ROOD, S. B. 1998. Streamflow requirements for cottonwood seedling recruitment - An integrative model. *Wetlands*, 18, 634-645.
- MARSTON, R. A. 2010. Geomorphology and vegetation on hillslopes: Interactions, dependencies, and feedback loops. *Geomorphology*, 116, 206-217.
- METCALFE, D. B., FISHER, R. A. & WARDLE, D. A. 2011. Plant communities as drivers of soil respiration: Pathways, mechanisms, and significance for global change. *Biogeosciences*, 8, 2047-2061.
- MONTEITH, J. L., HUDA, A. K. S. & MIDYA, D. 1989. RESCAP: A resource capture model for sorghum and pearl millet. In: VIRIMANE, S. M., TANDON, H. L. S. & ALAGARSWAMY, G. (eds.) *Modeling the Growth and Development of Sorghum and Pearl Millet*. Patancheru, India: ICRISAT.
- OSTERKAMP, W. R., HUPP, C. R. & STOFFEL, M. 2012. The interactions between vegetation and erosion: New directions for research at the interface of ecology and geomorphology. *Earth Surface Processes and Landforms*, 37, 23-36.
- PASQUALE, N., PERONA, P., FRANCIS, R. & BURLANDO, P. 2012. Effects of streamflow variability on the vertical root density distribution of willow cutting experiments. *Ecological Engineering*, 40, 167-172.
- POLLEN-BANKHEAD, N. & SIMON, A. 2009. Enhanced application of root-reinforcement algorithms for bank-stability modeling. *Earth Surface Processes and Landforms*, 34, 471-480.
- POLLEN-BANKHEAD, N. & SIMON, A. 2010. Hydrologic and hydraulic effects of riparian root networks on streambank stability: Is mechanical root-reinforcement the whole story? *Geomorphology*, 116, 353-362.
- POLLEN, N. 2007. Temporal and spatial variability in root reinforcement of streambanks: Accounting for soil shear strength and moisture. *Catena*, 69, 197-205.
- PREGITZER, K. & FRIEND, A. L. 1996. The structure and function of Populus root systems. In: STETTLER, R. F., BRADSHAW, H. D., JR., HEILMAN, P. E. & HINCKLEY, T. M. (eds.) *Biology of Populus and its Implications for Management and Conservation*. Ottawa, Ontario, Canada: National Research Council of Canada Research Press.
- RINALDI, M. & DARBY, S. E. 2007. Modelling river-bank-erosion processes and mass failure mechanisms: Progress towards fully coupled simulations. In: HELMUT HABERSACK, H. P. & MASSIMO, R. (eds.) *Developments in Earth Surface Processes*. Elsevier.
- ROOD, S. B., BIGELOW, S. G. & HALL, A. A. 2011. Root architecture of riparian trees: river cut-banks provide natural hydraulic excavation, revealing that cottonwoods are facultative phreatophytes. *Trees-Structure and Function*, 25, 907-917.
- ROOD, S. B., KALISCHUK, A. R., POLZIN, M. L. & BRAATNE, J. H. 2003. Branch propagation, not cladogenesis, permits dispersive, clonal reproduction of riparian cottonwoods. *Forest Ecology and Management*, 186, 227-242.
- SCHENK, H. J. & JACKSON, R. B. 2002. The global biogeography of roots. *Ecological Monographs*, 72, 311-328.
- SIMON, A. & COLLISON, A. J. C. 2002. Quantifying the mechanical and hydrologic effects of riparian vegetation on streambank stability. *Earth Surface Processes and Landforms*, 27, 527-546.
- SIMON, A., POLLEN, N. & LANGENDOEN, E. 2006. Influence of two woody riparian species on critical conditions for streambank stability: Upper Truckee River, California. *Journal of the American Water Resources Association*, 42, 99-113.
- TIBBETT, M. 2000. Roots, foraging and the exploitation of soil nutrient patches: The role of mycorrhizal symbiosis. *Functional Ecology*, 14, 397-399.
- TOCKNER, K., WARD, J. V., ARSCOTT, D. B., EDWARDS, P. J., KOLLMANN, J., GURNELL, A. M., PETTS, G. E. & MAIOLINI, B. 2003. The Tagliamento River: a model ecosystem of European importance. *Aquatic Sciences*, 65, 239-253.
- WELBER, M., BERTOLDI, W. & TUBINO, M. 2012. The response of braided planform configuration to flow variations, bed reworking and vegetation: The case of the Tagliamento River, Italy. *Earth Surface Processes and Landforms*, 37, 572-582.

Chapter 5

ASSOCIATIONS OF ROOT PROPERTIES WITH THE LOCAL ROOTING ENVIRONMENT

5.1 INTRODUCTION

The previous chapter investigated the hypothesis that riparian root distribution is influenced primarily by the large scale factors of inherited species traits and limiting hydrological conditions and how they vary within a river corridor. Significant relationships between root distributions and both depth and site moisture were identified. However, there was a considerable degree of variability in the data that was not explained by these relationships, and ‘hotspots’ of variability in root density were observed at particular depths within root profiles. These observations suggest that the variability in sediment characteristics, which are expressed in distinct layering within each profile may be another major factor influencing the local vertical distribution of rooting patterns. In this chapter, the influence of the local rooting environment, with particular focus on sediment calibre, is investigated.

Past and continuing urban and agricultural development on floodplains puts riparian zones under pressure, and the stabilisation of river banks in order to prevent erosion and fix the course of rivers has long been standard practice. Given the inherent unpredictability of river flows, bank engineering works typically incorporate an extremely generous factor of safety, often with the result that almost all the natural ecological functioning of these valuable land-water ecotones is lost behind durable, impermeable concrete or steel. As the benefits of ‘more natural’ river banks are increasingly appreciated, however, there is growing momentum behind approaches which incorporate vegetation (both live and dead) in ‘soft’ or bioengineering solutions. Furthermore, there are increasing efforts by responsible authorities to reduce the overall number of interventions, by better assessing the risks of bank failure.

The mechanical and hydraulic reinforcement of river banks by the roots of riparian vegetation is generally widely accepted at this point in time, and increasingly sophisticated models are being developed to represent the processes involved (Pollen-Bankhead et al., 2013). However, a fundamental barrier to the successful application of these models in the design of ‘soft’ bank revetments or the assessment of bank stability, is our limited ability to characterise the location and types of roots in a sufficiently realistic way (Pollen, 2007,

Docker and Hubble, 2008). Field sampling to gather this information is labour-intensive and so the few bank stability models which do incorporate roots tend to apply simple depth decline models such as those investigated in the previous chapter and selected to represent particular species or vegetation cover types (Rinaldi and Darby, 2007, Van de Wiel and Darby, 2007). As was demonstrated, these depth curves capture a rather limited degree of variability in root distributions and take little account of variations in environmental conditions within or between sites. The findings of Chapter 4 shed light on some differences in root profiles between and within sites and the important influence of broad hydrological conditions, but it would also be highly beneficial to better understand the more detailed environmental influences on root variability. Such information would not just inform the disciplines of civil engineering, but would make significant contributions to understanding the ecology and geomorphology of riparian zones, and potentially to management applications such as the design of riparian buffer strips.

Two potentially important influences on rooting characteristics at the local scale are the physical properties of the soil and the proximity and characteristics of the nearby trees. Abernethy and Rutherford (2001) showed that the depth distribution of root area ratio only reached a reasonably smooth vertically declining curve at distances of several metres from the trees they investigated, with differences in this distance dependent on species. For riparian black poplar – an early successional tree typically with access to plenty of light – root growth is likely to be limited by hydraulic (Karrenberg et al. (2003), Willms et al. (2006), Gurnell (2015 (in press)) and nutrient (Pregitzer and Friend, 1996) resources in the soil, and thus linked to root investment.

In natural, dynamic riparian zones, the vertical sediment profile is typically a complex inter-bedded mix of sediment types as a result of infill after the migration of active channels, the deposition of fines in slack-water areas and on the floodplain, and large-scale movement of coarser-grained material, for example as migrating bars (Huggenberger et al., 1998). The pattern of sediment types varies greatly in the horizontal plane as well as with depth, reflecting the complex patterns of sediment erosion and deposition that construct fluvial corridors. This three-dimensional patchwork of sediment is not only characterised by strong contrasts in sediment calibre but also in the chemical, biological and hydrological rooting environment available for riparian vegetation (Kyle and Leishman, 2009). For example, a backwater may accumulate thick deposits of fine silts and clays, as well as organic detritus, which, when buried by later deposits and subsumed into the soil profile, are likely to become nutrient- and moisture-rich yet oxygen-poor layers, which may even act to confine shallow groundwater. Conversely, the burial of a bar edge or riffle may result in a pebbly substrate

with large pore spaces and little fine material, very little nutrient availability but extremely high water transmissivity and oxygen availability. Both sediment types are visible within a few centimetres of each other in Figure 5.1.



Figure 5.1 An example of the diverse, layered and patchy sediment types found in riparian soil profiles on the river Tagliamento. Tape measure at left is extended to 1 m.

There is an extensive literature in plant science linking rooting and root properties to various soil properties, but in field studies it is often impossible to disentangle the relative influences of individual variables, owing to complementary, confounding and interacting effects. Nonetheless, there does appear to be a hierarchy of factors such that relationships with the most dominant drivers can sometimes be detected. In spite of the fact that the extreme heterogeneity of soil types would appear to make riparian zones an ideal system for exploring empirical root-soil relationships, and the important issue of the mediation of bank stability by vegetation, there are few studies of such natural systems.

The present study aims to identify relationships between a suite of tree, sediment and root variables for riparian root profiles in an active river corridor. It is not the intention to develop a predictive model of root distributions based on sediment and vegetation data – such an endeavour would require an extremely comprehensive sampling regime in terms of the range of variables, river styles, vegetation types, etc. to be successful, and of course feedbacks from roots to influence vegetation and sediment properties (rhizosphere development) cannot be ignored. The objective is instead to use data from a naturally functioning system (part of the middle reaches of the River Tagliamento in northeast Italy) to identify the relative strength of associations between root properties and a number of key tree and sediment variables,

which could later inform the development of such predictive tools. Piercy and Wynn (2008) developed regression models of root length density and volume ratio in stream bank faces in Virginia, USA, finding soil bulk density and tree density to be significant determining factors, but predictive power to be low except for the very finest roots. Working in a much more rapidly changing environment, the present study encompasses a substantially wider range of physical sediment properties (notably the inclusion of gravel-dominated substrates) and so avoids the complicating factor of sampling on the bank face itself, and investigates differences in the frequency distributions of root properties and types with greater depth resolution.

5.1.1 Research questions

Specific questions addressed in this chapter are as follows:

- i. What, if any, are the significant relationships between the proliferation and size distribution properties of roots in a bank profile and properties of nearby large trees?
- ii. What, if any, are the significant relationships between the proliferation and size distribution properties of roots and the organic content and grain size distribution properties of the sedimentary strata in which they are found?
- iii. What are the main dimensions of variability in the size distribution properties of roots in riparian sediment profiles?
- iv. What are the main dimensions of variability in the sediment properties of riparian bank profiles, and can they be summarised in a simplified classification?
- v. What are the relationships, if any, between broad sediment types (or classes) and measured root proliferation and size distribution properties, as well as higher order descriptors of the variability in rooting patterns?

5.2 METHODS

5.2.1 Field campaign

Field data collection and sampling were carried out on the River Tagliamento in July and August 2013, as detailed in Chapter 3. In summary:

- Duplicate bank profiles of 0.2 m width were excavated at 9 sites of varying regional environmental water availability and with *P. nigra* as the dominant bank-top vegetation, in the pre-Alpine to piedmont reaches of the river.
- On each profile, the diameters of all roots greater than 0.1 mm were measured and mapped within 0.1 m depth intervals.
- Sediment samples were taken from the mid-point of every distinct sediment layer that was identified in the field.
- The diameter, height and location of the largest poplar trees within 10 m of each of the profiles were also measured.

5.2.2 Data analysis

The collected root diameter data were used to calculate root density (number of roots per unit area of bank face) and root area ratio (RAR, the total sectional area of roots per unit area of bank face), as well as a number of other variables describing the root diameter and area distributions within each 0.1 m depth interval. A complete list of root variables can be found in Table 5.15. Furthermore, as they perform quite different physiological functions, some variables were recorded or calculated separately for coarse and fine roots.

Fine roots were defined as those with diameter less than or equal to 0.5 mm. Though the shortcomings of this simplistic dichotomous physiological categorisation, assumed from a relatively arbitrary morphological threshold, are increasingly recognised (see, e.g., McCormack et al., 2015), no alternative approach was possible with the root profile exposures used in the present study, in the absence of much more detailed data on root topology and anatomy. The threshold approach has, however, been the traditional standard, and so there is plenty of compatible supporting literature (see, e.g., Table 5.1 for a sample of values used in studies of poplar). The 0.5 mm value is low in comparison to the more common 2 mm, which maximises the probability that those roots categorised as ‘fine’ here were indeed absorptive in function, as opposed to being involved in transport or mechanical support. Moreover, the ‘fine root’ category here is directly comparable with the class of roots showing the strongest associations identified by Piercy and Wynn (2008).

Sediment samples were analysed for mineral particle size distribution, organic matter content and gravimetric field moisture content, using methods detailed in Section 3.4.2. Particle size data were analysed using GRADISTAT (Blott and Pye, 2001). Seven key sediment variables output from GRADISTAT were selected for further analysis, while output variables whose values were not well distributed among the samples, or which showed very high correlations with the selected variables, were omitted. The seven selected grain size variables (proportional content of gravel, sand and silt & clay, mean, median (d50), d90 and Sorting (according to methods of Folk and Ward, 1957) were combined with organic matter content to provide the eight sediment variables incorporated in the analyses described below. It is assumed here that the seven sediment physical properties representative of the grain size distribution are the fundamental drivers in the development of the diverse soil types found in riparian zones. Organic matter is also considered in recognition of the significant flood-related accumulations of buried organic material frequently encountered in the Tagliamento system, and the importance of this material for soil biological activity and water retention characteristics. Moisture content in the field at the time of sampling was considered separately (as it is only a transient property of the sediment), alongside the sampling depth.

Table 5.1 Some examples of threshold values used to define ‘fine roots’ in published studies of poplar. After Block et al., 2006.

Location and forest type	Target species	Threshold (mm)	Reference
Washington, plantation	(hybrid)	0.5	Heilman et al. (1994)
Wisconsin, plantation	(hybrid)	0.5	Coleman et al. (2000)
UK, greenhouse	<i>P. Canadensis</i>	2.0	Black et al. (1998)
Wisconsin, plantation	<i>P. tremuloides</i>	2.0	Coleman et al. (1996)
Northwest USA, Plantation	(hybrid)	2.0	Friend et al. (1991)
Michigan, plantation	<i>P. Canadensis</i>	2.0	Kosola et al. (2001)
Alaska, boreal forest	<i>P. balsamifera</i>	2.0	Ruess et al. (1996)
Iowa, riparian buffer	<i>P. euroamericana</i>	2.0	Tufekcioglu et al. (1998)
Wisconsin, southern boreal forest	<i>P. tremuloides</i>	3.0	Ruark and Bockheim (1987)
Saskatchewan, plantation	(hybrid)	2.0, 5.0	Block (2004)
Saskatchewan, boreal forest	<i>P. tremuloides</i>	5.0	Steele et al. (1997)
Manitoba, boreal forest	<i>P. tremuloides</i>	5.0	Steele et al. (1997)
Southern Quebec, boreal forest	<i>P. tremuloides</i>	10.0	Finer et al. (1997)

For tree variables, both average values for all trees sampled at an excavation site, and those of the nearest tree to the profile, were assigned to root samples.

The approach to investigating relationships between rooting patterns and local factors adopted here comprised three main stages:

- a. Matching sediment data to root data.
- b. Identifying correlations between measured variables. Associations with local above-ground tree characteristics were also investigated at this stage alongside sediment characteristics.
- c. Multivariate analysis of the datasets using both Principal Components Analysis (PCA) and Agglomerative Hierarchical Clustering (AHC). Associations were then investigated between individual variables, emergent component loadings and scores from PCAs and the main clusters extracted using AHC.

Directionality is assumed in this approach such that root variables are always considered dependent on sediment or tree factors, although there is likely to be some feedback with respect to organic matter content and certainly many of the tree variables. Statistical analyses were conducted using XLSTAT Pro 2015.

a Matching sediment samples to root samples

Whereas root profiles were sampled evenly within 0.1 m depth intervals, sediments were recorded and collected according to their natural stratigraphic distribution. It was necessary therefore to develop a method for matching the 366 root and 186 sediment samples. A simple association of the nearest stratum mid-point to the root interval midpoint was rejected as strata were frequently several times narrower than the 0.1 m root intervals. Instead, a weighted average approach was adopted.

Where sampled sedimentary strata completely overlapped a root sampling interval, sediment data were assigned without modification. Where multiple strata overlapped a root interval, average data for all strata were assigned, weighted according to their proportion of overlap across the 0.1 m depth increment within which the roots were sampled. Where one or more of the overlapping strata was not sampled, the weights of the other strata were equally increased to make up to a total of 100 %.

All subsequent analyses were performed on a dataset based on the 0.1 m depth increments of the 366 root samples, with associated weighted average sediment data. For 16 of these root intervals, no overlapping sediments were sampled, reducing the size of the final dataset to 350. Summary statistics for both the raw and the weighted average sediment datasets are presented in Section 5.3.1.

b Correlations between measured variables

Spearman rank correlation coefficients were calculated for all combinations of sediment and root variables as well as tree and root variables. This non-parametric measure was used as none of the variables were normally distributed (Anderson-Darling and Shapiro-Wilk tests at $\alpha = 0.01$), and most could not be transformed to approximate normality using a simple and interpretable transformation. Scatter plots of all combinations of variables were visually inspected for potentially significant non-linear relationships.

As tree data were found not to be particularly strongly associated with rooting patterns in these correlation analyses, and because of the significantly smaller sample size, they were excluded from subsequent analyses.

c Multivariate analyses

Multivariate analyses were selected to tackle the high variability in the data and substantial inter-correlations among variables, and thus to identify any higher order structure in the root and sediment datasets. PCAs were separately performed on Spearman rank correlation matrices of sets of root and sediment variables. Spearman rank correlations were used because the variables were far from normally distributed. In relation to root data, PCAs were separately conducted on parameters of root area and root diameter distributions and then the PCA on the root diameter distribution parameters was extended to include root density and root area ratio, given the importance of root sectional area and these aggregate measures (density and RAR), for existing models of bank stability.

In order to develop a more intuitive classification of the sediments sampled, AHC (Ward's method, based on Euclidean distance) was conducted on eight core sediment variables. Whether the emergent sediment clusters differed significantly with respect to the root and supplementary abiotic variables (field moisture and depth), as well as the root PCA dimensions, was investigated using Kruskal-Wallis tests. Significant differences among clusters were identified using the Steel-Dwass-Critchlow-Fligner procedure.

One outlier sediment sample 'S077' was removed from analyses owing to its extremely high organic matter content (22.4 %), which was more than ten standard deviations from the mean for this variable (see Table 5.6).

5.3 RESULTS

5.3.1 Correlations between measured variables

a Tree variables

Descriptive statistics for the root data are presented in Table 4.1, in the previous chapter. Statistics for the measured tree variables are presented in Table 5.2, and then as apportioned to the root sampling intervals, in Table 5.3. All correlations between root and tree properties can be found in Appendix B, whereas the strongest and most informative correlations are discussed below.

The strongest tree correlate of root density was the average vertical growth rate (annual increase in stem length) of the nearest (within 10 m) recorded poplar trees. The strongest correlation with the root area ratio of the root sampling intervals was an inverse relationship with the absolute distance to the base (at ground level) of the nearest large poplar stem. However, though statistically significant, Table 5.4 and Figure 5.2 reveal that the variance explained by these factors is very small. When considering fine and coarse roots separately, both fine root density and area behaved similarly to overall root density, being most strongly related to the average vertical growth rate. Coarse root density and area were both comparable with the overall root area ratio in being most strongly correlated with the proximity of the nearest poplar stem. Table 5.4 and Figure 5.3 show the relationships to be slightly stronger for fine roots than the bulk root data, and the weakest relationships were with coarse roots.

Table 5.2 Descriptive statistics for tree variables.

Statistic	Age (years)	Diameter at Breast Height (mm)	Stem Length (m)	Mean Radial Growth Rate (mm a ⁻¹)	Mean Vertical Growth Rate (m a ⁻¹)
Count	46	46	46	46	46
Maximum	27	488	27.5	12.2	2.0
Mean	14.7	177	14.9	6.0	1.1
Standard error of mean	0.548	14.5	0.721	0.361	0.051
Standard deviation	3.68	97.1	4.84	2.42	0.343
Median	15.0	165	15.0	5.86	0.971
Variance	13.5	9430	23.4	5.88	0.118
Coefficient of variation	0.251	0.550	0.324	0.407	0.328
Skewness	0.386	1.62	0.390	0.509	0.987
Kurtosis	1.39	3.06	-0.170	-0.204	0.553

Table 5.3 Descriptive statistics for tree variables as distributed among the 366 root sampling intervals.

Statistic	Age of Nearest Tree (years)	Stem Length of Nearest Tree (m)	Mean Radial Growth Rate of Nearest Tree (mm a ⁻¹)	Mean Vert. Growth Rate of Nearest Tree (m a ⁻¹)	Horizontal Distance to Nearest Tree (m)	Absolute Distance to Nearest Tree (m)	Mean Age of Nearest Trees (years)	Mean Stem Length of Nearest Trees (m)	Mean Radial Growth Rate of Nearest Trees (mm a ⁻¹)	Mean Vert. Growth Rate of Nearest Trees (m a ⁻¹)
Count	366	366	366	366	366	366	366	366	366	366
Maximum	19.0	21.5	8.73	1.43	4.74	4.84	20.7	24.7	9.33	1.30
Mean	14.1	13.9	5.60	0.979	1.78	2.13	15.2	14.6	5.89	0.973
Std. error of mean	0.166	0.248	0.100	0.014	0.054	0.047	0.170	0.207	0.094	0.010
Standard deviation	3.17	4.74	1.92	0.259	1.02	0.907	3.26	3.96	1.80	0.182
Median	15.0	15.0	6.00	0.938	1.73	2.06	16.3	14.0	6.31	0.988
Variance	10.1	22.5	3.67	0.067	1.05	0.822	10.6	15.7	3.25	0.033
Coefficient of variation	0.225	0.341	0.342	0.264	0.574	0.426	0.214	0.271	0.306	0.187
Skewness	-0.443	-0.153	-0.282	0.248	0.643	0.568	-0.390	0.844	-0.036	0.209
Kurtosis	-0.701	-1.02	-1.30	-0.909	0.627	0.685	-0.427	0.183	-0.717	-1.03

Table 5.4 Strongest correlations between root density and area and tree variables.

** $p < 0.0001$, * $p < 0.01$ R²: Spearman coefficient of determination expressed as percentage of variance explained; GR: growth rate.

Tree variable	Spearman's ρ	R ²	Tree variable	Spearman's ρ	R ²
<i>Root Density</i>			<i>Root Area Ratio</i>		
Mean vertical GR	0.298 **	8.9 %	Distance to nearest	-0.236 **	5.6 %
Distance to nearest	-0.215 **	4.6 %	Mean vertical GR	0.225 **	5.1 %
<i>Fine Root Density</i>			<i>Fine Root Area Ratio</i>		
Mean vertical GR	0.299 **	8.9 %	Mean vertical GR	0.317 **	10.1 %
<i>Coarse Root Density</i>			<i>Coarse Root Area Ratio</i>		
Distance to nearest	-0.248 **	6.2 %	Distance to nearest	-0.187 *	3.5 %

The strongest tree-root relationships were those between the fraction of the very finest roots (the first quartile of the fine root diameter distribution) and tree growth rates at a site (Table 5.5).

Table 5.5 Other informative significant correlations between tree and root variables.

** $p < 0.0001$ ** R²: Spearman coefficient of determination expressed as percentage of variance explained.

Root variable	Tree variable	Spearman's ρ	R ²
1 st Quartile of Fine Root Diameter Distribution	Vertical Growth Rate of Nearest Tree	0.355 **	12.6 %
1 st Quartile of Fine Root Diameter Distribution	Mean Radial Growth Rate of Nearest Trees	0.352 **	12.4 %

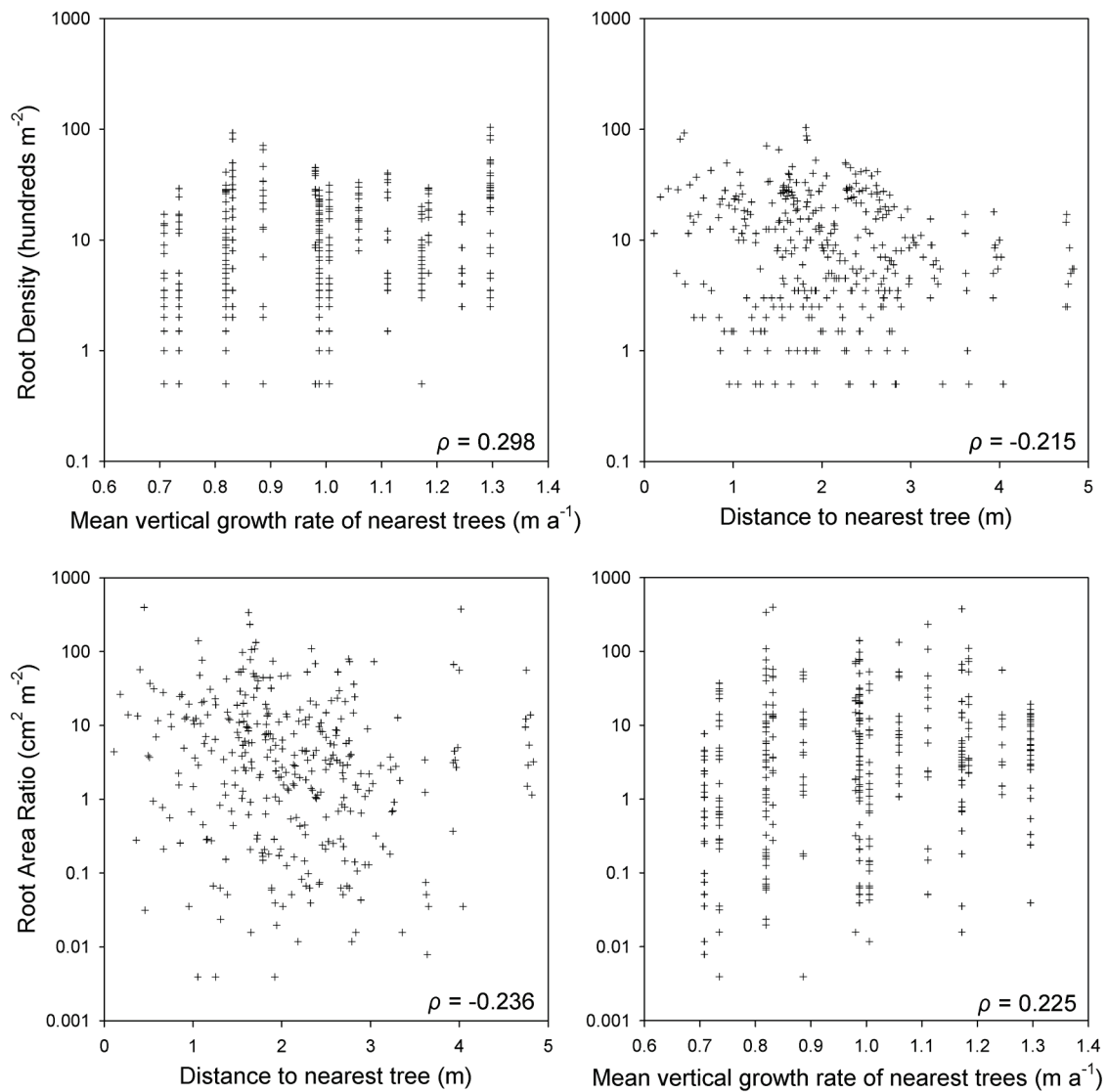


Figure 5.2 Scatter plots illustrating the strongest relationships between tree variables and root density (top) and root area ratio (bottom, both plotted on logarithmic axes). Spearman's correlation coefficient (ρ) is displayed for each relationship.

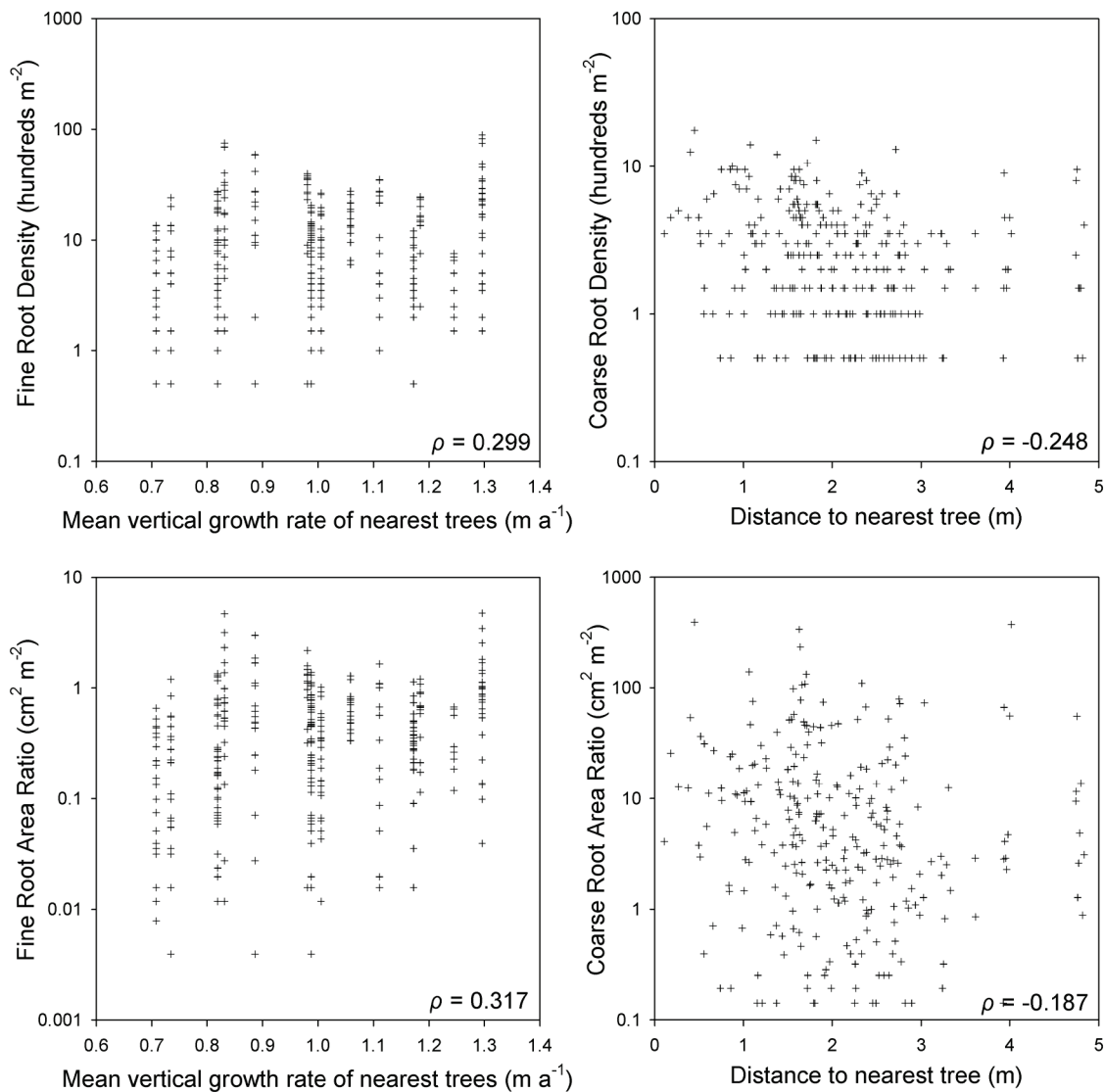


Figure 5.3 Scatter plots of the strongest relationships between tree variables and fine and coarse root density (top, left and right, respectively) and fine and coarse root area ratio (bottom, left and right, respectively). Root variables are plotted on logarithmic axes. Spearman's correlation coefficient (ρ) is displayed for each relationship.

While many combinations of the analysed variables showed peak variability at intermediate or extreme values of tree variables, only one potential non-linear relationship was detected from visual inspection of all the scatter plots: the skewness of the diameter distributions versus the mean radial growth rate of poplars at the site (Figure 5.4). While still exhibiting a great deal of variability ($R^2 = 12.7\%$, Root mean squared error (RMSE) = 1.72), the fitted third order polynomial in Figure 5.4 illustrates an apparent peak positive skew at growth rate values of around 4.9 mm a^{-1} . Whether or not there is actually a trough around 8 mm a^{-1} is impossible to determine with any confidence.

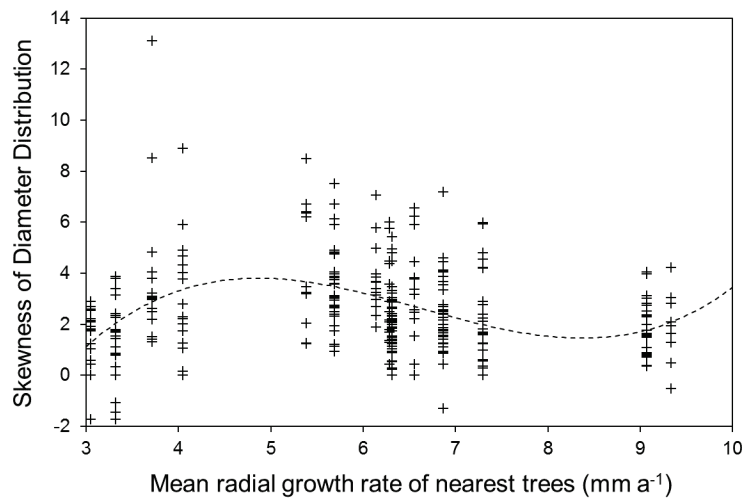


Figure 5.4 Potential non-linear relationship between the skewness of the root diameter distribution and the mean radial growth rate of poplars at the site. A fitted third order polynomial is plotted with a dashed line.

In summary, tree proximity, size, age and growth rates were not strongly related to root patterns, although many significant associations were detected.

b Sediment variables

Summary statistics for the eight selected sediment variables and field water content in the original sediment samples are presented in Table 5.6, and as weighted averages distributed among the 0.1 m root sampling intervals, in Table 5.7.

Table 5.6 Descriptive statistics for sediment samples (including sample S077, which was excluded from later analyses owing to extremely high organic content).

Statistic	% Gravel	% Sand	% Silt + Clay	% Organic Matter	Mean Particle Size (Φ)	d50 (Φ)	d90 (Φ)	Sorting (Φ)	% Water (in field)	Stratum Midpoint Depth (m)
Count	186	186	186	186	186	186	186	186	186	186
Maximum	96.7	90.3	86.4	22.4	6.30	5.80	10.1	3.25	36.0	3.60
Mean	26.1	40.8	33.1	1.68	2.64	2.10	5.63	1.61	7.10	1.51
Standard error of mean	2.75	1.82	1.85	0.146	0.170	0.185	0.220	0.054	0.623	0.064
Standard deviation	37.4	24.7	25.1	1.98	2.32	2.51	2.99	0.730	8.48	0.868
Median	0.00	37.6	30.5	1.50	3.57	3.13	6.67	1.84	3.10	1.63
Variance	1400	612	630	3.93	5.37	6.31	8.93	0.532	71.9	0.753
Coefficient of variation	1.43	0.606	0.757	1.18	0.878	1.20	0.531	0.452	1.19	0.574
Skewness	0.813	0.158	0.406	6.41	-0.508	-0.498	-0.842	-1.02	1.57	-0.026
Kurtosis	-1.26	-1.29	-1.07	63.6	-1.30	-1.43	-0.204	0.489	1.25	-0.831

Table 5.7 Descriptive statistics for weighted average sediment data as distributed among the 350 coincident root sampling intervals.

Statistic	% Gravel	% Sand	% Silt + Clay	% Organic Matter	Mean Particle Size (Φ)	d50 (Φ)	d90 (Φ)	Sorting (Φ)	% Water (in field)	Root Interval Midpoint Depth (m)
Count	350	350	350	350	350	350	350	350	350	350
Maximum	96.7	87.8	86.4	4.93	6.30	5.80	10.1	2.52	30.7	2.37
Mean	27.2	43.6	29.2	1.48	2.46	1.93	5.40	1.56	5.65	0.903
Standard error of mean	36.4	24.4	21.3	1.09	2.11	2.29	2.67	0.641	6.95	0.569
Standard deviation	36.4	24.4	21.3	1.09	2.11	2.29	2.67	0.641	6.95	0.569
Median	0.00	48.5	28.9	1.52	3.22	2.88	6.43	1.76	2.64	0.850
Variance	1322	596	453	1.18	4.47	5.24	7.14	0.411	48.3	0.324
Coefficient of variation	1.34	0.560	0.728	0.733	0.861	1.19	0.495	0.411	1.23	0.630
Skewness	0.746	-0.108	0.516	0.593	-0.472	-0.478	-0.917	-1.17	1.94	0.356
Kurtosis	-1.28	-1.29	-0.583	0.031	-1.29	-1.41	0.178	0.835	2.95	-0.758

All correlations between root properties and the eight sediment properties can be found in Appendix B, whereas the strongest and most informative correlations are discussed below. Overall, correlations between root density and area and sediment variables were much stronger than for tree variables (Figure 5.5 and Figure 5.6). For the bulk root dataset, sediment variables were more strongly correlated with root density than root area ratio (Table 5.8). Root density increased with smaller grain sizes, represented by high values in phi units of d90, d50 and the mean particle size. There were similar relationships with general grain size statistics for root area ratio, however, the degree of sorting was most strongly correlated with this variable, with greater root area associated with more poorly sorted sediments. As with the tree data, the fine root area ratio again exhibited stronger correlations than the coarse root area ratio, this time with finer grained sediments, and particularly with the d90 value (Table 5.8, Figure 5.7). Fine root density also showed similar associations with sediment properties to fine root area, but median particle sizes became more important. Coarse root

associations with sediment properties were weaker than those for fine roots but were broadly similar to those for the bulk root data. High coarse root density was most strongly associated with finer sediments (i.e. high values of d90 and mean grain size in phi units), while sediment sorting appeared as another significant correlate of coarse root area ratio.

Table 5.8 Correlations between the eight sediment variables and root area ratio and root density; and between the four strongest sediment correlates and fine and coarse root density and area. R² is the Spearman coefficient of determination expressed as percent variance explained.

** p < 0.0001 * p < 0.05

Sediment variable	Spearman's ρ	R ²	Sediment variable	Spearman's ρ	R ²
<i>vs Root Density</i>			<i>vs Root Area Ratio</i>		
d90 ϕ	0.559 **	31.3 %	Sorting ϕ	0.501 **	25.1 %
% Silt + Clay	0.555 **	30.8 %	d90 ϕ	0.500 **	25.0 %
d50 ϕ	0.550 **	30.2 %	Mean particle size ϕ	0.482 **	23.2 %
Mean particle size ϕ	0.543 **	29.5 %	% Silt + Clay	0.478 **	22.9 %
% Organic Matter	0.497 **	24.7 %	d50 ϕ	0.467 **	21.8 %
Sorting ϕ	0.484 **	23.4 %	% Organic Matter	0.434 **	18.8 %
% Gravel	-0.418 **	17.5 %	% Gravel	-0.424 **	17.9 %
% Sand	0.105 *	1.1 %	% Sand	0.245 **	6.0%
<i>vs Fine Root Density</i>			<i>vs Fine Root Area Ratio</i>		
% Silt + Clay	0.531 **	28.2 %	d90 ϕ	0.579 **	33.5 %
d50 ϕ	0.529 **	28.0 %	% Silt + Clay	0.577 **	33.3 %
Mean particle size ϕ	0.520 **	27.0 %	Mean particle size ϕ	0.577 **	33.3 %
d90 ϕ	0.516 **	26.6 %	d50 ϕ	0.576 **	33.2 %
<i>vs Coarse Root Density</i>			<i>vs Coarse Root Area Ratio</i>		
d90 ϕ	0.441 **	19.5 %	d90 ϕ	0.304 **	9.3 %
Mean particle size ϕ	0.412 **	17.0 %	Sorting ϕ	0.297 **	8.8 %
% Silt + Clay	0.398 **	15.8 %	Mean particle size ϕ	0.290 **	8.4 %
d50 ϕ	0.397 **	15.8 %	% Silt + Clay	0.276 **	7.6 %

Outside the eight main sediment variables, clay content also showed strong associations with both root density and area, and particularly fine root area and density (Table 5.9). Besides the aggregate root variables of density and RAR, the maximum root diameter in each sampling interval was reasonably strongly associated with the degree of sorting and the d90 of the grain size distribution. Note the similar dominance of these relationships to those of the bulk and coarse root area data.

Table 5.9 Other informative significant correlations between root and sediment variables.

R² is the Spearman coefficient of determination expressed as percent variance explained.

** p < 0.0001

Root variable	Sediment variable	Spearman's ρ	R ²
Fine Root Area Ratio	% Clay	0.574 **	32.9 %
Density	% Clay	0.552 **	30.4 %
Fine Root Density	% Clay	0.521 **	27.2 %
Root Area Ratio	% Clay	0.482 **	23.2 %
Maximum diameter	Sorting _φ	0.424 **	18.0 %
Maximum diameter	d90 _φ	0.419 **	17.6 %

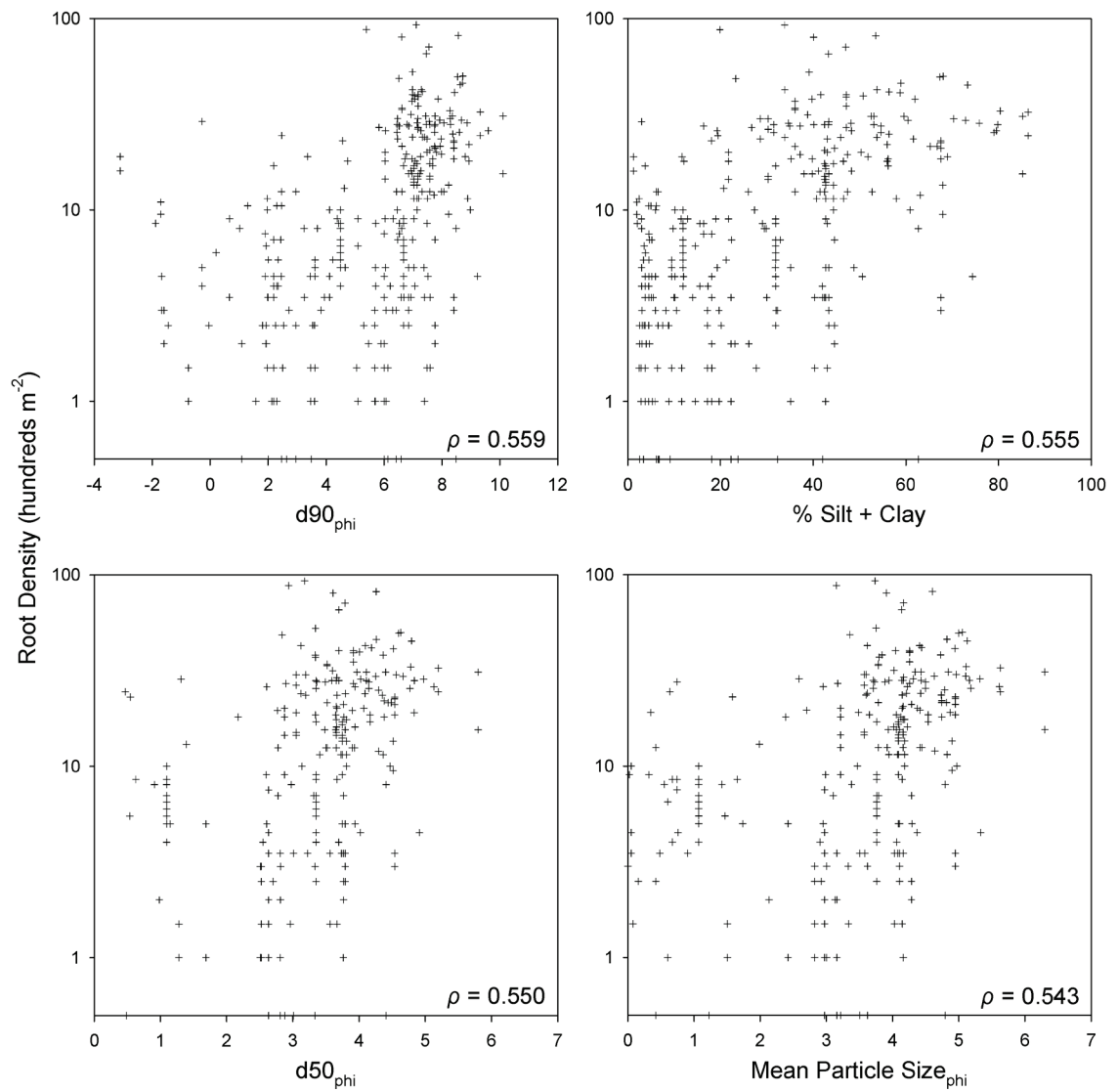


Figure 5.5 Scatter plots of the four strongest sediment correlates of root density (plotted on a logarithmic axis). Spearman's correlation coefficient (ρ) is displayed for each relationship.

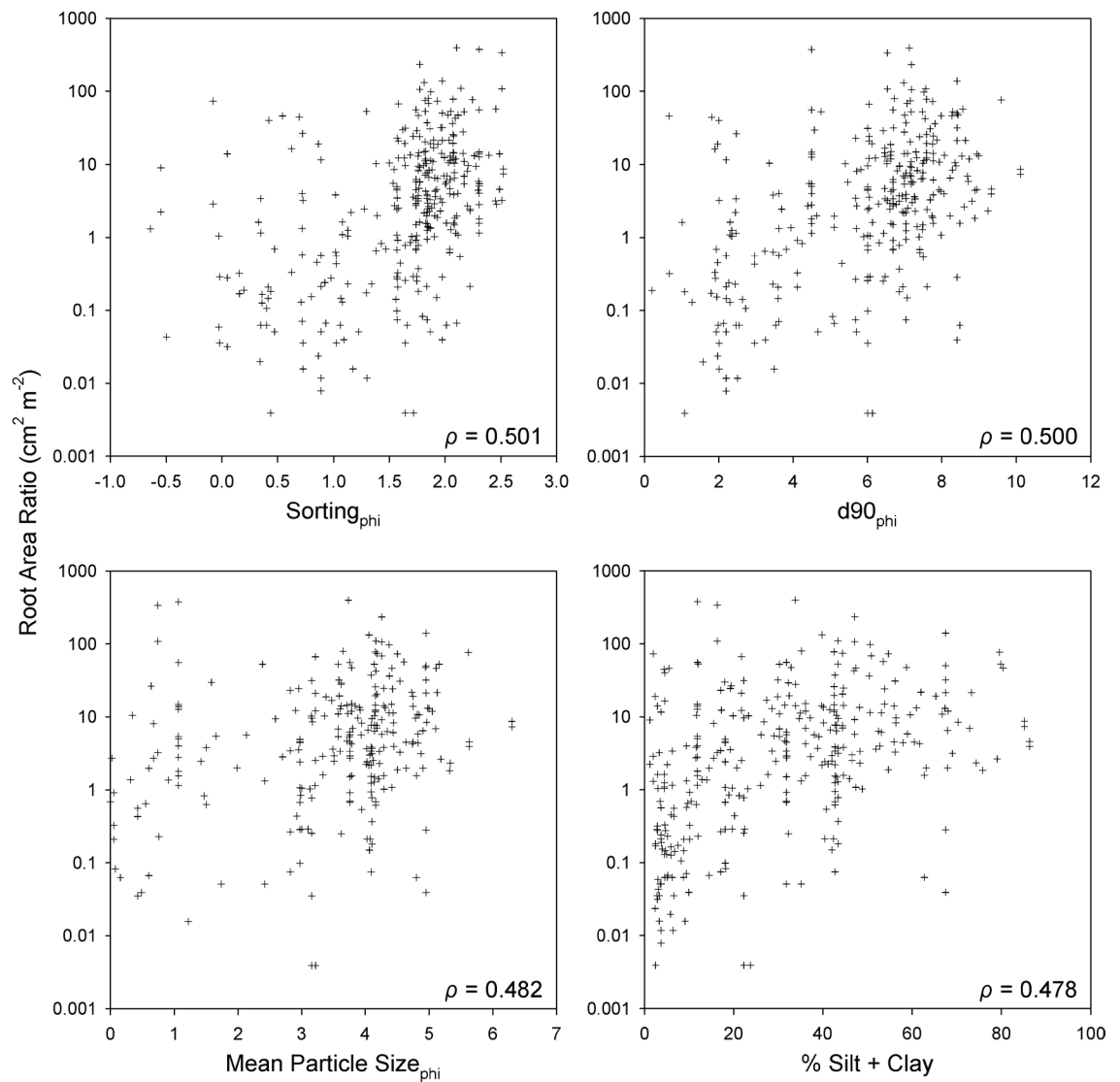


Figure 5.6 Scatter plots of the four strongest sediment correlates of root area ratio (plotted on a logarithmic axis). Spearman's correlation coefficient (ρ) is displayed for each relationship.

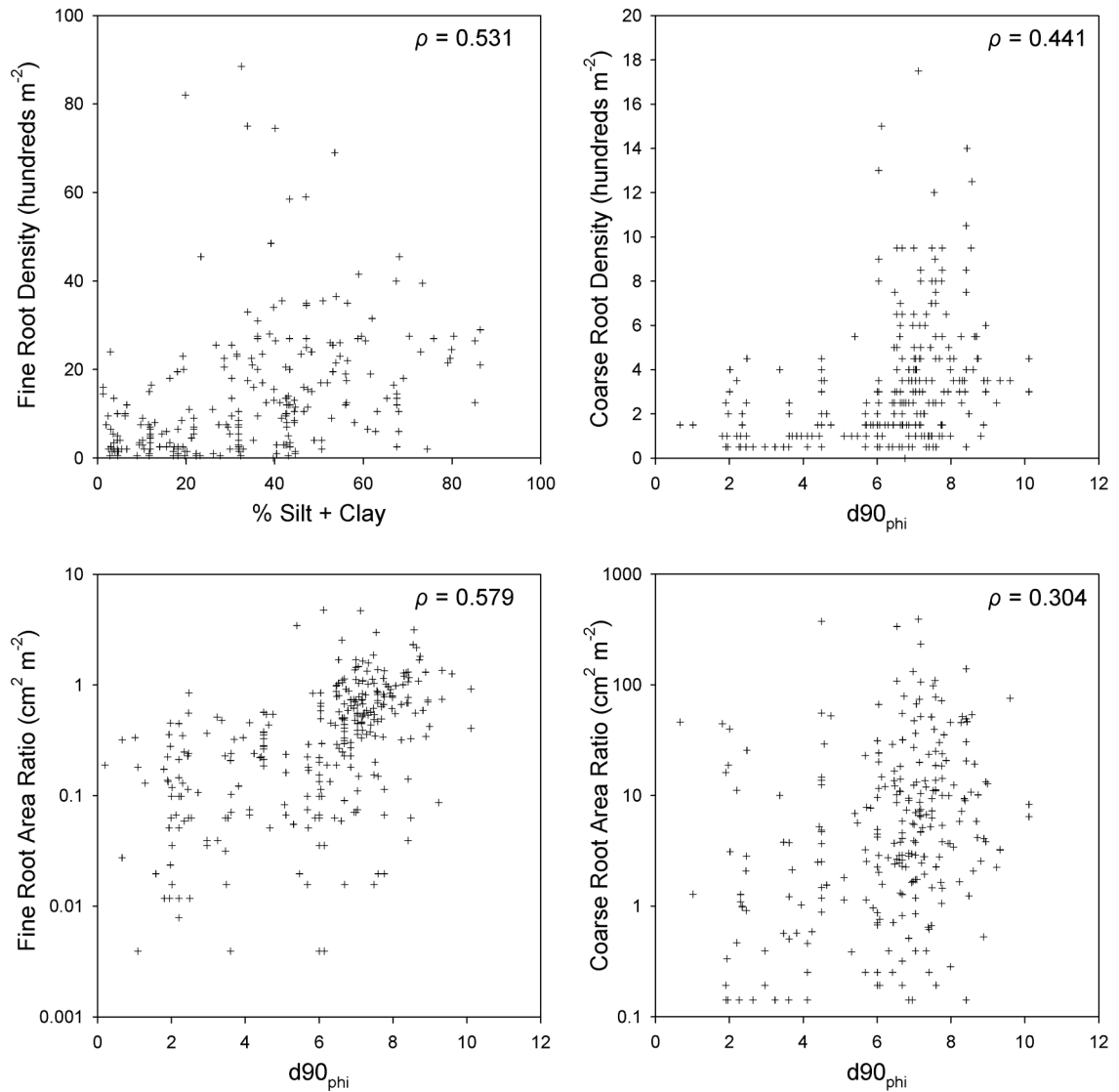


Figure 5.7 Scatter plots of the strongest relationships between sediment variables and fine and coarse root density (top, left and right, respectively) and fine and coarse root area ratio (bottom, left and right, respectively). Root variables are plotted on logarithmic axes. Spearman's correlation coefficient (ρ) is displayed for each relationship.

Visual inspection of the root-sediment scatter plots also identified potential non-linear relationships with skewness of the root diameter and area distributions, in this case, when these variables were plotted against percent sand content (Figure 5.8). Maximum positive skew appeared to be associated with approximately 50 % sand (for the diameter fit – $R^2 = 5.4$ %, RMSE = 1.81; for the area fit – $R^2 = 8.5$ %, RMSE = 2.21).

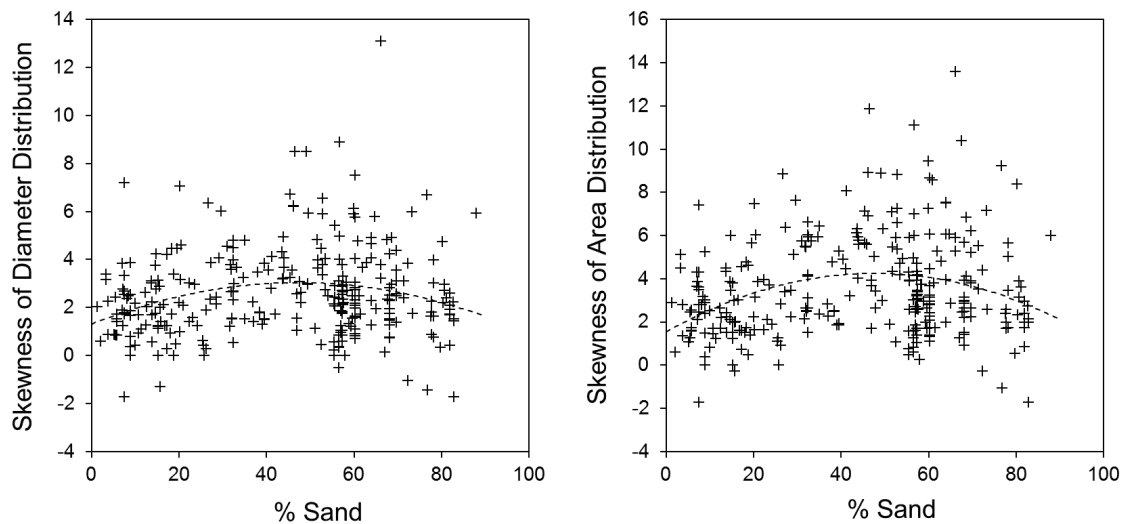


Figure 5.8 Potential non-linear relationship between sediment sand content and skewness of the root diameter and area distributions for root sampling intervals. Fitted second order polynomials are plotted with dashed lines.

5.3.2 Principal Components Analysis

a Root diameter and area

Root diameter distribution properties

Principal components analysis was applied to parameters of the bulk root diameter distributions (Table 5.10). The analysis identified two components with eigenvalues greater than 1, which accounted for approximately 89 % of the variability in the dataset. These components were subjected to a Varimax rotation in order to maximise the loadings of the original variables. Following the rotation, high loadings of variables summarising increasing spread (coefficient of variation, maximum diameter), peakedness (kurtosis) and length of high diameter tail (skewness) of the root diameter frequency distribution, indicate that factor 1 broadly represents the shape of the frequency distribution of root diameter for each 0.1 m depth interval (see also the vector plot in Figure 5.9). The second factor, explaining almost as great a proportion of the variability in the data as Factor 1, shows high loadings for measures of central tendency of the root diameter distributions, describing a gradient of increasing mean, median and quartile values. In the scatter plot of the sample scores on these two factors (Figure 5.9), a strong cluster is centred on small negative values of both factors, from which there is a reasonable degree of dispersion of samples in the positive directions along both factor axes.

Table 5.10 Eigenvalues, percent variability explained and loadings of variables on the first three factors (after Varimax rotation of the first two Principal Components (PCs)) of a Principal Components Analysis of the root diameter distribution parameters.

** Loadings > 90%, * > 80 %

	Factor 1	Factor 2	PC 3
Eigenvalue (before rotation)	4.505	3.496	0.529
Variability (%. after rotation)	45.13	43.77	5.875
Cumulative variability (%)	45.13	88.90	94.77
<i>Loadings</i>			<i>(without rotation)</i>
1 st Quartile	-0.232	0.829 *	0.404
Median	-0.139	0.890 *	0.258
3 rd Quartile	-0.025	0.937 **	-0.172
Mean	0.341	0.918 **	-0.116
Standard Deviation	0.721	0.645	-0.204
Maximum	0.864 *	0.470	-0.046
Coefficient of Variation	0.958 **	0.067	-0.195
Skewness	0.928 **	-0.228	0.263
Kurtosis	0.909 **	-0.216	0.324

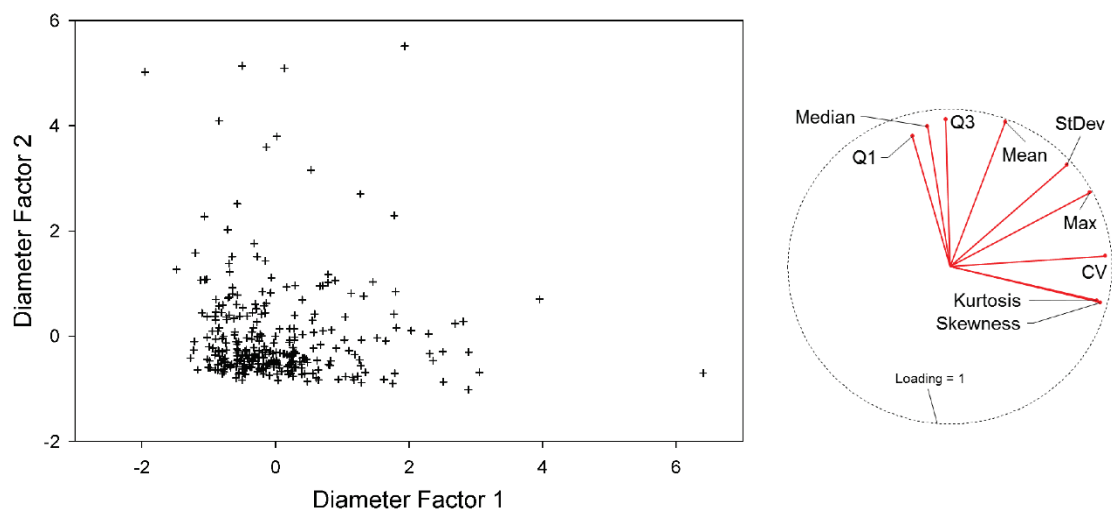


Figure 5.9 Scatter plot (left) of sample scores on the first and the second factors (after Varimax rotation of the first and second Principal Components) of an analysis root diameter distribution parameters, and the related plot of variable loadings on these factors (right). CV: Coefficient of Variation; Max: Maximum value; StDev: Standard Deviation.

Root diameter distribution properties, root density and root area ratio

In order to determine whether the aggregate measures of root density and root area ratio had associations with the root diameter distribution, these two variables were incorporated into the PCA. As can be seen in Table 5.11, this slightly altered the variability explained by each of the first two factors (following rotation), but total variability explained and the loadings of the root diameter distribution properties on the first two factors were broadly the same as in the previous analysis (Figure 5.10). Both root area ratio and root density showed reasonably strong loadings on the first factor, which remained indicative of root diameter distribution shape. This set of variables resulted in slightly tighter sample clustering around the same low negative scores on the two factors, but overall the plot of sample scores on the two factors (Figure 5.10) was very similar to the previous analysis, as were the outputs of PCAs applied to the properties of the root diameter distributions augmented by root density or root area ratio individually.

Table 5.11 Eigenvalues, percent variability explained and loadings of variables on the first three factors (after Varimax rotation of the first two Principal Components (PCs)) of a Principal Components Analysis of root diameter distribution parameters, root density and root area ratio. ** Loadings > 90%, * > 80 %

	Factor 1	Factor 2	PC 3
Eigenvalue (before rotation)	5.620	3.845	0.615
Variability (% , after rotation)	47.85	38.19	5.586
Cumulative variability (%)	47.85	86.04	91.63
<i>Loadings</i>			<i>(without rotation)</i>
Root Density	0.750	-0.258	0.465
Root Area Ratio	0.853 *	0.456	0.044
1 st Quartile	-0.229	0.826 *	0.297
Median	-0.113	0.879 *	0.330
3 rd Quartile	-0.015	0.934 **	-0.058
Mean	0.339	0.920 **	-0.113
Standard Deviation	0.708	0.649	-0.250
Maximum	0.872 *	0.467	-0.067
Coefficient of Variation	0.936 **	0.068	-0.277
Skewness	0.918 **	-0.238	0.107
Kurtosis	0.903 **	-0.228	0.169

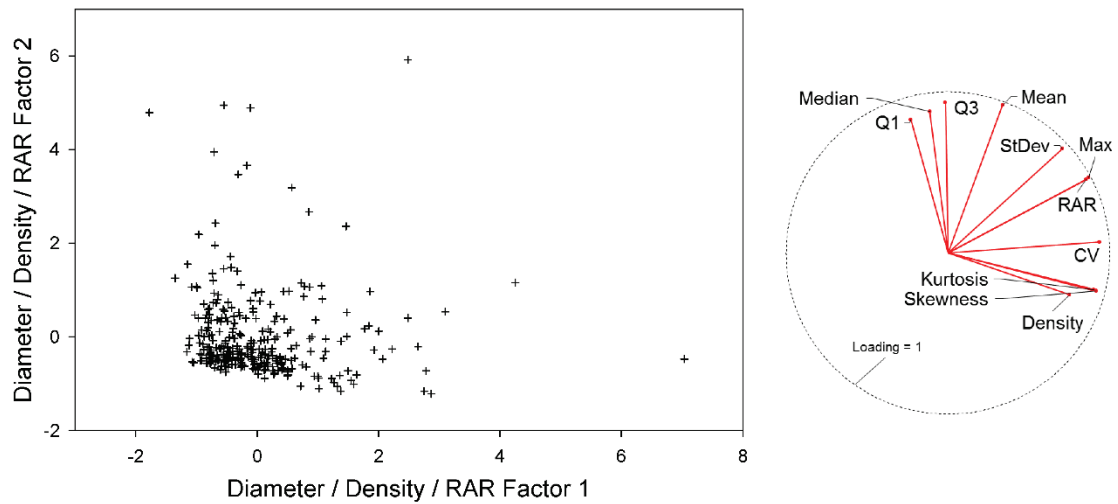


Figure 5.10 Scatter plot (left) of sample scores on the first and second factors (after Varimax rotation of the first and second Principal Components) of an analysis of root diameter distribution parameters, root area ratio and root density, and the related plot of variable loadings on these factors. CV: Coefficient of Variation; Max: Maximum value; RAR: Root Area Ratio; StDev: Standard Deviation.

Root area distributions

Though it is acknowledged that the root area distributions simply represent a square transform of those of root diameter, it was considered appropriate to investigate whether or not the parameters describing them possessed a significantly different structure, given the importance of root sectional area for sediment reinforcement models. However, application of the same analyses performed on the root density distribution parameters to those of the root area distributions (Table 5.12 and Figure 5.11) demonstrate that, with respect to the variable loadings, this was not the case. Similarly to the analysis of the root diameter parameter variables, only the first two components had eigenvalues greater than 1, these captured approximately 89 % of the variability in the dataset, and the loadings of the parameters on the first two factors were very similar to those of the root diameter analysis. The main differences to the root diameter analysis were that the mean had a smaller loading on Factor 1 and the samples clustered more closely on the second factor (Figure 5.11).

Table 5.12 Eigenvalues, percent variability explained and loadings of variables on the first three factors (after Varimax rotation of the first two Principal Components (PCs)) of a Principal Components Analysis of the root area distribution parameters.

** Loadings > 90%, * > 80 %

	Factor 1	Factor 2	PC 3
Eigenvalue (before rotation)	4.628	3.374	0.522
Variability (%. after rotation)	48.37	40.55	5.800
Cumulative variability (%)	48.37	88.92	94.72
<i>Loadings</i>			<i>(without rotation)</i>
1 st Quartile	-0.254	0.827 *	0.371
Median	-0.141	0.876 *	0.318
3 rd Quartile	-0.061	0.921 **	-0.106
Mean	0.544	0.795	-0.233
Standard Deviation	0.744	0.623	-0.215
Maximum	0.843 *	0.506	-0.128
Coefficient of Variation	0.980 **	-0.066	0.007
Skewness	0.939 **	-0.187	0.265
Kurtosis	0.929 **	-0.187	0.292

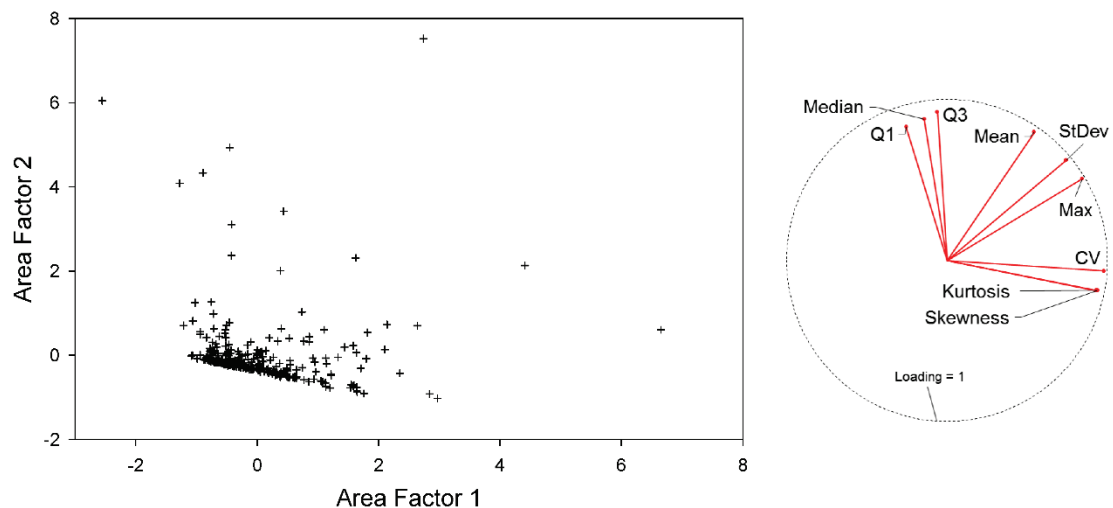


Figure 5.11 Scatter plot (left) of sample scores on the first and second factors (after Varimax rotation of the first and second Principal Components) of an analysis of root area distribution parameters, and the related plot of variable loadings on these factors. CV: Coefficient of Variation; Max: Maximum value; RAR: Root Area Ratio; StDev: Standard Deviation; CV: Coefficient of Variation; Max: Maximum value; StDev: Standard Deviation.

b Sediment

Analysis of data on the eight sediment variables revealed only one principal component with an eigenvalue greater than one, although the eigenvalue of the second component was very close to one (Table 5.13). These first two components together explained 92 % of the variability in the dataset. The first component described a gradient of decreasing particle size, with % Gravel having a high negative loading, and % Silt and Clay and the Mean Particle Size, d50 and d90 (in phi units, such that large values indicate small particles) having high positive loadings. In addition, Sorting and % Organic Matter showed high positive loadings, indicating increased sediment sorting and organic matter along this gradient of decreasing sediment size. The second component described a gradient of increasing % Sand, which is independent of the grain size gradient of PC1. When the scores of the samples on these two PCs are plotted (Figure 5.12), two distinct clusters of samples are apparent, illustrating a group of gravel-dominated samples on the left of the plot and finer samples on the right. These finer sediment samples cover a broad range of scores on the second component (sand content), whereas the gravel-dominated samples showed a much narrower range of scores on PC2.

Table 5.13 Eigenvalues, percent variability explained and loadings of variables on the first three Principal Components (PCs) of a Principal Components Analysis of the eight main sediment variables, as distributed among the root sampling intervals. ** Loadings > 90 %, * > 80 %

	PC 1	PC 2	PC 3
Eigenvalue	6.362	0.967	0.441
Variability (%)	79.53	12.09	5.516
Cumulative variability (%)	79.53	91.66	97.13
<i>Loadings</i>			
% Gravel	-0.905 **	-0.362	0.117
% Sand	0.520	0.845 *	0.072
% Silt + Clay	0.966 **	-0.203	-0.074
% Organic Matter	0.953 **	-0.063	-0.127
Mean Particle Size ϕ	0.980 **	-0.124	-0.076
d50 ϕ	0.948 **	-0.138	-0.198
d90 ϕ	0.971 **	-0.170	0.052
Sorting ϕ	0.794	-0.117	0.594

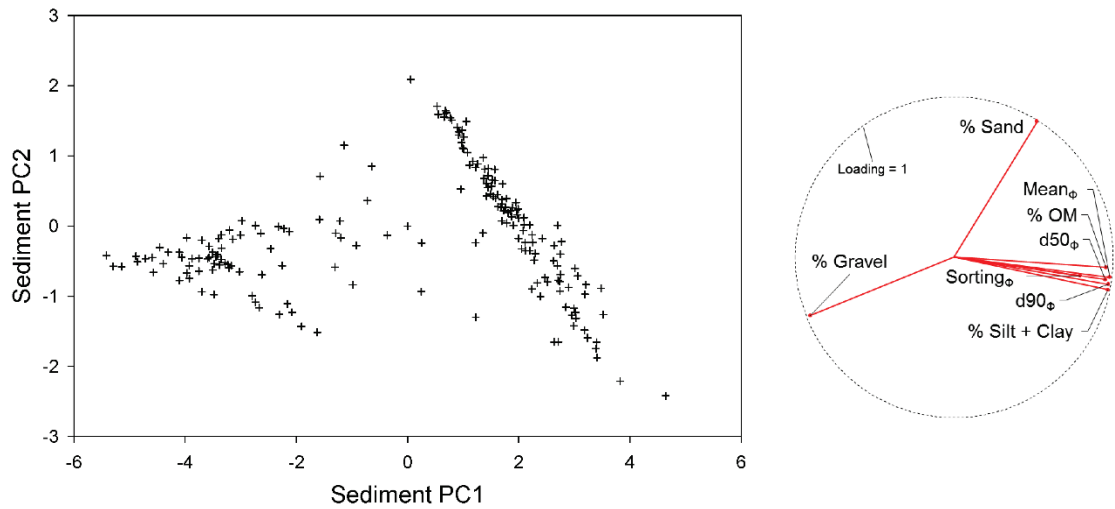


Figure 5.12 Scatter plot (left) of sample scores on the first and second PCs following a Principal Components Analysis of eight sediment properties, and the related plot of variable loadings on these factors. OM: Organic Matter.

These distinctive patterns within the sediment data provided a useful tool for visualising associations of sediment properties with other data. Figure 5.13 further aids interpretation of the sediment data structure by plotting high, intermediate and low values for the eight sediment variables in the PC space. The three classes were determined using Fisher's classification function.

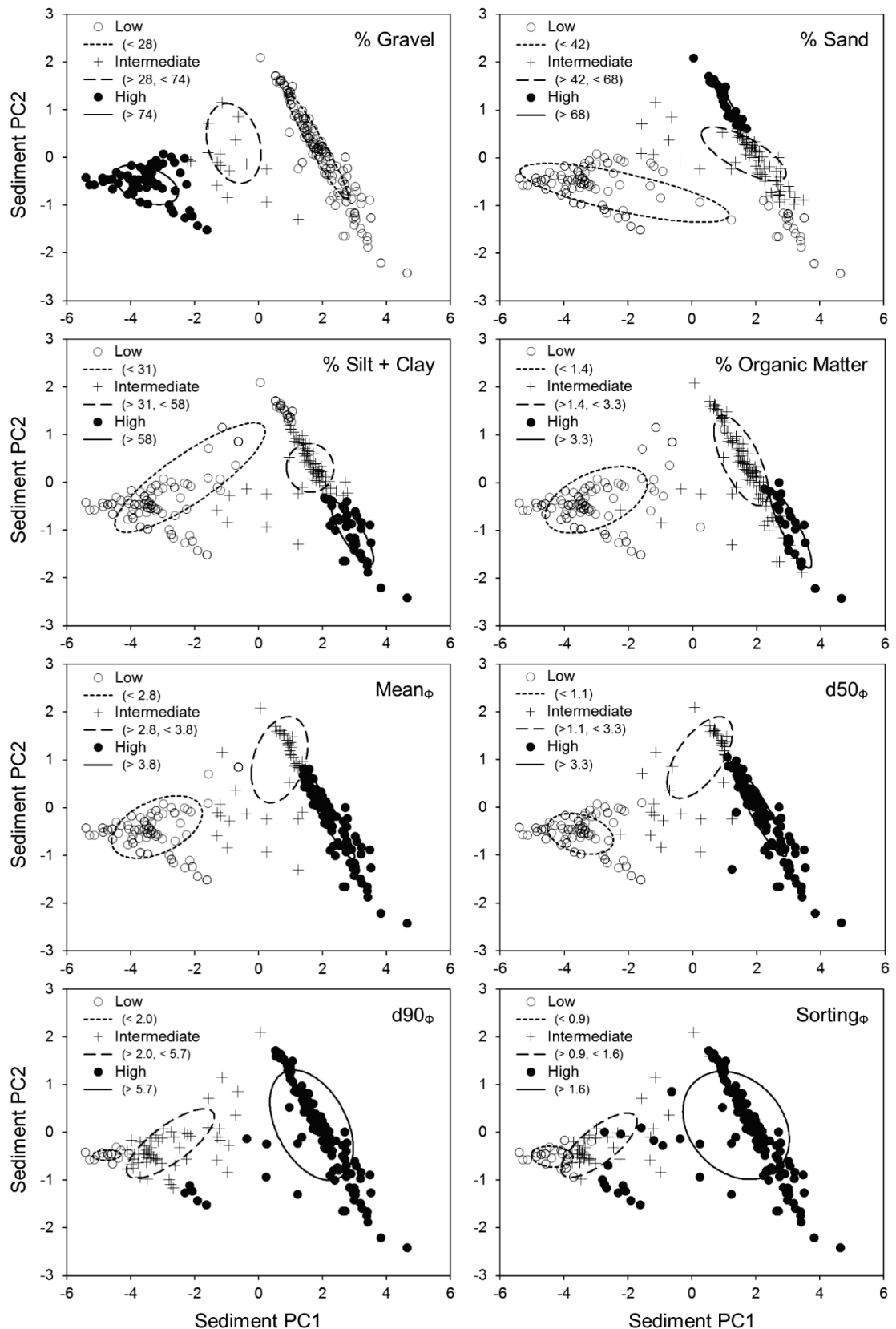


Figure 5.13 Distribution of the eight sediment variables with respect to PC1 and PC2. Areas characterised by high, intermediate and low values of each variable (see text for definition) are plotted separately, in the form of 50 % confidence ellipses.

5.3.3 Hierarchical Cluster Analysis

Following the PCA, which indicated distinct clustering of samples with similar characteristics within the sediment data, Agglomerative Hierarchical Clustering (AHC) was used to identify these sediment classes in a discrete way and allocate samples to classes. The AHC was applied to the eight core sediment properties using Euclidean distance as the distance measure and Ward's clustering algorithm, which tends to define fairly evenly-sized, compact clusters (e.g., Emery et al., 2003, Gurnell et al., 2006). The dendrogram in Figure 5.14 shows a clear distinction between finer (left) and coarser (right) grain dominated samples. Within these two broad groups, the coarser main group contains three clusters C, D and E, and the finer group divides into at least two clusters A and B (more easily visible in Figure 5.15). Further subdivisions of the clusters were investigated but a final set of five sediment classes was adopted (A, B, C, D and E), because this was the minimum number to provide a distinction between finer samples with higher and lower sand content (Classes A and B). These classes were also distinguished by differences in their organic matter and silt + clay content in the primary fine-grained cluster of the PC1-PC2 sample plot (Figure 5.16). Although five classes were selected (and subsequently found to be robust), further subdivision of class B could have yielded six clusters with three among the finer grained sediments. Table 5.14 shows centroid values for the eight core sediment variables in each of the five classes and also within the subdivisions of class B, which were also considered.

Table 5.14 Centroid values of the eight core sediment variables within the five sediment classes (A to E) and the two subdivisions of class B that were considered (in italics).

Class	% OM	d50 ϕ	d90 ϕ	% Gravel	% Sand	% Silt + Clay	Mean ϕ	Sorting ϕ
A	3.22	4.68	8.73	0.00	30.9	69.1	5.09	2.11
B	1.96	3.37	6.84	1.06	62.2	36.7	3.76	1.85
<i>B1</i>	<i>2.09</i>	<i>3.63</i>	<i>7.13</i>	<i>0.52</i>	<i>57.7</i>	<i>41.8</i>	<i>4.02</i>	<i>1.91</i>
<i>B2</i>	<i>1.56</i>	<i>2.57</i>	<i>5.92</i>	<i>2.73</i>	<i>76.4</i>	<i>20.9</i>	<i>2.96</i>	<i>1.63</i>
C	0.65	0.290	4.72	45.5	38.9	15.7	1.09	1.95
D	0.26	-1.24	2.43	77.2	16.7	6.04	-0.329	0.902
E	0.11	-1.16	-1.22	90.7	6.31	2.96	-1.12	-0.069

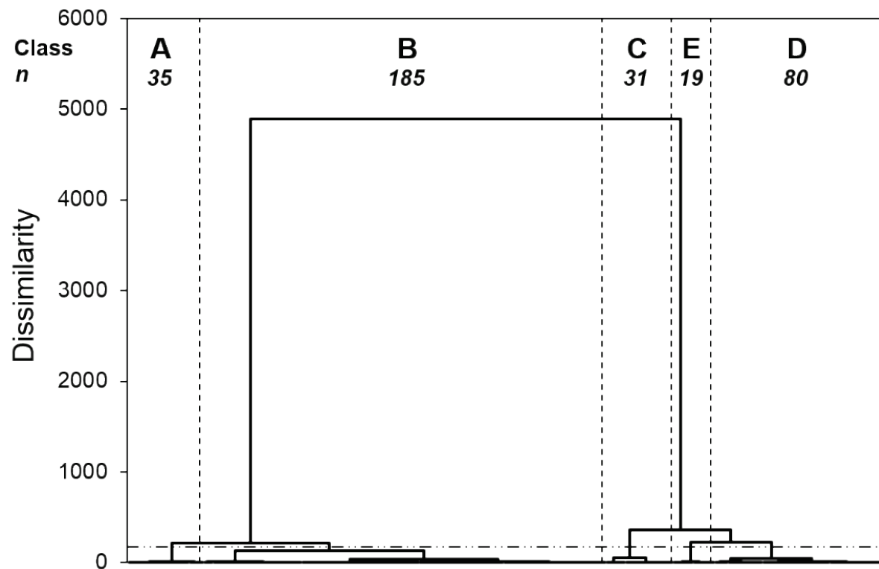


Figure 5.14 AHC cluster dendrogram locating the five main sediment classes (A, B, C, D, E) that were identified and the number of samples within each of these classes.

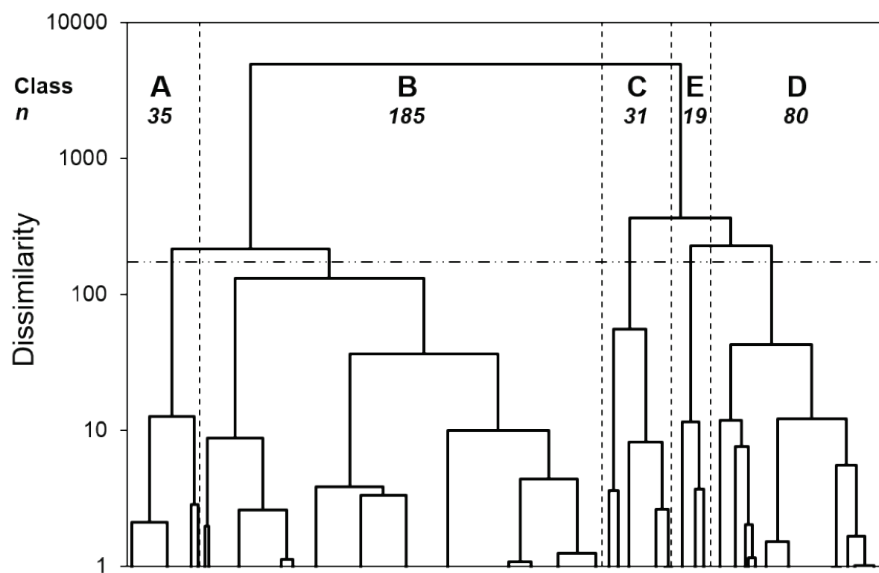


Figure 5.15 AHC dendrogram from Figure 5.14 with a logarithmically transformed dissimilarity axis to better illustrate sediment cluster structure.

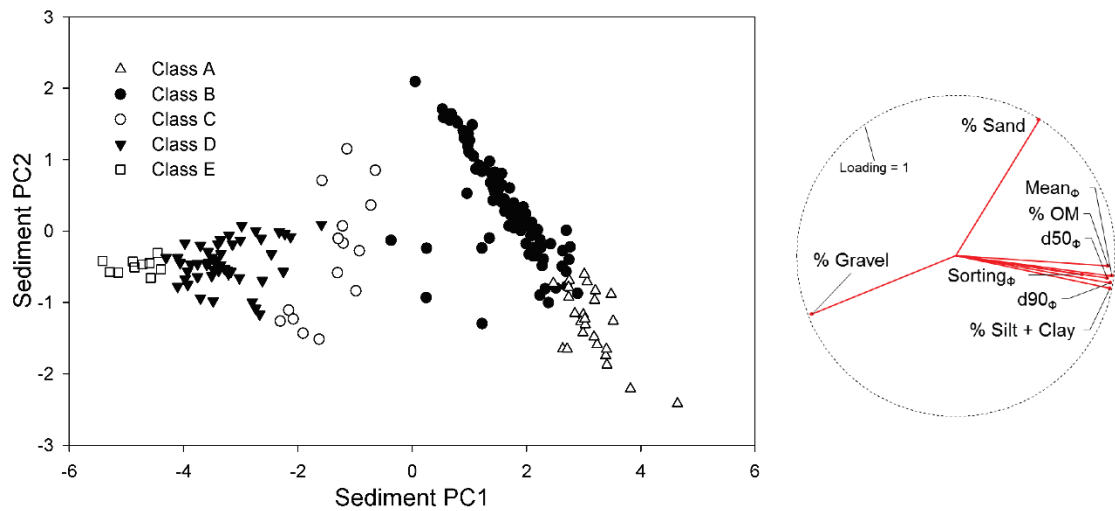


Figure 5.16 Scatter plot of sediment samples with respect to their scores on PC1 and PC2 (left), and shaded according to their membership of the five sediment classes (A, B, C, D, E) identified from the AHC analysis. Variable loading vectors are presented (right) to aid interpretation.

Figure 5.17 shows the differences between the five sediment classes with respect to class centroid values of the eight core sediment variables. All sediment properties of samples were found to vary significantly between the five classes (all $p < 0.0001$ in Kruskal-Wallis tests with 4 d.f.), and each class was significantly different from all others with respect to organic content, $d_{90\phi}$, silt + clay content and mean particle size ϕ (two-tailed multiple pairwise comparisons by Steel-Dwass-Critchlow-Fligner procedure at $\alpha = 0.05$). With respect to the other four variables, only one pair of classes was found to be not significantly different for each variable.

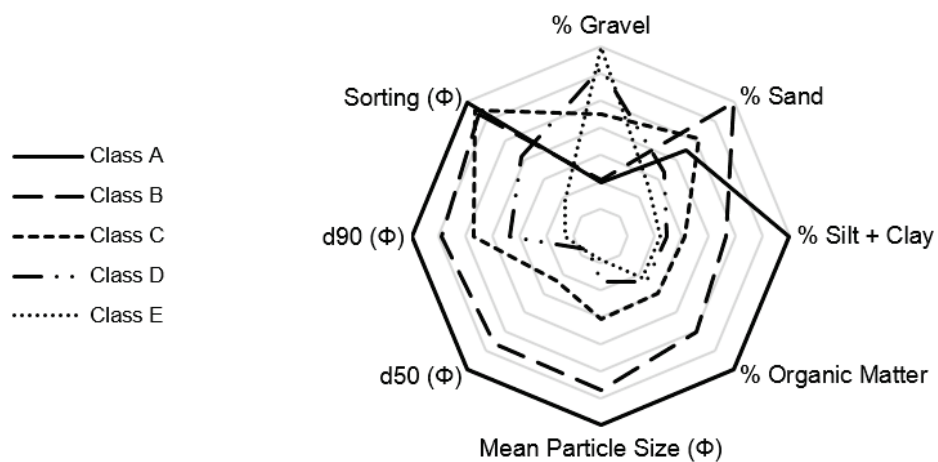


Figure 5.17 Radar chart summarising relative magnitude of sediment variable centroids in each sediment class.

5.3.4 Distribution of root and abiotic variables within the five sediment classes and PC space

Differences in the supplementary abiotic variables (field moisture content, sampling depth) and all root variables were investigated in relation to the sediment class membership of the samples. Kruskal-Wallis tests (Table 5.15) revealed that all five sediment classes contained significantly different ($p < 0.01$) root and supplementary abiotic variable values (including diameter and area distribution PC scores), except for the skewness, kurtosis and first quartiles of the fine root diameter distribution. Most of the variables showed statistically significant differences in their values across two or three distinct groups of classes ($p < 0.01$, Steel-Dwass-Critchlow-Fligner comparisons), with only the fine root area ratio distinguishable across four groups of classes. Table 5.15 reveals that coarse sediment Classes D and E always grouped together with respect to root and abiotic variables, except in the case of scores on Factor 2 of the PCA of the root area distributions.

Depending on the number of distinct groups identified by the pairwise comparisons, root distribution, PCA (factor) scores on root diameter and area distribution variables and abiotic variable data were categorised (high to low, with no, one or two intermediate levels) using the Fisher algorithm, and 50% confidence ellipses for each level were over-plotted on the scatter plot of sample scores on sediment PC1 and PC2. These plots are shown for the supplementary abiotic variables (Figure 5.18) and some key root density and root area ratio variables (Figure 5.19), as well as other variables showing the most distinct clustering with respect to the sediment PC axes (Figure 5.19 and Figure 5.20). Distinctions between high and low factor scores from the PCAs of root area and diameter frequency distribution parameters are plotted in Figure 5.21.

Table 5.15 Significant differences in non-sediment abiotic and root variables across five sediment classes, identified using Kruskal-Wallis tests with pairwise comparisons among the classes using the Steel-Dwass-Critchlow-Fligner procedure. * $p < 0.01$

	Variable	Kruskall-Wallis <i>K</i> (4 d.f.)	Distinct groups ($p < 0.01$)
Abiotic Variables	Depth	63 *	CDE > AB
	Field Moisture Content	155 *	A > B > CDE
Root Variables	Root Density	78 *	A > BC > DE
	Root Area Ratio	80 *	AB > C > DE
	Maximum Diameter	65 *	AB > C > DE
	Mean Diameter	46 *	BC > ADE
	Median Diameter	29 *	BC > A > DE
	Standard Deviation of Diameter Distribution	49 *	ABC > DE
	Coefficient of Variation of Diameter Distribution	34 *	ABC > DE
	Skewness of Diameter Distribution	31 *	AB > CDE
	Kurtosis of Diameter Distribution	34 *	A > B > CDE
	First Quartile of Diameter Distribution	21 *	BC > ADE
	Third Quartile of Diameter Distribution	25 *	BC > ADE
	Maximum Area	65 *	AB > C > DE
	Mean Area	53 *	ABC > DE
	Median Area	29 *	BC > A > DE
	Standard Deviation of Area Distribution	55 *	ABC > DE
	Coefficient of Variation of Area Distribution	45 *	A > BC > DE
	Skewness of Area Distribution	48 *	A > B > CDE
	Kurtosis of Area Distribution	49 *	A > B > CDE
	First Quartile of Area Distribution	21 *	BC > ADE
	Third Quartile of Area Distribution	23 *	BC > ADE
	Proportion Fine Roots by Number	30 *	DE > ABC
	Proportion Fine Roots by Area	36 *	DE > ABC
	Fine Root Density	59 *	A > B > CDE
	Fine Root Area Ratio	83 *	A > B > C > DE
	Mean Fine Root Diameter	27 *	BC > ADE
	Median Fine Root Diameter	19 *	C > ABDE
	Std. Dev'n of Fine Root Diameter Distribution	16 *	A > BCDE
	Coeff. Var. of Fine Root Diameter Distribution	14 *	A > BCDE
	Skewness of Fine Root Diameter Distribution	5.3	-
	Kurtosis of Fine Root Diameter Distribution	2.1	-
	1st Quartile of Fine Root Diameter Distribution	8.6	-
	3rd Quartile of Fine Root Diameter Distribution	22 *	ABC > DE
	Coarse Root Density	40 *	A > B > CDE
	Coarse Root Area Ratio	25 *	ABC > DE
	Mean Coarse Root Diameter	15 *	ABC > DE
	Median Coarse Root Diameter	17 *	BC > ADE
PC (Factor) Scores	(Root) Diameter Factor 1	32 *	ABC > DE
	(Root) Diameter Factor 2	23 *	C > AB > DE
	(Root) Area Factor 1	39 *	A > BC > DE
	(Root) Area Factor 2	15 *	CD > ABE

There appears to be a tendency for gravel-dominated sediments to occur at greater depth than finer sediments (Figure 5.18), and for higher field moisture content in sediments to be associated with finer sediments with higher organic matter and lower sand content.

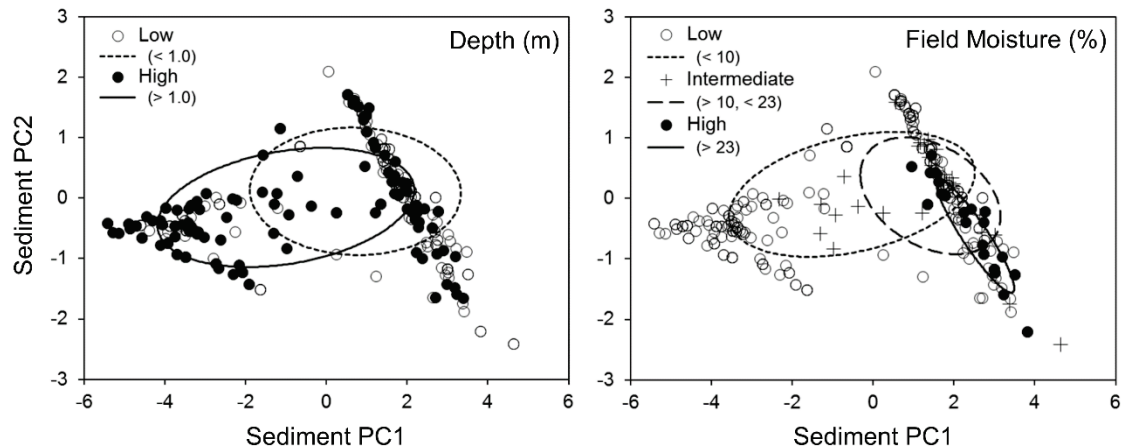


Figure 5.18 Distribution of the two supplementary abiotic variables of sample depth (left) and field moisture at time of sampling (right) in relation to sediment PC1 and PC2. Significantly different classes (see text for definition) are plotted separately, each with 50 % confidence ellipses.

The lowest values for the root variables were not strongly associated with any particular sediment type, but rather showed a broad distribution (Figure 5.19). However, the highest values of bulk root density, and fine root density and RAR, were strongly associated with the area of the plots occupied by samples in sediment class B, that is, those samples which are fine-grained, but with a relatively higher sand content than Class A (Figure 5.19). However, when considering bulk root area ratio (Figure 5.19, top right) and maximum root diameter (Figure 5.19, bottom left), extremely high values appeared not to be confined to any particular sediment type, although the density of coarse roots was greatest in fine sediments with intermediate sand content (Figure 5.19, middle right).

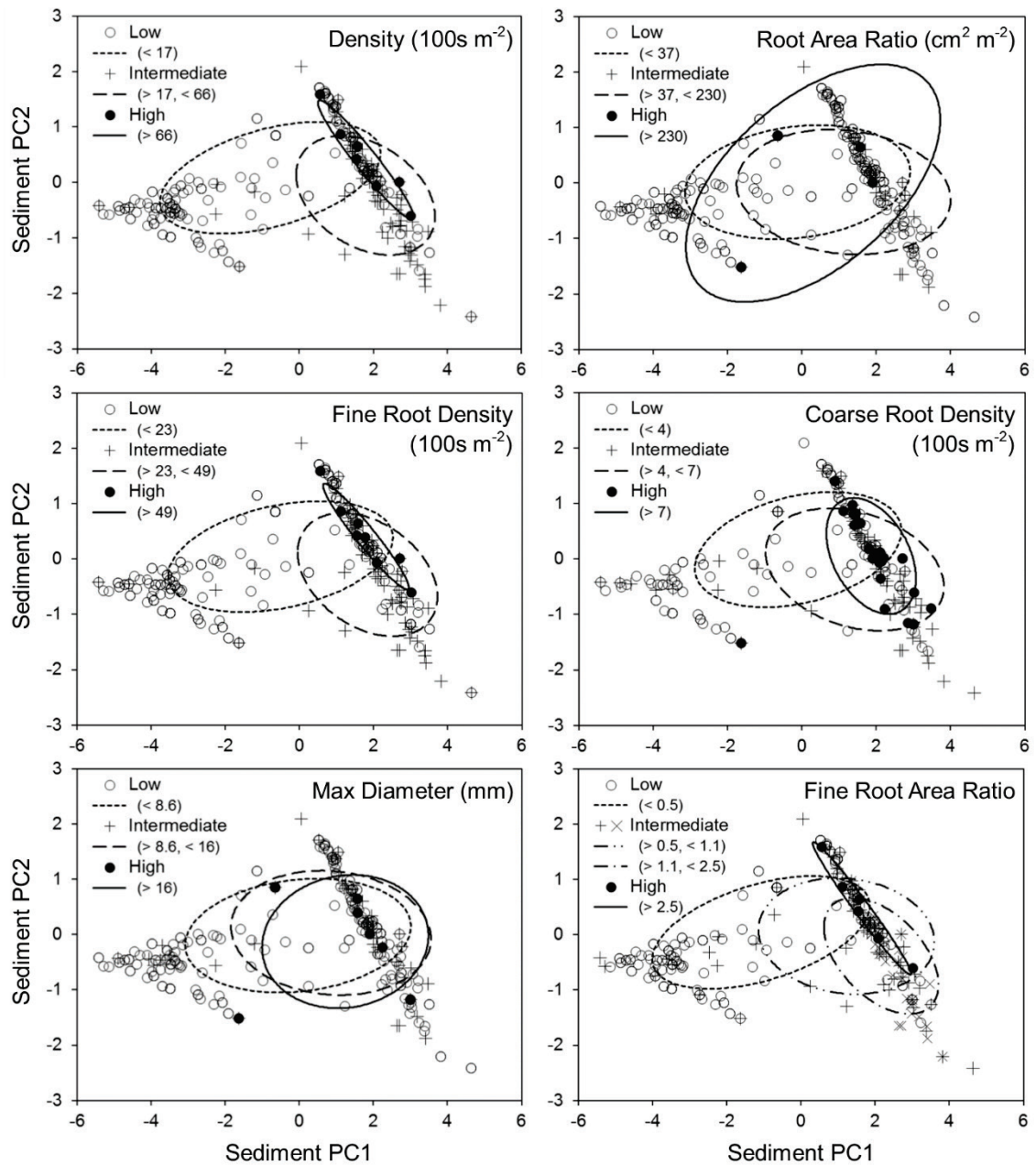


Figure 5.19 Distribution of key root variables in relation to sediment PC1 and PC2. Significantly different classes (see text for definition) are plotted separately, each with 50 % confidence ellipses.

As with the root variables, the lowest values of several properties of the root diameter and area distributions (Figure 5.20) were not strongly associated with any particular sediment type, but showed a broad distribution across the sediment PC scatter plot. Some of the most distinct clustering of these root frequency distribution parameters reflected the shape of the distributions (kurtosis, skewness, coefficient of variation), discriminated by the first sediment PC, which describes a sediment size gradient (Figure 5.20). The most leptokurtic root diameter and root area distributions were found in fine sediments (Figure 5.20, top left and

bottom right). Very similar patterns were observed for the coefficient of variation and the degree of positive skew of the root area distribution (Figure 5.20, top right and bottom left).

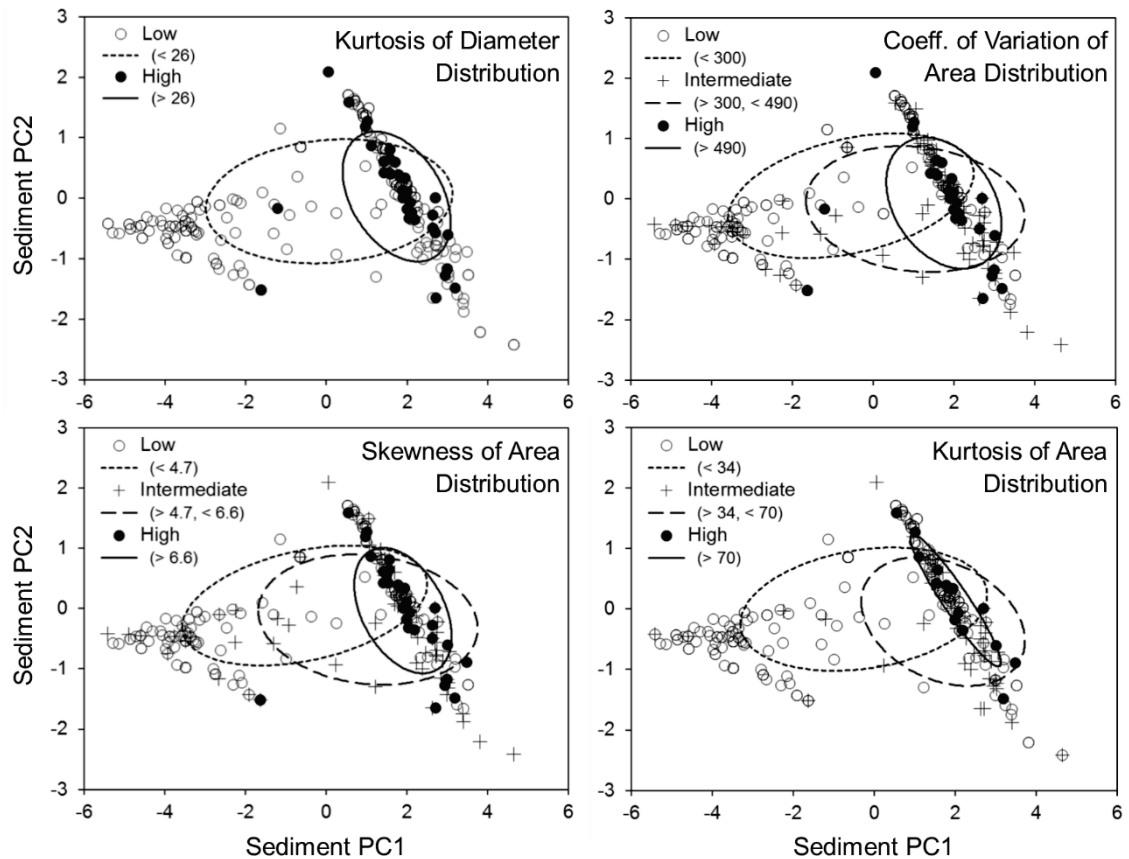


Figure 5.20 Position of root diameter and root area distribution shape parameters with respect to sediment PC1 and PC2. Significantly different classes (see text for definition) are plotted separately, each with 50 % confidence ellipses.

Plots of scores on the first two factors of the root area and density PCAs in relation to sediment PC1 and PC2 present an integrated view of the associations between root diameter and area distributions and the various types of sediment sampled (Figure 5.21). Noting the similarities in the frequency distribution parameter loadings on root diameter and root area Factors 1 and 2, the shape of the distributions (Factor 1) appeared more sensitive to the overall dominant grain size (Sediment PC1), whereas, central tendency values (Factor 2) appeared more sensitive (in finer sediments, at least), to the relative sand content (Sediment PC2). A summary of the observed distributions of the main sediment and root variables across sediment Classes A to E is presented in Table 5.16.

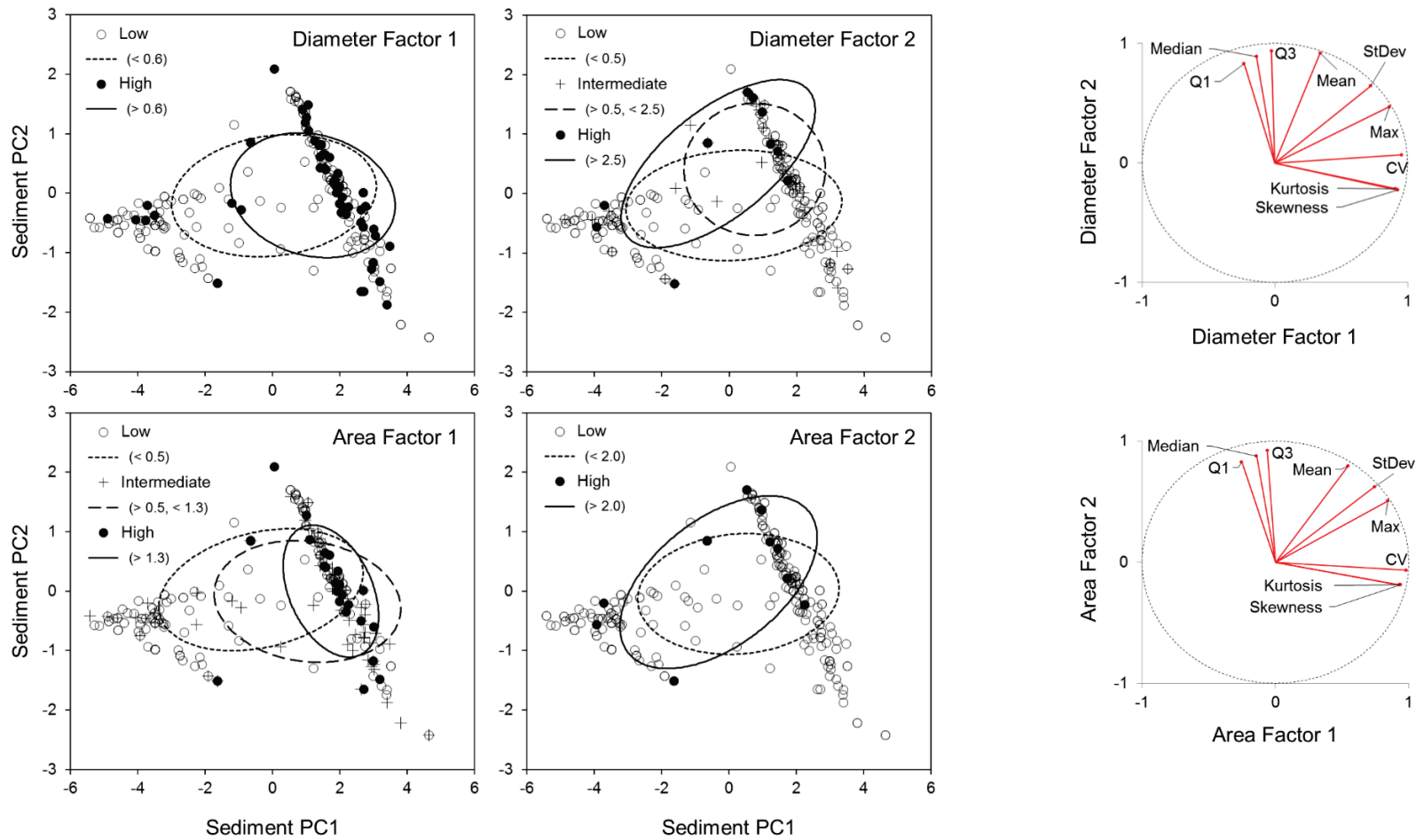


Figure 5.21 Root diameter (top) and area (bottom) factor classes plotted with respect to sediment PC1 and PC2, with 50 % confidence ellipses. The loadings of the root diameter (above) and area (below) frequency distribution parameters on the first two factors of the root PCAs are presented at right to aid interpretation.

Table 5.16 Summary of key features of the five sediment classes, including guideline values based on centroids (sediment) or median values (roots).

<i>Sediment class</i>		A	B	C	D	E
Sediment characteristics	Gravel content	← — — — — None — — — — →		Intermediate, variable (~ 40 %)	High (> 75 %)	Very high (> 90 %)
	Sand content	Intermediate (~ 30 %)	High (~ 60 %)	Intermediate, variable (~ 40 %)	← — — — — Low — — — — → (~ 10 %)	
	Silt & clay content	High (~70 %)	Intermediate (~ 35 %)	← — — — — Low — — — — → (< 15 %)		
	Sorting	← — — — — Poorly sorted — — — — → (~ 2 Φ)			Moderate (~ 0.9 Φ)	Very good (~ 0 Φ)
	Organic content	Relatively high (~ 3 %)	Intermediate (~ 2 %)	← — — — — Low — — — — → (< 1 %)		
	Typical moisture content	High (> 10 %)	Intermediate (~ 5 %)	← — — — — Low — — — — → (< 3 %)		
Root characteristics	Density	High (~ 2500 m ⁻²)	← — — — — Intermediate — — — — → (~ 1000 m ⁻²)		← — — — — Low — — — — → (~ 400 m ⁻²)	
	Root Area Ratio	← — — — — High, variable — — — — → (~ 5 - 10 cm ² m ⁻²)			Extremely variable (~ 3 - 30 cm ² m ⁻²)	← — — — — Low — — — — → (~ 0.2 cm ² m ⁻²)
	Average root diameter	← — — — — Intermediate — — — — → (~ 0.3 - 0.4 mm)			Relatively high (~ 0.5 mm)	← — — — — Low — — — — → (~ 0.2 mm)
	Spread of the diameter distribution	← — — — — Higher — — — — → (Coeff. Variation ~ 120)			← — — — — Lower — — — — → (Coeff. Variation ~ 70)	
	Peakedness and positive skew of the diameter distribution	High (Kur. ~ 12, Ske. ~ 3)	Intermediate (Kur. ~ 8, Ske. ~ 2.5)	Intermediate (Kur. ~ 5, Ske. ~ 2)	Relatively low (Kur. ~ 2, Ske. ~ 1.5)	Intermediate (Kur. ~ 5, Ske. ~ 2)
	Area of absorptive fine roots	High (~ 1 cm ² m ⁻²)	Relatively high (~ 0.5 cm ² m ⁻²)	Intermediate (~ 0.3 cm ² m ⁻²)	← — — — — Low — — — — → (~ 0.1 cm ² m ⁻²)	
	Density of coarse roots	High (~ 400 m ⁻²)	Intermediate, variable (~ 200 - 400 m ⁻²)		← — — — — Relatively low — — — — → (~ 150 m ⁻²)	
	Dominance of fine roots	← — — High in terms of numbers, Low in terms of area — — → (~ 80 % of density, ~ 10 % of area)			Very high numbers, ~ Equal share of area (~ 90 % of density, ~ 50 % of area)	

5.4 DISCUSSION

The present study sought to identify relationships between root distribution properties and vegetation and sediment characteristics in the riparian zone of a large, highly dynamic river which shows strong morphological interaction with the dominant tree species, *Populus nigra* L. Correlation analyses on pairs of variables was subsequently supplemented with multivariate approaches, to penetrate beyond the considerable variability in the data and inter-correlation among variables to extract significant broad and informative associations between the sets of rooting and sediment parameters.

5.4.1 Single variable correlates of root density and total area

In spite of many known – and presumably also unknown – interactions among groups of variables and other complicating factors, the simple approach of investigating correlations between pairs of variables identified a large number of significant relationships, although the highest coefficient of determination was 33.5 % (fine RAR vs sediment $d_{90\phi}$). The fact that root properties were more strongly associated with sediment properties than with tree properties was probably due in part to the smaller sample size of the latter, and the fact that only the ‘absolute distance to nearest tree’ variable also varied with depth (other variables applied a single value to the whole profile).

Nonetheless, tree growth rates, and in particular, the stem elongation rate (vertical growth rate) emerge as key variables, strongly associated with both root density and area, but particularly with fine root properties. As speculated in the introduction to this chapter, this provides further support for the notion that growth of poplar in such early successional environments is more closely linked to root, rather than above-ground investment, particularly investment in fine, absorptive roots. The relatively large influence of the proximity of the nearest mature stem on root area ratio and coarse root parameters is most likely due to the occurrence of relatively infrequent, extraordinarily large roots which are primarily mechanical in function. Note also that the maximum root diameters are most significantly correlated with the same variables as RAR (Sorting ϕ and $d_{90\phi}$, Table 5.8 and Table 5.9). This skew due to large roots is reported by other authors (e.g., Abernethy and Rutherford, 2001) and is supported by the later multivariate analyses (maximum root diameter and RAR plot together on Factor 1 of the root diameter distribution PCA, Table 5.11) and highlights the potential for overestimation of root reinforcement by taking into account RAR alone, high values of which can be due to just one or two roots with extremely high sectional area.

Similar to the tree data, sharing of sediment samples across a greater number of root samples is likely to have diluted relationships between sediment and root properties to some degree. Nevertheless, correlation coefficients were remarkably high, and although many sediment variables had similar correlations with root variables – and were indeed significantly correlated with each other – a high $d_{90\phi}$ (i.e., a high relative content of the finest-grained material) and a low degree of sorting were all consistently associated with high root density and RAR. Furthermore, clay content was also clearly an important factor for the ramification of roots, which is not particularly surprising as the cation exchange capacity of this mineral fraction is likely to be at a premium in the gravel-dominated Tagliamento system. The particularly strong association of clay content with fine root variables supports the hypothesis that this is a nutritional relationship, but further work on this issue would certainly benefit from investigating availability of macronutrients in various bank sediment types, and their relationships with rooting. Sand content did not in itself appear to be an important factor for the aggregate root density and RAR values – the significance of the sand fraction appears to lie in the variability of root diameter distributions, as discussed below.

In general, the distinction between fine and coarse roots appears to be useful, particularly for providing greater insight into the diameter class composition and driving factors behind root area. As found by Piercy and Wynn (2008), fine (or ‘very fine’ under their classification) roots show the strongest relationships with sediment and vegetation parameters, and this perhaps demonstrates that such factors are stronger drivers of the year-to-year physiological adaptations of tree root systems (acknowledging the vast turnover rates of such absorptive roots). The system of coarser roots, obviously of increasing age with increasing diameter, may be more sensitive to factors which exert influence over larger timescales – a hypothesis explored in the following chapter.

5.4.2 Multivariate associations between roots and sediments

It is clear from the PCA that the major distinction between sediments sampled on the Tagliamento is between coarse gravels and finer deposits, and the classification adopted from AHC analysis reflects this, but also distinguishes two apparently important categories within the fine-grained deposits. The higher sand content of Class B sediments indicates deposition by water with slightly higher average velocity than that of Class A, and so the former may be interpreted as more typical floodplain deposits, whereas Class A sediments may have accumulated in still ponds and backwaters and may even contain a wind-blown component (Gurnell et al., 2008). These finest Class A sediments are also likely to have contained organic material. This is borne out by the position of Class A sediment samples in the sediment PC

space with respect to the organic matter loading vector (Figure 5.12) and the 50% confidence ellipse for the highest % Organic Matter (Figure 5.13). As can be seen in Table 5.15, Classes D and E almost always group together with respect to root variables, and so it seems this distinction between gravels with slightly different degrees of sorting is not particularly relevant for tree rooting patterns. The dendrograms (Figure 5.14 and Figure 5.15) suggest a system based on six clusters (splitting class B into two subclasses) may be appropriate given the somewhat larger dissimilarity difference between six and seven, versus five and six clusters. This would give more resolution within the fine-grained classes, but it would probably be prudent to combine some of the coarse-grained clusters, particularly D and E, to provide a sediment classification that may be even more strongly attuned to rooting patterns.

In spite of the wide range of root parameters investigated, the aggregate variables of root density and RAR – particularly fine RAR – show the greatest distinction among the five sediment classes (Table 5.15). This is valuable from the point of view of understanding root reinforcement, given that RAR forms the basis of bank stability models, and particularly given the fact that fine roots are disproportionately strong (Gray and Barker, 2004, Tosi, 2007, De Baets et al., 2008). It can thus be broadly concluded that fine sediments are particularly well reinforced by roots in this system. However, note that such sediment classes are also associated with a wider distribution of root diameters (Table 5.16). This may suggest that root reinforcement predictions in fines may be associated with a wider degree of uncertainty, although the somewhat counterintuitive association between kurtosis and coefficient of variation indicates that a narrower diameter class of roots may be more dominant in spite of a wider overall spread of the root size distribution. Investigation of other variables such as redox status and macronutrient availability may shed light on the processes leading to these distribution characteristics and aid interpretation of root exploitation of these fine sediment classes.

Root density generally increased along the sediment PC1 axis, but note in Figure 5.19 that the very highest values of fine root density and area occurred in Class B sediments. Figure 5.21 suggests that the distinctiveness of this class and associations with its higher sand content appears to be related to the second root PC factor (central tendency). Higher median and mean diameters in these sediments may indicate perhaps a trade-off between slightly higher moisture stress relative to Class A material, but a more favourable environment in terms of oxygen and nutrient availability (due to aerobic microbial activity), making exploitation of these sediments worthwhile, but requiring thicker, more lignified and protected roots on average. This association may also indicate lower investment in the finest

roots, alternatively implying little actual exploitation of soil resources, but perhaps more roots involved in transit of resources from more favourable zones.

The high variability of density of coarse roots in Class B sediments may be due to the variable occurrence of the specialist long, horizontal, suckering adventitious roots associated with clonal expansion of poplar. A central tenet of the biogeomorphologic life cycle (BLC) of riparian black poplar (Corenblit et al., 2014) is expansion into finer floodplain deposits via these roots, and Class B sediments appear to display the characteristics of such material. Such adventitious roots may also account for a large degree of the dominance of sectional area by coarse roots in the fine-to-intermediate sediment classes (Table 5.16), but under the diameter classification used here, it is difficult to distinguish between the effect due to these roots versus those which are more mechanical in function. The relationships with sand tentatively implied by Figure 5.8 (greater occurrence of larger roots in strata with intermediate sand content) are rather more difficult to interpret and also warrant further investigation.

Despite the high variability within the datasets and inter-correlations among many of the variables investigated in this chapter, a combination of multivariate analyses has revealed numerous important associations between alluvial sediments and roots. These are summarised in Table 5.16 by describing the properties of five sediment classes and then associating these sediment classes with key properties of their contained roots. The table shows how sediment calibre is associated with organic content, moisture retention and sorting, and that there are clear trends in key root properties along a gradient from predominantly coarse to fine sediment calibre. These trends in root properties do not simply reflect root size, area, and density but also the shape of the root diameter frequency distribution. The above discussion has built on these associations by attempting to explain them in relation to other likely properties of the sediment environment and the likely function of roots within sediments of different type or class. Given the sample sizes involved, the features summarised in Table 5.16 are robust, at least for the case of the Tagliamento river and its riparian poplars.

5.4.3 Implications and further work

The BLC concept for poplars as advanced by Corenblit et al. (2014) is based around the expansion of root systems into successive layers of fine sediments deposited over gravels, and the subsequent stabilisation of this fine material. The present study has demonstrated that there are at least two distinct types of fine sediment in the Tagliamento system, which are characterised by root populations of different character. Figure 5.18 demonstrates an overall tendency for fine sediments to be found at shallower depths, but it also demonstrates

that gravels and finer material can be found at all depths, and that the sediment profiles exposed in the context of this work display common and complex interbedding of sediment of widely varying calibre. The strong associations between sediment calibre and root properties revealed here imply that root reinforcement of fines can occur at any depth (within the limit of sampling) where they occur, and the BLC model is not limited simply to the situation of fine flood deposits atop gravels. Given the importance of suckering adventitious roots for the vegetation dynamics of riparian poplar, and the observation that these roots mostly appear to occupy a particular diameter range in the order of 10 - 35 mm, it is suggested that future studies on this system include a third root diameter category to be able to account for them separately.

With regards to the general issue of the prediction of root reinforcement in river banks, the sediment associations identified with the most important root variables from a mechanical point of view are encouraging. However, this study does highlight the enormous variability still unaccounted for, and predicting the distribution of RAR among roots of different diameter and thus tensile strength remains difficult. The relationships observed open the door to the development of slightly more detailed modelling of the enhancement of bank stability, however. For example, the Bank Stability and Toe Erosion Model (BSTEM) developed by Pollen-Bankhead and Simon (2009) and others already includes explicit treatment of sedimentary strata and simple root depth distributions, and so it may be relatively straightforward, given more detailed data on root-sediment associations, to modify the root depth distributions using the stratigraphic data.

5.5 CONCLUSIONS

With respect to the specific questions outlined in Section 5.1.1, the following conclusions can be made from observations on the Tagliamento and its black poplars:

- i. The density and sectional area of roots in bank profiles are most closely related to the mean vertical growth rates of the nearest trees and the proximity of the nearest large stem, respectively. However, though many significant relationships were found, tree properties account for a very low amount of variability in rooting patterns. Fine roots are more strongly influenced by tree growth rates, whereas coarse roots, by the proximity to large trees.
- ii. With respect to sediment variables (which were all more strongly associated to root data than tree variables) high d_{90} (on the phi scale) is consistently associated with high root density and sectional area. Poorly sorted sediments with a high proportion

of silt and clay also show prolific rooting, and the strongest relationships identified apply to fine roots.

- iii. Root size distributions vary primarily in terms of their range and evenness, and secondarily in terms of their central tendency (median and mean).
- iv. Sediments in this dynamic, gravel bed river system vary mostly in one dimension related to their mean and median grain size, degree of sorting and organic matter, forming two main clusters. However, fine sediments also vary significantly in terms of their sand content. Based on these dimensions, a four class system is proposed: (A) very fine-grained with significant organic material, (B) fine grained with sand, (C) intermediate grain size and (D+E) gravel-dominated.
- v. Class A sediments show the highest root density and area, with frequent very large roots as well as very high numbers of fine roots. Class B and C sediments have intermediate root density, but the root area in B types can be high due to many coarse roots. Class C sediments show extremely variable root properties, but relatively low numbers of coarse roots. Roots are scarce in D+E types, but occasional large roots occur, and fine roots still account for half of the sectional area of the roots which are found. Classes mostly differ in terms of the first principal components of variability of both sediment and root data, but Class B is distinctive in terms of the second components (sand content and central tendency of the root size distribution).

The most significant distinction in this system is that of fine (sand, silt and clay) versus coarse (gravel and pebble) sediments, with higher root density and area in the former, relatively independently of depth in the upper couple of metres of sediment studied here. This study demonstrates, however, that a lot more information pertinent to the physical and ecological functioning of the riparian tree-root-sediment system is gleaned from analysis of the distribution of root sizes, rather than simply the aggregate value of RAR (or root volume ratio) typically studied for the purposes of applying models emerging from the engineering disciplines. The functional insight gained from the separate treatment of fine and coarse roots is valuable, but insufficient to explain some of the other dimensions of variability uncovered, particularly with respect to the differences in coarse root distributions within the different types of fine sediments. Chapter 6 investigates coarse root structure of riparian poplars in greater detail, with particular emphasis on the disturbance events which lead to the complex sediment profiles and directly modify the development of the overall sub-aerial structures of trees in such dynamic environments.

5.6 REFERENCES

- ABERNETHY, B. & RUTHERFURD, I. D. 2001. The distribution and strength of riparian tree roots in relation to riverbank reinforcement. *Hydrological Processes*, 15, 63-79.
- BLACK, K. E., HARBRON, C. G., FRANKLIN, M., ATKINSON, D. & HOOKER, J. E. 1998. Differences in root longevity of some tree species. *Tree Physiology*, 18, 259-264.
- BLOCK, R. M. A. 2004. Fine root dynamics and carbon sequestration in juvenile hybrid poplar plantations in Saskatchewan, Canada. MSc, University of Saskatchewan.
- BLOCK, R. M. A., VAN REES, K. C. J. & KNIGHT, J. D. 2006. A review of fine root dynamics in *Populus* plantations. *Agroforestry Systems*, 67, 73-84.
- BLOTT, S. J. & PYE, K. 2001. Gradstat: A grain size distribution and statistics package for the analysis of unconsolidated sediments. *Earth Surface Processes and Landforms*, 26, 1237-1248.
- COLEMAN, M. D., DICKSON, R. E. & ISEBRANDS, J. G. 2000. Contrasting fine-root production, survival and soil CO₂ efflux in pine and poplar plantations. *Plant and Soil*, 225, 129-139.
- COLEMAN, M. D., DICKSON, R. E., ISEBRANDS, J. G. & KARNOSKY, D. F. 1996. Root growth and physiology of potted and field-grown trembling aspen exposed to tropospheric ozone. *Tree Physiology*, 16, 145-152.
- CORENBLIT, D., STEIGER, J., GONZÁLEZ, E., GURNELL, A. M., CHARRIER, G., DARROZES, J., DOUSSEAU, J., JULIEN, F., LAMBS, L., LARRUE, S., ROUSSEL, E., VAUTIER, F. & VOLDOIRE, O. 2014. The biogeomorphological life cycle of poplars during the fluvial biogeomorphological succession: a special focus on *Populus nigra* L. *Earth Surface Processes and Landforms*, 39, 546-563.
- DE BAETS, S., POESEN, J., REUBENS, B., WEMANS, K., DE BAERDEMAEKER, J. & MUYS, B. 2008. Root tensile strength and root distribution of typical Mediterranean plant species and their contribution to soil shear strength. *Plant and Soil*, 305, 207-226.
- DOCKER, B. B. & HUBBLE, T. C. T. 2008. Quantifying root-reinforcement of river bank soils by four Australian tree species. *Geomorphology*, 100, 401-418.
- EMERY, J. C., GURNELL, A. M., CLIFFORD, N. J., PETTS, G. E., MORRISSEY, I. P. & SOAR, P. J. 2003. Classifying the hydraulic performance of riffle-pool beforms for habitat assessment and river rehabilitation design. *River Research and Applications*, 19, 533-549.
- FINER, L., MESSIER, C. & DE GRANDPRE, L. 1997. Fine-root dynamics in mixed boreal conifer-broad-leaved forest stands at different successional stages after fire. *Canadian Journal of Forest Research*, 27, 304-314.
- FOLK, R. L. & WARD, W. C. 1957. Brazos River bar: a study in the significance of grain size parameters. *Journal of Sedimentary Petrology*, 27, 3-26.
- FRIEND, A. L., SCARASCIA-MUGNOZZA, G., ISEBRANDS, J. G. & HEILMAN, P. E. 1991. Quantification of two-year-old hybrid poplar root systems: morphology, biomass, and ¹⁴C distribution. *Tree Physiology*, 8, 109-119.
- GRAY, D. H. & BARKER, D. 2004. Root-soil mechanics and interactions, Washington, Amer Geophysical Union.
- GURNELL, A. 2015 (in press). Trees, wood and river morphodynamics: results from 15 years research on the Tagliamento river, Italy. In: GILVEAR, D., GREENWOOD, M., THOMS, M. & WOOD, P. (eds.) *River Science: Research and Applications for the 21st Century*. Hoboken, NJ: John Wiley and Sons.
- GURNELL, A. M., BLACKALL, T. D. & PETTS, G. E. 2008. Characteristics of freshly deposited sand and finer sediments along an island-braided, gravel-bed river: The roles of water, wind and trees. *Geomorphology*, 99, 254-269.
- GURNELL, A. M., MORRISSEY, I. P., BOITSIDIS, A. J., BARK, T., CLIFFORD, N. J., PETTS, G. E. & THOMPSON, K. 2006. Initial adjustments within a new river channel: Interactions between fluvial processes, colonizing vegetation, and bank profile development. *Environmental Management*, 38, 580-596.
- HEILMAN, P. E., EKUAN, G. & FOGLE, D. 1994. Above-ground and below-ground biomass and fine roots of 4-year-old hybrids of *Populus trichocarpa* X *Populus deltoides* and parental species in short-rotation culture. *Canadian Journal of Forest Research*, 24, 1186-1192.
- HUGGENBERGER, P., HOEHN, E., BESCHTA, R. & WOESSNER, W. 1998. Abiotic aspects of channels and floodplains in riparian ecology. *Freshwater Biology*, 40, 407-425.

- KARRENBERG, S., KOLLMANN, J., EDWARDS, P. J., GURNELL, A. M. & PETTS, G. E. 2003. Patterns in woody vegetation along the active zone of a near-natural Alpine river. *Basic and Applied Ecology*, 4, 157–166.
- KOSOLA, K. R., DICKMANN, D. I., PAUL, E. A. & PARRY, D. 2001. Repeated insect defoliation effects on growth, nitrogen acquisition, carbohydrates, and root demography of poplars. *Oecologia*, 129, 65–74.
- KYLE, G. & LEISHMAN, M. R. 2009. Plant functional trait variation in relation to riparian geomorphology: The importance of disturbance. *Austral Ecology*, 34, 793–804.
- MCCORMACK, M. L., DICKIE, I. A., EISSENSTAT, D. M., FAHEY, T. J., FERNANDEZ, C. W., GUO, D., HELMISAARI, H. S., HOBBIE, E. A., IVERSEN, C. M., JACKSON, R. B., LEPPÄLAMMI-KUJANSUU, J., NORBY, R. J., PHILLIPS, R. P., PREGITZER, K. S., PRITCHARD, S. G., REWALD, B. & ZADWORNÝ, M. 2015. Redefining fine roots improves understanding of below-ground contributions to terrestrial biosphere processes. *New Phytologist*, 207, 505–518.
- PIERCY, C. & WYNN, T. 2008. Predicting Root Density in Streambanks. *JAWRA Journal of the American Water Resources Association*, 44, 496–508.
- POLLEN-BANKHEAD, N. & SIMON, A. 2009. Enhanced application of root-reinforcement algorithms for bank-stability modeling. *Earth Surface Processes and Landforms*, 34, 471–480.
- POLLEN-BANKHEAD, N., SIMON, A. & THOMAS, R. E. 2013. *The Reinforcement of Soil by Roots: Recent Advances and Directions for Future Research*. Treatise on Geomorphology. Elsevier Inc.
- POLLEN, N. 2007. Temporal and spatial variability in root reinforcement of streambanks: Accounting for soil shear strength and moisture. *Catena*, 69, 197–205.
- PREGITZER, K. & FRIEND, A. L. 1996. The structure and function of *Populus* root systems. In: STETTNER, R. F., BRADSHAW, H. D., JR., HEILMAN, P. E. & HINCKLEY, T. M. (eds.) *Biology of Populus and its Implications for Management and Conservation*. Ottawa, Ontario, Canada: National Research Council of Canada Research Press.
- RINALDI, M. & DARBY, S. E. 2007. Modelling river-bank-erosion processes and mass failure mechanisms: progress towards fully coupled simulations. In: HABERSACK, H., PIEGAY, H. & RINALDI, M. (eds.) *Developments in Earth Surface Processes*.
- RUARK, G. A. & BOCKHEIM, J. G. 1987. Below-ground biomass of 10-, 20-, and 32-year-old *Populus tremuloides* in Wisconsin. *Pedobiologia*, 30, 207–217.
- RUESS, R. W., VAN CLEVE, K., YARIE, J. & VIERECK, L. A. 1996. Contributions of fine root production and turnover to the carbon and nitrogen cycling in taiga forests of the alaskan interior. *Canadian Journal of Forest Research*, 26, 1326–1336.
- STEELE, S. J., GOWER, S. T., VOGEL, J. G. & NORMAN, J. M. 1997. Root mass, net primary production and turnover in aspen, jack pine and black spruce forests in Saskatchewan and Manitoba, Canada. *Tree Physiology*, 17, 577–587.
- TOSI, M. 2007. Root tensile strength relationships and their slope stability implications of three shrub species in the Northern Apennines (Italy). *Geomorphology*, 87, 268–283.
- TUFEKCIOGLU, A., RAICH, J. W., ISENHART, T. M. & SCHULTZ, R. C. 1998. Fine root dynamics, coarse root biomass, root distribution, and soil respiration in a multispecies riparian buffer in Central Iowa, USA. *Agroforestry Systems*, 44, 163–174.
- VAN DE WIEL, M. J. & DARBY, S. E. 2007. A new model to analyse the impact of woody riparian vegetation on the geotechnical stability of riverbanks. *Earth Surface Processes and Landforms*, 32, 2185–2198.
- WILLMS, C. R., PEARCE, D. W. & ROOD, S. B. 2006. Growth of riparian cottonwoods: A developmental pattern and the influence of geomorphic context. *Trees - Structure and Function*, 20, 210–218.

Chapter 6

BURIED LIVELIWOOD AND COARSE ROOT SYSTEMS OF RIPARIAN BLACK POPLAR

6.1 INTRODUCTION

Research presented in the preceding chapters has described the great variability in root density, size and distribution in riparian sediment profiles, and has identified and investigated the influences of moisture availability and sediment properties, which are overlain on fundamental depth distributions. However, in spite of an increasingly comprehensive understanding of the patterns of riparian tree root growth, much variability still remains to be explained, and significant and often extreme deviations from the expected root distributions were frequently encountered in the previously analysed datasets. It is hypothesised that these anomalies are due to atypical coarse root architecture which forms the higher order structural framework from which the great numbers of lower order roots develop. Moreover, it is proposed that such irregular gross structure is due to sporadic physical disturbance by floodwaters and the particular adaptations of poplars which enable them to survive and exploit such events.

Riparian poplar and willow species are typified by high growth rates and the ability to propagate readily from vegetative fragments, even when these are very small. These characteristics appear to have evolved in response to the particular selection pressures experienced in riparian zones (Eckenwalder, 1996). High root growth rate of seedlings permits establishment on newly deposited fluvial sediments with rapidly declining water tables (Mahoney and Rood, 1992, Barsoum and Hughes, 1998, Guilloy-Froget et al., 2002). High stem elongation rates in established plants confers tolerance to burial by flood-deposited sediment, and the propensity for vegetative reproduction from fragments permits survival of destructive flow events (Barsoum et al., 2004).

Furthermore, poplars produce vast networks of adventitious roots which give rise to new stems by suckering. Consequently, natural poplar stands usually consist of genetically uniform patches of clonal stems, often with a large, shared root network (Pregitzer and Friend, 1996). This vast underground biomass, which is particularly significant in younger trees (Shepperd and Smith, 1993), constitutes a large store of readily mobilised carbohydrate (Nguyen et al., 1990, Pregitzer and Friend, 1996) and can permit rapid replacement of stems

destroyed by major disturbances as well as rapid colonisation of newly deposited fine sediments and the exploitation of their nutrient and moisture storage resources. The labile photosynthate driving new growth is contained within the recalcitrant structural carbohydrate infrastructure of these large, woody roots (Nguyen et al., 1990). The previously overlooked carbon store constituted by fluvial wood is beginning to be appreciated (e.g., Wohl et al., 2012), however, the significance of buried *living* wood as a carbon source in dynamic riparian environments, where buried dead organic material can decompose rapidly, remains to be evaluated.

Poplar growth forms and dynamics are reciprocally linked with fluvial geomorphology and given the associated acceleration of sediment deposition (by increasing channel roughness) and retardation of erosion (by root-mediated sediment reinforcement and soil development), riparian poplars can be considered physical ecosystem engineers (Gurnell, 2014). The bidirectional physical and biological influences have been conceptualised in a cyclical ‘fluvial biogeomorphic succession’ (FBS) model (Corenblit et al., 2007), within the latter phases of which, stem burial and adventitious root production play key roles (Figure 6.1). There has, however, been little investigation into whether the sub-aerial poplar structures in mature stands (corresponding with the ‘Ecological Phase’) really match the assumptions of the model.

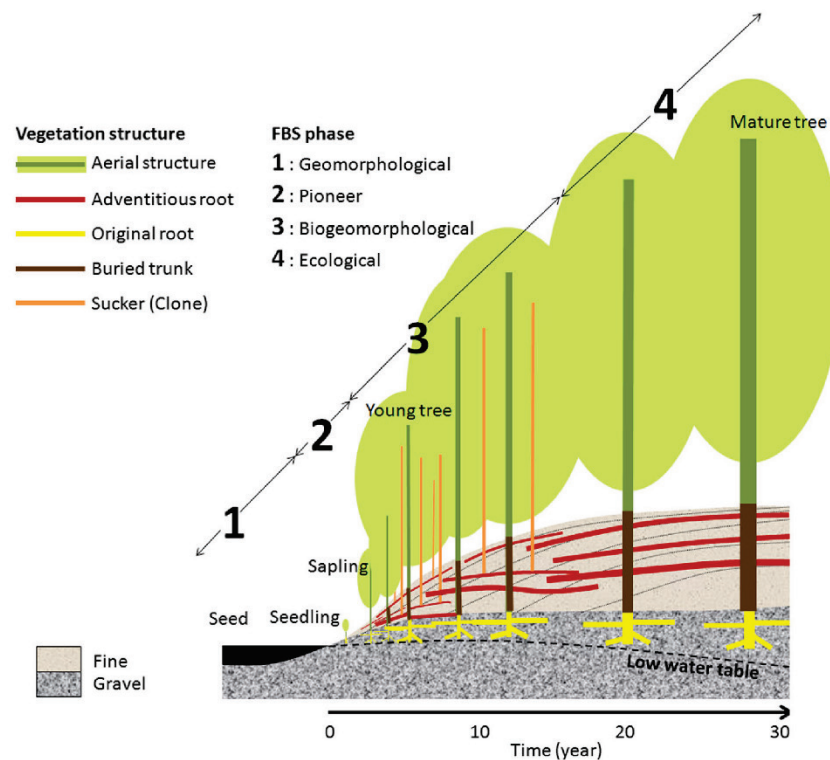


Figure 6.1 Spatiotemporal sequence of the four phases of the fluvial biogeomorphic succession model of riparian poplar ecosystem engineering. Corenblit et al. (2014)

The hitherto unknown depth, longevity and growth of buried stems and associated roots have major implications for landform stability and turnover. Should such structures be deep, well-anchored and active, hysteresis in the BGS cycle and landform stability will be more likely, with increased resilience against returning to the initial states of bare gravels and pioneer vegetation. In the event that mature trees are able to withstand major disturbances and avoid wholesale removal from the landforms established in association with their presence, the earlier stages of the BGS cycle are effectively bypassed, and the resulting buried stem and root architecture is likely to be dramatically altered. Locally, even small patches of resilient trees under repeated disturbance and burial may constitute recalcitrant 'hard points' in the floodplain (*sensu* Collins et al., 2012), acting as nuclei for long-term island survival. Such a phenomenon, described by Collins et al. (2012) for rafts of dead wood associated with decomposition-resistant conifers in the Pacific Northwest of America, would be unlikely to occur in rivers where Salicaceae such as poplars are the dominant ecosystem engineers, unless buried wood remained alive and able to resist degradation.

Coarse root structures are also of importance to the transport and deposition dynamics of trees. Ease of erosion and entrainment is clearly related to the form of the root system and associated strength of its anchorage within the banks of islands and floodplain margins. Furthermore, attached root structures affect the deposition and retention of mobilised wood (Bertoldi et al., 2014) as well as the orientation of wood upon deposition and the resulting volume of gravels scoured and organic material trapped (Ravazzolo et al., 2015), with knock-on effects for the early stages of island formation.

Given the many and varied ways in which the gross root architecture of riparian trees may influence the dynamics of both fluvial landforms and riparian vegetation, there are clear gains to be made in developing understanding of their potential forms and the processes by which they are generated. Of course, predictive plant-focused developmental models (see, e.g., Collet et al., 2006) would be of great value, particularly considering the effort required for the excavation and study of large root systems. However, even if such models explicitly accounted for the dramatic heterogeneity in soil resources, it is likely that they would be of very limited application in the present context, where physical disturbance plays such a pivotal role. It is hypothesised that survival of exhumation, displacement and other forms of disturbance results in peculiar, variable and largely unpredictable sub-aerial forms. It remains to be seen how much of the original structures survive these events.

The research presented in this chapter represents a first step in describing and understanding the diversity and common features of sub-aerial structures of riparian black poplar. This is achieved through detailed study of the root systems of eight case study trees, coupled with

additional observations of rooting patterns and buried livewood from the central island-braided, gravel bed reaches of the Tagliamento River in northeast Italy.

6.1.1 Research questions

Specific questions addressed in this chapter are as follows:

- i. To what extent do current models of root system development – particularly those assumed in the fluvial biogeomorphic succession of Corenblit et al. (2007) – agree with field observations of coarse root structures along the central Tagliamento River?
- ii. How extensive is buried poplar livewood in the Tagliamento River system?
- iii. What common features are shared by all riparian poplar coarse root systems?
- iv. To what extent are the sub-aerial structures of riparian trees influenced by flood events and hydrogeomorphological change?
- v. Is it possible to reconstruct the development of coarse root architecture from available information on river flow, sedimentation and hydrogeomorphological change?

6.2 METHODS

6.2.1 Field methods

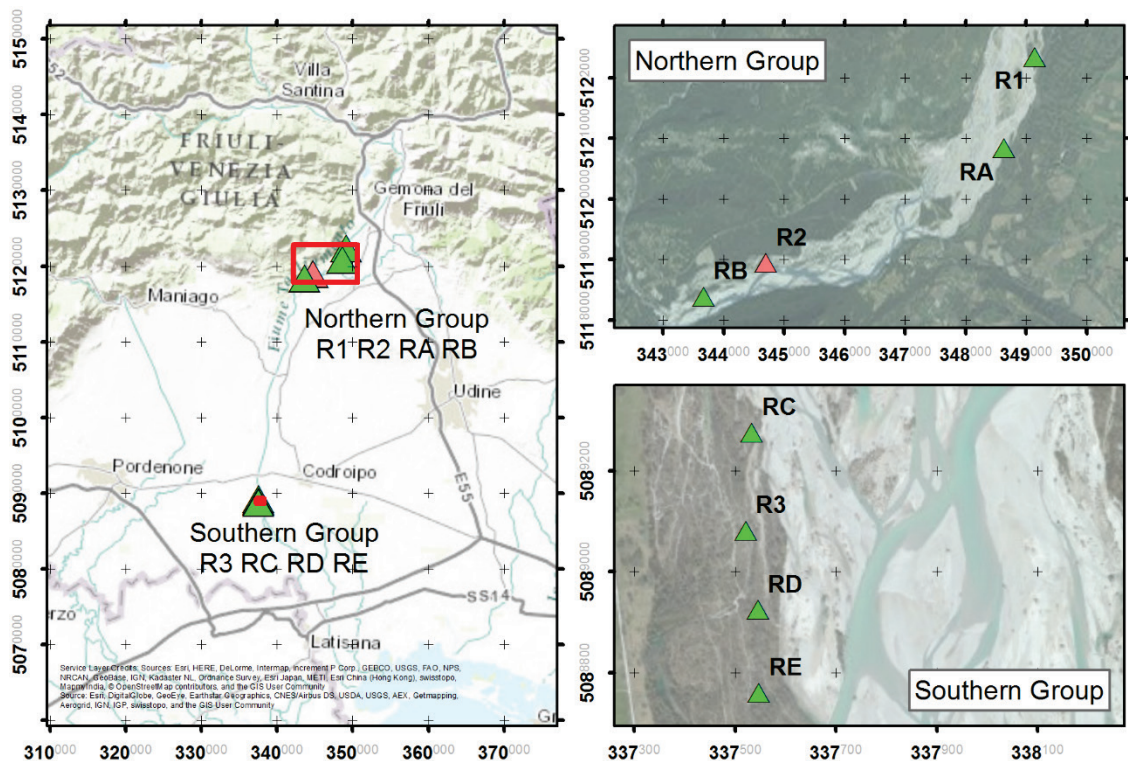


Figure 6.2 Locations of case study poplar trees. Reference grid values are UTM eastings and northings in m. Only a partial dataset is available for case study R2.

The root systems of eight mature poplars situated on eroding banks of the Tagliamento River were excavated in two separate field campaigns: July – August 2014 (trees R1 – R3), and March 2015 (trees RA – RE). The trees were located within the same areas as the studies reported in Chapters 4 and 5, and so were in two geographically distinct clusters, hereafter referred to as the North and South Groups. This subdivision ensured that the trees were subject to the differences in moisture availability and sediment calibre and complexity previously identified in these two areas. Note that the North Group case study trees were much more widely distributed than the South Group.

Twenty candidate trees were identified in initial walk-over surveys, and each was scored according to the ease of access for excavation (1, 2, or 3) and the apparent complexity of bank sediment profile (1, 2 or 3). The highest ranking trees according to the sum of scores (with ‘ease of access’ given half the weighting of apparent complexity of the bank sediment profile) were selected for excavation, which was carried out according to the procedure outlined in Chapter 3. In summary, the dimensions and location of each tree were recorded before sediments were excavated to expose a minimum of half of the root system, trimming back smaller roots in the process. The excavated structures were then photographed from multiple angles for photogrammetric modelling (mean 217 JPEG images per tree). Cores and sections were taken for tree ring dating of various key points on the buried structures. Finally, the extent and broad sediment calibre class (occurrence of silt, sand, gravel and pebbles) of the main strata within the exposed sediments were visually assessed and recorded.

A moderately large flow event (1.19 m stage recorded at Villuzza) occurred during excavation works on 13th of August 2014, resulting in the re-burial and destabilisation of R2 and a fourth tree (R4). Work on the latter was abandoned, but it was possible to collect a partial dataset from R2.

Note that upon burial, annual growth rings often become indistinct (see, e.g., Friedman et al., 2005), and this phenomenon was frequently encountered here. In consideration of this, together with errors associated with sample collection and preservation, ages estimated from wood cores and slices represent minima, and thus wood structures must have established on or before any dates reported.

6.2.2 Data analysis

The geometry of buried structures was recorded by creating three-dimensional models using a commercial Structure from Motion (SfM) photogrammetry interface (Agisoft PhotoScan 1.1.6; see Appendix D for further details). The method was initially trialled with root systems

where finer roots were not trimmed, but the point-matching algorithm was not able to run successfully in these cases.

Historical contextual information on the trees was obtained from available daily mean river stage records from Villuzza (46.181° N, 12.958° E; January 1982 – October 2014, see chapter 3 for further information on this monitoring station) and aerial imagery (see Table 6.1). Hereafter, all water surface heights reported are as recorded at the Villuzza gauge.

In order to identify likely periods where the case study trees may have established, a modified version of the ‘recruitment box’ model of Mahoney and Rood (1998) was applied to the stage record. The main modification was to remove the condition for a particular time window (originally included to represent seed release and viability), thereby extending the model to capture potential recruitment from vegetative propagules, assuming that root growth rate was still the main limiting factor in these cases. The possibility of faster root growth due to mobilisation of larger carbohydrate stores in deposited wood (Francis et al., 2006, Francis, 2007) is acknowledged, but the original, conservative growth rate was retained here in order to continue to account for seedlings to a certain extent. Recruitment was assumed most likely when all of the following conditions were satisfied:

- Declining water level at a rate no greater than 25 mm d⁻¹ (maximum root growth rate)
- Period of at least 300 days to next flood above 2.5 m (complete growing season)
- Water surface elevation between one and two metres (elevation band balancing moisture availability and flood disturbance probability, assuming summer base flow stage of 0.5 m)

The southern cluster of trees was approximately 28 km downstream of the Villuzza monitoring station, and channels in the intervening reach lose water to the alluvial aquifer (see Chapter 3). The tree located furthest upstream (R1, at 10 km) was also in a losing reach, but close to a small spring. Owing to these complications, the Villuzza record is not assumed to be an accurate representation of stage fluctuations at all sites. However, it was assumed adequate for identifying the largest peak flows and their timing.

Bertoldi et al. (2009) have previously identified critical water surface levels for biogeomorphic activity in the North Cluster, using the same Villuzza stage record. Bankfull stage is considered to be approx. 3.0 m, at which point all island surfaces are inundated and there is often extensive erosion of large trees. At approximately 2.5 m, the active width approaches 50 % that of total potential, and there are many and variable changes around vegetated patches in the active channel. While even relatively modest peak flow events (circa 1.0 m) are capable of causing morphological change in this reach, the most significant

interaction with vegetation occurs at these higher elevations, and so these values were used to identify important floods for the purposes of the present analysis.

Ortho-rectified aerial and satellite images were obtained from a number of sources (Table 6.1) and visually compared in order to track the establishment and erosion of vegetation, as well as any obvious sediment or tree deposition. A subset of images showing the most significant changes is presented in Section 6.3.2, and all the images listed in Table 6.1 may be found in Appendix C.

Table 6.1 Sources and dates (where known) of aerial and satellite imagery analysed.

Image ID	Date	Source
1944-07	July 25, 1944	The Aerial Reconnaissance Archives, Keele University
1946-??	<i>No date available</i>	The Aerial Reconnaissance Archives, Keele University
1954-04	April 11, 1954	Istituto Geografico Militar
1954-05	May 15, 1954	Istituto Geografico Militar
1966-11	November, 1966	Autorita` di Bacino dei fiumi dell'Alto Adriatico
1970-??	<i>No date available</i>	Autorita` di Bacino dei fiumi dell'Alto Adriatico
1986-12	December 24, 1986	Istituto Geografico Militar
1988-11	November 21, 1988	Regione Friuli Venezia Giulia
1991-10	October 8, 1991	Rossi s.r.l. REVEM Brescia
1993-05	May 10, 1993	Regione Friuli Venezia Giulia
1993-07	July 16, 1993	<i>Original source unknown</i>
1996-??	<i>No date available</i>	AIMA del Ministero delle Politiche Agricole Alimentari e Forestali
1997-06	June 16, 1997	Autorita` di Bacino dei fiumi dell'Alto Adriatico
1997-09	September 16, 1997	Autorita` di Bacino dei fiumi dell'Alto Adriatico
1999-09	September 11, 1999	Autorita` di Bacino dei fiumi dell'Alto Adriatico
2001-04	April 9-13, 2001	Autorita` di Bacino dei fiumi dell'Alto Adriatico
2002-07	July 21, 2002	DigitalGlobe
2002-09	September 14, 2002	DigitalGlobe
2002-11	November 30, 2002	Autorita` di Bacino dei fiumi dell'Alto Adriatico
2003-09	September 14/27, 2003	Regione Friuli Venezia Giulia, DigitalGlobe
2005-05	May 23, 2005	Natural Environment Research Council UK
2006-06	June 13, 2006	Department of Geography, University of Padova
2007-04	April 12, 2007	Department of Geography, University of Padova
2008-06	June 25, 2008	European Space Imaging
2009-05	May 14, 2009	Department of Geography, University of Padova
2011-05	May 19, 2011	DigitalGlobe
2012-03	March 2, 2012	DigitalGlobe
2012-10	October 23, 2012	Department of Geosciences, University of Padova

6.2.3 Qualitative and secondary observations

Given the extensive time and resources required for excavating entire root systems (see, e.g., Smit et al., 2000, Danjon and Reubens, 2008), fieldwork conducted in 2014 and 2015 was also supplemented with observations made by the author during surveys of trees and landforms on the River Tagliamento during 2012 and 2013, and by A.M. Gurnell and colleagues during regular field campaigns between 2002 and 2015. A selection of these observations, supported by photographs, is presented and discussed in Section 6.3.3, below.

6.3 RESULTS

For each of the case study trees, an annotated screen capture of the SfM point cloud is first presented and key features of the buried structures are described. The panel on the right of these figures indicates presence of various mineral particle size classes in the main strata below the main stem (unless otherwise indicated); whether or not the sediment is strongly consolidated or loose (filled or empty box, respectively); the presence of organic inclusions; and of orange patches due to oxidation of iron. Some images have been mirrored to maintain a consistent river flow direction in all figures, which is left to right. Red markings on the staff(s) are found every other 50 cm. Further screen captures from the SfM analysis, including different viewpoints of the point clouds and triangulated surface models, are presented in Appendix D.

Major changes in the vegetation structure and channel migration in the vicinity of the tree are then described using selected aerial images. Image excerpts are oriented with north at the top. Inset in each figure is an approximate date, scale bar, miniature cropped hydrograph indicating the timing of the image (red line and circle) with respect to major floods (red (> 3.0 m stage) and orange (> 2.5 m) square symbols), as well as a larger scale magnification, the extent of which is indicated by the outline on the main image.

Tree ring age estimates (latest year of origin) are then indicated on the SfM screen capture, and finally a discussion section attempts to link all the observations, and presents a summary diagram of a proposed trajectory of development of the structures unearthed. In these diagrams, the colour-coded event summaries relate to the colour of the image mark-up.

6.3.1 Recent formative flood events

Over the period of the Villuzza record (Figure 6.3), bankfull events occurred in 2004, 2002, 2000, 1996, 1993, 1990, 1984 and 1982, with no severe flood of this magnitude (> 3.0 m) in the last ten years. Fourteen smaller but biogeomorphologically important events (> 2.5 m)

occurred, while 2013, 2005, 2001, 1997, 1994-5 and 1986 were notably ‘quiet’ years (NB. There were several gaps in the stage record up to 1993).

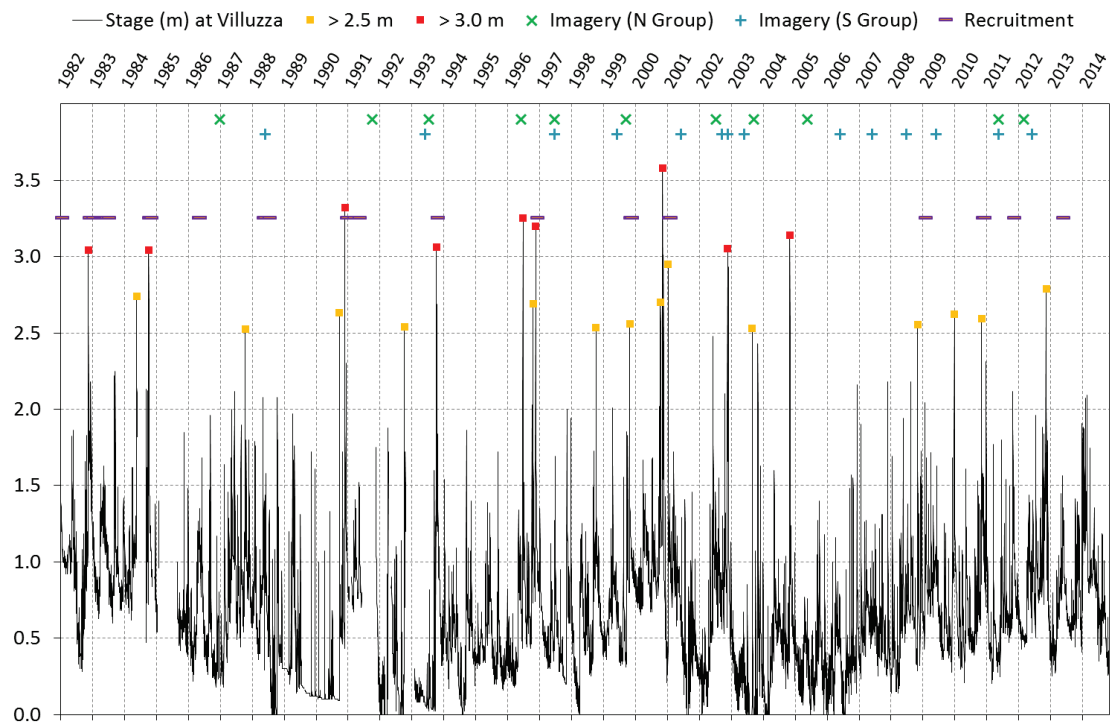


Figure 6.3 Daily average stage record from January 1982 to October 2014 recorded at Villuzza. Biogeomorphologically significant peaks are identified and availability of aerial imagery is indicated. Periods with stage patterns suitable for recruitment of vegetation as identified using the modified ‘recruitment box’ model are indicated at the 3.25 m line.

Most of the severe floods occurred in October and November, with one notable exception in the summer of 1996. These autumn floods were usually part of a cluster of flow peaks, with the exception of late October 2004 (Figure 6.4). The floods of November 2002 were the longest in duration, with approximately 5 days of inundation above 2.5 m.

The recruitment modelling identified suitable periods for vegetation establishment more-or-less every two-to-three years (Figure 6.3). Between 2001 and 2009, however, flow conditions appeared to be less favourable.

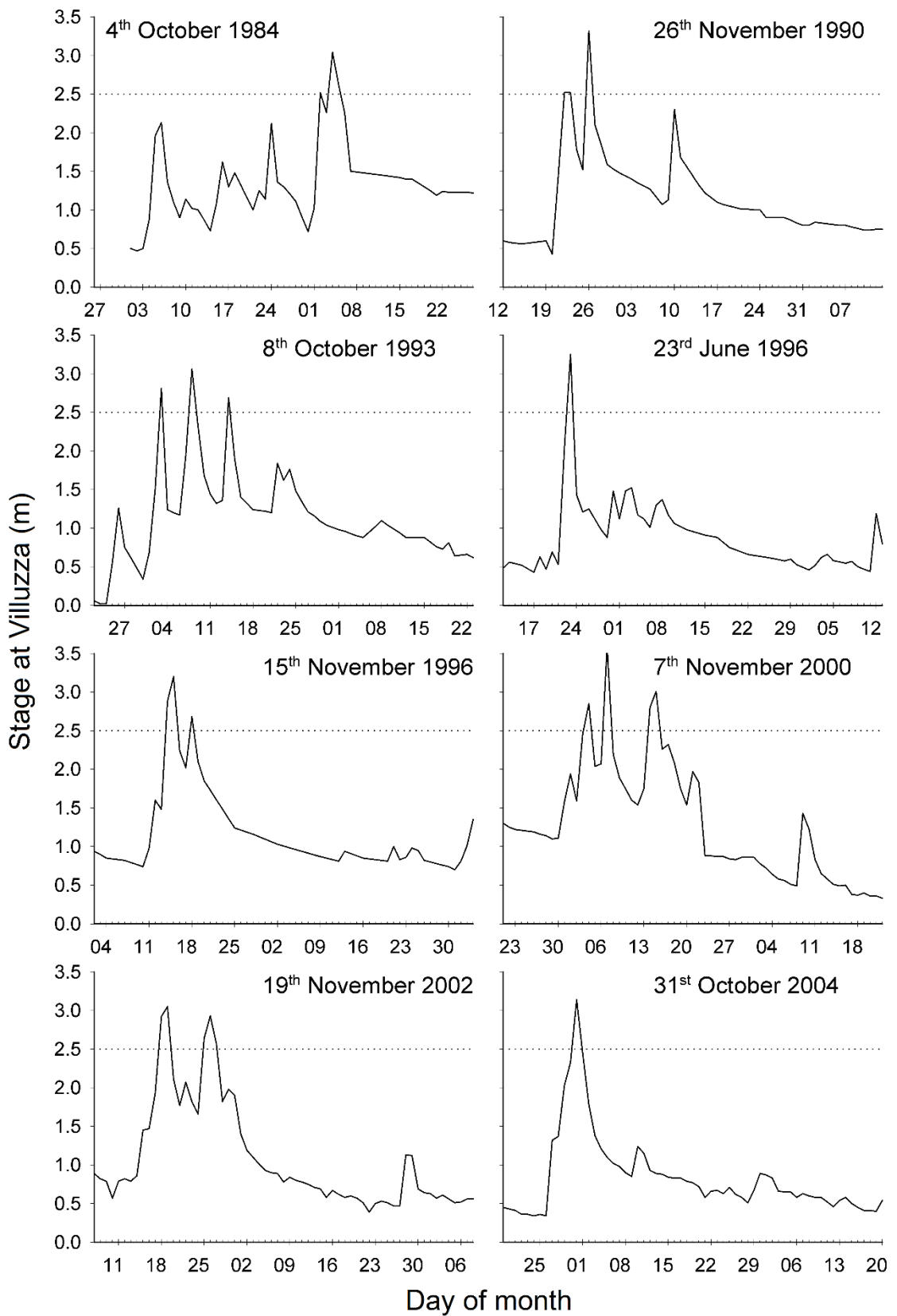


Figure 6.4 Hydrographs of the eight most recent large floods (> 3 m at Villuzza). The 2.5 m stage line (nominal threshold for significant interaction with vegetation) is plotted for reference.

6.3.2 Case studies from excavations

a Summary information for case study trees

The main stems of all the trees excavated were of a similar age and size (

Table 6.2), though average growth rates were more variable. Closely associated pairs of stems were often encountered. An overview of the trees and their roots is provided in Figure 6.5 and Figure 6.6. Note that in these Figures, none of the images has been mirrored, but mirroring has been used to orient images such that upstream is left and downstream, right, when the case study trees are discussed individually in subsections 6.3.2 b onwards. Unfortunately it was not always possible to get far enough from the tree to photograph its full height for Figure 6.5 and Figure 6.6.

Table 6.2 Key features of aerial stems of the case study trees. Where there are two main stems, measurements relate to the larger.

Case Study ID	Number of stems	Stem age at 1.2 m (a)	Diameter at 1.2 m (cm)	Stem length (m)	Radial growth rate (mm a ⁻¹)	Vertical growth rate (m a ⁻¹)
R1	1	20	23	17	5.8	0.9
R2	1	13	15	13	5.8	1.0
R3	2	14	16	11	5.7	0.8
RA	1	19	13	13	3.4	0.7
RB	1	12	12	13	5.0	1.1
RC	2	16	20	13	6.3	0.8
RD	1	13	15	13	5.8	1.0
RE	2	17	15	17	4.4	1.0
<i>Mean</i>		15.5	16.1	13.8	5.3	0.9

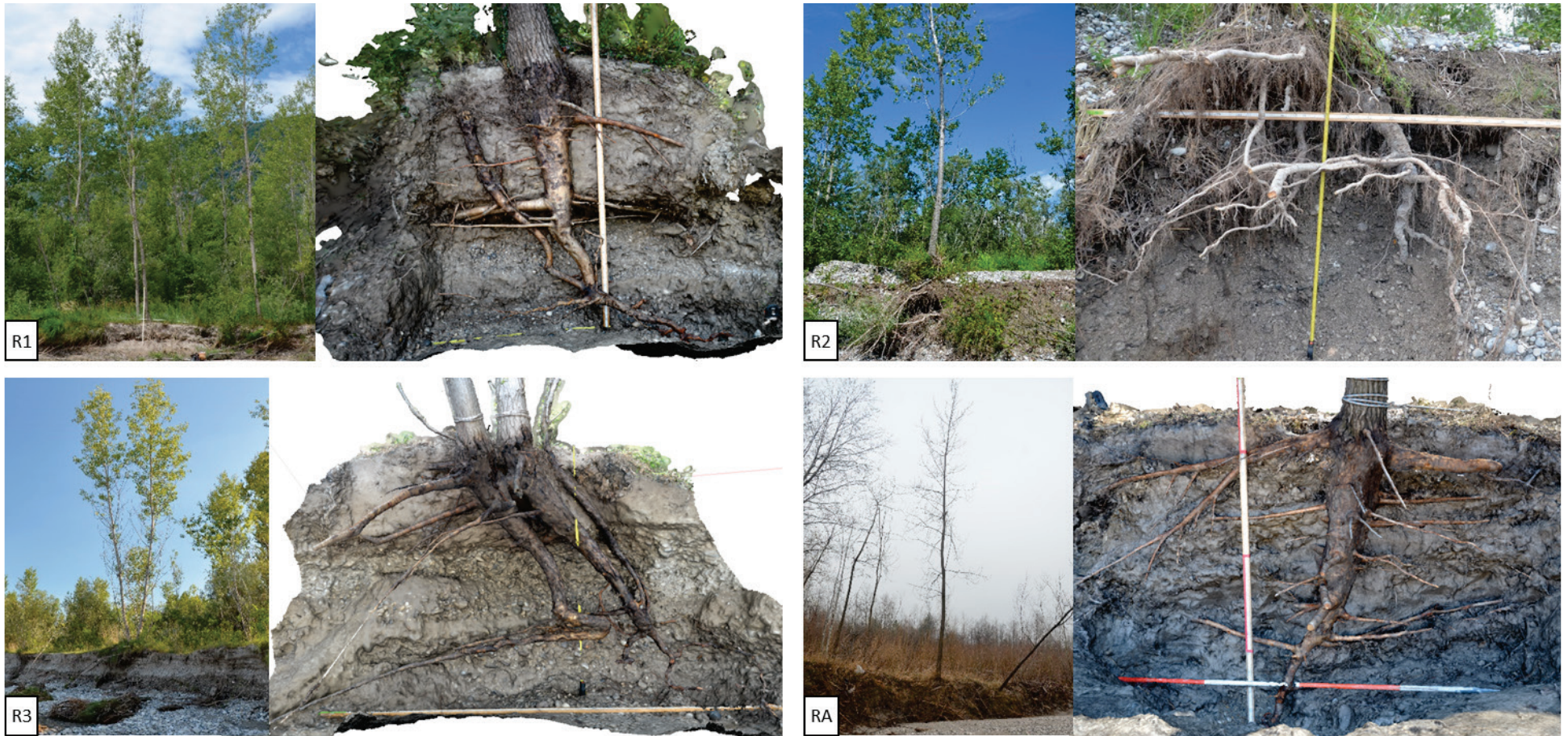


Figure 6.5 Case study trees R1-3 (sampled summer 2014) and RA (sampled early spring 2015). A wide angle photo is presented alongside a screen capture of the SfM model (except in the case of R2). Flow in the main channel is from right to left in all cases except RA.

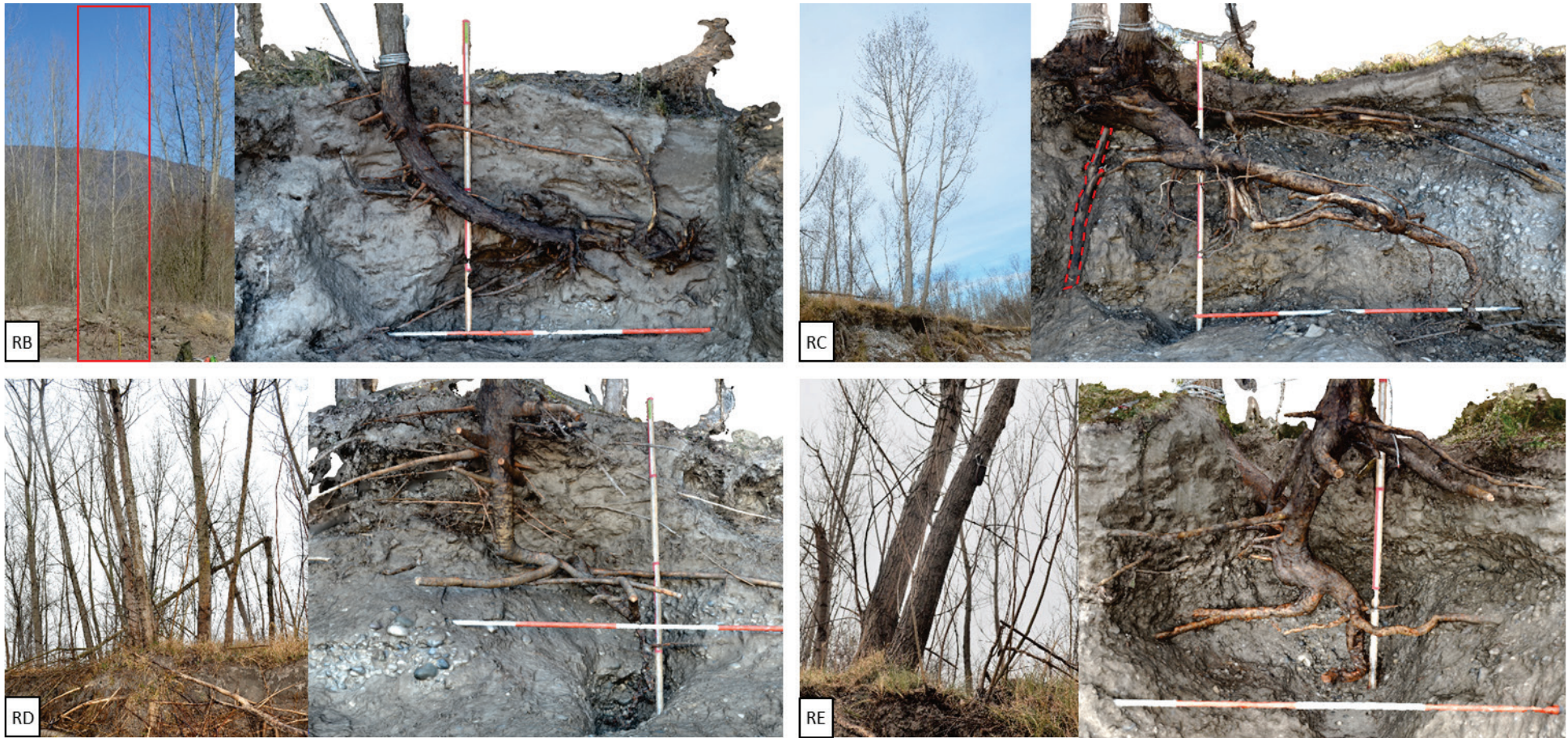


Figure 6.6 Case study trees RB-RE (sampled early spring 2015). A wide angle photo is presented alongside a screen capture of the SfM model. Note that none of these images have been mirrored. Flow in the main channel is from right to left in all cases. The component outlined in red in the RC model is a prop installed during excavation.

b Case study “R1”

Overall form, key features and sedimentology



Figure 6.7 Front perspective view of R1 model with key features and main sedimentary strata identified.

Above-ground, this tree had a single stem of 17 m and 23 cm DBH. Describing the structure down from ground level, the main axis had three main parts: a relatively upright, large diameter section with horizontally-radiating laterals (A); a slightly curved section with few laterals, pointing downstream (B); and a straight section lying at approximately 30° to horizontal (C). There was a proliferation of lateral roots from the junction of sections B and C, and a subsidiary stem (D) originating from the distal end of section C, which had died and no longer emerged at ground level. One particularly large lateral root is also noteworthy (E). The cavity below the junction of A and E was caused by loss of unconsolidated gravels during excavation. Gravels were found only at the lowest elevations, except for a seam coincident with section B, which also included organic debris.

Vegetation and channel change from aerial imagery

All available aerial images are presented in Appendix C, but the most significant changes over the period of the flow record in the locality of this case study tree are presented in the images below. Flow is from top (north) to bottom.

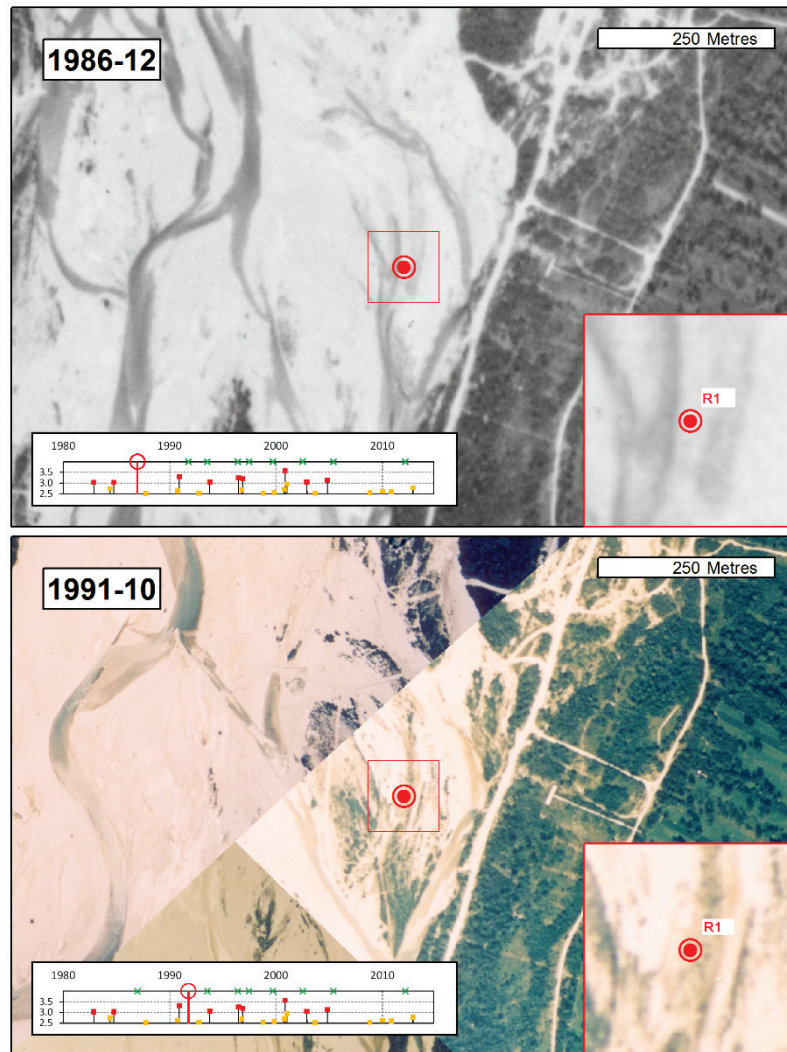


Figure 6.8 Key aerial images of the R1 neighbourhood, 1986-1991. Image sources in Table 6.1.

In the December 1986 image, the site was bare of vegetation, but on the margin of a channel which was seeping from the gravel. By October 1991, low and sparse vegetation had established along the lines of the channel margins. The channel configuration around the vegetated patches was broadly the same as in the image taken four years earlier.

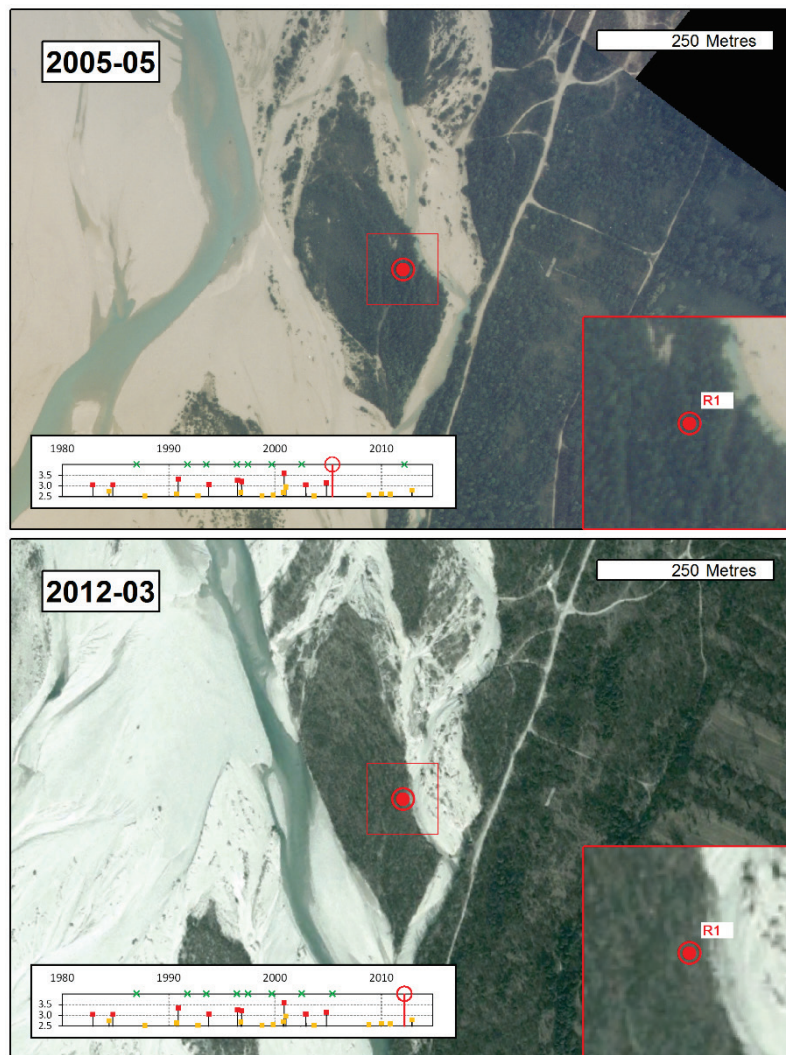


Figure 6.9 Key aerial images of the R1 neighbourhood, 2005-2012. Image sources in Table 6.1. Lower panel © 2015 DigitalGlobe.

Fourteen years later, in May 2005, the patches of vegetation had matured and coalesced to form a distinct island. The path of one or two earlier channels is visible through the middle of the island, and it is likely that these relict channels flowed in times of flood. The northeast edge of the island had begun to be eroded by a side channel which separated it from the unbroken floodplain forest to the east by a reasonably open gravel expanse. Further erosion was evident on the eastern margin of the island in March 2012, and also on the western edge of the downstream tail, adjacent to where the main channel had migrated. It is likely that the bank erosion which exposed the buried structures of this tree occurred in the flood experienced later in that year (12 November 2012, 2.79 m).

Age structure

The latest possible dates of origin of various parts of the root system, determined from annual rings in cores and sections, are presented for the main axis (A) and lateral roots and subsidiary stem (B) below.

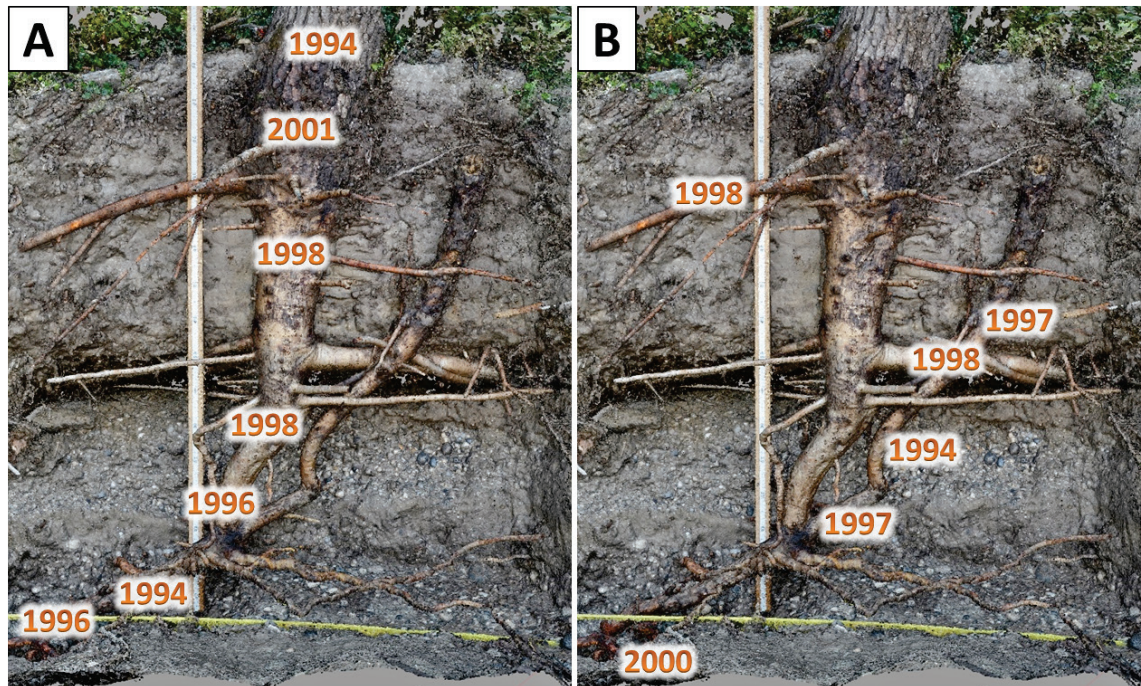
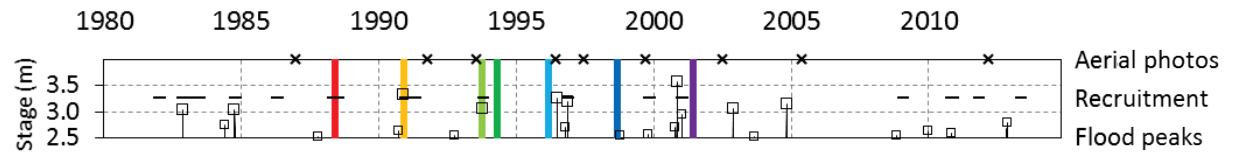
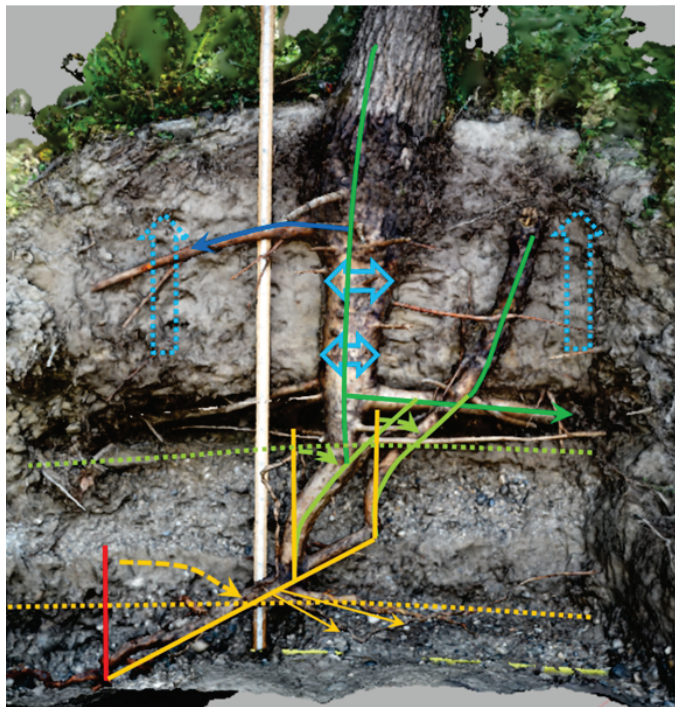


Figure 6.10 Estimates of latest possible dates of origin of different parts of the main axis (A) and lateral roots and the subsidiary stem (B) of the R1 root system, from dendro-chronological analysis.

The oldest part of this root system appeared to have established in or before 1994. This limiting date was associated both with the basal part of the main axis and the stem at 1.2 m from the ground surface, as well as the lower part of the subsidiary stem. The large lateral root appeared to date to 1998 or earlier.

Discussion and summary

The presence of two, connected, downstream-deflected sections and two distinct gravel deposits suggests that development of this tree's coarse root system was due mainly to two large floods. It is proposed that the extant components originated near the lower limits of the excavation (just above the water table at the time of sampling) and the main axes are buried stems, as opposed to taproots. The length and shape of the lower deflected section suggests that the sapling was at least one metre tall and quite inflexible at the time of the first flood. With the main stem having been knocked down and mostly buried in gravels, lateral buds or existing small branches near the new bar surface would have become the dominant vertical stems. Two of these stems survived to the time of excavation. Perhaps only a few years later, a second disturbance event again caused a deflection and burial of the two surviving stems. This timing is suggested by the limited accumulation of fine sediments beneath the second gravel layer and the fact that the new stems must still have been flexible enough to result in the curve evident in these components. Following these relatively violent events, the deep and upwardly fining sediment deposited is consistent with an increasingly sheltered site and increasingly dense vegetation, as demonstrated by the aerial imagery. The limiting 1994 date of the extant (undeflected) above-ground trunk dictates that both floods must have occurred before this time, which makes the flow events of late 1993 and late 1990 the most likely candidates. Consequently, the growth season of 1988 would appear to be a probable period for the original establishment of this case study tree (identified from recruitment modelling).



Aerial photos show channel margin colonisation between 1986 and 1991. Recruitment model suggests 1988 a good year, though oldest roots only pre-1994. However, original roots may have died.

Stem knocked down by flood. Gravel deposited. Two surviving vertical shoots carry on up from lateral buds. Horizontal roots track along top of gravel as fines are deposited above

Two stems deflected by flood and embedded in further gravel deposits

Lateral bud becomes dominant on upstream shoot as apex dies back. This new shoot sends out major new adventitious roots into accumulating fines. So does downstream shoot, but to a lesser extent

Site becomes increasingly sheltered as vegetation thickens considerably. Fine sediment accumulates

Highest large lateral root from main stem

Growth and deposition slow as canopy closes

Figure 6.11 Summary of the proposed potential development trajectory of case study R1. Text box colours relate to events marked on the SfM model and timeline.

c Case study "R2"

As described above, a high flow event resulted in bank slumping and the re-burial of this case study during excavation. As a consequence, not all the structures were easily visible, no SfM model was produced and fewer dendrochronological samples were taken.

Overall form, key features and sedimentology

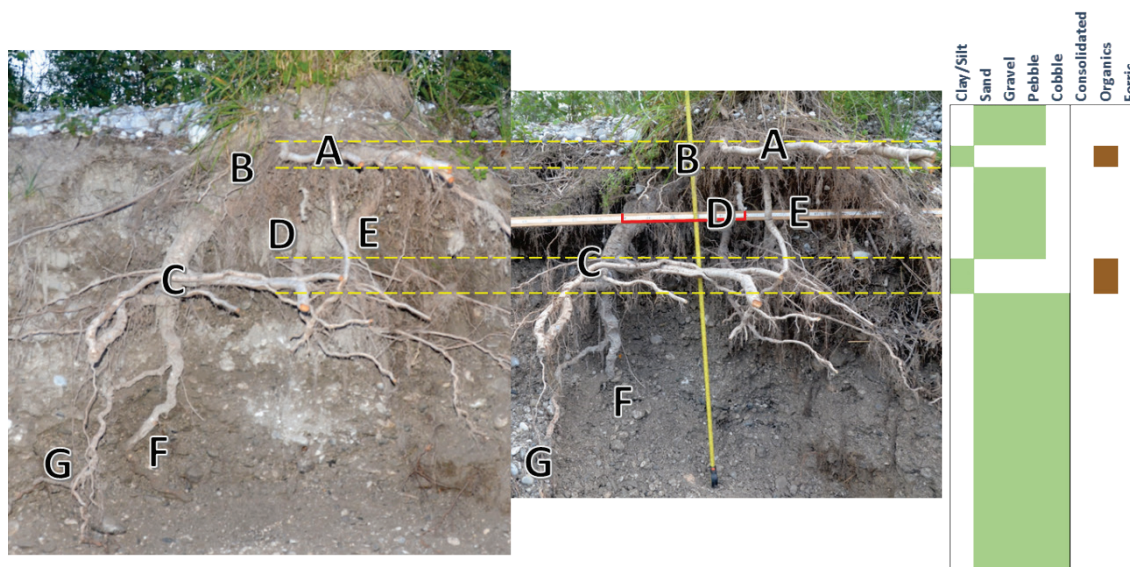


Figure 6.12 Two images of the R2 root system at a later (left) and earlier (right) stage of excavation, with key features labelled and main sedimentary strata identified.

The lean on this single stem of approximately 13 m length and 15 cm DBH suggested that the bank had previously slumped slightly, and this was exacerbated by further erosion when the site was inundated during excavation. Just below the base of the main stem, the main buried axis was initially almost horizontal, lying on top of or just within a narrow band of fine sediment (A-B). Many lateral roots of considerable size emerged from what appeared to be a node on the main axis at A. Below the near-horizontal section was a portion with a downstream lean of around 35° from the vertical (B-C), defined at its base by another node with prolific lateral roots (C) emerging into a second narrow fine sediment layer. Many of these horizontal adventitious roots were weakly grafted to each other. Below the upper near-horizontal portion of the main axis were at least two stout, near vertical roots (D and E), which are slightly more easily visible in Figure 6.13. Below the second fine sediment layer, the main axis took a wandering, near-vertical course through the gravels (F), down beyond the limits of excavation, with one notable lateral (G), which also followed a downward course.

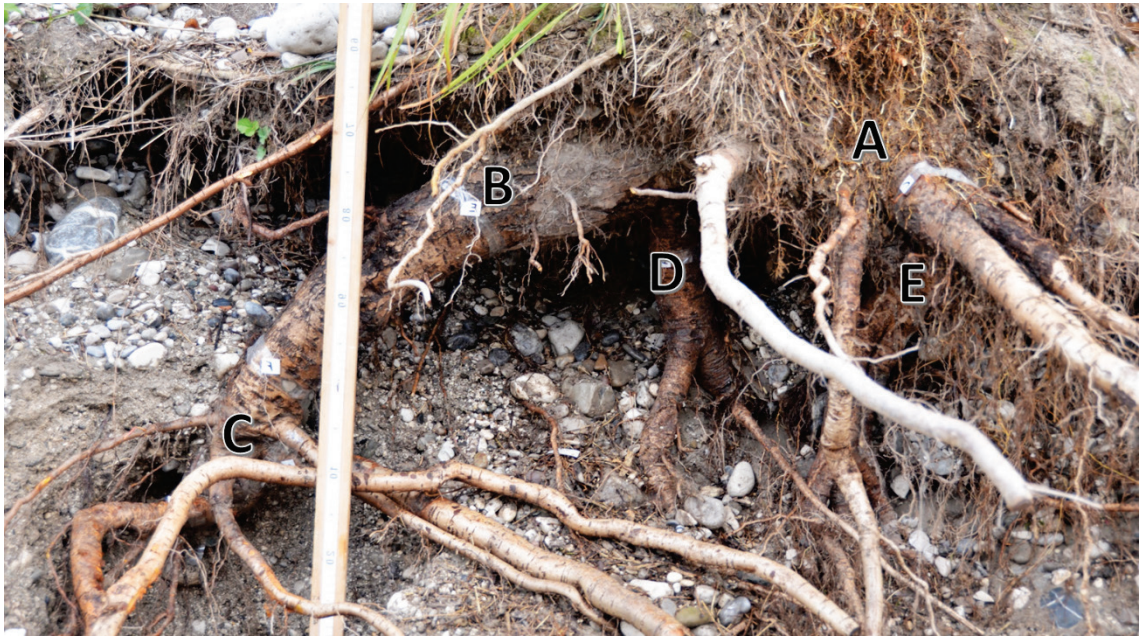


Figure 6.13 Detail of the upper part of the R2 root system, with key features labelled as in the preceding figure. Note that this was taken after the flood and subsequent slumping of the bank. Length of measuring staff visible is approx. 0.75 m.

Vegetation and channel change from aerial imagery

Major changes over the period of the flow record are presented below. All available images are presented in Appendix C. The main channel flows from right (east) to left.

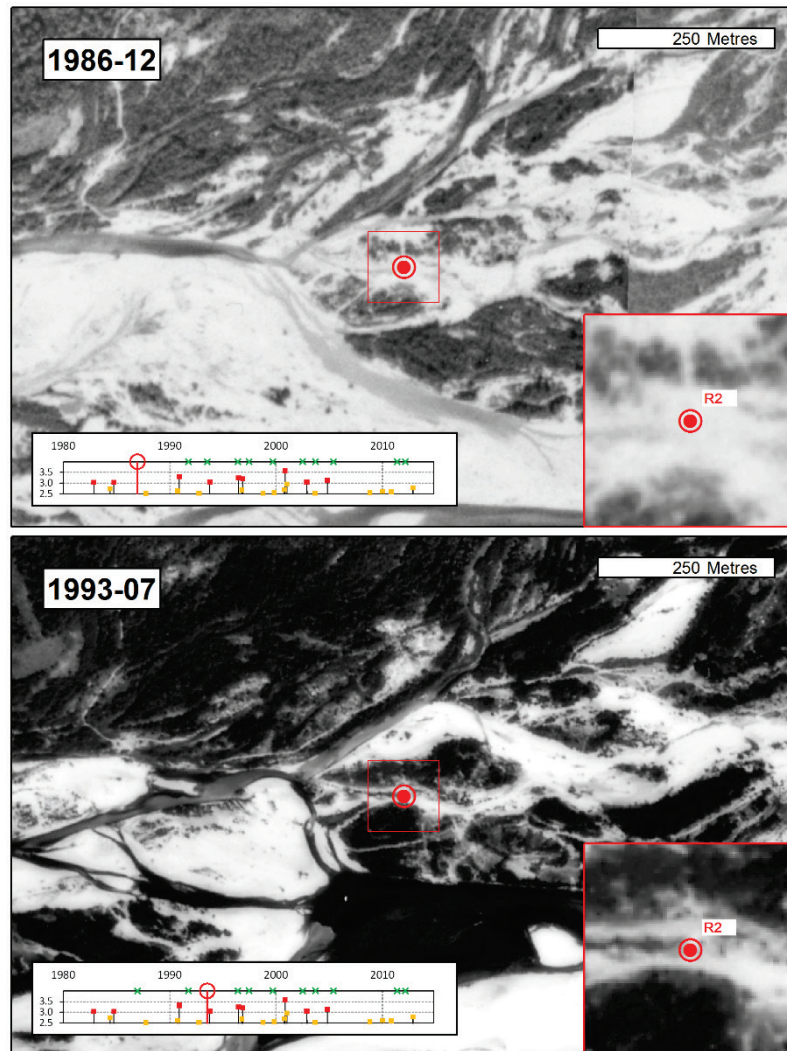


Figure 6.14 Key aerial images of the R2 neighbourhood, 1986-1993. Image sources in Table 6.1.

The site appeared in 1986 to be on or adjacent to (geolocation of this image is subject to at least five metres of error) what was probably an intermittently flowing channel (note the difficulty of distinguishing small areas of water and vegetation in this grayscale image) which bisected a patchwork of vegetation of various different stages of maturity. By 1993, sparse vegetation patches in the area had thickened and were at the early stages of island formation. Again, it was difficult to determine whether the dark area in the exact location of the case study tree was a wet area or vegetation. Its irregular edge hints at vegetation, however.

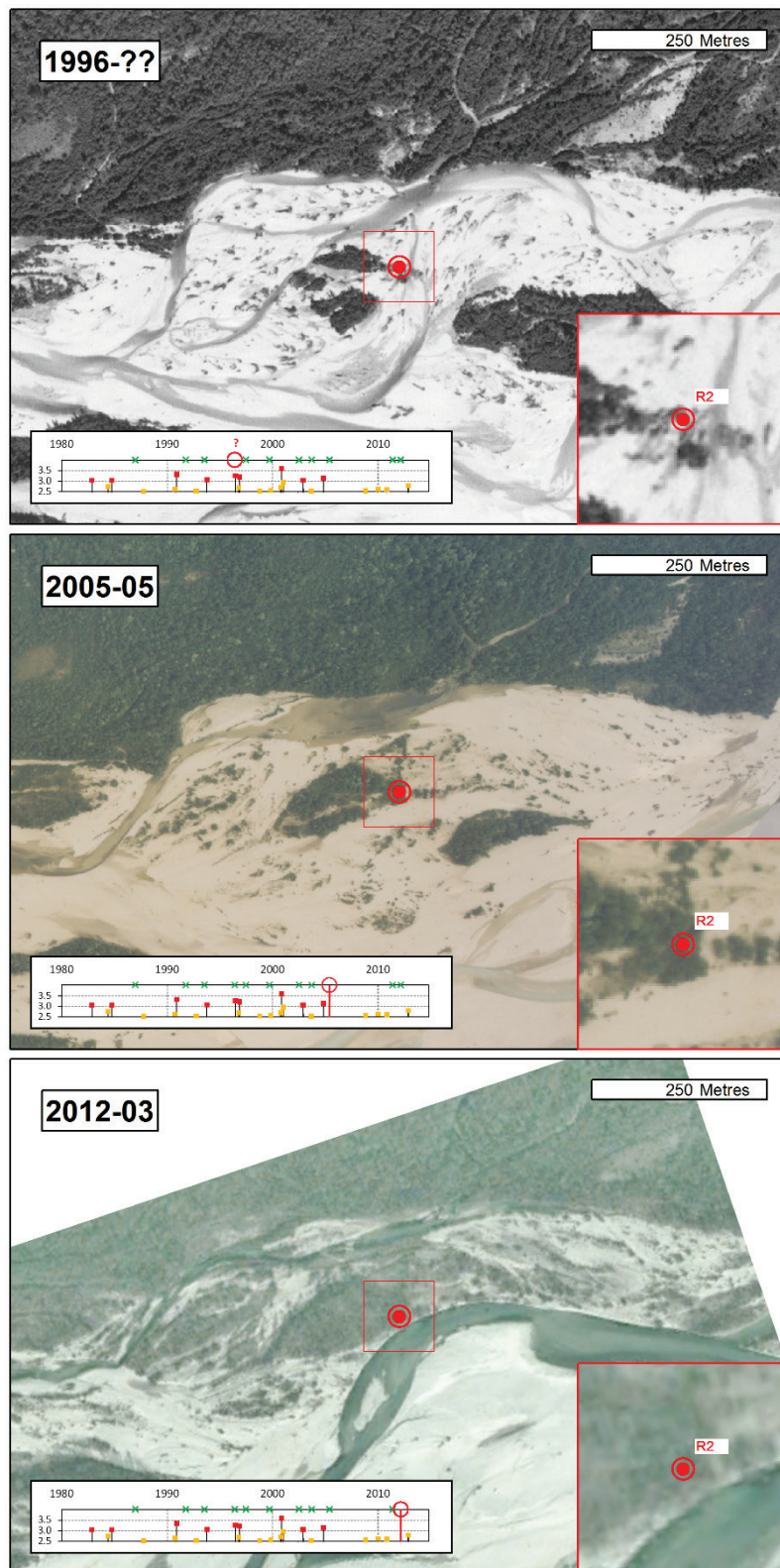


Figure 6.15 Key aerial images of the R2 neighbourhood, 1996-2012. Image sources in Table 6.1. Lower panel © 2015 DigitalGlobe.

The 1996 image appeared to show recent island turnover and scattered deposition of eroded trees, presumably due to the late summer flood of that year (June 23rd, 3.25 m). The large upstream lobe of the island as it appeared in the previous image had been completely

removed. The case study tree may have been among the survivors of this event, which in 1996 formed an upstream prominence of the island remnant. Nine years later, in 2005, channels between the three small islands in the vicinity had in-filled and become colonised with trees, resulting in one larger island, albeit with a channel remnant still visible. The four large (> 3.0 m) flood events in the intervening period appeared to have kept colonisation of the open gravels to a minimum, interrupting the biogeomorphic succession from deposited trees at the pioneer island stage. Most of the large island to the southeast of the area of focus had been eroded away as a bend of the main channel of the Tagliamento migrated north- and westwards. Progressive migration of the river's main channel had entirely eliminated the island to the south and east by early 2012, and had begun to encroach on the island of focus. In the absence of large floods, there had been expansion of vegetation between the pioneer islands visible in 2005.

Age structure

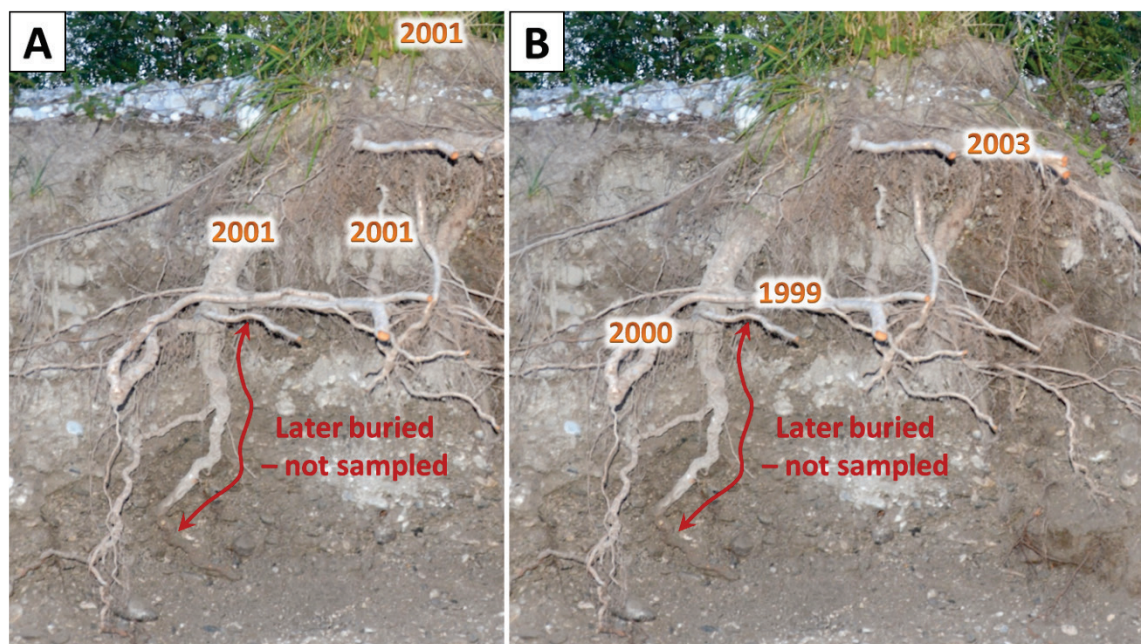


Figure 6.16 Estimates of latest possible dates of origin of different parts of the main axis and supporting vertical root (A) and lateral roots (B) of the R2 root system, from dendrochronological analysis.

Though it was only possible to take a few wood samples from this tree, 1999 (lower set of laterals in Figure 6.16) appeared to set a limiting date on its origin. This main buried axis was established before 2001, and the upper set of laterals, by 2003.

Discussion and summary

Examination of the aerial imagery alone might suggest that this is an interesting example of the establishment of a line of vegetation in fine (lentic) deposits at the bottom of a channel relic, *sensu* Stella et al. (2011). This is in contrast to other patterns of linear establishment on channel margins and locally elevated areas such as ‘scroll bars’ (Ward et al., 2002, Hupp and Rinaldi, 2007) and natural levées formed by overbank deposition (Steiger et al., 2001, Gurnell, 2014). Though subject to interpretation, the imagery does appear to show this phenomenon, but the root samples of the case study tree date it to a later phase in the history of this site. Instead, it is proposed that this stem originated on top of coarse bar deposits in 1999, at the elevation of ‘C’ in Figure 6.12. Given the well-established vegetation at the site at this time, it seems plausible that this was a sucker from adventitious roots expanding into the fine silt and clay deposits which had accumulated in the absence of any severe flooding since 1996, existing vegetation having acted to slow over-bank flows. The crooked path of the main axis below this point, and the angle of branching with the lateral root ‘G’ in Figure 6.12, suggest that this is not a buried stem, but a downward-tracking root. Indeed, there may be deeper ramification below the limits of excavation, into fines associated with the relict channel referred to at the beginning of this paragraph.

The deflection and burial of the young stem (C-B) in gravel most likely occurred in the extreme event of late 2000. The next, more horizontal section of buried stem (B-A) appears to have been deflected in this same event, because the extant aerial stem, as well as the stout sinker root beneath it, date to the 2001 growing season. This perhaps occurred in the third flow peak around a week after the maximum water level (see Figure 6.4). The long duration of the 2002 flood makes it a strong candidate for being a significant contributor to the deposition of the upper layers of fine sediment, into which further adventitious roots appear to have grown in the following year. The tree appears to have changed little since 2004, in the absence of extreme floods. The lack of a build-up of fines in this period may be accounted for by the somewhat exposed position at the upstream point of an island, and more recent position on the outside of a bend in a main channel.

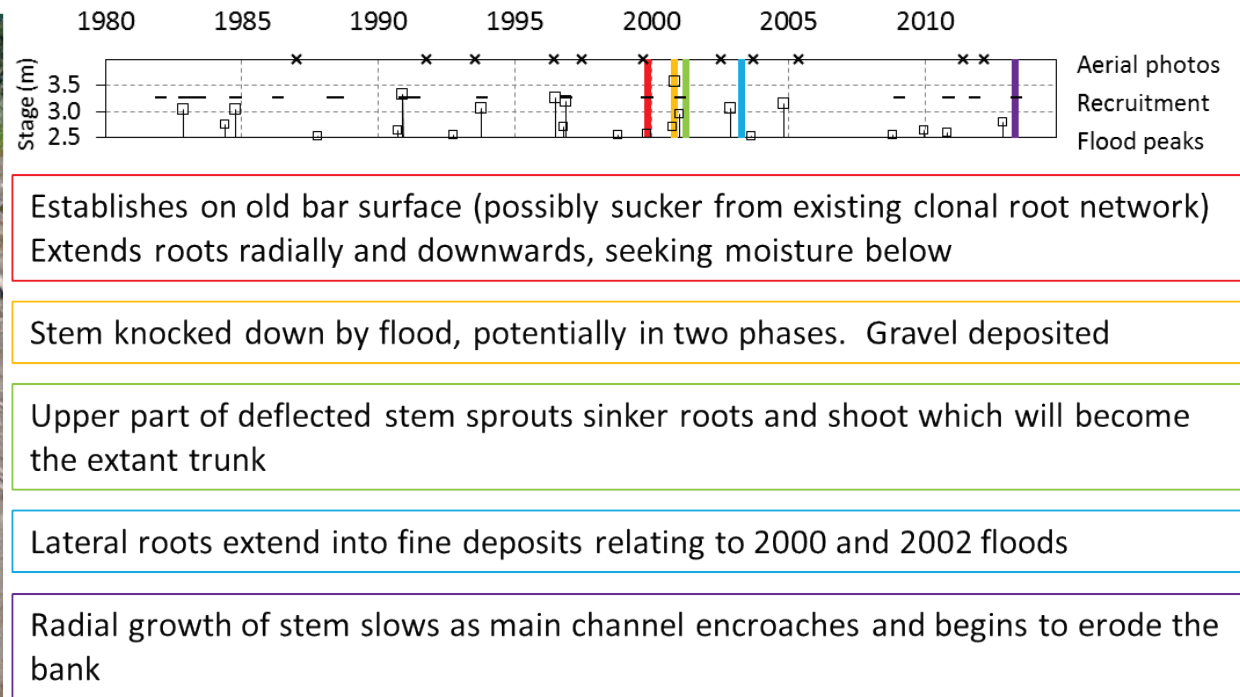
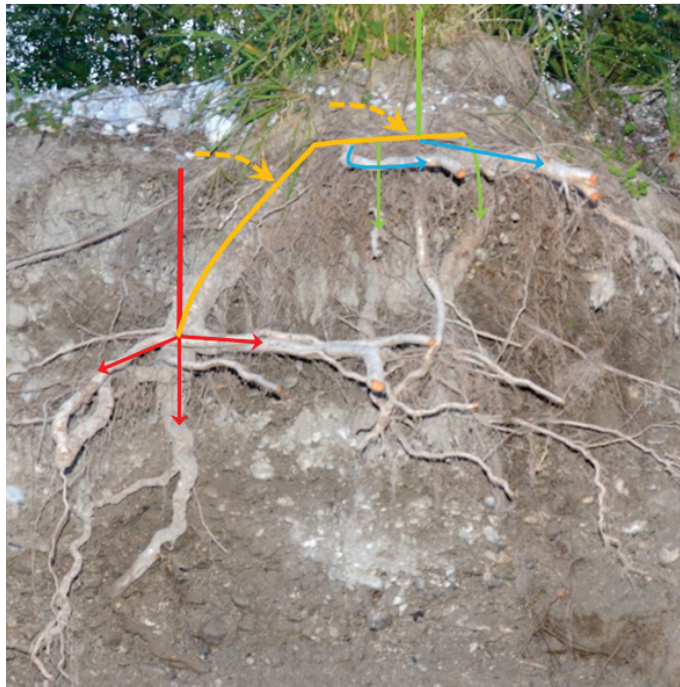


Figure 6.17 Summary of the proposed potential development trajectory of case study R2. Text box colours relate to events marked on the photograph and timeline.

d Case study “R3”

Overall form, key features and sedimentology

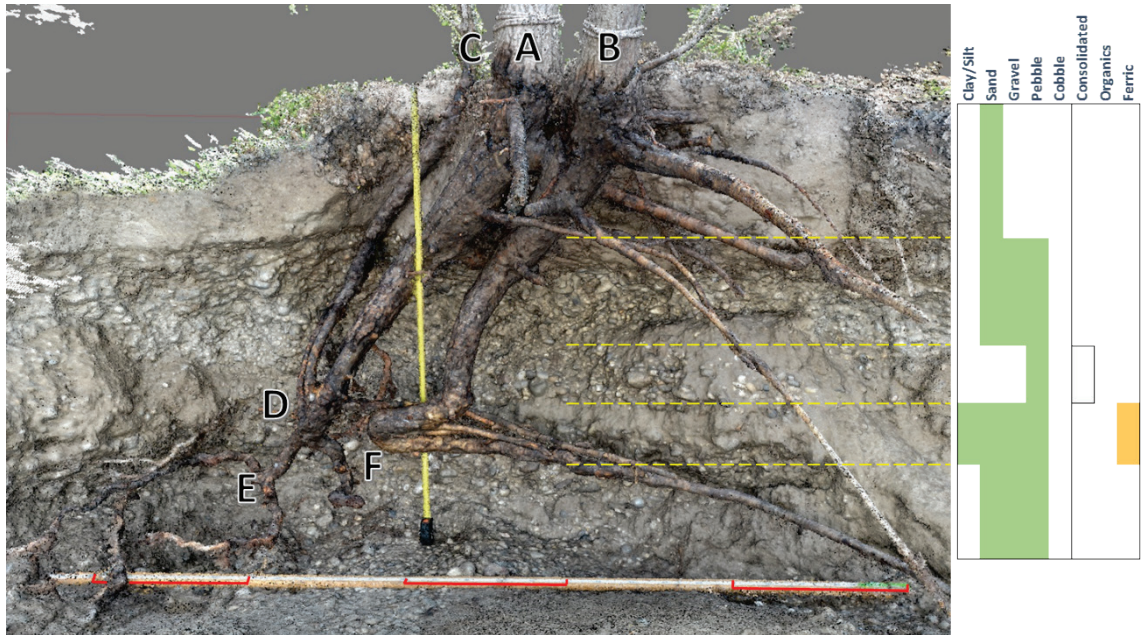


Figure 6.18 Front perspective view of R3 model with key features and main sedimentary strata identified.

Three stems (A, B, C) emerged at the ground surface, the largest of which (A) measured approx. 11 m in height from the ground surface, with a diameter of 16 cm at breast height. It was not possible to determine whether stems A and B had grafted near the soil surface, but they were intimately associated. These stems all penetrated the upper fine deposits and a thick gravel layer, originating in a deep layer containing much siltier material below loose pebbles. Stem C was dead at the time of excavation. Many shoots had emerged from the base of stem B, but had since died, and this stem also possessed large, downstream-leading lateral roots in both of the fine sediment-dominated layers. Stems C and A both originated from a node (D) which had also sprouted roots, and this in turn was connected to a slightly deeper node with a complex, spreading root system (E). Stem B originated from an entirely separate structure (F), which possessed many large horizontal, downstream-pointing roots, emerging from a large diameter horizontal stem. The lower parts of the main buried axes (in the upper gravel layer) were actually deflected both downstream and back in towards the bank as viewed in Figure 6.18, while the upper sections, in finer sediment, were deflected only in the downstream direction of the main channel (Figure 6.19).

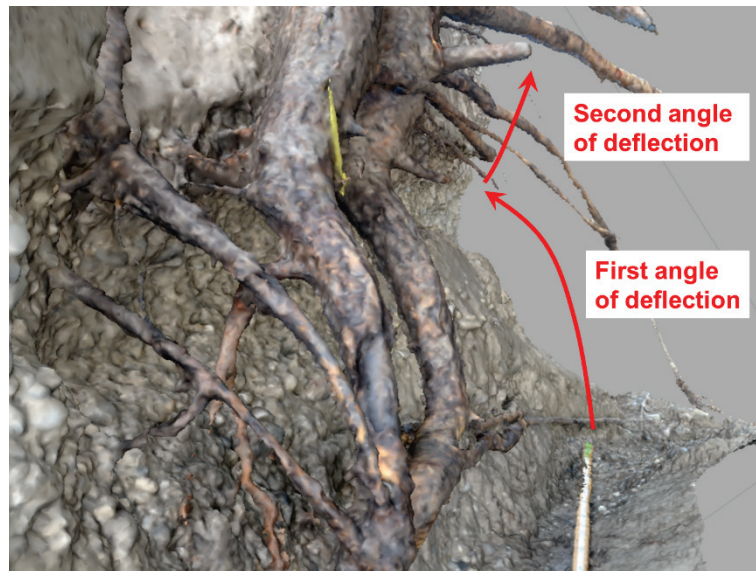


Figure 6.19 Side view (from upstream) of R3 model, showing deflection into the bank of the lower buried stems.

Vegetation and channel change from aerial imagery

Major changes in the vicinity of this tree and RC (200 m to the north) over the period of the flow record are presented below. All available images are presented in Appendix C. The main channel flows from top (north) to bottom. Note that the scale bars relate to the main images, not the magnified areas.

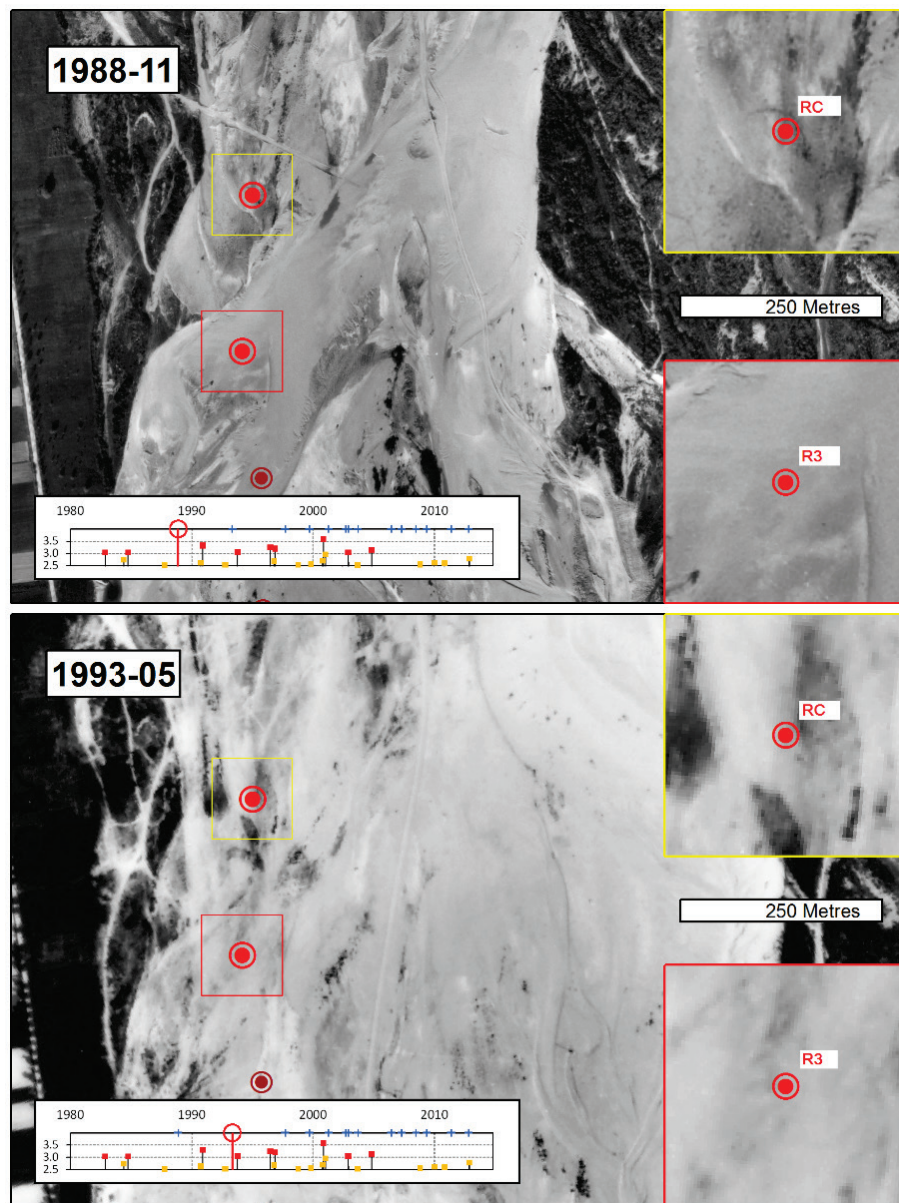


Figure 6.20 Key aerial images of the R3 and RC neighbourhood, 1988-1993. Image sources in Table 6.1.

While in the 1988 image the site of R3 was quite clearly devoid of vegetation and near the middle of a major channel, the image hinted at the establishment of some vegetation – perhaps seedlings or suckers in the vicinity of one or two stranded trees – near RC. It could be surmised with a greater degree of confidence that there was at least some form of landform development in this latter area. Vegetation in the areas of focus was still hard to distinguish in the image taken in 1993, however, it appeared that at least the eastern side of the landform with which RC may be associated had survived, probably with a limited cover of early successional plants. There appeared to be some bar stabilisation at R3, but probably with little or no vegetation cover.

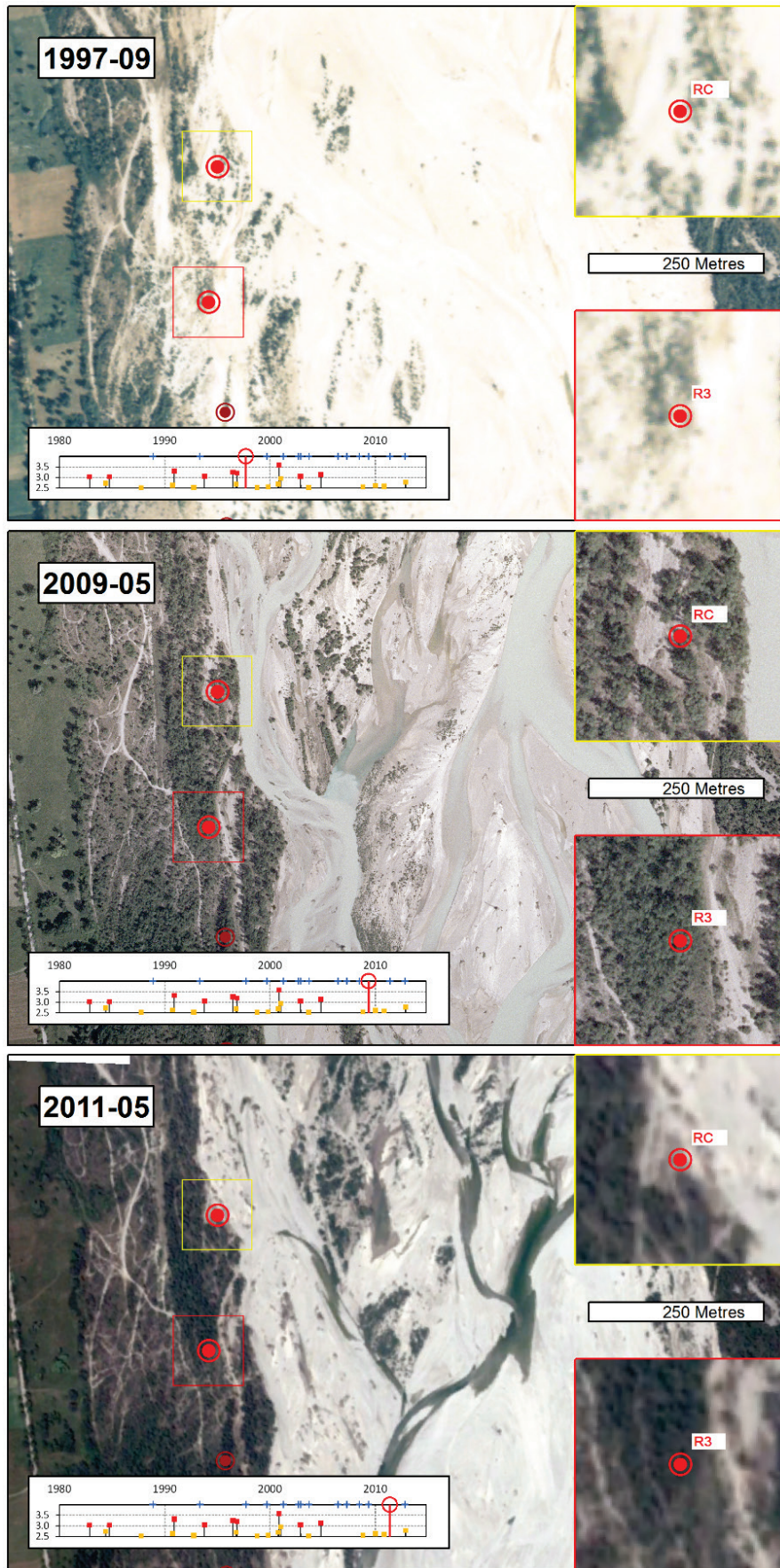


Figure 6.21 Key aerial images of the R3 and RC neighbourhood, 1997-2011. Image sources in Table 6.1. Lower panel © 2015 DigitalGlobe.

With three large flood events between 1993 and 1997, there is a chance that there was complete turnover of vegetation near the case study trees, though the shapes of the patches in 1993 broadly matched those in 1997. This suggested that the latter had their provenance in plants established at least four years earlier. This also held true for vegetated areas across the wider braid plain. Some twelve years later, vegetation at the sites of interest had persisted, and the area around R3 had developed into a mature forest stand. A little further north, RC showed signs of more regular disturbance, with overbank flow and deposition from what was clearly a rather active nearby channel. The situation was much the same in 2011, though the RC site had experienced some bank erosion. It is likely that the buried structures of this case study tree were exposed in the following flood, in 2012 (12 November 2012, 2.79 m).

Age structure

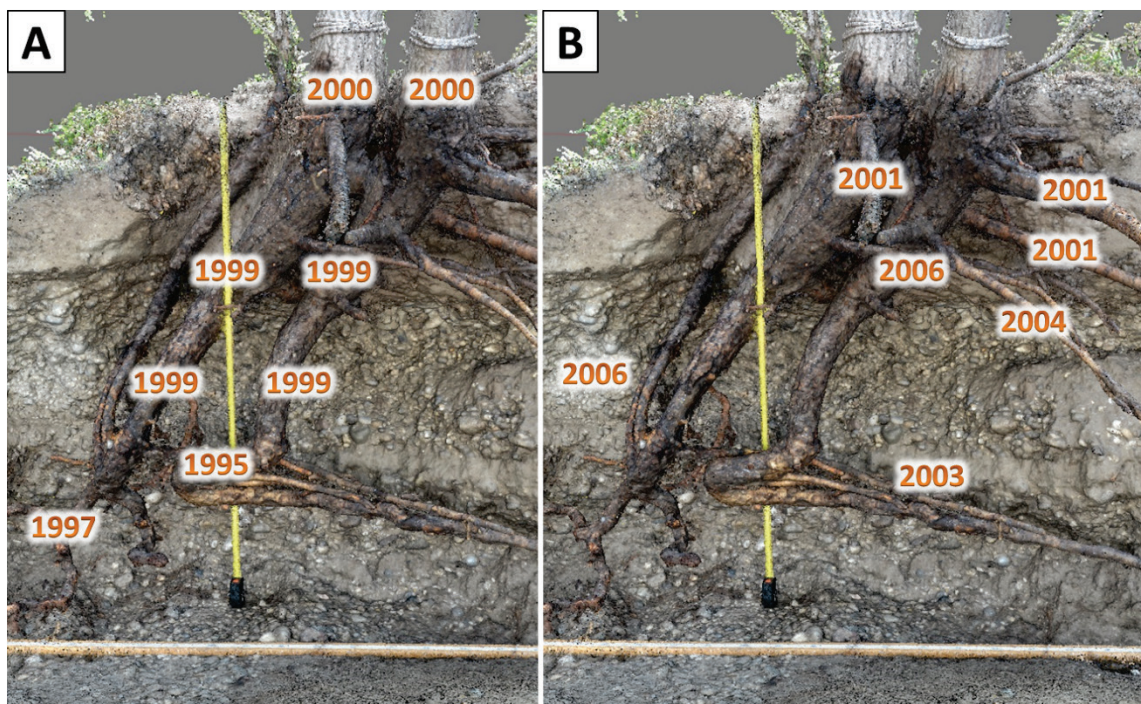


Figure 6.22 Estimates of latest possible dates of origin of different parts of the main axes (A) and lateral roots (B) of the R3 root system, from dendrochronological analysis.

The two aerial stems were established before 2000, and the buried axes beneath them, a year earlier. Lowest parts of the system dated back beyond 1995, while lateral roots extending into the upper layer of fine sediments appeared more recently. The age of the small upstream-most buried axis (part of ‘C’ in Figure 6.18) is likely to have been underestimated as this stem was dead when sampled.

Discussion and summary

Aerial imagery suggests most geomorphic activity occurred at this site between 1993 and 1999, which makes the two flood events of 1996 strong candidates for the deposition of the first gravel stratum and formation of the lower part of this case study's buried structure. The earliest wood dates to 1995 at the latest, and it is proposed that this represents a portion of an original stem, flattened in the summer 1996 flood. It seems three nodes may have sprouted on this deflected axis, but only the lower two established roots successfully, while the upper and lower were responsible for the stems which survived until excavation (Figure 6.23). It may have been that a shoot from node F was destroyed in the later November 1996 flood, and roots did not develop from node G owing to its elevation above the sediment surface. Whatever the course of events, while D became an independent plant with roots and shoots, nodes F and G were interdependent, remaining connected while the rest of the original stem decomposed.

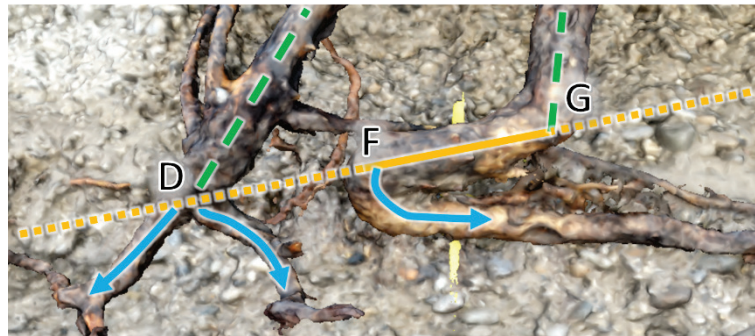


Figure 6.23 Proposed development trajectory of the lower part of the R3 buried stem system. Original stem knocked down and buried by flood is marked in gold (extinct portions dotted), initial stem sprouts in dashed green and main adventitious roots, blue arrows. Nodes labelled D and F correspond to Figure 6.18.

Shoots from the wood deposited in 1996 then appear to have been buried in gravel and deflected downstream and in towards the bank, and then afterwards only in the downstream direction, buried in fine sediments. Both of these events must have occurred before 2000, which is the date of origin of the extant, vertical, aerial stems. In the 1997 aerial photo, the site appears exposed and flow paths are visible from the main channel out to the right bank (Figure 6.21). It is therefore proposed that this initial deflection and deposition occurred in the October 1998 flood, while the second deflection and deposition of fines is related to the October 1999 flood, when the site was more sheltered by thickening vegetation. Horizontal roots then spread (mostly downstream) into the deposited sand and silt.

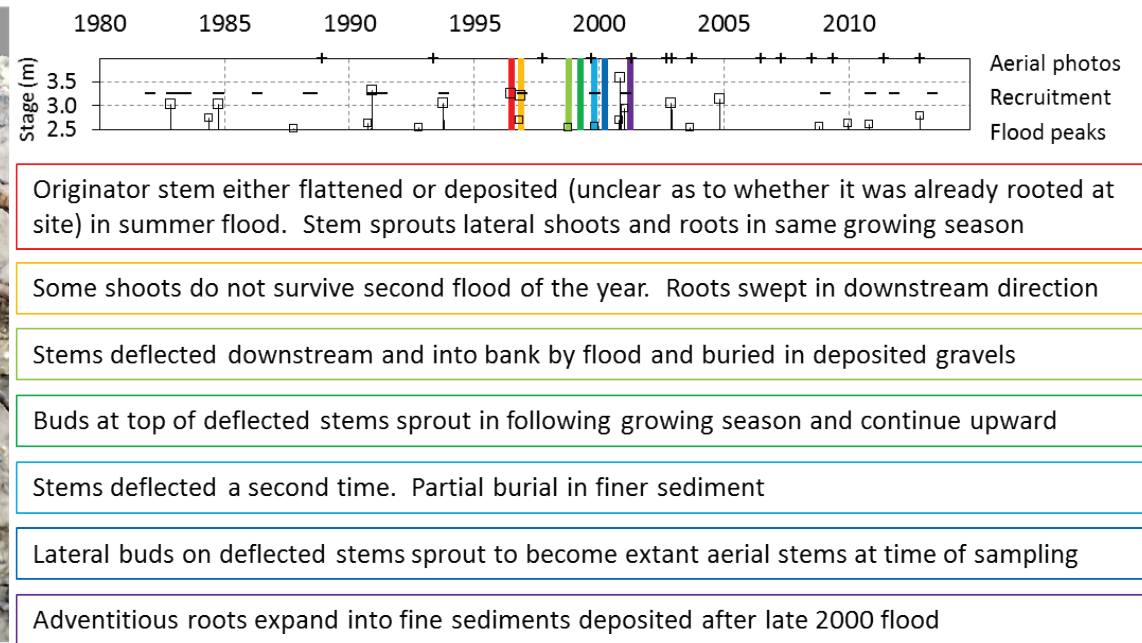
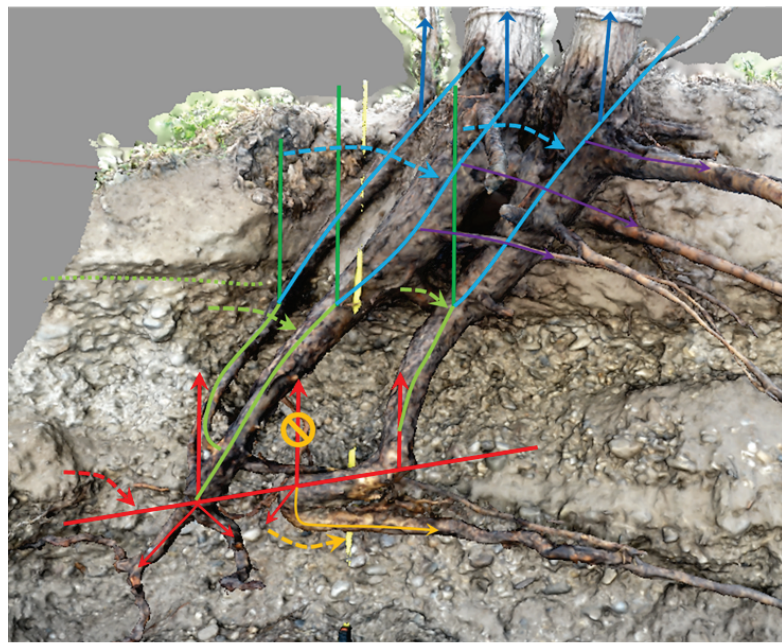


Figure 6.24 Summary of the proposed potential development trajectory of case study R3. Text box colours relate to events marked on the SfM model and timeline.

e Case study “RA”

Overall form, key features and sedimentology

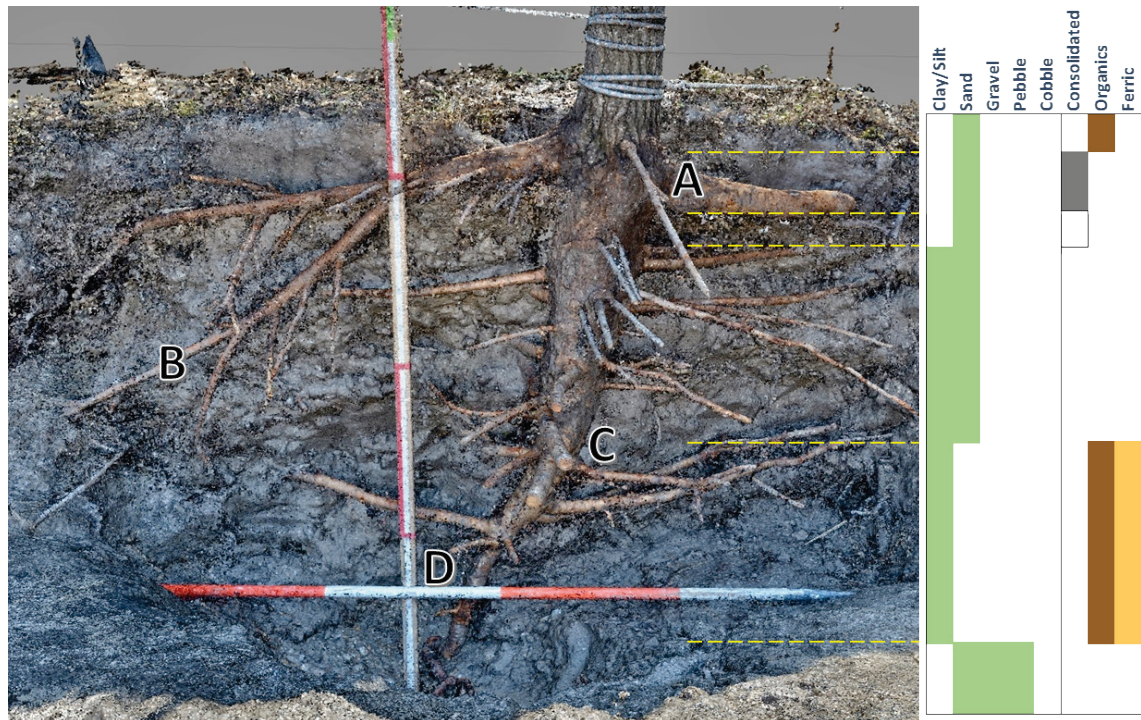


Figure 6.25 Front perspective view of RA model with key features and main sedimentary strata identified.

This tree was a single stem of 13 m from the bank top, with a DBH of 13 cm. It comprised a single main axis, with large structural lateral roots (asymmetric due to compression wood) ten or so centimetres below the ground surface (A). Notably, one of these excavated shallow laterals had branched to exploit deeper layers of the thick fine sediment deposits (B). Lateral roots were relatively evenly distributed along the rest of the main axis, though a few more were observed just below a sandy horizon than elsewhere (C). The main axis had a gentle lean downstream, which increased slightly between C and D. The bottom of this principal axis was rooted in the lower, gravelly stratum, at approximately the level of the water table at the time of excavation.

Vegetation and channel change from aerial imagery

Major changes over the period of the flow record are presented below. All available images are presented in Appendix C. The main channel flows from top (north) to lower left (southwest).

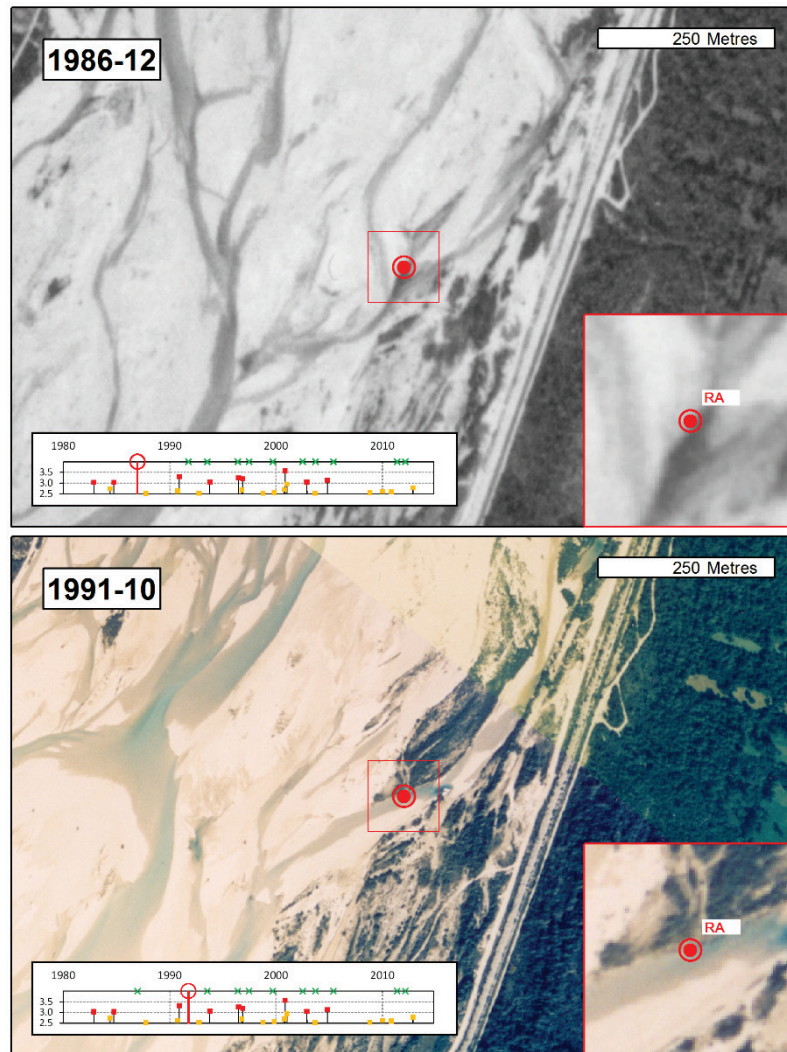


Figure 6.26 Key aerial images of the RA neighbourhood, 1986-1991. Image sources in Table 6.1.

The earliest image of the RA site coincident with the flow record showed a point of flow concentration at the meeting of three channels, with no vegetation in the immediate area. By 1991 there had been extensive colonisation from the case study tree upstream, with the greatest density on the northern margin of the central channel of the three mentioned above.

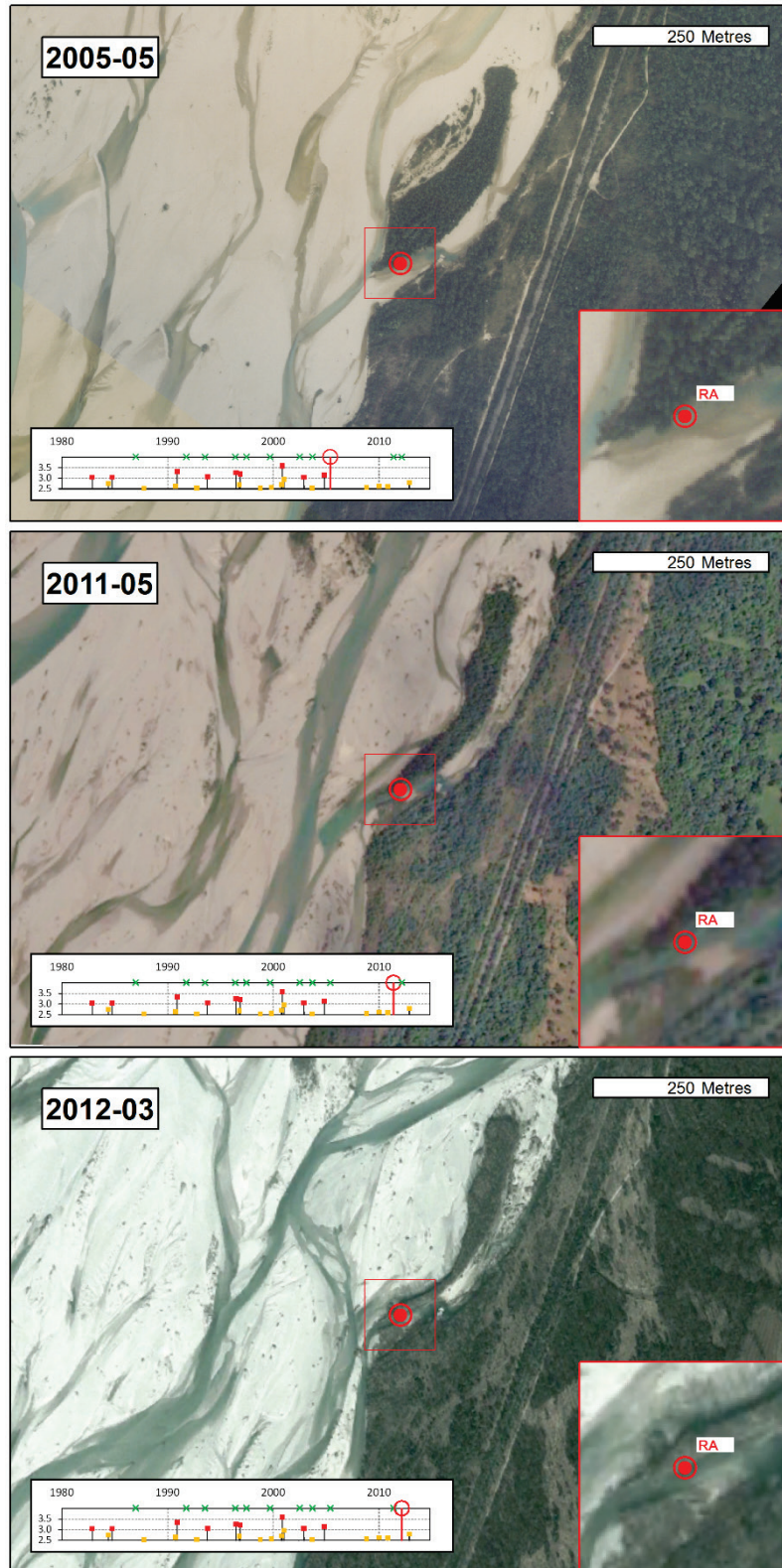


Figure 6.27 Key aerial images of the RA neighbourhood, 2005-2012. Image sources in Table 6.1. Middle and lower panels © 2015 DigitalGlobe.

Throughout the years 1991 to 2005, in spite of seven major floods, the island containing tree RA remained undisturbed, developing almost continuous forest cover. The channel separating it from the wider left bank floodplain forest fringe had continued to flow, however, being situated on the inside of the gentle curve in this channel, the case study tree is unlikely to have experienced significant disturbance or exposure. Lateral migration of the more major channels of the Tagliamento had resulted in significant erosion of the western side of the island in the image captured in 2011. The case study tree remained sheltered though, on the narrowing downstream tail of the island. The 2012 image illustrates the progressive nature of the erosion of the western edge of the island in the area of focus. The degree of shelter afforded to RA by the island was gradually reducing here.

Age structure

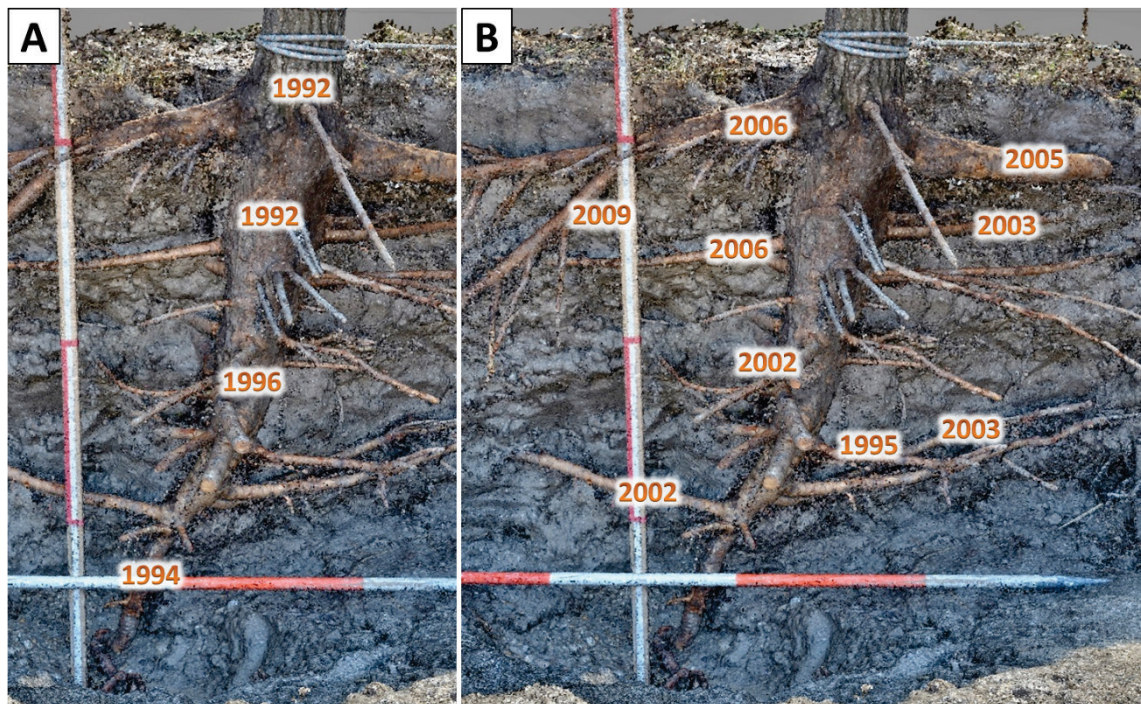


Figure 6.28 Estimates of latest possible dates of origin of different parts of the main axis (A) and lateral roots (B) of the RA root system, from dendrochronological analysis.

This tree was one of the oldest studied, with the main stem dating back beyond 1992. Cores were difficult to read, but this age appeared to apply to the whole main axis, though the lowermost sample pre-dated 1994. Many of the lower lateral roots developed before 2003, and one, before 1995, whereas laterals in the uppermost stratum were mainly in the region of ten years old at the time of excavation.

Discussion and summary

The aerial imagery suggests colonisation of this site by the end of 1991, and the dates, recruitment modelling and simple single-stem morphology of this tree are all compatible with it being a seedling in this first wave of colonisation. An alternative hypothesis may be that it was a sucker from deep adventitious roots, but there were no older 'parent' trees in the area at the time of origin to sustain it. The simple form and relatively well-distributed lateral roots of RA reflect its sheltered position and relatively gradual burial of the stem. However, there is still a downstream lean to the main axis, which is greater in the lower half. Both the main stem age and a lateral dated to 1995 (Figure 6.28) putting limits on the date of this disturbance, and aerial images show vegetation was not dense in the immediate locality until sometime between 1993 and 1996. The strongest candidate event is therefore the flood of November 1990. The lack of coarse material associated with the sediment at this site may be due to the fact that its position was in the lee of a patch of established vegetation. The lack of deposition due to the absence of many very large floods in recent years is evident from the fact that the very highest laterals, just below the ground surface, date to before 2006. Overall, this tree exemplifies one of the simplest development trajectories possible.

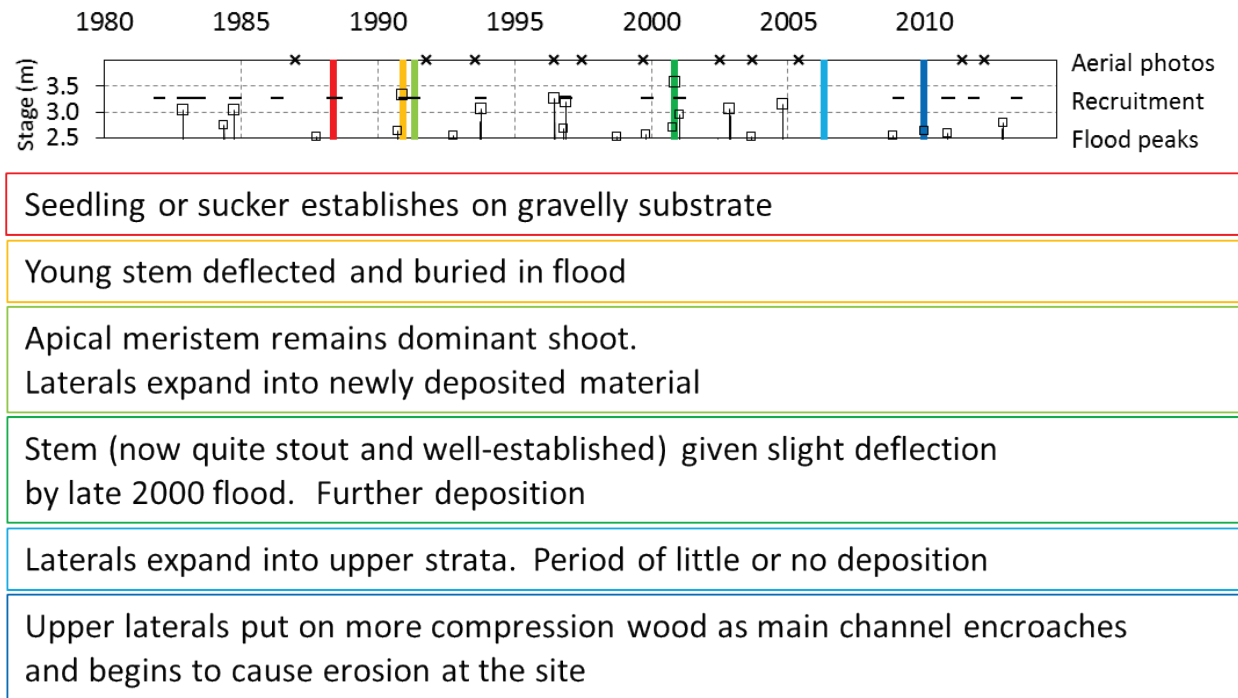
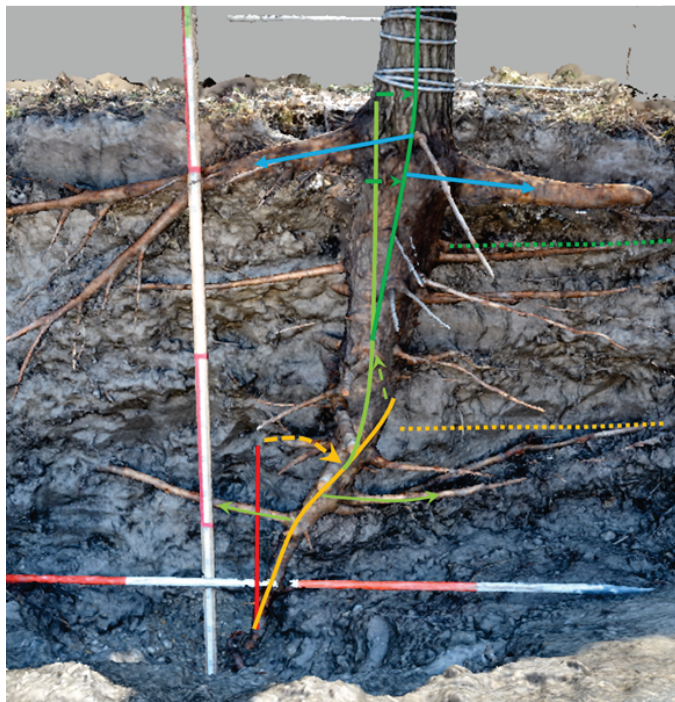


Figure 6.29 Summary of the proposed potential development trajectory of case study RA. Text box colours relate to events marked on the SfM model and timeline.

f Case study “RB”

Overall form, key features and sedimentology



Figure 6.30 Front perspective view of RB model with key features and main sedimentary strata identified.

This tree comprised a single main stem of 13 m height above the ground surface, and 12 cm DBH. There was however a smaller stem (A), oriented with the first tilted section of buried stem (D-E). The buried structure comprised a single, curved axis, attached to a large, branching mass of dead wood (B). An old piece of nylon cord had been tied round the main axis at the junction between the living and dead wood (just upstream of C), and the lower extremity of the living part of the axis had a proliferation of roots emerging from the lower side (C), some leading downstream. A second area with many large adventitious roots occurred just above a point at which the main axis turned more steeply upwards (D). Again, most of these roots were on the lower and downstream-facing side and grew into a layer of finer material above loose sand. E (long dead) may have represented an extension of the C-D stem. Point F, where the main axis turned to a vertical orientation, was also associated with a collar of lateral roots, a large one of which is visible pointing upstream in Figure 6.30. Gravels only occur at depth, and strata are sloping roughly parallel to the ground surface.

Vegetation and channel change from aerial imagery

Major changes over the period of the flow record are presented below. All available images are presented in Appendix C. The main channel flows from right (east) to lower left (southwest).

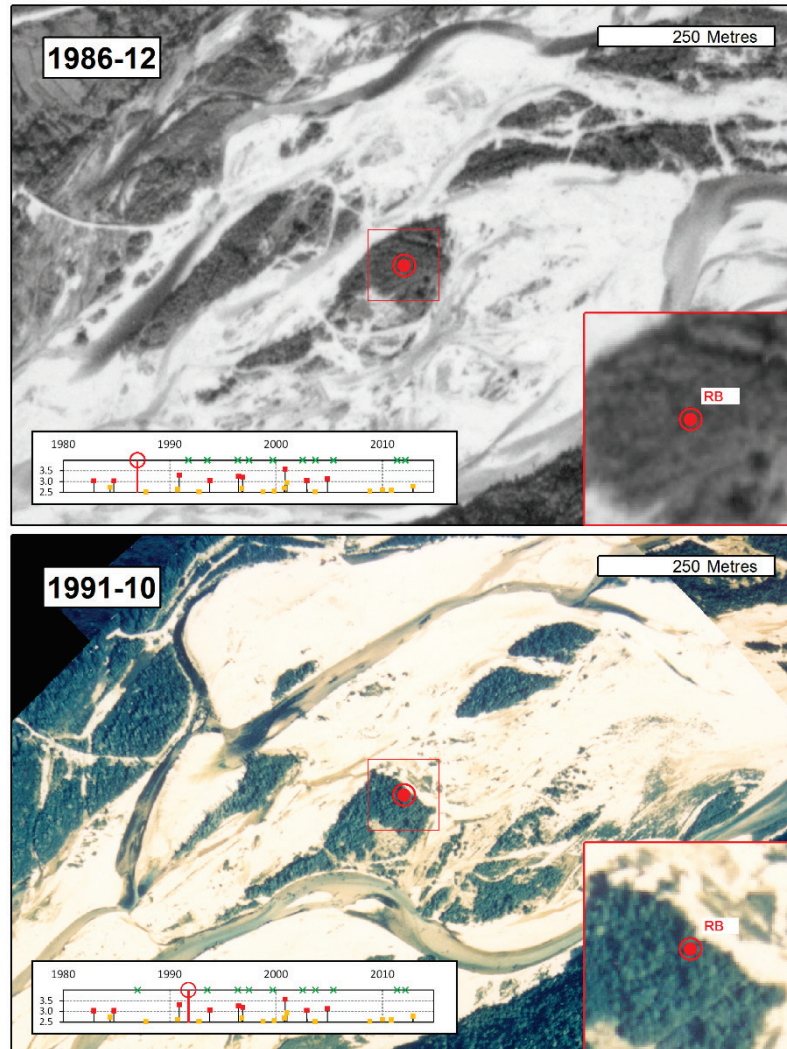


Figure 6.31 Key aerial images of the RB neighbourhood, 1986-1991. Image sources in Table 6.1.

The site in 1986 was occupied by a large, relatively uniform and apparently well-established island. Many such late-successional islands existed in the braid plain. Large floods and lateral channel migration had eroded the upstream part of the island of focus by 1991, along with large areas of vegetation on the entire right half of the braid plain. The RB site appeared to be just within the extent of the remaining forest, however. There had been extensive re-vegetation to the southeast of the site, around one or two isolated mature trees visible in the previous image.

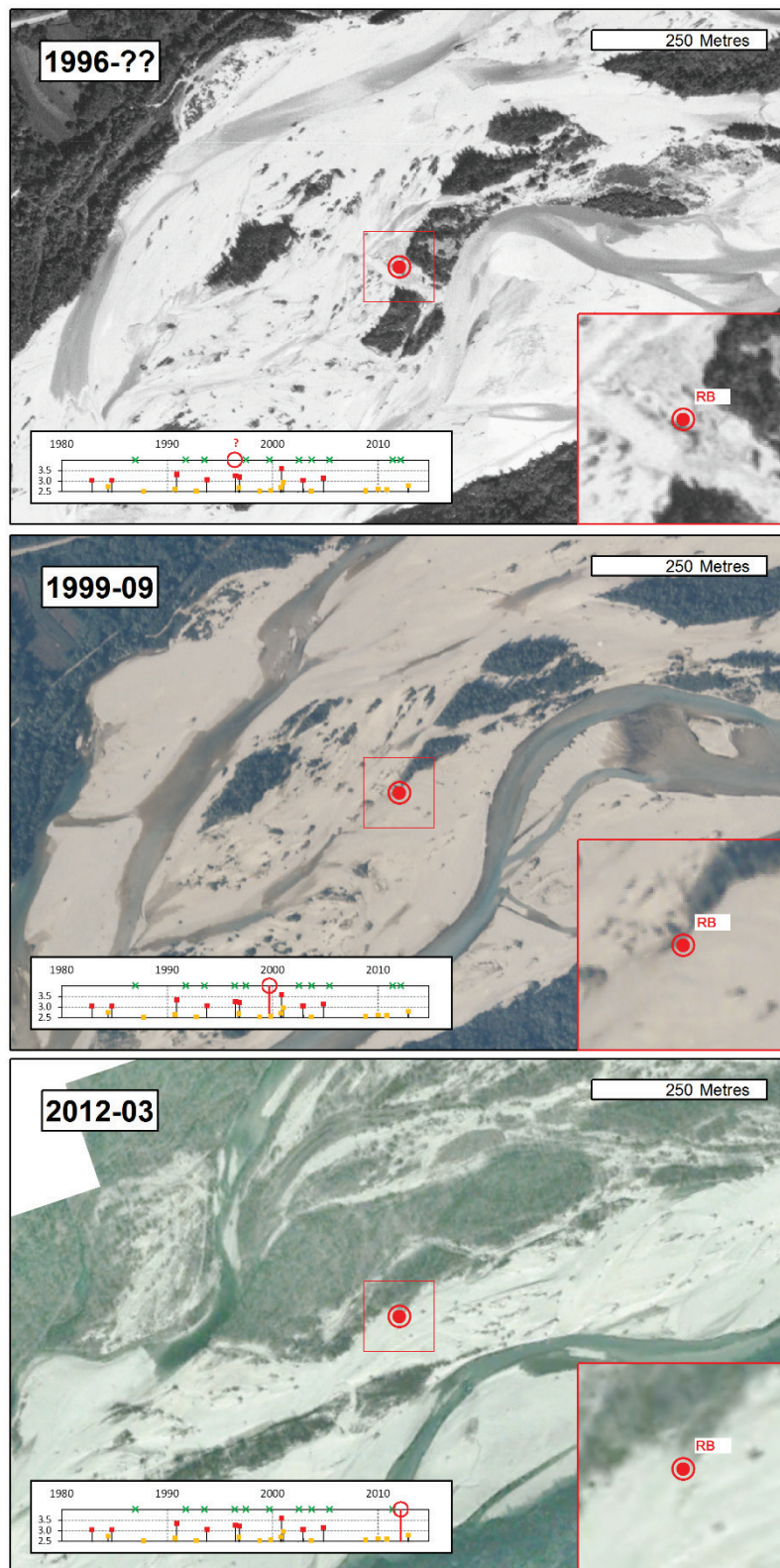


Figure 6.32 Key aerial images of the RB neighbourhood, 1996-2012. Image sources in Table 6.1. Lower panel ©2015 DigitalGlobe.

The two large floods of 1993 (8 October, 3.06 m) and summer 1996 (23 June, 3.25 m) resulted in widespread reorganisation of the active tract, including almost complete removal of trees at the RB site. This appeared to have been caused by the downstream migration of

the transverse erosion front which removed the north-easternmost part of the island in the 1991 image. Some trees appeared to have been deposited in the vicinity of the case study tree, however, and vegetation had begun to in-fill between patches to the northeast. Many scattered deposited trees were assumed a result of the floods of this year. A highly active migrating main channel appeared to have removed all trace of mature vegetation to the south of the site of RB by 1999. Many isolated deposited trees remained from the 1996 floods, though there had been little deposition and in-fill of vegetation between them. Large floods in the intervening thirteen years appeared to have resulted mainly in deposition of fine sediment and vegetation expansion on the northern (right bank) side of the braid plain, as opposed to the flow disturbance and resetting of vegetation succession as observed in the previous decade. The study tree remained in an exposed position, however, and is likely to have been disturbed several times by fast flowing water during floods, particularly as the active tract constricts to a little over 100 m just two kilometres downstream.

Age structure

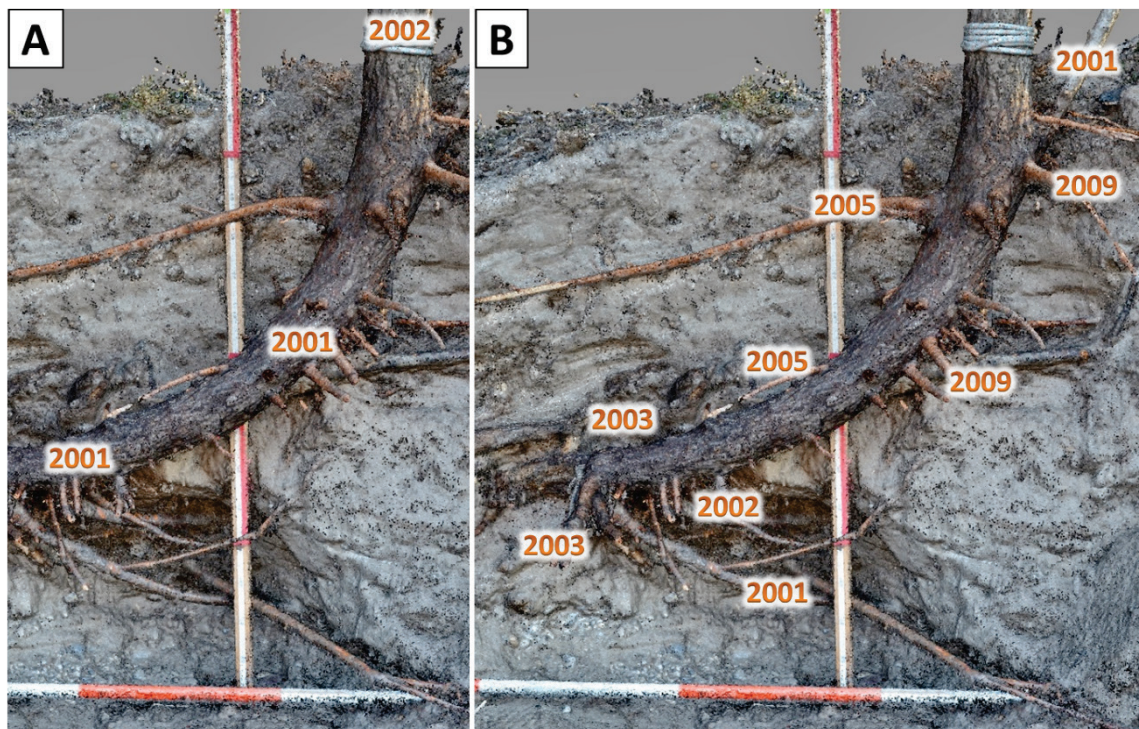


Figure 6.33 Estimates of latest possible dates of origin of different parts of the main axis (A) and lateral roots (B) of the RB root system, from dendrochronological analysis.

The main axis of this tree dated back to at least 2001 along its full living length, with the aerial portion of the stem perhaps being a year younger. The small subsidiary aerial stem dated to 2001. Most of the lowest laterals appeared to have originated in around 2002, while the mid and high lateral roots were dated to 2005 and 2009.

Discussion and summary

After very large scale erosion of vegetation at this site between 1997 and 1999, the aerial images show the island dynamics to be rather static up to the time of sampling, with just gradual deposition and in-fill of vegetation to the north. However, the position of this particular tree has since remained exposed, on the very edge of an island, facing the open, active tract of the main channel. It appears that the buried stem was the apical part of a larger young tree, upright before 2001, which was probably eroded from the island edge and redeposited. The overall, gently upwardly-curving form of the main axis could be explained by gradual deflection and burial by successive events, keeping pace with phototropic apical growth. Each time the apex of the main stem took a turn upward, it would have been deflected downstream and buried slightly deeper in fine sediment. However, the axis can also be considered in two distinct sections (C-D and D-F in Figure 6.30) and the date associated with the long, upstream-pointing lateral root parallel with the bank top suggests that almost all deposition occurred before 2005. Furthermore, axes A and E in Figure 6.30 appear to be remnants of original apical shoots. It is therefore suggested that the initial deposition of the 'parent' tree occurred in the late 2000 flood, at which point a lateral bud from node D became the dominant shoot (of which A is a remnant). The 2002 flood then buried and put a second deflection on the main axis and the extant main aerial stem sprouted from node F. The fact that most of the lateral roots appear to date to periods slightly later than the year following burial of the main sections may be due to provision of sufficient resources by the system below node C. The nylon cord tied round the stem just below this node appears to have led to the mortality of the lower portion of the system sometime around 2006/7, judging by changes in wood properties in the lower lateral roots.

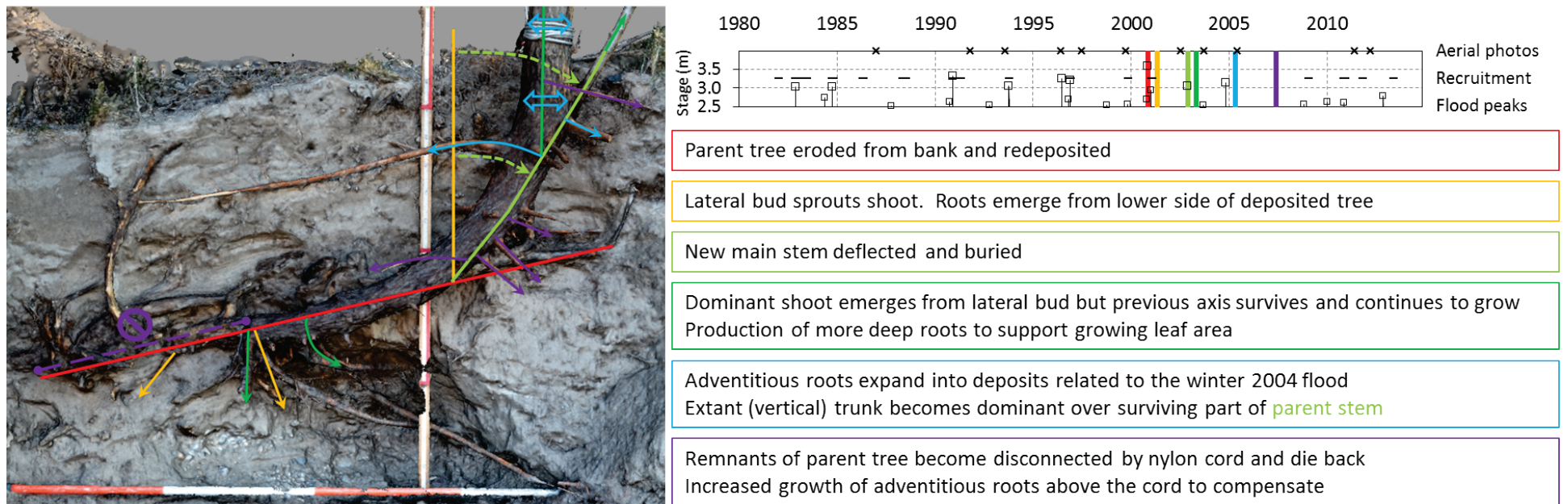


Figure 6.34 Summary of the proposed potential development trajectory of case study RB. Text box colours relate to events marked on the SfM model and timeline.

g Case study “RC”

Overall form, key features and sedimentology

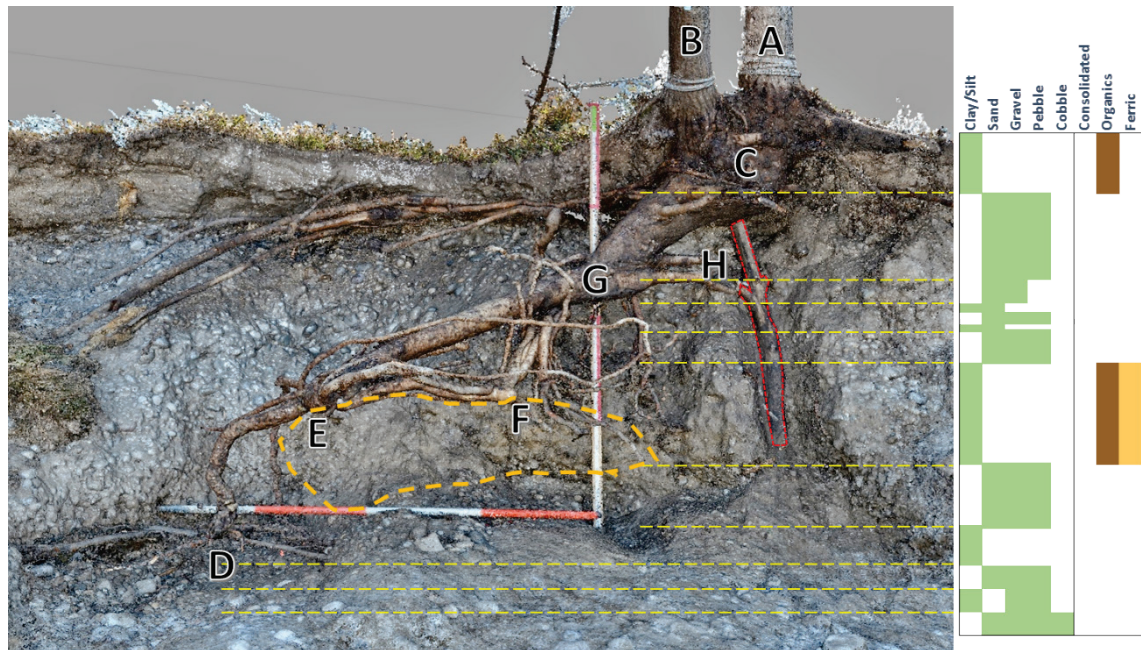


Figure 6.35 Front perspective view of RC model with key features and main sedimentary strata identified. Outlined in red is a log installed during excavation in order to support the weight of the stems.

Above ground, this tree comprised two relatively large stems, the larger of which (A) was 13 m high and 20 cm DBH. These were both attached (at C) to one main buried axis of approximately 3 m in length, with an overall angle of around 25° from horizontal. This originated from a deep later of silt and clay at D, from which horizontal roots spread in all directions. From this node, the main axis deviated from the vertical in the downstream direction, and another major node occurred at E, with many large, downstream-swept adventitious roots. Most of these became deflected and contorted at F. A local patch of silt and clay is outlined in dashed gold. The main axis was virtually uninterrupted by adventitious roots until a third major node at G, where a thick lateral branch took a 45° course up to C and became dominant. Two large roots were observed continuing along the line of the original axis, however (H). The near-surface node (C) was also associated with long lateral roots extending in all directions in the finer surface sediments. The stratigraphic profile was complex beneath this tree, containing mainly gravel but many silt, clay and organic inclusions.

Vegetation and channel change from aerial imagery

(see images and commentary for R3, above)

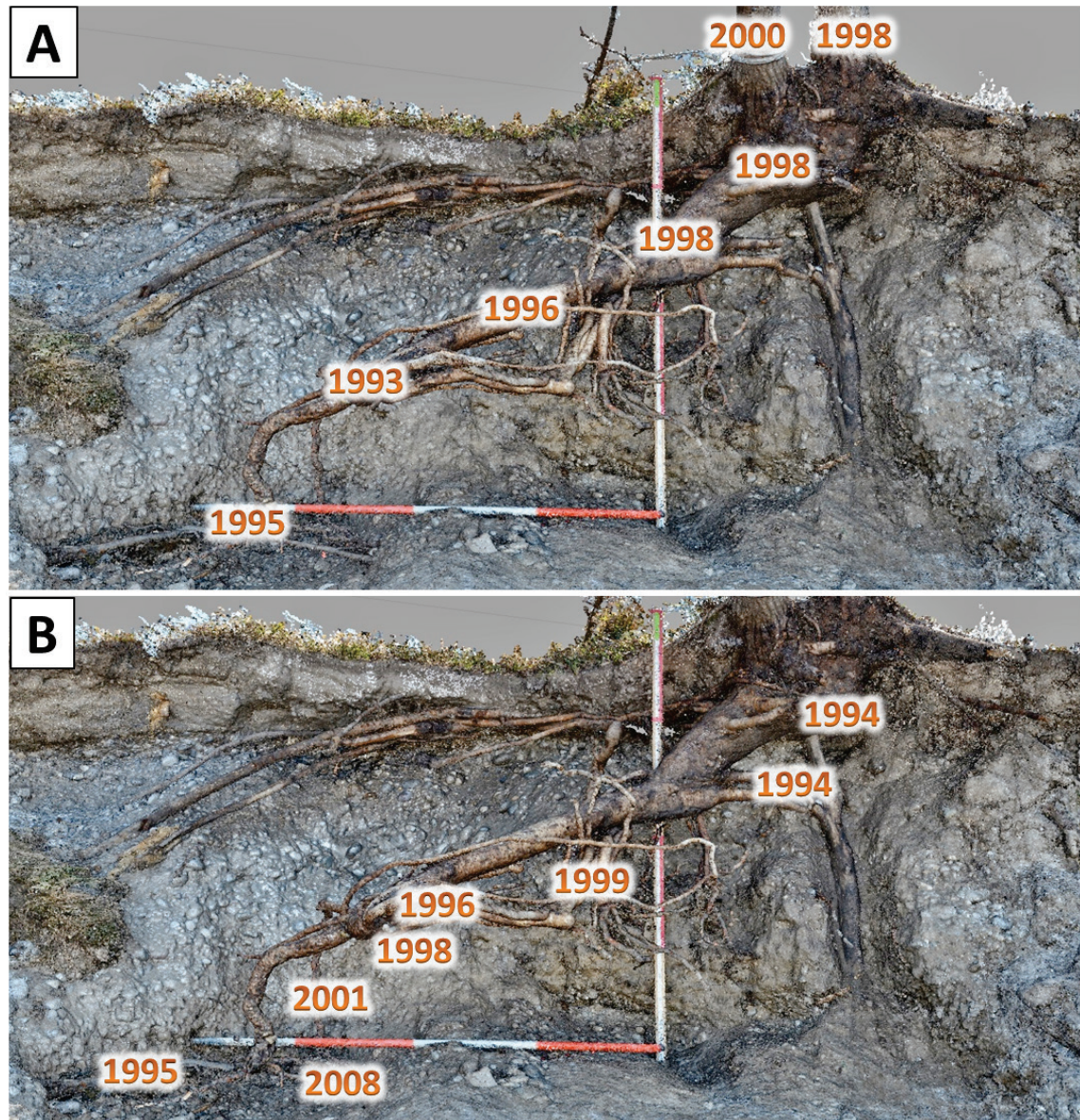


Figure 6.36 Estimates of latest possible dates of origin of different parts of the main axis (A) and lateral roots (B) of the RC root system, from dendrochronological analysis.

Sections from the buried structures of RC dated it to before 1993. There was no clear pattern of increasing or decreasing age limits along the main axis, but the extant aerial stems appeared significantly younger, predating 1998. At least one of the lateral roots in the upper gravel layer appeared to be rather old, dating to 1994 or earlier. Other adventitious roots covered a range of potential ages, dating to between 1996 and 2008.

Discussion and summary

The sequence of aerial images suggest an early provenance of this tree by comparison to the other case studies. The 1988 image does show possible vegetation at the site, and recruitment modelling suggests this to be a likely year, but the alternative recruitment period identified in 1991 seems more appropriate in correspondence with the dendrochronology dates. This may perhaps represent a round of secondary colonisation by expansive suckering among a patch of established plants. It is suggested that this young tree was flattened in the October 1993 flood, creating the lowermost curve in the main axis, and potentially leading to the trapping of fine sediments and organic material in its canopy, resulting in the development of the patch of silt and clay outlined in Figure 6.35. At this point it appears the node E sprouted a shoot which later became the dominant axis. Scars in the growth rings suggest that the next major event was the summer 1996 flood, bending the tree almost flat once again and creating the kink in the main axis seen in Figure 6.37. However, much of the canopy appears to have survived this event, with the apical stem and a branch probably giving rise to the axes G-H and G-C, respectively. In the following period up to the late 2000 flood, it is proposed that the uppermost node (C) sprouted new shoots, and many of the long adventitious roots emerged from the buried node E. It is difficult to explain the severe distortion of these adventitious roots at point F, but one potential explanation is that the extreme floods of November 2000 caused wholesale movement of the buried structures, dragged by their aerial stems, downstream, causing bunching of these roots. There appear to be no major changes at the site over the following ten-to-fifteen years, except that bank erosion starts to encroach between 2009 and 2011. The resulting instability from loss of sediment is seen in the production of compression wood by upper laterals in recent years.



Figure 6.37 Detail of the RC model, showing node E (as labelled in Figure 6.35) viewed from above. Note the kink in the main axis (outlined). This image has been mirrored to be consistent with other figures. Flow direction is from the bottom to the top of the image.

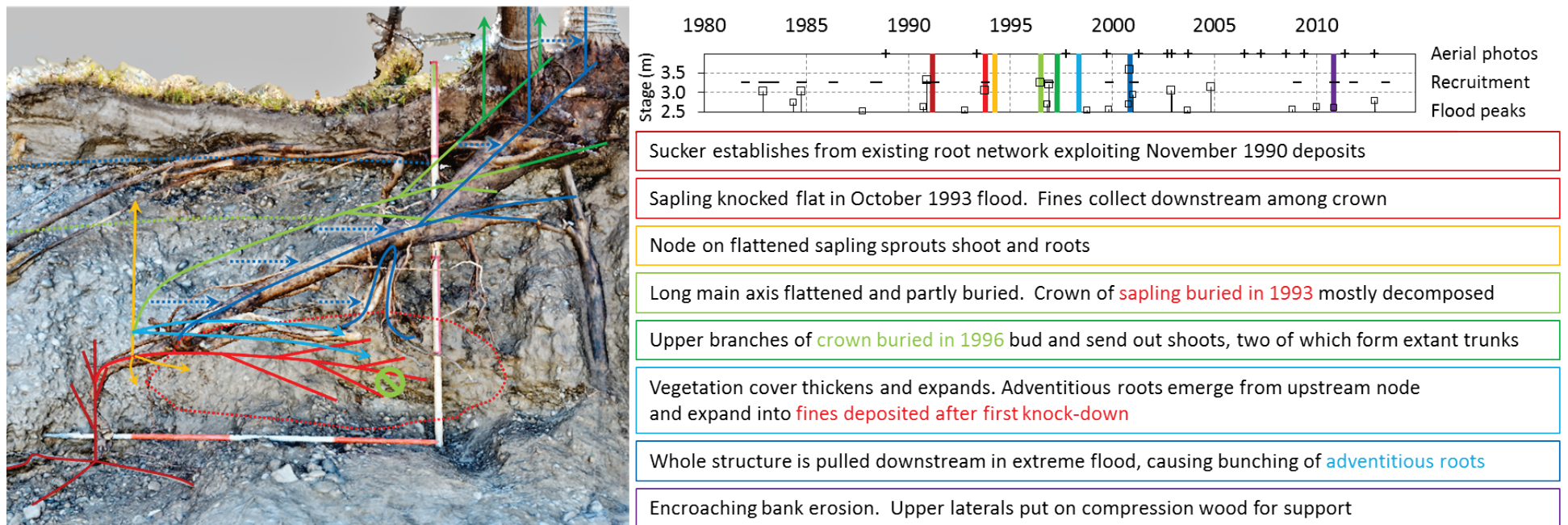


Figure 6.38 Summary of the proposed potential development trajectory of case study RC. Text box colours relate to events marked on the SfM model and timeline.

b Case study “RD”

Overall form, key features and sedimentology

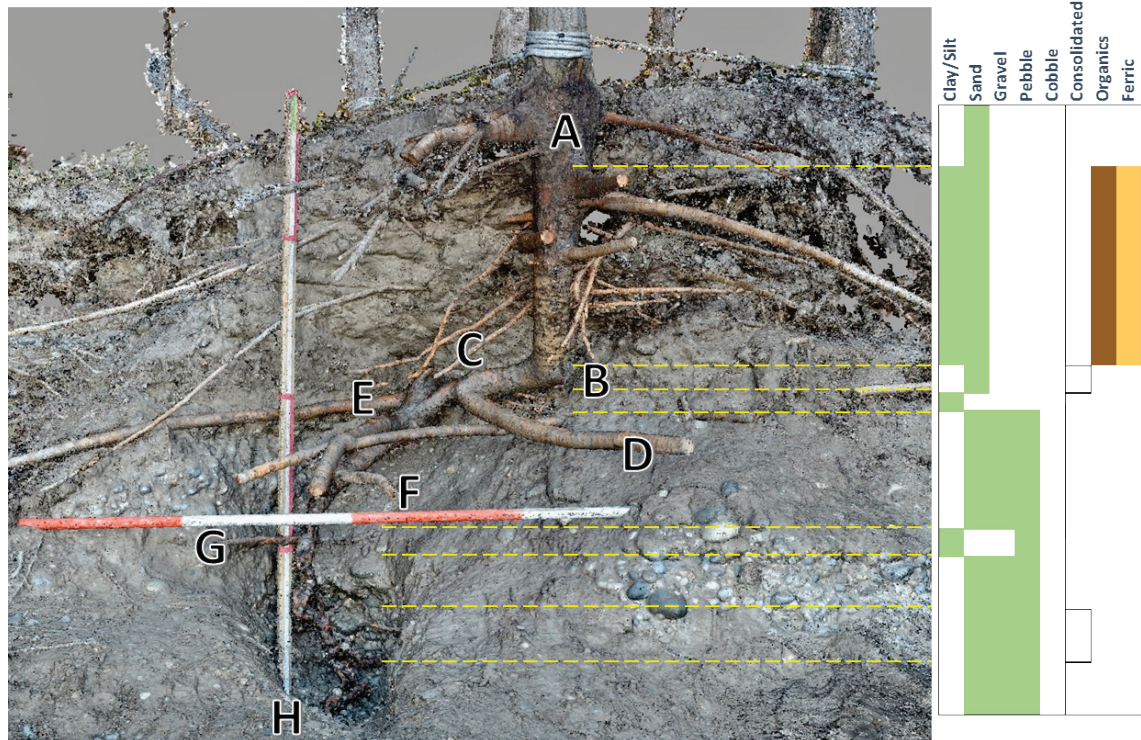


Figure 6.39 Front perspective view of RD model with key features and main sedimentary strata identified.

This tree was part of a patch of approximately five stems of similar size, additionally with one or two large dead stems. The stem excavated measured 13 m above the surface, with a DBH of 15 cm. The tree possessed several large supporting laterals just below the surface (A), below which there was a metre-long vertical section with intermittent adventitious roots. Below this, a large diameter, near-horizontal and upstream-pointing section was dominant at a node (B) which also had remnant stubs of several other horizontal roots and one or two stems, pointing back into the bank. This level was coincident with the top of a gravel-dominated layer. A short distance upstream on this dominant horizontal axis was a junction (C) with a major downstream-pointing horizontal root (D). Again, just a short distance (approx. 20 cm) further along the upstream-pointing axis, were several strong grafts with roots from other stems, emerging from the bank (E, with close-ups in Figure 6.40). Below this, the main axis penetrated the thick gravel deposits in a wandering but more-or-less vertical course, with significant laterals in the surface of the gravel (F) and coincident with a silty inclusion deeper down (G). The bottom of this root system extended beyond the limits of excavation (H).



Figure 6.40 Details of grafting (E1, E2) observed between roots of RD and other stems in the cluster. The photograph has been mirrored to maintain consistency with other figures.

Vegetation and channel change from aerial imagery

Major changes over the period of the flow record are presented below. All available images are presented in Appendix C. The main channel flows from top (north) to bottom. Note that the scale bar relates to the main images, not the magnified areas.

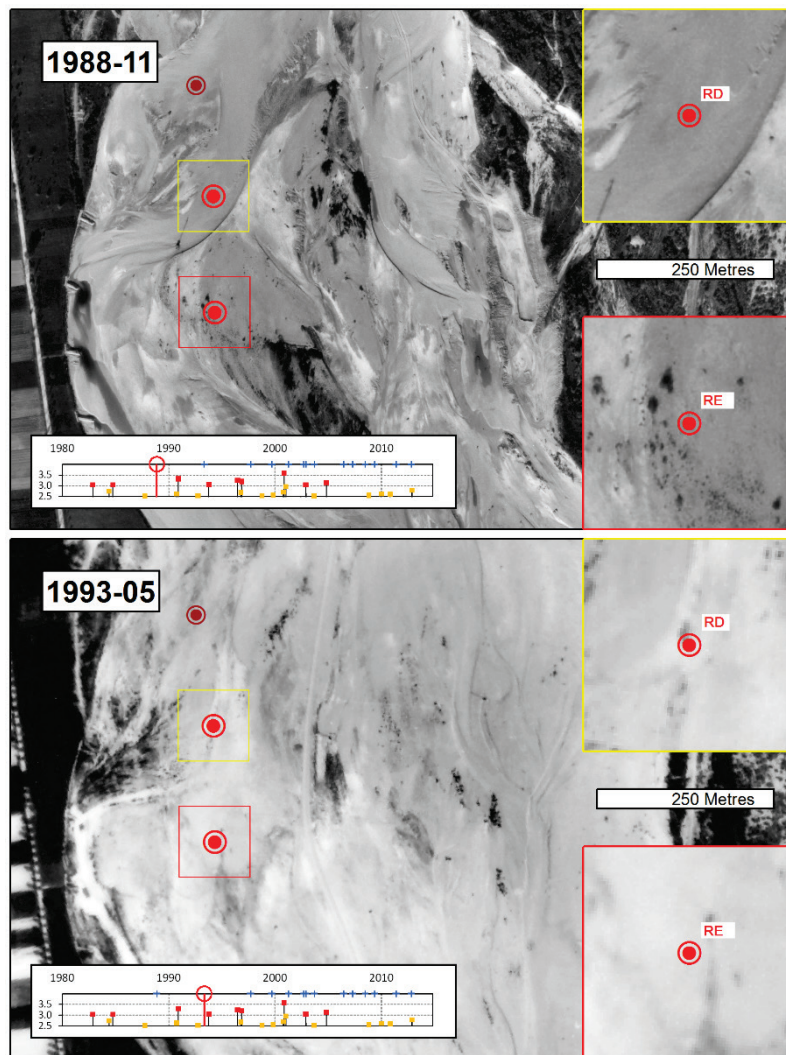


Figure 6.41 Key aerial images of the RD and RE neighbourhood, 1988-1993. See further explanation at the beginning of this Section. Image sources in Table 6.1.

The sites in question were both in highly active channel areas in 1988 (note groynes constructed on right bank). Scattered young trees and shrubs were present in the area of RE and may have been stems which survived burial on top of a bar. However, the pattern of patches visible in this image was not preserved in later images, suggesting these stems were not directly related to the case study tree. The 1993 image was the first to show a pattern of sparsely vegetated patches which is conserved in later images. RD appeared to show colonisation along a channel margin. The area downstream of RE appeared to have remained as a bar feature since the previous image, with establishment of perhaps seedlings and some deposited live wood at the upstream focus. The active tract of the river was in general rather devoid of vegetation.

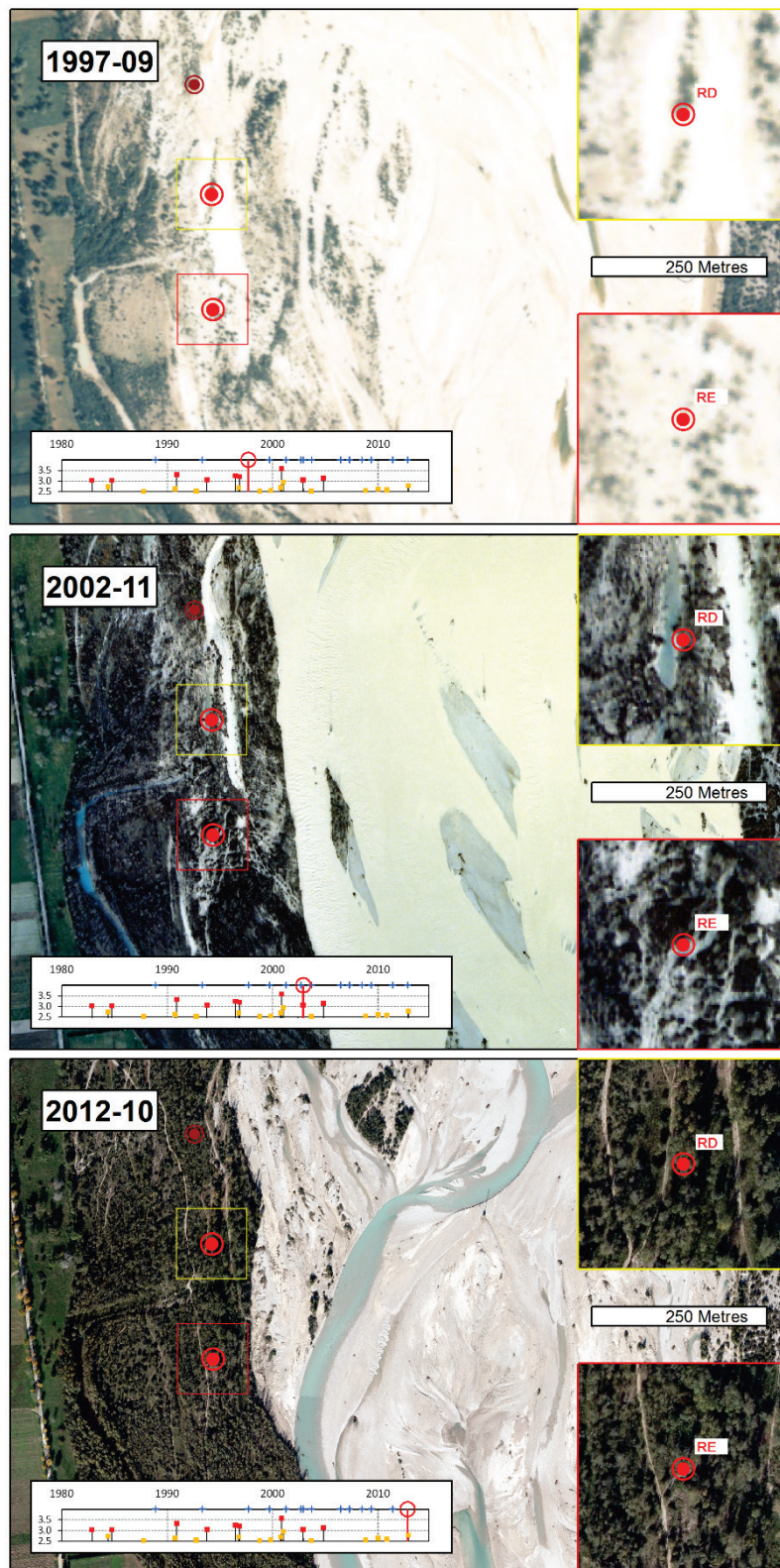


Figure 6.42 Key aerial images of the RD and RE neighbourhood, 1997-2012. Image sources in Table 6.1.

In the four years after 1993, which included 3 large floods, the main channel migrated towards the left bank, allowing significant vegetation regeneration on the western half of the active tract by 1997. There had been expansion of the linear feature of which RD is a

component, though it seemed a significant volume of water still flowed either side of this in floods. At RE there was a patchy distribution of trees, perhaps resulting from regular sediment deposition, burial and mortality of intervening stems. The 2002 image essentially showed the same pattern of trees as before, but the trees were more mature. There had been only limited in-fill of woody vegetation between the older stems, but perhaps an increased cover of grass and herbaceous plants. The patch around RD had expanded eastwards and the stem (or set of stems) immediately north of RE had grown significantly. Taken during a substantial flood, this image showed that minor channels adjacent to the trees of interest were still active at high flow. The sites of focus remained effectively undisturbed over the next decade, and the 2012 image showed only in-fill of stems between older trees, presumably by clonal expansion.

Age structure

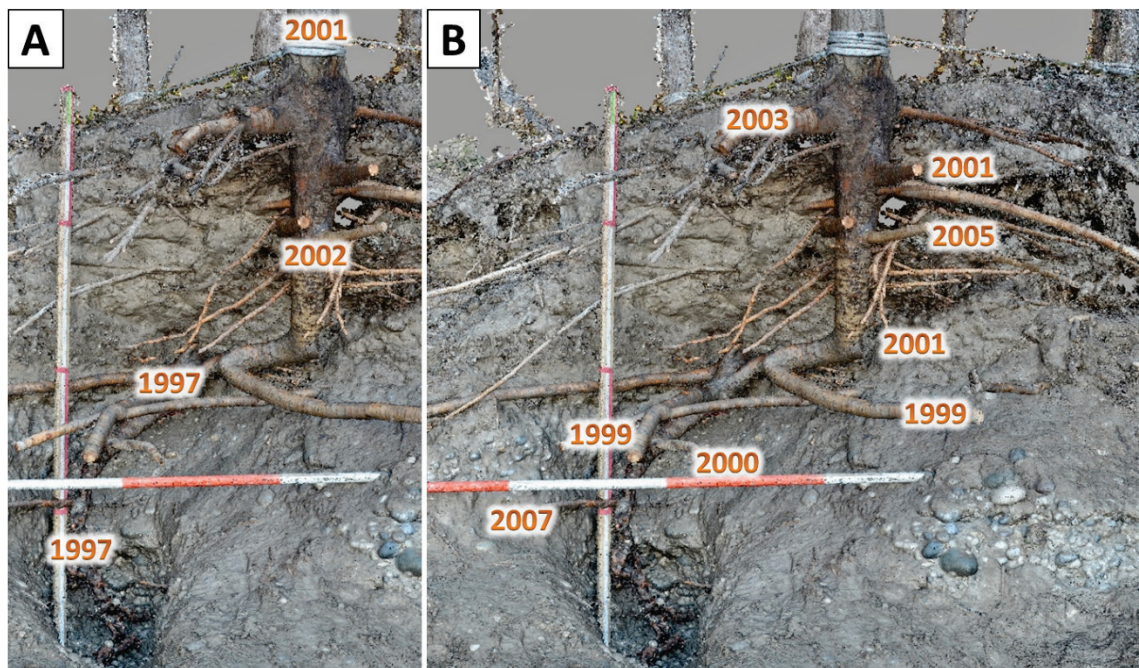


Figure 6.43 Estimates of latest possible dates of origin of different parts of the main axis (A) and lateral roots (B) of the RD root system, from dendrochronological analysis.

The extant aerial stem at the time of sampling dated back to 2001 or earlier, and a similar date was found for the buried portion of this vertical axis. Beyond the node labelled B in Figure 6.39, the main axis pre-dated 1998. Lateral roots were a variety of ages, with one of the uppermost established by 2003, and most of the horizontal roots associated with the grafting layer (C, D, E) seemed to originate in or before 1999.

Discussion and summary

Early aerial images suggest that vegetation at this site developed as part of a linear channel margin feature. The fact that roots have very readily grafted suggest that the stems here are all the same clone, and the 1993 image appears to show a single deposited tree at the site. While the slightly later dates of the structures excavated suggest that they may not be original parts (or closely connected to parts) of this deposited wood, it is proposed that all the stems and their associated sub-aerial structures have developed from this 'parent tree'. Although no 1997 adventitious root was sampled, it seems likely that this system developed from expansion of horizontal roots into fine deposits associated with the 1996 floods (coincident with point G in Figure 6.39). The wandering course of the axis below this point suggests it was a sinker root, while the straight but downstream deflected axis above suggests it was a stem. This stem appears to have been flattened and buried in the October 1998 flood, with a proliferation of adventitious roots then expanding in 1999 into fines deposited on the flood's falling limb. Indeed, the aerial imagery shows considerable deposition between 1997 and 1999. Other parts of the clonal root system appear to have similarly expanded horizontally at this time, grafting where their paths crossed. The last major phase of deposition at this site appears to have occurred during the late 2000 flood, and the major vertical axis seems to be a sucker which has grown up through the associated silty sand layer. The second highest lateral root labelled in Figure 6.43 conveniently dates the upper limit of this layer, whereas the distinctly sandier stratum atop this looks likely to have been associated with the November 2002 flood, dated by the highest labelled lateral root.

This case study shows the markedly different behaviour of a clonal, suckering, well-developed planar root network, in contrast to structures related to the early developmental phases of single deposited trees, fragments or seedlings, which may later produce such an expansive horizontal network.

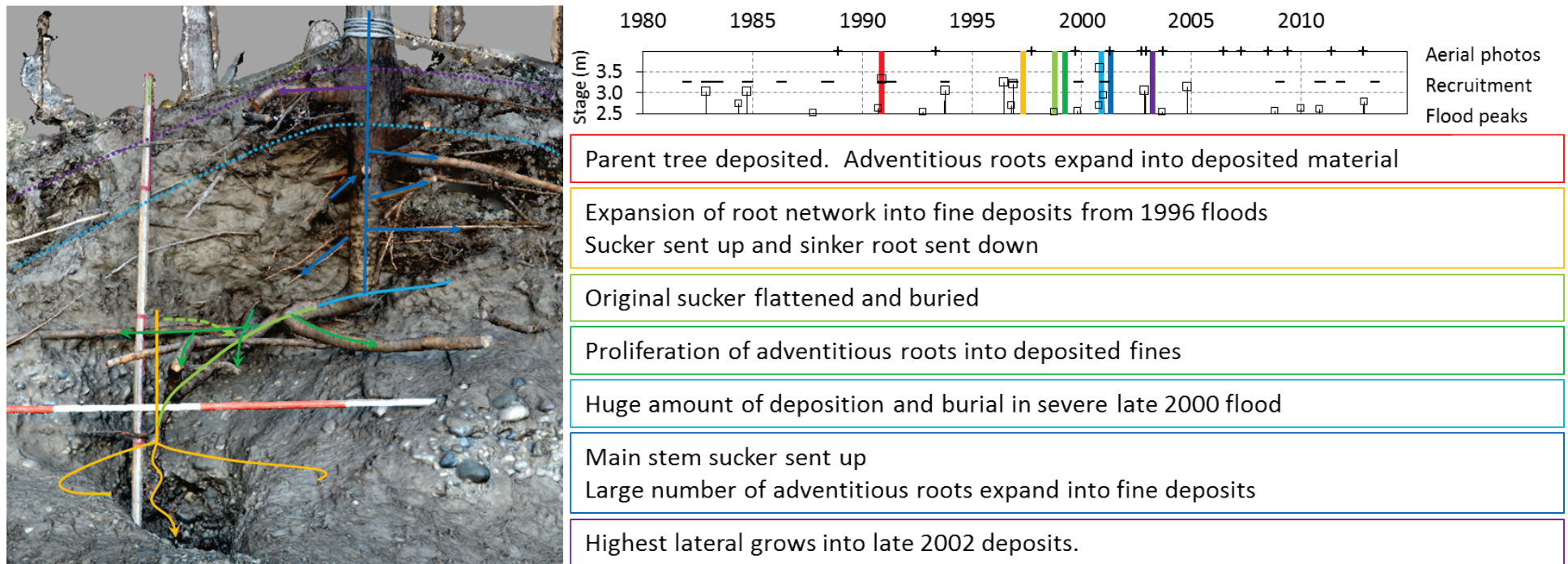


Figure 6.44 Summary of the proposed potential development trajectory of case study RD. Text box colours relate to events marked on the SfM model and timeline.

i Case study “RE”

Overall form, key features and sedimentology



Figure 6.45 Front perspective view of RE model with key features and main sedimentary strata identified. The image has been mirrored such that flow is left to right. See further explanation below and in the introduction to this Section.

This specimen comprised a pair of stems, the smaller of which was closer to the bank and was excavated. This stem was 17 m in length and had a diameter of 15 cm at 1.2 m above the bank top, with many supporting laterals just below the ground surface, supporting the upstream lean of this stem. The two stems were connected by a large diameter (approx. 20 cm) buried trunk (A) which took a straight, gently angled course from the larger to the smaller stem, turning more steeply downward to connect at B (see Figure 6.46). One other small stem (dead) emerged from this connecting section (C). The node B, associated with the top of the gravels, also possessed many large horizontal roots projecting downstream. Below this node, the very massive main axis lay at an angle of about 20° from horizontal, with a substantial root emerging halfway along this section (D), proceeding downstream along the top of an unconsolidated gravel layer. A vertical section then occurred below this, with another major node (E) at the top, producing four large horizontal roots spreading in all directions, following the same sediment horizon as D. The bottom of this vertical section was marked by a near 90° bend in the main axis (F) which then continued horizontally out towards the channel (towards the observer in Figure 6.45).

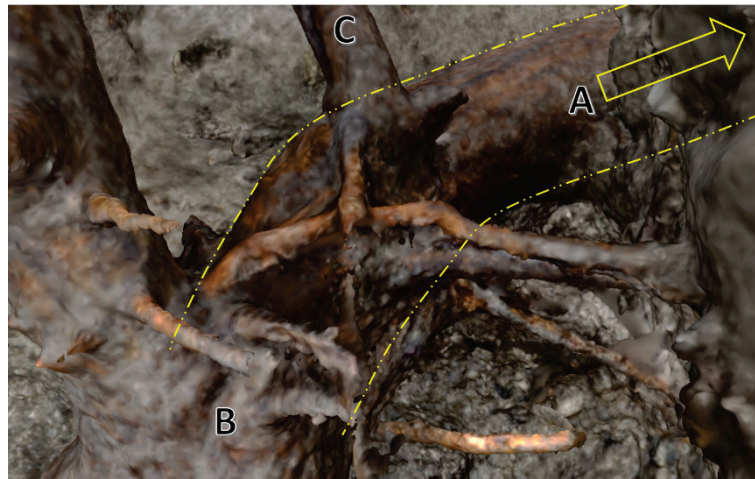


Figure 6.46 Detail of RE model showing the connecting axis (A) bending downwards prior to connecting with the main stem axis being excavated (B). Labels correspond with features in Figure 6.45. Model image has been mirrored to maintain consistency with other figures.

Vegetation and channel change from aerial imagery

(see images and commentary for R3, above)

Age structure

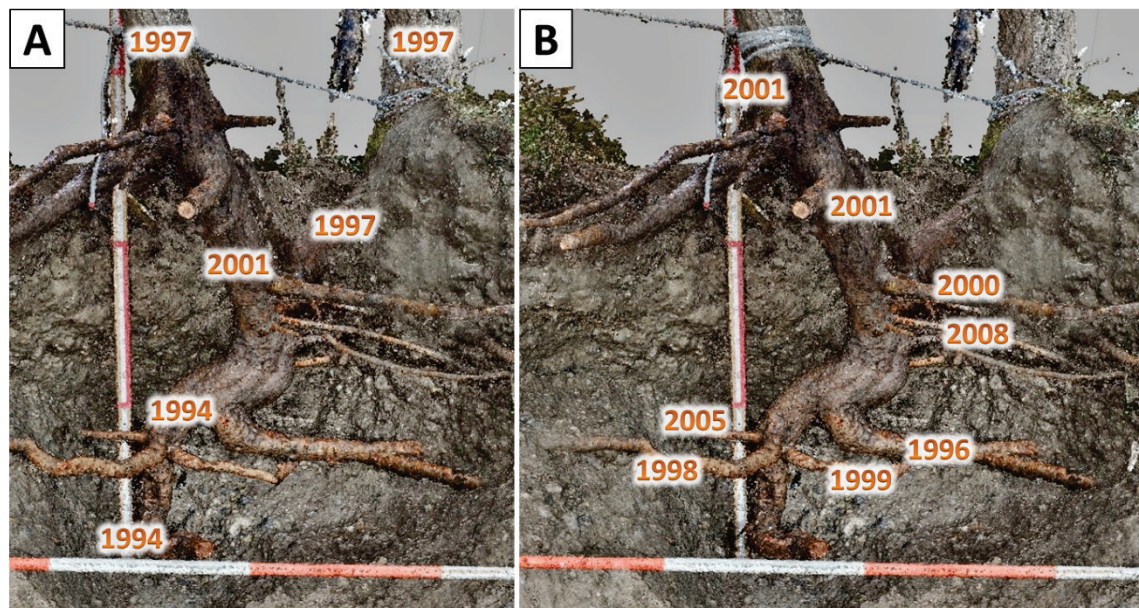


Figure 6.47 Estimates of latest possible dates of origin of different parts of the main axes (A) and lateral roots (B) of the RE root system, from dendrochronological analysis.

The deepest and oldest parts of this system were established in 1994, while the two aerial stems dated back to 1997 or earlier. The large connecting axis also pre-dated 1998. Lateral roots in the upper sand pre-dated 2002, while lower laterals dated to the mid-to-late 1990s.

Discussion and summary

There is, unfortunately, a substantial gap in the aerial imagery for this site around the probable years of establishment for this tree as based on the dendrochronological samples. However, the recruitment model suggests that 1993 is a likely year for its initiation and it seems quite possible for it to have developed from seeds or vegetative propagules deposited on the emerging landform visible in the May 1993 image, taken 5 months before a significant flood. In fact the sparse, patchy structure of vegetation in the following 1997 image suggests the deposition of wood, rather than seedlings, which are more often encountered in a coherent block (Corenblit et al., 2014). The main axis below node E has irregularly-shaped annual rings through its entire section, indicating that this originated as a root, tracking down between gravel particles, and suggesting that node E is the point of origin of this tree. This is also borne out by the regularly distributed lateral roots tracking out in all directions from this point. This first taproot turned 90° on encountering the deeper, more consolidated gravel deposit, and continued to track along its upper horizon. The date of the large root labelled D in Figure 6.45 suggests that the original shoot was flattened in the summer 1996 flood. Indeed, the 1997 aerial image does show it to be in a rather exposed position on the braid plain, and a large amount of gravel deposition is evident. A new shoot from node B then presumably became the dominant stem, only to be knocked down again, this time back towards the bank, later that year in the second major flood. This appears to constitute a lot of formative action and sediment deposition in a short period of time, but the 1997 limiting date on the extant aerial stems dictates that the connecting axis from which they originate (vertically) must have been in position by this time. Unfortunately, as previously mentioned, potentially corroborating aerial photo evidence is lacking. However there is very substantial change depicted more generally between 1993 and 1997 in this part of the braid plain. The sharp bend angle of the deflected stem (Figure 6.46) also suggests that it was particularly young and flexible at the time. Following the major disturbance in 1996, the deflected axis seems to have sprouted a strong distal shoot (the larger, more downstream of the two trunks standing at the time of excavation), a shoot immediately at its base (B – the second trunk standing at excavation), and another at the point of bending (C), which later died.

This is merely one potential explanation of the complex form of the buried structures of these trees, but the evidence would imply that this case study demonstrates that many morphogenic processes can occur in just a few years.

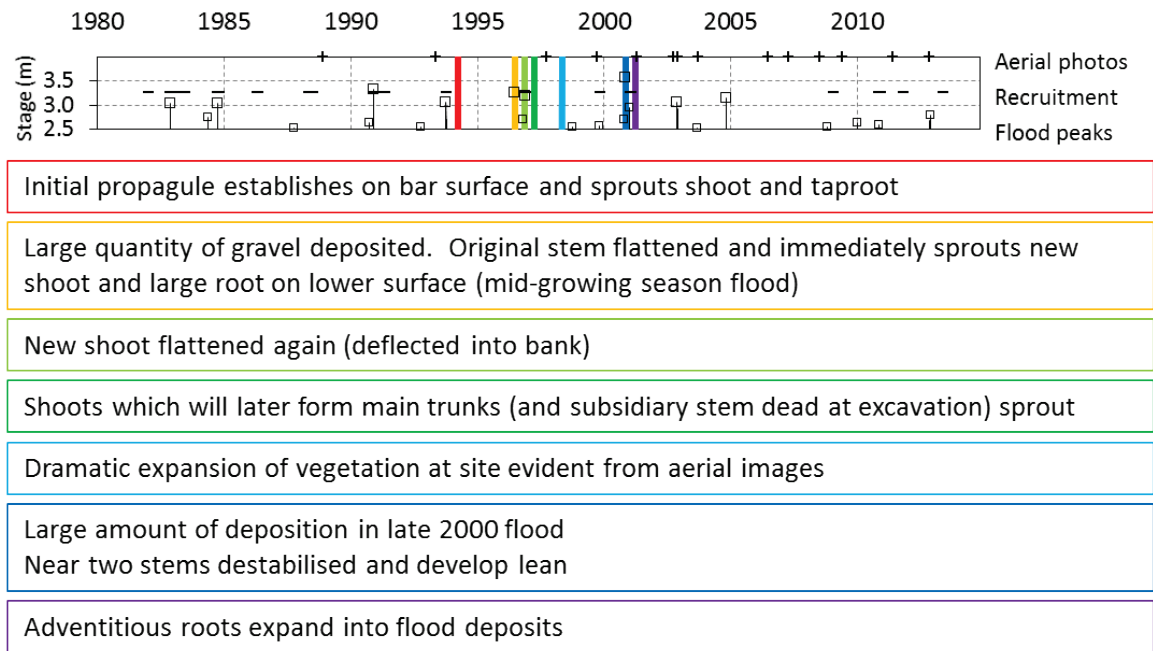
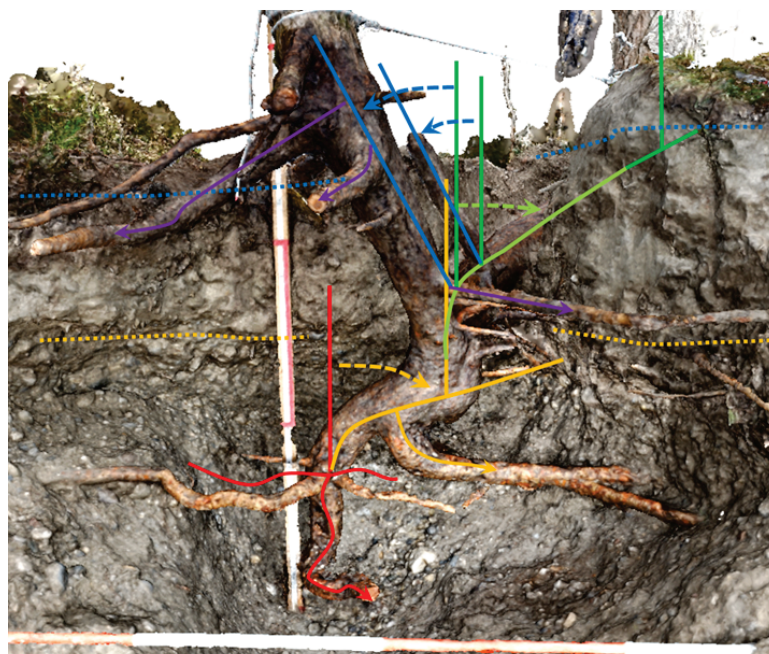


Figure 6.48 Summary of the proposed potential development trajectory of case study RE. Text box colours relate to events marked on the SfM model and timeline.

6.3.3 Compiled observations from this and other studies

a Adventitious roots

Structures and properties

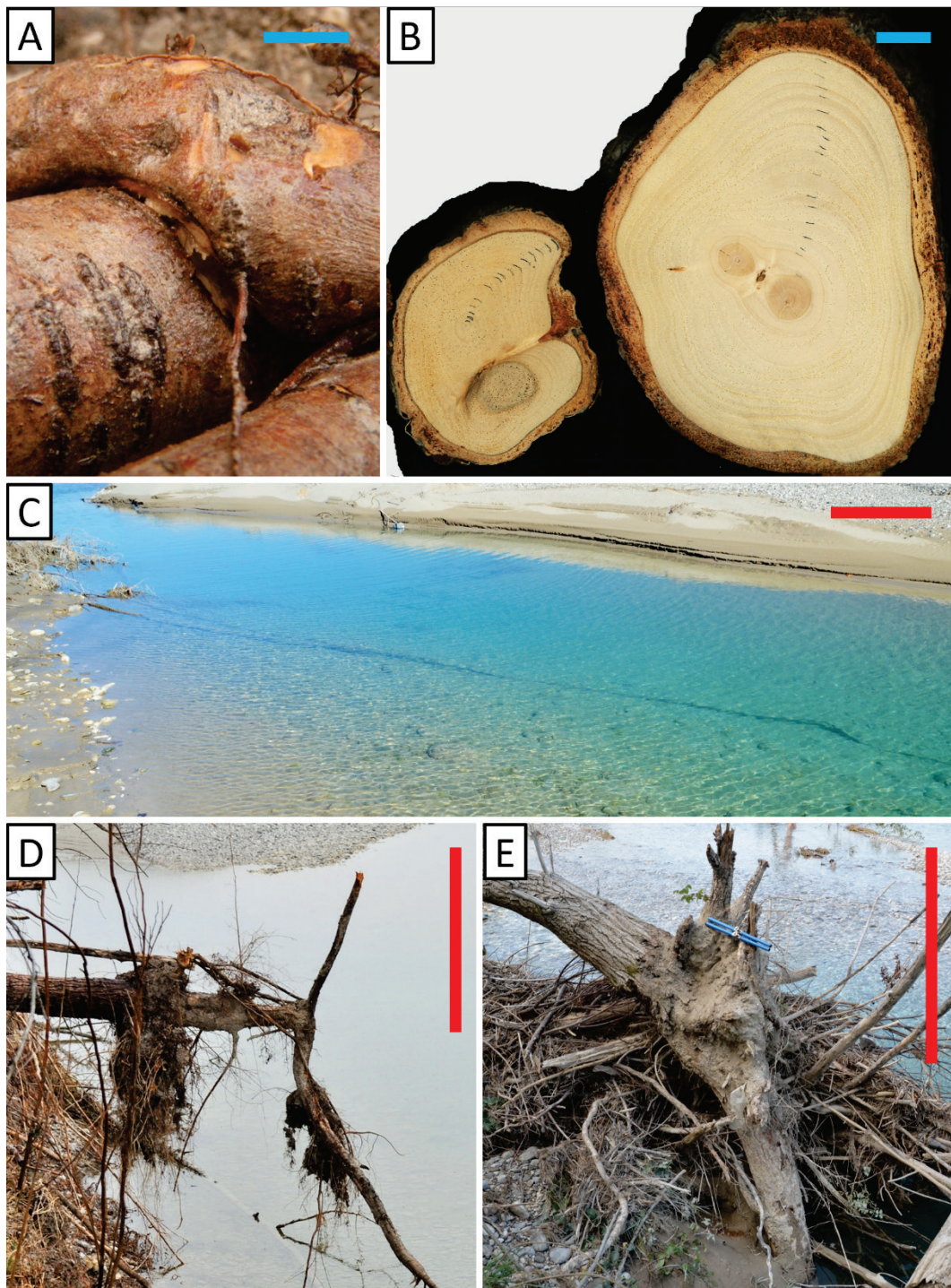


Figure 6.49 Adventitious root structures and properties. A: Weak grafting. B: Strong grafting. C: Extremely long root. D: Classic sucker root structure (deposited tree snagged on bank). E: Ambiguous root structure which may be related either to suckering or flood disturbance. Blue scale: approx. 1 cm. Red scale: approx. 1 m on feature of interest.

The proliferation of adventitious roots is a fundamental adaptation of black poplar to the unstable and heterogeneous riparian environment. Several features of these specialised structures pertaining to riparian vegetation dynamics, which are not necessarily prominent in the literature, were noted in the field and are highlighted here.

Two types of grafting of roots were observed. The first (Figure 6.49 A) was a weak association of the root wood, which could readily be pulled apart. Stronger grafting, with fusion of the vascular cambium (Figure 6.49 B) was seen in several sections taken for tree ring analysis. It is acknowledged that the weak examples were most often seen in younger roots (< 5 years) and may represent an early stage in the same process, however, complete fusion appears to be possible within this early period, as seen in many root sections.

Figure 6.49 C provides a dramatic example of the possible extent of these exploratory horizontal roots. This particular specimen, unlike most other long lengths which become exposed, probably resisted dying back by being submerged in well-oxygenated water. The nearest stem was more than twenty metres from the tip of the root in the Figure.

Suckers borne from adventitious roots produce a characteristic ‘inverted T’ root architecture, as seen in Figure 6.49 D. Authors have previously noted preferential wood development on the side of the horizontal root furthest from the parent tree in deteriorating aspen (*P. tremuloides* Michx) stands (Schier, 1982), and examples encountered in this study certainly show such asymmetry. This T-shaped structure was only noted in young trees, however. It seems likely that as stems grow and increase their photosynthetic capability (and thus independence) and/or are released from dominance by a parent stem, secondary root growth will outpace that of the original connecting root, and the form exemplified in Figure 6.49 D will become less apparent. Another common type of gross root architecture encountered was a more ‘J-shaped’ form as depicted in Figure 6.49 E and Figure 6.50. Although it is recognised that such a form may have originated from the classic root sucker architecture, the extreme asymmetry and larger angle between stem and dominant root axis suggest deflection and burial in floods to be a more likely cause, in this dynamic riparian context.

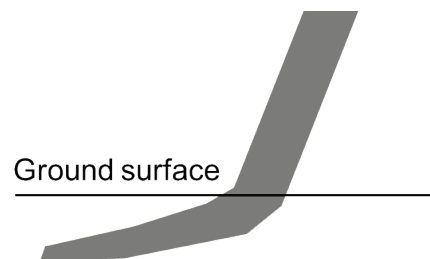


Figure 6.50 Basic representation of the commonly encountered ‘J-shaped’ form of the main tree axis.

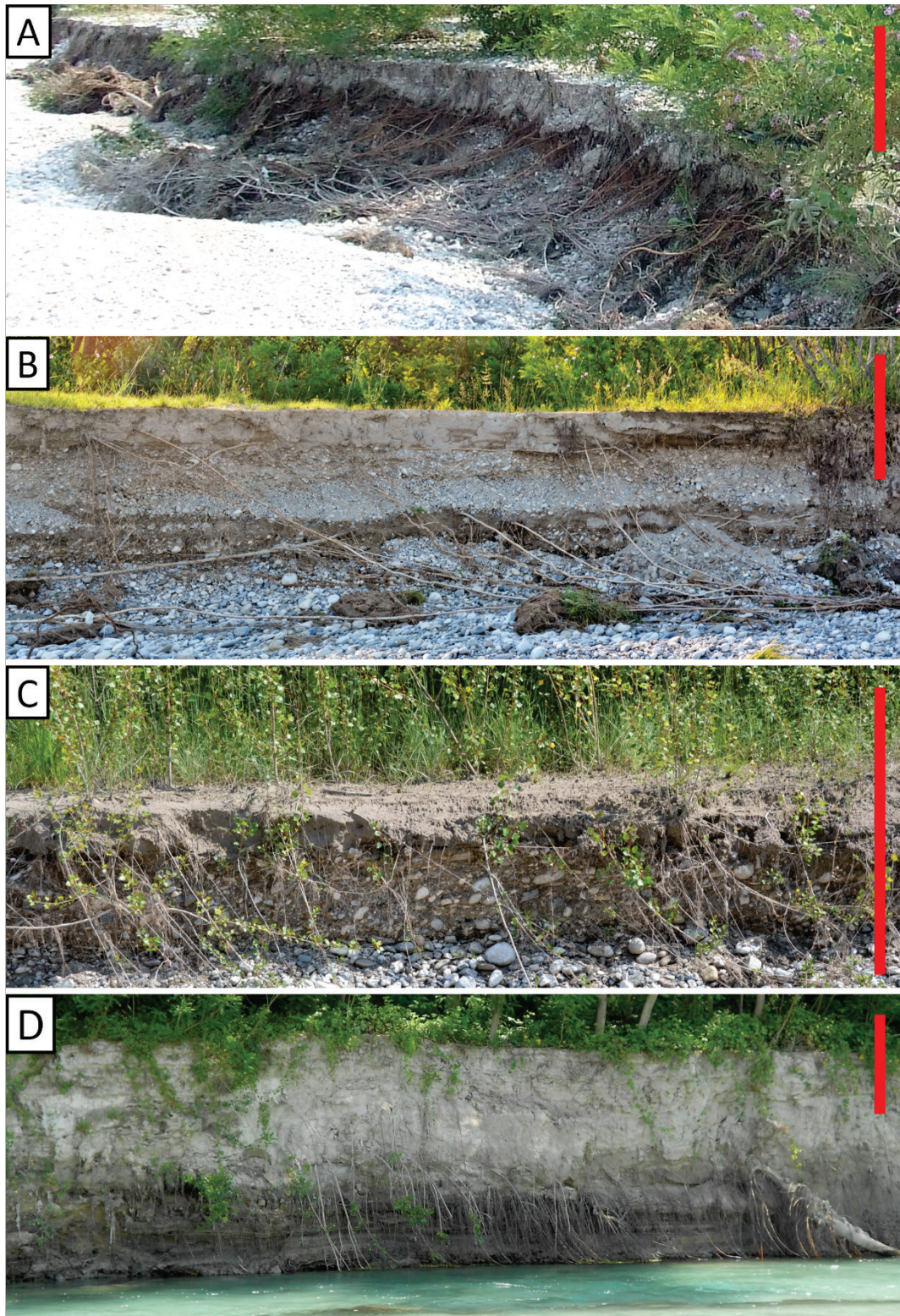


Figure 6.51 Adventitious root distributions. A: Thin, dense mat confined by gravels. B: Long, coarse roots proliferating in surface fine sediments and even more so in a buried fine-grained stratum. C: A mass of young (approx. 1 year) poplar stems interconnected by a dense web of suckering roots in a thin (approx. 10 cm) surface layer of fines. D: Maximum density at the top of the capillary fringe. Scale bar: 1 m (approx.). Flow: left to right.

Chapters 4 and 5 of this this thesis analyse root distributions quantitatively, but without explicit consideration of the diameter class into which most extensive, horizontal, adventitious roots fall (approx. 7 – 35 mm). This type of root is particularly obvious to any casual observer in the field, however, and the photographs in Figure 6.51 exemplify some recurring phenomena, which are described in more qualitative terms below.

Conspicuous protruding roots are frequently very clearly confined to fine-grained sedimentary layers and nearly completely absent from intervening gravel seams. Where the fine sandy and/or silty layer is narrow, extremely high densities of roots of all diameters are often apparent, as in Figure 6.51 A. In more substantial deposits (such as in Figure 6.51 B), fewer but larger diameter roots appear to dominate.

Figure 6.51 C demonstrates that such an expansive network of suckering roots can also be associated with very young trees, early in the establishment phase. The rather uniform size of stems here and the thin fine sandy sediment deposits suggest that suckering may also occur as a mechanism of in-filling among a patch of germinated seedlings. The lack of large diameter roots in this case implies that these stems are not dependent on established mature trees, but rather on each other in this newly colonised flood deposit.

Rood et al. (2011) concluded that North American poplars (cottonwoods) were variously phreatophytic depending on the growing season evaporative demand. Figure 6.51 D supports this conclusion, very clearly showing peak root density at the edge of the low flow capillary fringe. Indeed, the location of this photograph is at one of the downstream sites on the Tagliamento, where rainfall is relatively low and average temperatures relatively high. Among the full set of sites sampled in the field campaign for the current study, however, such deep, uniform fine-grained sediment deposits were rarely encountered, and so such a clear association with the water table was not easily observed. Instead, local seams of fine-grained material constituted hotspots of moisture availability and retention within the bank profile, and the heterogeneous distribution of this water is noticeable as darker patches in Figure 6.51 B.

b Results of gradual burial

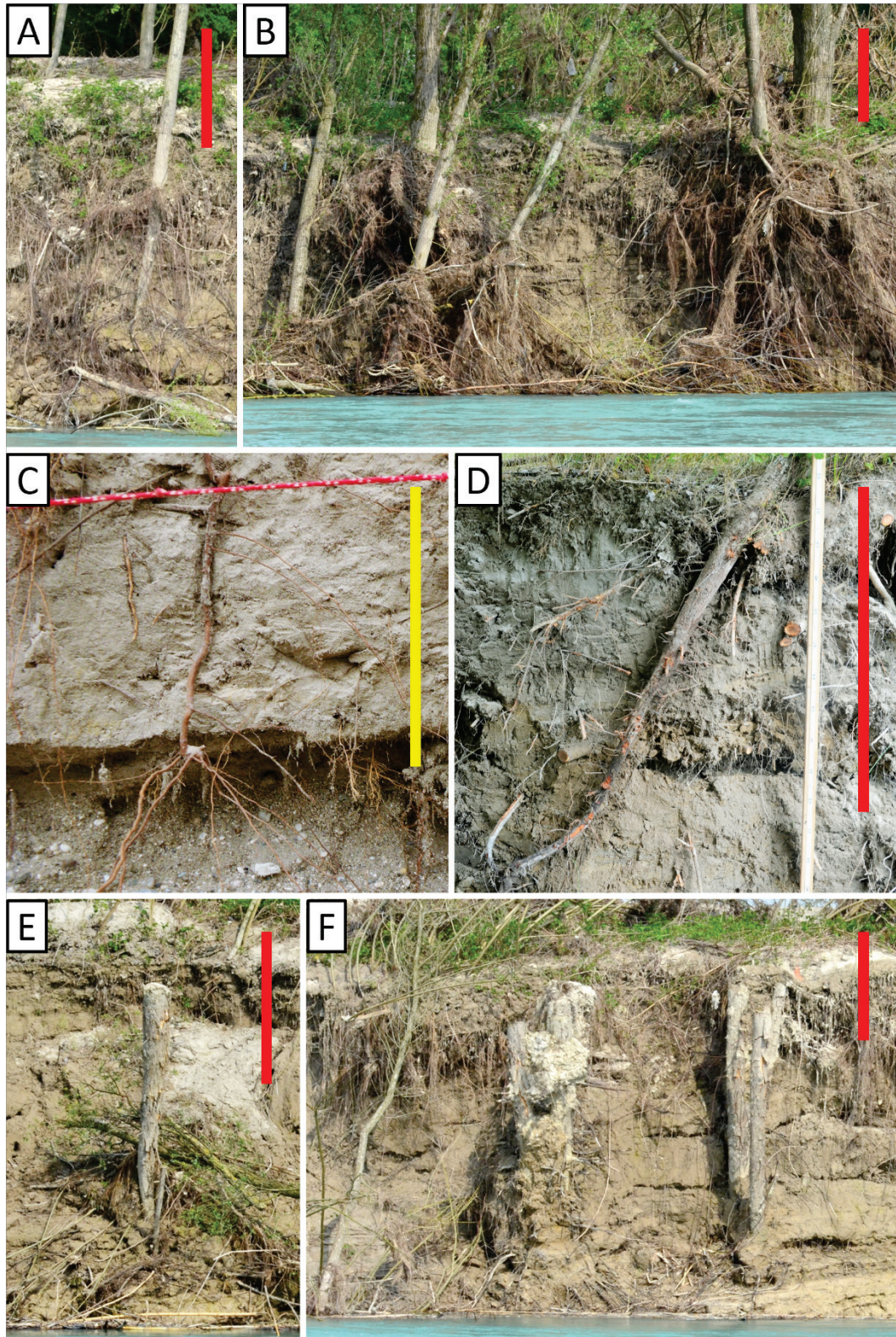


Figure 6.52 Deeply buried stems in fine sediments. A, B: Surviving poplars with deep, straight, buried stems. C: Dead *Salix* spp. seedling, germinated on gravel, with adventitious roots visible in overlying fines. D: Deeply buried *Salix* spp. with many adventitious roots (trimmed). E, F: Large dead buried stems. Red scale: 1 m approx. Yellow scale: 10 cm approx. Flow is left to right.

Central to the fluvial biogeomorphologic succession, particularly in its later stages, is the trapping of fine sediments by riparian trees, and the tolerance – and indeed exploitation – of stem burial in this material. Figure 6.52 provides some examples of just how extensive this can be.

Even accounting for the fact that the trees in Figure 6.52 A and B appear to have slipped down the bank somewhat, bank erosion has revealed that large diameter, straight, buried stems can extend two metres or more down into riparian sediments. Figure 6.52 A demonstrates proliferation of finer roots in a ‘collar’ in the upper, organic soil layers, but reasonably large, well-distributed coarse roots all the way down the main axis below this. The second and third fallen stems from the left of Figure 6.52 B illustrate that these deeper roots can also be more numerous – an assertion further supported by the deep, dense root systems of the group of stems on the right of the Figure, which have yet to slip down the bank.

Figure 6.52 C and D show this process occurring at smaller scales, on younger sites, and in this case in *Salix*, the sister genus of *Populus*. C clearly shows germination on the top of a gravel and sand bar, with adventitious roots emerging at right angles from the stem above. The age of this specimen demonstrates the speed with which burial may occur. The willow in Figure 6.52 D shows a concentration of adventitious roots in the lower half of the buried stem, coincident with a particular sediment layer.

Such buried stems can clearly leave a significant legacy of buried organic material long after the death of the aerial stem under certain conditions, as exemplified by Figure 6.52 E and F.

c Features associated with deposition of transported wood

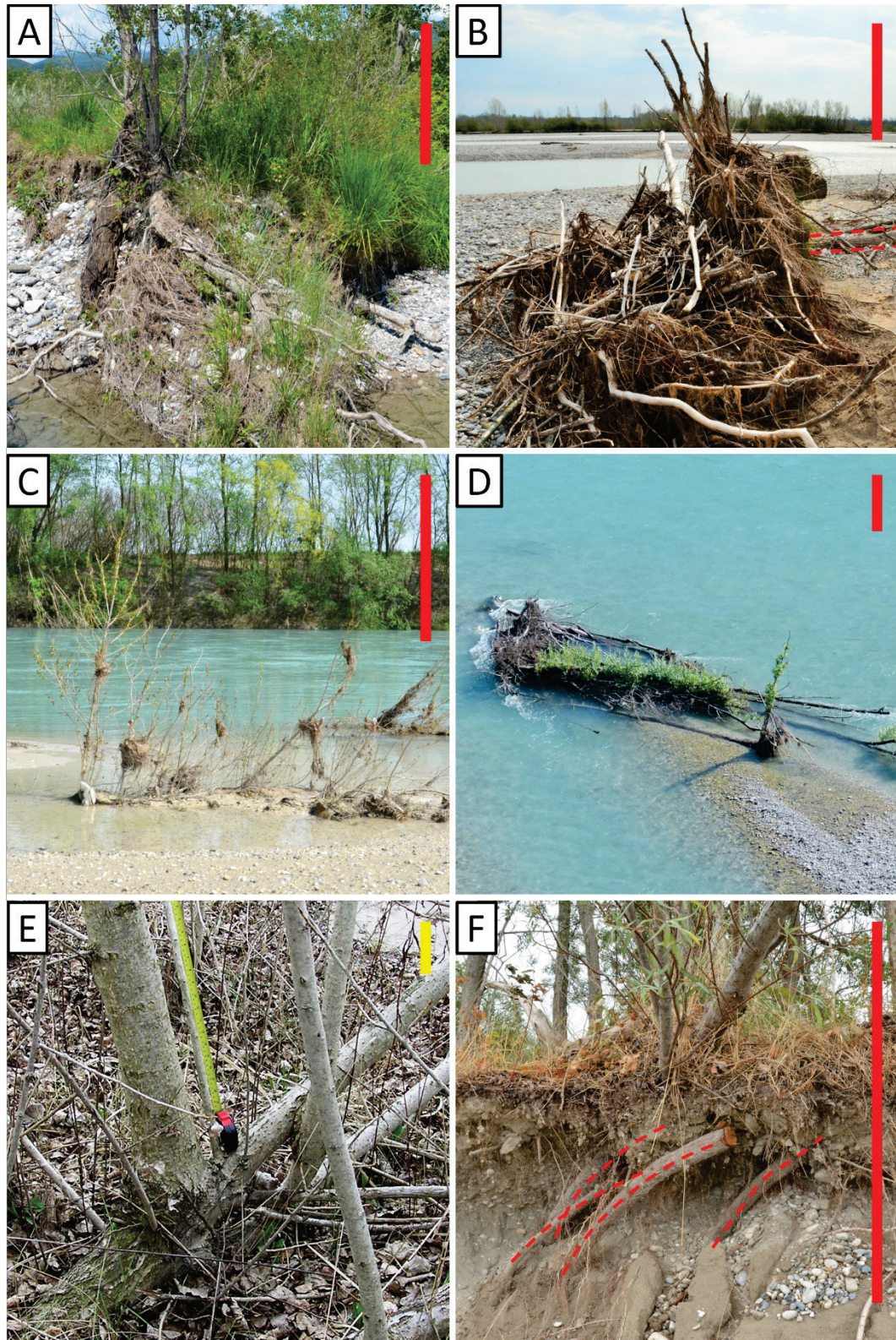


Figure 6.53 Features resulting from deposition of wood. A: Deflected stem at upstream end of pioneer island. B: Root plate of deposited tree (trunk indicated) acting as large debris trap. C, D: Dominance of closest branch to root wad on deposition (D appears to be lateral root). E: Characteristic geometry of branch union in surviving deposited crown. F: buried crown of *Salix* spp. preserved in gravels. Red scale: 1 m approx. Yellow scale: 10 cm approx.

Interpretation of the case study trees attributed many features to the action of large volumes of flowing water, and the deposition of live wood. The examples in Figure 6.53 provide evidence for these morphogenic processes, seen in their early stages, before burial.

Many of the case studies incorporated a long, downstream-swept large diameter axis at a low angle from the horizontal. Figure 6.53 A provides an example of this in context, at the upstream point of a pioneer island (a landform attributed to a single key tree). In this case, the island is at quite a well-developed stage. While lateral sprouts from the original deposited axis are now well-developed, probably independent trees with a good rooting resource immediately below them, this original, long sloping stem may have been retained as it connects the extant stems with a persistent water source – a pond collected in the upstream scour hole.

Figure 6.53 B demonstrates how effective a large root plate on a deposited tree may be at collecting and trapping flood-transported debris. Upon later burial, it is easy to see how such a concentration of organic material could constitute a valuable nutrient and moisture hotspot, and may help explain the retention of upstream roots in buried and re-sprouted trees.

Most of the case studies above implied survival of only the lowermost one or two shoots emerging from a deposited or deflected aerial stem. The examples in Figure 6.53 C and D appear to support this. In the case of C, it seems many lateral stems initially sprouted but perhaps the upstream-most branch monopolised the existing root resource. In example D (where, unusually, the tree has been deposited with roots downstream), it appears that a protruding lateral root has in fact sprouted leaves.

Figure 6.53 E demonstrates another potential development mechanism for the ‘J’ or asymmetric ‘T-shaped’ stem base structures seen in Figure 6.49 E and Figure 6.50 (cf. root suckering). Here, radial growth of the original deposited branch (now lying diagonally bottom left to top right) has slowed above the node, but continued below it, to support the now dominant lateral sprout (just off-vertical). This particular pattern of relative diameters around a node was encountered on several occasions during excavations.

The survival of many of the original branches of a deposited and buried tree or shrub crown appears to be a regular occurrence. The shrub form of many *Salix* species on the Tagliamento (as seen in Figure 6.53 F) better lends itself to this process which may then result in a patch of multiple secondary stems. By comparison, poplars tend to show much more apical dominance, and so the crown is much more diffuse along the main axis. However, where young poplars are buried, there appears to be a greater chance of the development of this multi-stem form among the resulting regrowth.

d Effects of bank dynamics

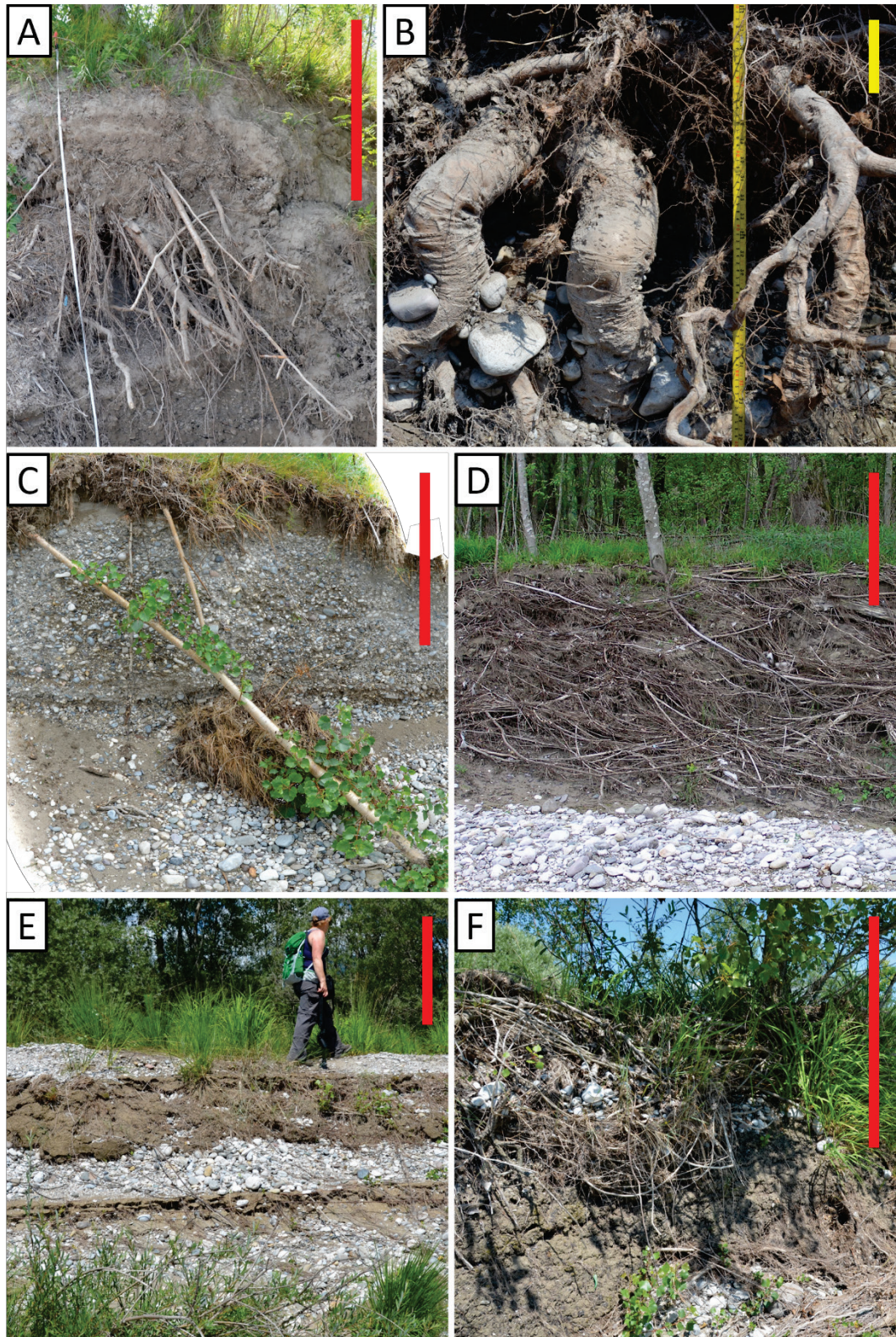


Figure 6.54 Interactions between bank dynamics and roots. A, B: Adventitious roots pulled downwards by bank failure. C: Re-sprouting adventitious root exposed by erosion. D: Bank protected by mass of adventitious roots. E, F: Bank protected by exposed flaps of thin, matted roots in silt and clay. Red scale: 1 m approx. Yellow scale: 10 cm approx.

For the purposes of excavation, the trees selected in the case studies above were necessarily situated close to the bank edge. Figure 6.54 demonstrates some particular interactions between roots and bank dynamics, which are explained below.

Given the large horizontal extent of poplar roots, even when the main stem is at a significant distance from the bank, mass failure can modify the form of roots. In the case of Figure 6.54 A, a large, cohesive block of upper, root-reinforced sediment has been undermined and fallen down the bank face, re-orienting the major tree roots it has dragged within it. In Figure 6.54 B, it is presumed that a similar event occurred when the bent roots were much younger and more flexible, leaving them with the distinctive angles seen here.

Many of the Figures in this Sub-section show adventitious roots exposed by bank erosion. While the majority of exposed roots gradually die back, many also re-sprout near the bank face, as in Figure 6.54 C. If the supply of resources from the connected root system is sufficient, or particularly when bank slumping leaves a good fine-textured bank face into which new roots may develop, stems emerging from these exposed roots may become sufficiently large to encourage deposition and reverse the effects of the initial erosive event.

Extremely high densities of exposed adventitious roots are often encountered, and when in such numbers as in Figure 6.54 D, may form an effective protective high roughness layer, again providing resistance against further erosion.

Finally, it was also frequently observed that, where particularly narrow seams of fines are exploited by roots as in Figure 6.51 A, gravels either side of this layer are sometimes eroded at a much faster rate, causing the exposed silty root layer to flap down onto the stony bank face, as in Figure 6.54 E and F. This phenomenon may present another erosion resistance mechanism, with the enmeshed roots acting in a similar way to a man-made geotextile, particularly if the matted layer becomes adhered to the coarse sediments through re-wetting of clays by rain and/or root growth into the underlying gravels. Additionally, such root mats may limit the down-cutting of channel avulsions, maintaining a higher number of shallower channels.

6.4 DISCUSSION

This study has shown that black poplar, in such a geomorphologically active system as the island-braided Tagliamento, regularly supports a large, deep and bulky unseen biomass within riparian sediments. Buried stems account for the gross structural framework of root systems, and are found in forms representing a continuum from virtually no disturbance to multiple violent exposures to fast-flowing water and transported sediment and debris. These large structures often occupy the full depth of the soil profile down to the low flow water table.

Using a variety of primary and secondary sources of information, attempts have been made to explain the development of buried structures of eight case study trees, showing the dramatic effect of exposure to floods. It must be acknowledged that interpretation of the very limited data available introduces a significant degree of uncertainty to these speculative reconstructions of the past. Indeed, there is virtually no precedent for this type of work and analyses could be taken much further – particularly with regard to the examination of samples taken for tree ring analysis. However, the approach adopted here is believed to have been conservative in recognition of limitations in the data, always with the most parsimonious explanation accepted for signals observed across multiple sources.

The novel application of SfM photogrammetry has been exceptionally useful, particularly for post-hoc exploration of hypotheses to explain certain structural characteristics which may not have been noted in the field. Though the method is not currently workable for capturing fine root architecture at the whole tree scale, there will no doubt be further improvements in technology and software allowing more detailed model construction in the future. The method certainly allows for much reduced time in the field; there is no requirement for removal and storage of roots (as in, e.g., Vennetier et al., 2015); and the automatically constructed, highly detailed model is then permanently available for analysis with new methods as they may be developed in the future. Furthermore, it is also possible to distinguish broad sediment types in the SfM model.

6.4.1 Features common to most or all case studies

As stated above, buried stems appear to make up the obvious bulk of the buried structures. It was originally anticipated that the year of burial could have been pinpointed from changes in the wood vessel structure, but the clear contrasts described by Friedman et al. (2005) in *Tamarix ramosissima* Ledeb. and *Salix exigua* Nutt. annual rings were not easily distinguishable in the poplar samples. Therefore there is still a small chance that these structures were misinterpreted roots rather than buried stems, but the weight of other evidence – particularly the consistent angle observed with respect to streamflow – supports the alternative

hypothesis. Should the main axes indeed be remnants of the original, rapidly downward-growing seed root, one potential explanation for the additional upstream growth vector may be a slightly higher water table at the upstream end of the deposited sediment, relating to the head difference driving interstitial flow. However, whether such a presumably subtle water table gradient could produce such dramatic root forms remains to be tested.

All the main buried stem axes exhibited a downstream deflection, even in the most sheltered case (RA), and the most likely explanation for this is exposure to flowing water in the first few years of life of the shoot, while it was still relatively flexible. Indeed, the reconstructed timelines of all case studies suggest that almost all of the morphogenesis occurs within the first ten years. It is also possible that some of the deflection in sheltered sites may be due to an additional planar shear effect in saturated fine sediments, with drag from surface vegetation causing some slight slippage of sediment layers over one another. The buried stems, particularly when close to vertical, all displayed a downward tapering in diameter, in spite of an increase in age. Annual radial growth increments were smaller at depth, and it is assumed that this is due to the overburden and physical resistance to diameter expansion. Alternatively, this may have reflected a reduction in the conductivity requirement from deeper roots over time, with the stem becoming more reliant on the upper parts of the underground system as they developed.

Tree ring dates indicated many young roots at depth, and surprisingly few roots contemporary with the establishment of the main axis. This would suggest that even deep parts of the root systems remain active, maintaining constant turnover. It is presumed that one of the main factors driving the maintenance of the deep axes is phreatophyty – securing access to water when precipitation and storage in upper soil layers is low. This is something which could be investigated in future, comparing growth of deep axes with the precipitation record and testing for different strategies between sites of dissimilar soil moisture regime.

6.4.2 Differences between case studies and uncommon features

Differences between the root systems uncovered here are best described by contrasting the most and least disturbed trees, the extreme ends of this gradient perhaps being best represented by RC and RA, respectively. The most immediately apparent difference is the angle of deflection of the buried stem. In the most extreme cases, fast-flowing water is likely to cause such extreme deflection that the stem is snapped, and it will either die back or become detached. Neither of these two scenarios would leave a buried trace, however. The different angles observed must be the result of a combination of both differing stem

flexibility and drag forces (relating to water velocity and canopy structure), but also different rates of burial and calibre (i.e., density) of the material under which the stems are buried. For an extreme angle to be preserved, for example, there must be a sufficient weight of overburden, deposited while the stem is being displaced, in order to resist its elastic recoil. Consequently (but also reflecting the flow velocity and transport capacity), the steeper angles are observed in thicker layers of the more dense gravels. It follows that little or no deflection is associated with more gradual burial in fine sediments which tend to be deposited at higher elevations or in more sheltered sites.

Another obvious difference is that some case studies have multiple main axes, while others have only one axis. The emergence of multiple stems appears to be associated with originator stem deflection of more than 45° from vertical. This suggests that the degree of contact with fine sediments, deposited perhaps on the falling limb of a flood or in lower amplitude events, and the resulting opportunities for root development from multiple nodes on the flattened stem, is a limiting factor on the survival of new shoots. Though the sample size here is small, it appears that new shoots are only sustainable over the long term if they have sufficient sediment resources to develop their own independent root systems, close to the points of origin on the parent stem. Note that the subsidiary stem of case study R1, which formed from a bud embedded at higher elevation in gravel and which was only connected to roots by the remnant parent stem, did not survive. This scenario seems counter-intuitive in a species which is known for producing many stems from a shared root system, but perhaps highlights physiological shortcomings of buried (near-horizontal) stems in this underground connectivity role, as compared to the specialised adventitious roots which connect suckers. Only one sucker stem appears to have been encountered in the present study, in case study RD. This example would appear to show that such stems require a particularly extensive root system to support them. Other stems encountered may have originated as suckers, but the lack of any clear surviving parent roots appears to show that most stems quickly develop their own independent root systems, as opposed to the scenario in the aspen depicted in Figure 3.5.

The distribution of lateral adventitious roots also differs between the disturbed trees in more gravel-dominated substrates (as typical for the Southern Group) and the stems which have been buried more gradually in fine sediments (as is more common for the Northern Group, and in particular, in the uppermost strata). Adventitious roots are clearly associated with fine sediments in the profile (in agreement with the findings of Chapter 5), and this leads to the development of particular nodes of proliferation along the main buried axis in sites with more complex stratigraphy. Conversely, the distribution is more even in less-disturbed trees.

Even within deep fine sediments, however, patterns are observed. Particularly high densities of adventitious roots appear to be associated with the lower portions of silt and clay-rich layers, presumably representing initial expansion into newly deposited, nutrient-rich material. Both the density and size of lateral roots also increase near the top of deep fine sediments, and it is hypothesized that this represents both an increasing dependence on nutrient cycling in upper organic layers as soil development progresses, and a response to the increasing requirement for mechanical support as the tree continues to grow.

6.4.3 Implications

This study has demonstrated that the survival of frequent disturbance leads to a more complicated, and generally more massive, underground structure, with particular nodes of prolific adventitious rooting which connect the main axis to the bank. This fact, together with field observations that a much greater proportion of transported large wood appears to have root systems of the simple, straight, single buried axis type (Figure 6.55) than more complex gross root system structure, suggests that trees which have already survived disturbance may be more resistant to entrainment and transport than trees developing in more sheltered sites. Such tenacious trees may represent a ‘cul-de-sac’ or at least temporary pause in the biogeomorphic cycle as hypothesized in the introduction to this Chapter.



Figure 6.55 Typical examples of root systems evident on fluvially transported wood.

Consequently, the development of geomorphologic ‘hard points’ related to persistent trees, similar to those postulated in relation to slow-decaying dead wood by Collins et al. (2012), seems a distinct possibility. Repeated flattening, burial and re-sprouting effectively leads to the phenomenon of a progressive ‘downstream walk’ of the stems of these resilient trees. Even upon death, any remaining structures of well-embedded trees may become effective ‘snags’ for transported debris upon exhumation, as demonstrated in Figure 6.52, potentially presenting nuclei for landform development. This more complex picture is somewhat in contrast to the idealised schematic of Corenblit et al. (2014) (Figure 6.1), but may in fact be conceived as the superposition of the same processes illustrated, occurring recurrently, following disturbance events.

6.5 CONCLUSIONS

With respect to the specific questions outlined in Section 6.1.1, the following conclusions can be made from observations on the black poplars of the Tagliamento system:

- i. The fundamental root architecture assumed within the fluvial biogeomorphic succession model – of buried vertical stems giving rise to horizontal, suckering adventitious roots – is indeed observed, but the buried stems are often connected at depth, always exhibit some degree of longitudinal deflection, and adventitious roots are often irregularly distributed along them.
- ii. The buried livewood resource on the Tagliamento is clearly extensive and highly significant, and appears to be directly related to rates of accretion and the depth of perennial groundwater. Although quantitative estimates are problematic owing to complex geometry, all trees observed possessed a far greater underground biomass than would be expected for non-riparian trees. The emergence of young roots from even the deepest buried structures proves that they can remain active throughout the life of the aerial stem.
- iii. All coarse root systems seem to possess one or more main buried stem axis with a downstream angle of deflection and a downward taper in diameter. The main axis deflection may vary from a slight lean, to completely horizontal, to contorted in multiple directions. Adventitious roots often tend to be associated with particular nodes of proliferation on the main axes, coincident with fine-grained strata (which may occur anywhere in the sediment profile, contrary to the idealised fluvial biogeomorphic succession model). Only in sheltered sites do adventitious roots radiate in all directions; otherwise they tend to extend horizontally downstream of the main axis.

- iv. Secondly to the fundamental, inherited ‘buried stem-horizontal adventitious root’ architecture, flood events are the main influence on the shape and volume of buried livewood. Influence is strongest and most direct near the channel, where flood flows lead to the rapid sequestration of large diameter stems by flattening and burial in often significant depths of gravel. At greater distances into the floodplain or established islands, there is little direct mechanical influence, but the deposition of fines in floods indirectly leads to sequestration of biomass in smaller diameter but more numerous adventitious roots, as well as the more gradual burial of large diameter vertical stems. Note that the strength of such influences varies over time as channel patterns evolve and the relative positions of trees to the active channels change. The indirect effect of flood-related sediment deposition has dramatic influence over the shape and distribution of all roots, as demonstrated in Chapter 5.
- v. Obviously it is not possible objectively to assess the accuracy of the type of developmental reconstructions attempted here without intensive monitoring but, informed also by wider observations, reasonable agreement between the various sources of evidence has been achieved. However, there are likely to be a great many possible explanations for the observed signals in such limited data. Flow records and dendrochronology (in spite of its complications in *Populus* spp.) have perhaps proved to be the most useful sources of information.

The methodologies developed here have helped to highlight a significant and perhaps overlooked component of riparian vegetation dynamics, and present many open questions for future investigation. For example, further application of SfM photogrammetry will readily lead to a more quantitative treatment of fluvial buried livewood. The following chapter synthesises results of the studies reported in this thesis and explores some future possibilities.

6.6 REFERENCES

- BARSOUM, N. & HUGHES, F. M. R. 1998. Regeneration response of Black poplar to changing river levels. In: WHEATER, H. & KIRBY, C. (eds.) *Hydrology in a Changing Environment*. John Wiley & Sons Ltd.
- BARSOUM, N., MULLER, E. & SKOT, L. 2004. Variations in levels of clonality among *Populus nigra* L. stands of different ages. *Evolutionary Ecology*, 18, 601-624.
- BERTOLDI, W., GURNELL, A., SURIAN, N., TOCKNER, K., ZANONI, L., ZILIANI, L. & ZOLEZZI, G. 2009. Understanding reference processes: Linkages between river flows, sediment dynamics and vegetated landforms along the Tagliamento River, Italy. *River Research and Applications*, 25, 501-516.
- BERTOLDI, W., WELBER, M., MAO, L., ZANELLA, S. & COMITI, F. 2014. A flume experiment on wood storage and remobilization in braided river systems. *Earth Surface Processes and Landforms*, 39, 804-813.
- COLLET, C., LÖF, M. & PAGÈS, L. 2006. Root system development of oak seedlings analysed using an architectural model. Effects of competition with grass. *Plant and Soil*, 279, 367-383.
- COLLINS, B. D., MONTGOMERY, D. R., FETHERSTON, K. L. & ABBE, T. B. 2012. The floodplain large-wood cycle hypothesis: A mechanism for the physical and biotic structuring of temperate forested alluvial valleys in the North Pacific coastal ecoregion. *Geomorphology*, 139, 460-470.
- CORENBLIT, D., STEIGER, J., GONZÁLEZ, E., GURNELL, A. M., CHARRIER, G., DARROZES, J., DOUSSEAU, J., JULIEN, F., LAMBS, L., LARRUE, S., ROUSSEL, E., VAUTIER, F. & VOLDOIRE, O. 2014. The biogeomorphological life cycle of poplars during the fluvial biogeomorphological succession: a special focus on *Populus nigra* L. *Earth Surface Processes and Landforms*, 39, 546-563.
- CORENBLIT, D., TABACCHI, E., STEIGER, J. & GURNELL, A. M. 2007. Reciprocal interactions and adjustments between fluvial landforms and vegetation dynamics in river corridors: A review of complementary approaches. *Earth-Science Reviews*, 84, 56-86.
- DANJON, F. & REUBENS, B. 2008. Assessing and analyzing 3D architecture of woody root systems, a review of methods and applications in tree and soil stability, resource acquisition and allocation. *Plant and Soil*, 303, 1-34.
- ECKENWALDER, J. E. 1996. Systematics and evolution of *Populus*. In: STETTLER, R. F., BRADSHAW, H. D., JR., HEILMAN, P. E. & HINCKLEY, T. M. (eds.) *Biology of Populus and its implications for management and conservation*. Ottawa, ON, Canada: NRC Research Press, National Research Council of Canada.
- FRANCIS, R. A. 2007. Size and position matter: riparian plant establishment from fluvially deposited trees. *Earth Surface Processes and Landforms*, 32, 1239-1243.
- FRANCIS, R. A., GURNELL, A. M., PETTS, G. E. & EDWARDS, P. J. 2006. Riparian tree establishment on gravel bars: interactions between plant growth strategy and the physical environment. In: SAMBROOK SMITH, G. H., BEST, J. L., BRISTOW, C. S. & PETTS, G. E. (eds.) *Braided Rivers: Process, Deposits, Ecology and Management*. Blackwell.
- FRIEDMAN, J. M., VINCENT, K. R. & SHAFROTH, P. B. 2005. Dating floodplain sediments using tree-ring response to burial. *Earth Surface Processes and Landforms*, 30, 1077-1091.
- GUILLOY-FROGET, H., MULLER, E., BARSOUM, N. & HUGHES, F. M. R. 2002. Dispersal, Germination and Survival of *Populus nigra* L. (Salicaceae) in Changing Hydrologic Conditions. *Wetlands*, 22, 478-488.
- GURNELL, A. 2014. Plants as river system engineers. *Earth Surface Processes and Landforms*, 39, 4-25.
- HUPP, C. R. & RINALDI, M. 2007. Riparian Vegetation Patterns in Relation to Fluvial Landforms and Channel Evolution Along Selected Rivers of Tuscany (Central Italy). *Annals of the Association of American Geographers*, 97, 12-30.
- MAHONEY, J. M. & ROOD, S. B. 1992. Response of a hybrid poplar to water table decline in different substrates. *Forest Ecology and Management*, 54, 141-156.
- MAHONEY, J. M. & ROOD, S. B. 1998. Streamflow requirements for cottonwood seedling recruitment - An integrative model. *Wetlands*, 18, 634-645.
- NGUYEN, P. V., DICKMANN, D. I., PREGITZER, K. S. & HENDRICK, R. 1990. Late-season changes in allocation of starch and sugar to shoots, coarse roots, and fine roots in two hybrid poplar clones. *Tree Physiology*, 7, 95-105.

- PREGITZER, K. & FRIEND, A. L. 1996. The structure and function of *Populus* root systems. In: STETTLER, R. F., BRADSHAW, H. D., JR., HEILMAN, P. E. & HINCKLEY, T. M. (eds.) *Biology of Populus and its Implications for Management and Conservation*. Ottawa, Ontario, Canada: National Research Council of Canada Research Press.
- RAVAZZOLO, D., MAO, L., PICCO, L., SITZIA, T. & LENZI, M. A. 2015. Geomorphic effects of wood quantity and characteristics in three Italian gravel-bed rivers. *Geomorphology*, 246, 79-89.
- ROOD, S. B., BIGELOW, S. G. & HALL, A. A. 2011. Root architecture of riparian trees: river cut-banks provide natural hydraulic excavation, revealing that cottonwoods are facultative phreatophytes. *Trees-Structure and Function*, 25, 907-917.
- SCHIER, G. A. 1982. Sucker regeneration in some deteriorating Utah aspen stands: development of independent root systems. *Canadian Journal of Forest Research*, 12, 1032-1035.
- SHEPPERD, W. D. & SMITH, F. W. 1993. The role of near-surface lateral roots in the life-cycle of aspen in the central Rocky Mountains. *Forest Ecology and Management*, 61, 157-170.
- SMIT, A. L., BENGOUGH, A. G., ENGELS, C., NOORDWIJK, V., PELLERIN, S. & VAN DE GEIJN, S. C. 2000. *Root Methods: A Handbook*, Springer Berlin Heidelberg.
- STEIGER, J., GURNELL, A. M., ERGENZINGER, P. & SNELDER, D. 2001. Sedimentation in the riparian zone of an incising river. *Earth Surface Processes and Landforms*, 26, 91-108.
- STELLA, J. C., HAYDEN, M. K., BATTLES, J. J., PIÉGAY, H., DUFOUR, S. & FREMIER, A. K. 2011. The Role of Abandoned Channels as Refugia for Sustaining Pioneer Riparian Forest Ecosystems. *Ecosystems*, 14, 776-790.
- VENNETIER, M., ZANETTI, C., MERIAUX, P. & MARY, B. 2015. Tree root architecture: new insights from a comprehensive study on dikes. *Plant and Soil*, 387, 81-101.
- WARD, J. V., TOCKNER, K., ARSCOTT, D. B. & CLARET, C. 2002. Riverine landscape diversity. *Freshwater Biology*, 47, 517-539.
- WOHL, E., DWIRE, K., SUTFIN, N., POLVI, L. & BAZAN, R. 2012. Mechanisms of carbon storage in mountainous headwater rivers. *Nature Communications*, 3.

Chapter 7

SYNTHESIS, CONCLUSIONS AND OUTLOOK

The investigations reported in this thesis have demonstrated that the root systems of trees in a dynamic riparian setting are not readily described by simple patterns, but are instead highly dependent on their topographic history and the characteristics of the sediments in which they grow. This chapter summarises the main findings, places them in the context of the contemporary understanding of riparian vegetation dynamics and highlights the main management implications. Potential avenues for further research are then presented, integrating some preliminary data from supplementary fieldwork.

7.1 SUMMARY OF KEY FINDINGS

7.1.1 Root depth distributions

The density and area of roots at poplar-dominated bank sites clearly declined with depth, but across the large dataset that was collected across multiple sites, only 17 % of the variability in root density could be explained by depth, and the patterns were weaker for the area of the bank section occupied by roots. All attempts at modelling the distributions of root area ratio were much less successful than those describing root density. Contrasting sites with different water availability revealed distinct differences in the distribution of roots, with wetter sites showing a much stronger depth relationship and higher density and area in shallow layers, as opposed to a deeper and more evenly spread pattern of root density in more water-limited environments. Wetter sites also had significantly higher root area overall throughout the bank profiles. When comparing individual sites, the slope of the depth distributions (when log-transformed) was more often conserved, with differences mainly due to the surface (depth = 0) intercept values.

Overlying these trends in absolute root density and area, relative measures highlighted differences in the shape of the root distributions observed in the contrasting soil moisture zones. Though results should be interpreted with caution because sampling did not always continue down to maximum rooting depth, there was an indication that plants at drier sites invested a greater proportion of their root system in shallow sediments. Root distributions showed a large amount of variability in shallow layers, and at drier sites an additional deep 'hotspot' of variability was observed (below one metre). Roots were generally slightly thicker overall at drier sites. While the very finest roots (~ 0.1 mm diameter (\emptyset)) were predominant

in terms of numbers, most of the root sectional area was due to roots in the size range 6.4 – 25.6 mm Ø (particularly at drier sites), which corresponds with the horizontal adventitious suckering roots characteristic of black poplar.

7.1.2 Associations with sediment and tree variables

Poorly sorted sediments with a high proportion of clay and silt were consistently associated with high root density and sectional area, and associations were always stronger with fine roots (note larger sample size of fine roots, however). Sediment $d_{90\phi}$ was the strongest single sediment predictor of root density and was also a very close second to $Sorting_{\phi}$ as a predictor of root area ratio. The strongest single pairing was $d_{90\phi}$ and fine root area ratio ($\rho = 0.579$, $R^2 = 33.5\%$, $p < 0.0001$). Tree variables were all poorly associated with root variables, but the strongest predictors were growth rate and proximity to the sampling site.

Sediments encountered on the Tagliamento essentially belonged to one of two primary types (coarse- and fine-grained), differing mostly in terms of the mean particle size, but also with a continuum of varying sand content in the finer types. The variability of root size distributions across samples was due primarily to differences in the range and evenness of spread of root diameters in a sampling interval, but there was a second, almost equally important, factor relating to the central tendency of the root diameter distribution. The major dimension of sediment variability (coarse to fine) mapped reasonably well onto that of root diameter, such that wider, more peaked and positively skewed root diameter distributions could be said to be associated with finer sediments in general, though certainly not without exceptions. The sand content also appeared to have a reasonable correspondence with the second root diameter factor, higher median and mean root diameters being more common in fine sediments with a higher proportion of sand.

A sediment classification system proved an effective framework for summarizing sediment associations with root data, though most root variables formed only two or three statistically distinct groups among the five sediment classes investigated. The distinction between moderately and very well sorted gravels appeared to be irrelevant for the interpretation of root distributions and so a four class system was proposed: (A) very fine-grained with significant amounts of organic material, (B) fine grained with sand, (C) intermediate grain size, and (D+E) gravel-dominated. High root density appeared more sensitive to sand content within the fine-grained deposits than did root area ratio (Classes A and B grouped together with respect to RAR). However, the root area ratio of *fine* roots was the most sensitive of all root variables to differences between sediment classes (including the differing sand content of Classes A and B).

7.1.3 Coarse structures

Burial of stems in flood deposits was a key process in all the trees investigated, and all sub-aerial stems had also experienced some degree of deflection due to moving water, giving them a characteristic ‘downstream lean’. The overall mass of the coarse root system appeared to be related to the extent of this deflection (i.e., the length of main stem buried for each incremental increase in sediment overburden) and was generally far greater than would be expected for a tree of equivalent size growing in an undisturbed environment. Multiple, connected stems were commonly encountered, and strongly grafted lateral roots were common among patches of (presumably clonal) stems. Young roots at depth indicated that even the deepest parts of the root systems, often at the low flow water table, remained active. Horizontal adventitious roots appeared to be associated with boundaries in the stratigraphy and, except in the most sheltered sites, were particularly prevalent in fines deposited over coarse gravels. This resulted in a general pattern of lateral roots emanating from nodes on the main axes, extending mostly in a downstream direction (except in the most sheltered sites). Flood events were evidently extremely influential on the form of the root systems, and the degree of sheltering by established vegetated landforms (identified from historic aerial imagery) related clearly to the size and shape of the buried structures. Dendrochronological analyses indicated that the major formative flow events usually occurred in the first few years after establishment. Interestingly, the findings suggested that increased flood exposure increases the extent and complexity of the root system and therefore anchorage of exposed trees.

7.2 THIS STUDY WITHIN THE WIDER SCIENTIFIC CONTEXT

The limitations due to the observational nature of this necessarily restricted field study are acknowledged, but every attempt has been made to account for variability in the main uncontrolled variables. The model systems were selected to exemplify processes which will be important across many different riparian settings, and the results are relevant to general models of interaction between vegetation and hydrogeomorphology. Whilst many previous studies have investigated multiple species, the results here demonstrate extensive variability within just one.

It is proposed that there is a degree of scale-related functional differentiation of plant roots in riparian zones, particularly with regard to *Populus* spp., and this is used to frame discussion of the findings of this research:

Fine roots (< 2 mm Ø, approx.)

- Absorptive roots with rapid turnover rates
- Regulate plant growth rates, nutrient and water cycling
- Important for soil aggregation and resistance to **erosion**

Medium roots (2 – 25 mm Ø, approx.)

- Form the framework for dynamic fine roots and include adventitious, suckering roots
- Determine the root system extent and mediate exploration and expansion
- Important for bank **mass failure** resistance and clonal **patch dynamics**

Coarse roots and buried stems (> 25 mm Ø, approx.)

- Structural components providing mechanical support
- Confer resistance and resilience to massive flow disturbances
- Important for fluvial **landform dynamics**

7.2.1 Riparian plant growth and bank stability

Rather than discussing them separately, fine and medium diameter roots, and their influences on riparian plant ecophysiology, bank erosion and mass failure, are considered together in this section. This is because, although the main functional significance of two size classes may differ, the investigations reported in Chapters 4 and 5 did not explicitly distinguish between them *ab initio*. The vertical profile excavations encountered coarse roots very infrequently, however, and so they are considered separately.

As observed by other researchers (e.g., Stromberg, 2001, Harner and Stanford, 2003) the over-riding control of water in what might at first appear to be a moisture-rich environment for plants, was confirmed by this study. Comparisons between the wetter and drier sites in Chapter 4 identified lower total root area and tree growth rates where water is less available, with the implication of reduced sediment reinforcement and bank stability, when considering the broad scale. However, it is clear that sediment calibre, moisture availability and plant growth are inextricably linked, and large-scale differences in water distribution due to precipitation and groundwater may be enhanced by feedback among these linked factors. Lower regional water availability will lead to slower plant growth, in turn reducing the rate of fine sediment accumulation and related moisture storage. It is suggested that this storage capacity is vital in riparian zones, where total water supply may be high, but extremely episodic. Indeed, hydraulic lift and redistribution of water by large root systems to isolated buried or surface fine-grained strata (Hao et al., 2013, Yu et al., 2013, Singer et al., 2014), with its consequences for the rest of the vegetation community (Prieto et al., 2012a, Prieto

et al., 2012b), may constitute a major and hitherto under-appreciated dimension of ecosystem engineering by riparian trees.

Though explicit associations with soil hydraulic properties were not explored, the strong associations of root area ratio and density with fine-grained sediments strengthens the case for moisture control of root distributions in mature riparian vegetation, for which much evidence has been gathered from work on cuttings (e.g., Snyder and Williams, 2007, Imada et al., 2008, Nakai et al., 2009, Pasquale et al., 2012). This is also supported by the fact that field moisture content on the day of sampling formed the most distinct grouping among the sediment classes (Table 5.15). However, further work is required to disentangle this influence from other factors such as nutrient availability. While this study found the strongest sediment associations for fine roots, Pollen et al. (2004) reported *coarse* root distribution to be more associated with specific strata. However, note also that high maximum root diameter was strongly linked with fine sediments on the Tagliamento (Table 5.15), and so this may illustrate a similar phenomenon, not apparent in the aggregate root density and RAR variables. However, whether through a high density of fine roots, fewer but larger roots or a combination of the two, where they occur at depth, distinct fine sediment layers are clearly particularly important for bank stability and reinforcement.

In light of the strong sediment, climate and streamflow dependence and high variability demonstrated within a single species, it is proposed that some effort is directed towards improving the representation of root system structure in the ever more sophisticated bank erosion and stability models which are being developed. It seems that root description in many models is a rather dark art and little information is available on the details of the distributions assumed within, for example, the bank erosion hazard index (BEHI, Kwan and Swanson, 2014) or bank stability and toe erosion model (BSTEM, Pollen-Bankhead and Simon, 2010). Though it will require considerable data collection, further efforts to determine the extent of variability of parameters of *simple* root models, such as employed by Van de Wiel and Darby (2007) (e.g., maximum rooting depth and minimum and maximum rooting density), and their dependence on climate, for example, may be better rewarded than attempts to represent an ever-increasing range of species and vegetation types. With more in-depth analysis of root-sediment associations, models which already require explicit stratigraphic data input could, in time, model some degree of sediment influence on the root system architecture. The widely observed deeper maximum rooting depth of trees in more water-limited environments is an effect which could be included quite easily, and should be accounted for, as it is likely to have major bank stability implications.

7.2.2 Vegetation and landform dynamics

In large and medium-sized rivers, the dynamics of vegetated landforms is governed by the establishment, expansion and erosion of patches of plants (Gurnell, 2014). The medium-sized adventitious roots studied here are key agents of the establishment, expansion and erosion resistance of poplar-engineered landforms, whereas coarse roots and buried stems are perhaps more important with regard to the resilience of vegetation in the face of erosion. The root systems described in Chapter 6 show distinct differences in structure depending on the level of exposure to flow disturbance, with more sheltered sites showing a wide depth distribution of adventitious roots, as opposed to the restriction of such horizontal roots to narrower, buried fine-grained strata in exposed locations. The implications for clonal expansion and patch dynamics require deeper and more focused investigation of these specialised roots (as discussed below in Section 7.4.3). However, it is clear that they comprise extremely far-reaching networks (the potential extent of which has probably been underestimated in the past) from which new stems may originate when conditions are favourable.

The implications for landform dynamics of the large and complex buried stem and coarse root systems uncovered are perhaps more immediately apparent. Considering that the depth, mass and complexity (in terms of number of nodes of proliferation of adventitious roots) of these systems appear to increase with increasing exposure to flowing water and soil moisture limitation; such harsh conditions are likely to harbour fewer, but more resilient trees which become increasingly better anchored with each flood disturbance they are able to survive. Though such isolated stem axes themselves may not be particularly hydraulically disruptive, these key trees will snag other transported material and re-start the process of landform generation when surrounding plants are removed. Furthermore, attached masses of adventitious roots (often observed having been swept back after exposure to flowing water, e.g., in case studies R3, RB and RC) will help to create hydraulic ‘dead zones’ in the lee of stems, promoting fine sediment accumulation.

The implied effect of such resilient trees (or small stem clusters), which are able to hang on while their neighbours are eliminated, is that vegetated landforms may repeatedly form around them in the same position in exposed parts of the active channel of large rivers. While there is turnover of the dependent vegetation and accumulated sediment, the stable ‘hard point’ persists through several formative flood events (or at least gradually ‘walks’ a small distance downstream as the main stem is flattened by each event). Unfortunately, this effect may not be immediately apparent in published studies of island turnover, as the analysis is typically on a ‘by area’ basis from aerial imagery, and the key trees themselves occupy too

small an area to be counted. However, comparative and longitudinal studies (e.g., Zanoni et al., 2008, Picco et al., 2015, Surian et al., 2015) could be reanalysed to look for such small features and whether there is indeed a trend of repeated patch formation with either increasing exposure and/or moisture limitation (and implied rooting depth).

There is of course the potential for the retention of such large buried living structures if their location becomes increasingly ‘terrestrialised’ and removed from the critical zone of interaction with flowing water identified in the conceptual model of Gurnell et al. (2015). They may then later be geomorphologically ‘reactivated’ upon exposure by channel avulsions or lateral erosion into the floodplain, acting in the same way as the dead wood hard points identified by Collins et al. (2012). The fundamental implication is that such large, key pieces of buried wood – living or dead – act to shortcut the initial pioneer stages of island dynamics, bypassing the need for the creation, *de novo*, of vegetation nucleation sites.

These aspects of vegetation dynamics are all in marked contrast to those of more sheltered marginal riparian forest, where trees are much more likely to behave as a coherent patch, conforming to the idealised biogeomorphological succession concept (Corenblit et al., 2014). Whereas complex and deeply rooted vegetation likely leads to more heterogeneous erosion patterns in more exposed sites, the shallower rooting observed in the thicker moisture- and nutrient-rich fine sediment deposits in sheltered areas seems more likely to lead only to surface sediment reinforcement and thus complete removal, of vegetation. This probably still holds true even when the rich sediments are extremely deep, owing to the rooting depth limits imposed by oxygen availability in such substrate types

7.2.3 Applicability beyond the Tagliamento / black poplar system

While the model system studied as part of this research was selected because it exemplifies a wide range of features and strong interaction between riparian plants and fluvial processes, there are a number of aspects of the Tagliamento and *Populus nigra* which will mean that some findings are not directly transferable to all other systems. The breadth of the *Populus* genus and its rather well-defined ecological niche (Stettler et al., 1996) means that many other riparian tree species are likely to exhibit broadly similar rooting behaviour. Outside the genus, however, clonal suckering and adventitious rooting are likely to be absent or rather different in character. Although *Salix* spp. are closely related to poplars and cottonwoods, and show many similar traits, observations from the fieldwork conducted as part of this study suggest that overall root system structure is markedly different (usually a single, stout taproot with laterals almost exclusively in shallow layers), and this may partly be explained by co-

occurrence with *Populus* spp. and thus niche separation. Encouragingly, however, Zanetti et al. (2015) found tree species to be much less important than soil type and water availability for the distributions of non-specialised roots and gross root system architecture.

The occurrence of deep, coarse-grained and highly permeable sediments in the aggrading, mountain-fed Tagliamento is likely to influence root growth significantly, owing to strong sub-aerial hydrological connectivity and reasonably good oxygen penetration. Rooting patterns are likely to be much reduced in depth in systems with banks comprising cohesive, fine-grained material, but there should be good transferability to most dynamic, gravel-bed systems. Urban river banks containing demolition rubble may represent an interesting contrasting system but with similar sediment properties. Finally, the large and laterally unconfined nature of the Tagliamento system undoubtedly has a great deal of influence on vegetation dynamics, and one would expect different effects in rivers of contrasting sizes with respect to vegetation (*sensu* Gurnell et al., 2002). However, the sub-aerial patterns and processes are not likely to be scale-dependent.

7.3 IMPLICATIONS FOR RIVER MANAGEMENT

While it is generally accepted that riparian forest improves deep bank stability at the reach scale (e.g., Lyons et al., 2000, Rood et al., 2015), the key message of this research is that root-mediated bank reinforcement is likely to vary within a catchment even when the plant community is relatively uniform, as root distribution and architecture is dependent on regional (climate-related) and local (sedimentology and morphodynamic history) conditions. Furthermore, the characteristic responses of key tree species to these conditions may also cause variability between sites with contrasting dominant vegetation.

Many of the vital issues relating to bank stability are introduced in Section 7.2.1 and relate to the use of models. It is clear that simple determinate root depth distributions should only be assumed with supporting stratigraphic evidence. Several opportunities for improving root distribution models present themselves from the findings of this research. The strong associations identified between sediment types and fine root area ratio are particularly promising for root reinforcement prediction, as this may be one of the most important metrics for existing geotechnical models, given the disproportionate strength of fine roots. Furthermore, the identification of potential predictors of parameters of the root diameter distribution (as opposed to aggregate root area ratio) may improve stability modelling by better describing properties of the 'fibre bundle' (Pollen and Simon, 2005). An important implication of preliminary further work on root strength (Section 7.4.2) is that the natural

process of root die-back upon the erosion of banks may be causing over-prediction of in-situ root strength as determined from trench-derived measurements.

The root-sediment associations also suggest some prudent approaches to bio-engineering design. A key message is that, when the objective is to maximise root density and reinforcement (as is usually the case), the substrate must be selected carefully, to balance oxygen supply with nutrient and moisture availability. Coarse gravels are often used in such operations owing to the high shear stresses required for their erosion. Such a rooting medium may be well aerated, but will not encourage root growth unless some finer sands (for moisture retention) and silts and clays (for nutrient supply and exchange capacity) are also included. One potential way forward may be to imitate the heterogeneous sediments found in systems such as the Tagliamento, with layering and/or patchy in-filling of coarse and finer materials. To obtain particularly deep root system structure with poplar or willow cuttings, another approach would be multi-stage construction, again imitating natural, periodic deposition dynamics. In such an approach, the plants would be given time to establish roots at low elevation, and the stems would later be buried in further mineral and organic material to encourage adventitious rooting at higher elevation into the new deposits. Given the abundance of reasonably large diameter adventitious roots where poplars grow, and their ability to resprout fairly readily (Figure 6.54 C), the use of sufficiently large fragments of these roots may be explored as an alternative to stem cuttings where poplars are already established. However, this practice would require further investigation and experimentation: the low wood density of these roots may indicate that the production of new shoots is dependent on being connected to the resource pool of a large, integrated root network.

In assessing the risk of tree failure and wood loading for management purposes, the observation that poplars in more frequently disturbed areas often have larger and better anchored root systems implies that such trees, somewhat counter-intuitively, may actually present lower risk than trees which have grown in more favourable, sheltered conditions. The considerable buried biomass of these specimens is perhaps an under-valued resource which should also be appreciated in carbon storage assessments.

7.4 FURTHER RESEARCH POSSIBILITIES: COMPLETING THE MODEL OF RIPARIAN ROOT FUNCTIONS AT ALL SCALES

The investigations reported in this thesis have demonstrated the great potential extent of variability in root distributions and structures, and thus the associated reinforcement of sediments, in a single, little-disturbed, naturally functioning riparian ecosystem. However, limits to this variability and some of the key driving factors have been identified, improving our model of the riparian tree root realm. A highly dynamic system is observed, intrinsically linked to the dynamism of the hydraulic and hydrological environment. The cycling of trees in floodplains and riparian zones is a phenomenon which may be beneficial to wildlife and humanity in many ways, and is a concept with which we should become culturally familiar and better understand. This research advances knowledge of several different ways in which roots influence this cycle, and demonstrates the relevance of scale for a functional understanding of the implications of these fractal systems in the riparian context.

All the studies described would benefit from expansion (i.e., by including more profiles, refining the root-sediment analysis and classifications, and excavating more case study trees), but these investigations on the Tagliamento have also given rise to many further questions regarding the characteristics and behaviour of roots in riparian zones and their significance.

Whilst comparison between species has previously been an area of prolific research (particularly for geotechnically-oriented studies), the present study has demonstrated that enormous variability may be observed within a single species in a single river system, and most of the suggested future avenues below could usefully be explored using the Tagliamento/black poplar model system. However, the extension of investigations to cover one or two representative *Salix* species would also be feasible and beneficial for widening the applicability of findings to more riparian systems. Of particular value for the Tagliamento may also be a comparative study of the roots of the invasive *Amorpha fruticosa* L., which is of rapidly increasing dominance in the riparian plant community (Dumitrascu et al., 2013, Takagi and Hioki, 2013).

A number of additional datasets were collected in the course of the fieldwork for this thesis, though were not included in the previous chapters owing either to problems with field sampling or limited time for adequate sample preparation, quality control, processing and analysis. Methods employed are detailed in Appendix E. Opportunities for these data to be incorporated within, or extended for the purposes of further investigations, are highlighted below, and preliminary results are presented. Methodological issues encountered are also addressed.

7.4.1 Fine root associations with soil hydraulic properties, nutrients and mycorrhizae

For a more complete understanding of the empirical associations identified in the present study, there must be deeper investigation of the mechanistic relationships between roots and soil in the riparian zone, mediated by the activity of fine roots. Nutrient and hydrological properties have been implicitly assumed to be related to organic matter content and particle size distribution in the present study (an assumption based on work by previous authors such as Steiger and Gurnell (2003)).

Firstly, given the identified importance of moisture availability, and the association between sand content (Sediment PC2) and central tendency of the root diameter distribution (Diameter Factor 2 (Figure 5.21)), analysis of soil moisture release curves in the finer sediments should provide further insight with regard to the influence of sand, which is expected to be related to drainage. Note also the potential non-linear relationships tentatively identified between some root properties and sand content (see, e.g., Figure 5.8).

Secondly, explicit analysis of sediment nutrient content is likely to refine and strengthen the associations between sediments and root distributions significantly, particularly in light of the contrasting dynamics of nitrogen and phosphorus and their relationships with mycorrhizae and the successional stage of the vegetation and soil. Steiger and Gurnell (2003) found nutrient availability to be directly linked to sedimentation volumes, which vary across complex riparian zones, and decaying leaves and sediment release carbon, phosphorus and nitrogen differentially during inundation (Ostojić et al., 2013). Thus, different nutrients are likely to be limiting and controlling root growth in more mature landforms (with a well-developed litter layer), versus more nascent colonisation sites with more extreme sediment dynamics. Furthermore, root system responses to nutrients depend on inundation and oxygen availability (Neatrou et al., 2007) and root system plasticity is likely to be traded-off with flood tolerance (Jansen et al., 2005).

Mycorrhizal associations are a third factor modulating the root-sediment relationship, and inundation and oxygen are again key structuring factors for the distribution of their occurrence. The symbioses formed by black poplar with arbuscular (AMF) and ectomycorrhizal fungi (EMF) at different stages in the biogeomorphic succession (Gryta et al., 2006, Piotrowski et al., 2008) have contrasting effects on growth and soil processes, divergent environmental tolerances and appear to be antagonistic (Lodge, 1989). Further sampling and analysis of relationships between roots, sediment properties and mycorrhizae is likely to aid the prediction of root length density and root system properties as well as the vigour of

vegetation growth. More intensive study of patterns with depth is required to identify the primary controlling factors.

Mycorrhizal associations may not only be important indirectly for sediment reinforcement (via establishment and resilience of vegetation), but also directly, owing to their physical binding effect, analogous to roots, at a microscopic scale (Tisdall, 1991, Rillig and Mummey, 2006, Mardhiah et al., 2014, Lehmann and Rillig, 2015). In preliminary additional fieldwork, depth distributions of soil hyphae were sampled at three, widely dispersed sites on the Tagliamento and two bank profiles at a mature poplar-dominated site on the Noce River where the morphology is virtually completely static and the hydrology dominated by approximately daily hydropeaking. Sampling was conducted under baseflow conditions. More information on the sites and methods is provided in Appendix E.

Harner et al. (2011) previously found a steady decrease with depth in hyphal length density of AMF in the soil, down to the summer water table at a single fine grain-dominated Tagliamento mature island site. The aim of the additional sampling here was to extend this depth profile dataset to other sites and to investigate hydrological influences by comparing distributions with the morphologically stable, hydropeaking site. Unfortunately it was not possible to distinguish mycorrhizal hyphae from other fungal types owing to sample degradation, and so Figure 7.1 and Figure 7.2 describe total length of all soil fungi per gram of sediment. There are likely to be mechanical differences between types of hyphae, and this may have implications for sediment reinforcement, but investigating such variability is beyond the scope of this preliminary investigation. The total hyphal length is more relevant from a sediment stabilisation point of view. However, further work on the mechanical properties of fungal mycelium from the point of view of soil stabilisation (current foci are related to commercial batch culture (e.g., Stocks and Thomas, 2001, Zhao et al., 2005) and biomaterial (e.g., Thomas et al., 2000) technologies) may shed light on the relevance of these differences.

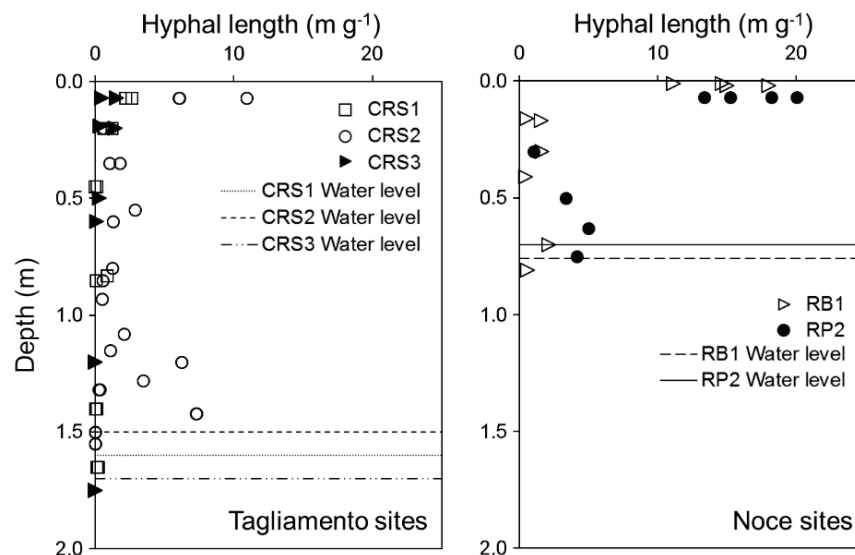


Figure 7.1 Soil hyphal length depth profiles at three bank sites on the Tagliamento (left) and two sites on the Noce river at Biotopo La Rupe (right). The water table level at the time of sampling is also indicated. See text for assumptions and further description.

Contrary to the steady decline observed in AMF hyphae in the study by Harner et al. (2011), total hyphal length dropped off dramatically from surface layers, particularly at the more established Noce sites (Figure 7.1). The extreme near-surface values are likely due to saprotrophic fungi, not evaluated by Harner et al. (2011). Otherwise, values are broadly comparable with the 2011 study, suggesting AMF contribute significantly. Site CRS2 on the Tagliamento showed significantly greater hyphal length than the other two sites throughout the profile and, like the RP2 site on the Noce, an increase approaching the water table. The higher overall values at CRS2 may be attributed to site maturity, high vegetation density and high moisture availability (in common with the Noce river sites) and also dominance of fine-grained sediments. However, the increase above the water table, observed to some extent in all but the youngest, most gravel-dominated profiles (at site CRS3), appears to be a hydrological effect which warrants further investigation. Another interesting result was that hyphal length appeared to remain significant even below the water table at all but the CRS3 site ($50 - 200 \text{ cm g}^{-1}$ on the Tagliamento and $0.5 - 4 \text{ m g}^{-1}$ on the Noce), possibly supported by soil water exchange with nearby well-oxygenated river water.

An attempt was made to identify relationships between root properties and soil hyphal length, but no effective method for obtaining intact fixed-volume samples of gravel-dominated sediments could be found for calculating bulk density, so that samples could be standardised on a volumetric basis. However, an initial analysis, assuming constant soil bulk density and thus a proportional relationship of mass to volume, appeared to identify different

relationships between soil root and hyphal length densities for the dynamic (Tagliamento) and static (Noce) sites (Figure 7.2). Potential explanations for this may include differential ratios of ecto- and endo-mycorrhizae between more and less mature riparian forest (Kikvidze et al., 2015, Piotrowski et al., 2008), or perhaps hydrological influences (e.g., Lodge, 1989).

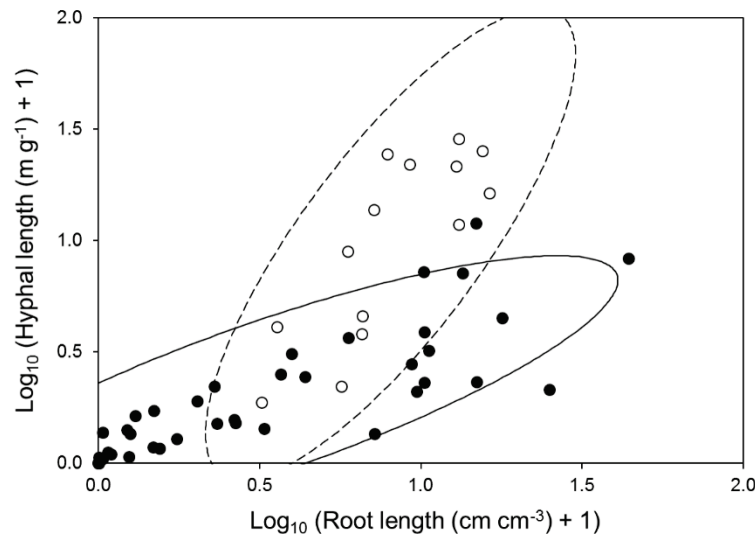


Figure 7.2 Relationships between hyphal length density in fine sediment fraction (< 4 mm) and root length density at Tagliamento (filled symbols, solid line) and La Rupe sites (open symbols, dashed line). Lines represent 90 % confidence intervals. Please note the assumptions implicit in this plot, detailed in the text.

Further work is needed to investigate associations between sediment properties, soil hyphae and roots, similarly to the analyses reported in Chapter 5. The use of optical root analysis (as in the preliminary data collection) would permit rapid through-put of samples, simple generation of secondary variables such as root surface area and reduced time spent in the field. However, the issue of fixed-volume sampling of the stony Tagliamento sediments must first be resolved.

7.4.2 Additional influences on root strength

Root mechanical properties are fundamental to the understanding of riparian sediment reinforcement, and the dependence of breaking stress on root diameter and species is well-established. However, strength-diameter relationships are usually extremely noisy, and though much of this scatter may be due to measurement error and apparatus (see below) relatively little attention has been directed towards trying to understand some of the potential physiological explanations for this variability. Thus it is suggested that there should be further investigation into some of the potential causes of within-species variability. Furthermore, strength-diameter investigations are currently rather limited by practical issues

to the medium diameter range of roots (around 1 - 10 mm), and so the development of methods to measure both fine and coarse root strength more effectively should be pursued.

Root strength varies due to different relative cross-sectional dominance of fibrous tissue and other structural carbohydrates in roots of different diameters (Hathaway and Penny, 1975, Genet et al., 2005, Zhang et al., 2014). However, the production of these strength-imparting compounds and tissues in roots is likely to vary in response to stresses such as drought, hypoxia, herbivory and microbial infection, and so investigation of the effects of such stresses may explain a large degree of the observed variability in strength-diameter relationships. Root strength testing was undertaken at most of the Tagliamento profile sites, but was later dropped, as too great a proportion of exposed roots at the eroding bank sites were dead, even when roots were selected from deeper into the bank (see Appendix E). This did, however, permit comparison of the strength characteristics of live and dead roots (Figure 7.3). In spite of the large degree of scatter, the plotted log-linear regressions suggest that dead roots are somewhat weaker for a given diameter. However, the effect was not quite statistically significant for the interaction term of 'dead' dummy variable and diameter ($\chi^2 = 2.95$, 1 d.f., $P = 0.08$) in regression analysis, and certainly not so for the 'dead' dummy variable itself ($\chi^2 = 0.63$, 1 d.f., $P = 0.43$).

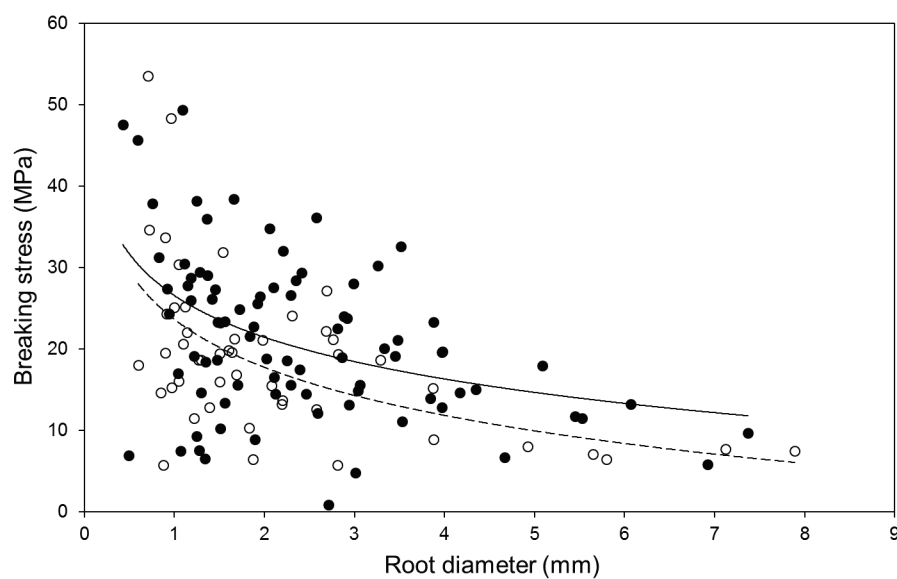


Figure 7.3 Poplar root breaking stress as a function of diameter from tests conducted on Tagliamento bank exposures. Filled symbols and solid line: live roots and log-linear regression; open symbols and dashed line: dead roots and log-linear regression.

From a methodological point of view, a novel method of attachment of root strength testing equipment was developed in the course of these investigations, involving the use of metal rigging thimbles as illustrated in Figure 7.4. Hales et al. (2013) relate the experience of many

investigators who typically have to disregard a large proportion of root strength tests owing to stress concentration in the root near to the clamp, and subsequent failure purely as a result of the method of attachment. Another common problem is the stripping of the cortex off the root stele by the clamp, which may actually occur in natural bank failures, but is not the desired outcome of the loading tests. By wrapping the entire root around a metal thimble of sufficient radius, forces are more evenly distributed and breaking is more likely elsewhere along the root length, as is desired. There is usually sufficient friction to secure the thimble when the tail end of the root is wrapped several times around the loaded section, and then either back on itself if sufficiently flexible (Figure 7.4, left and middle), or secured with, e.g., strong tape (Figure 7.4, right).



Figure 7.4 Use of rigging thimbles for applying load to roots more evenly.

7.4.3 Adventitious roots and poplar clonal patch dynamics

The diameter range coincident with suckering, adventitious (medium diameter) roots was found to dominate root sectional area across the data reported in Chapter 4 (see Figure 4.17). As these roots are the main agents of clonal patch dynamics in poplar – a process influencing both bank stability via root system structure and fluvial landform construction – variability in their distribution and its control warrant further investigation. As the 0.2 m wide profiles measured in the initial field campaigns did not encounter large numbers of medium and coarse diameter roots at individual sites, three more extensive, 5 m wide bank profile exposures were prepared in order to obtain larger sample sizes of the larger diameter roots. Here, only roots > 1.5 mm \varnothing were recorded, and mapped in two dimensional space. See Appendix E for further information on sites and methods.

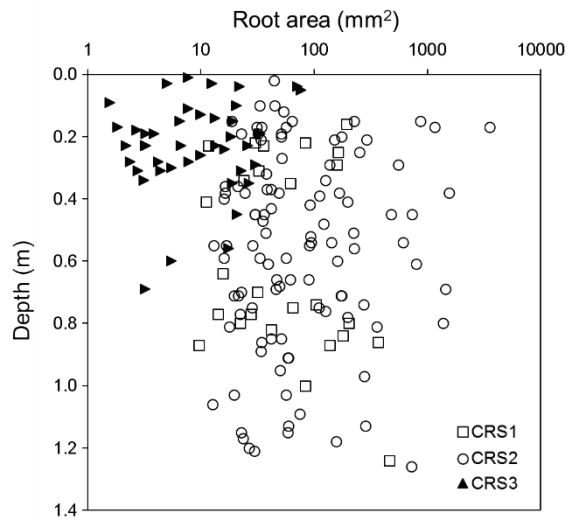


Figure 7.5 Depth distribution of the areas of individual coarse roots (> 1.5 mm Ø) at three sites on the Tagliamento.

As evident in Figure 7.5, the ranges of root sectional area differ dramatically between sites and vary over four orders of magnitude. Interpretation of the differences is aided by further description of site conditions. Site CRS3, occupying the lower end of the range of root areas, comprised recently deposited fine sediments, colonised primarily by a mass of poplars less than two years old (Figure 6.51 C). Site CRS2 presented a well-established island profile, with moist, favourable growing conditions, and dense vegetation. Here, many roots of a wide range of diameters were encountered. Site CRS1, in the much drier, southern group of sites (Figure 6.2) had much more widely spaced and slower-growing but well-established trees. Here, the narrower range of root sectional areas relates more closely to suckering, cable-like adventitious roots, and suggests that resource limitation may trigger expansion and exploratory rooting phenomena. The two-dimensional plots in Figure 7.6 show the between-site contrasts more dramatically and illustrate that the roots at CRS1 were limited almost exclusively to two buried fine-grained strata.

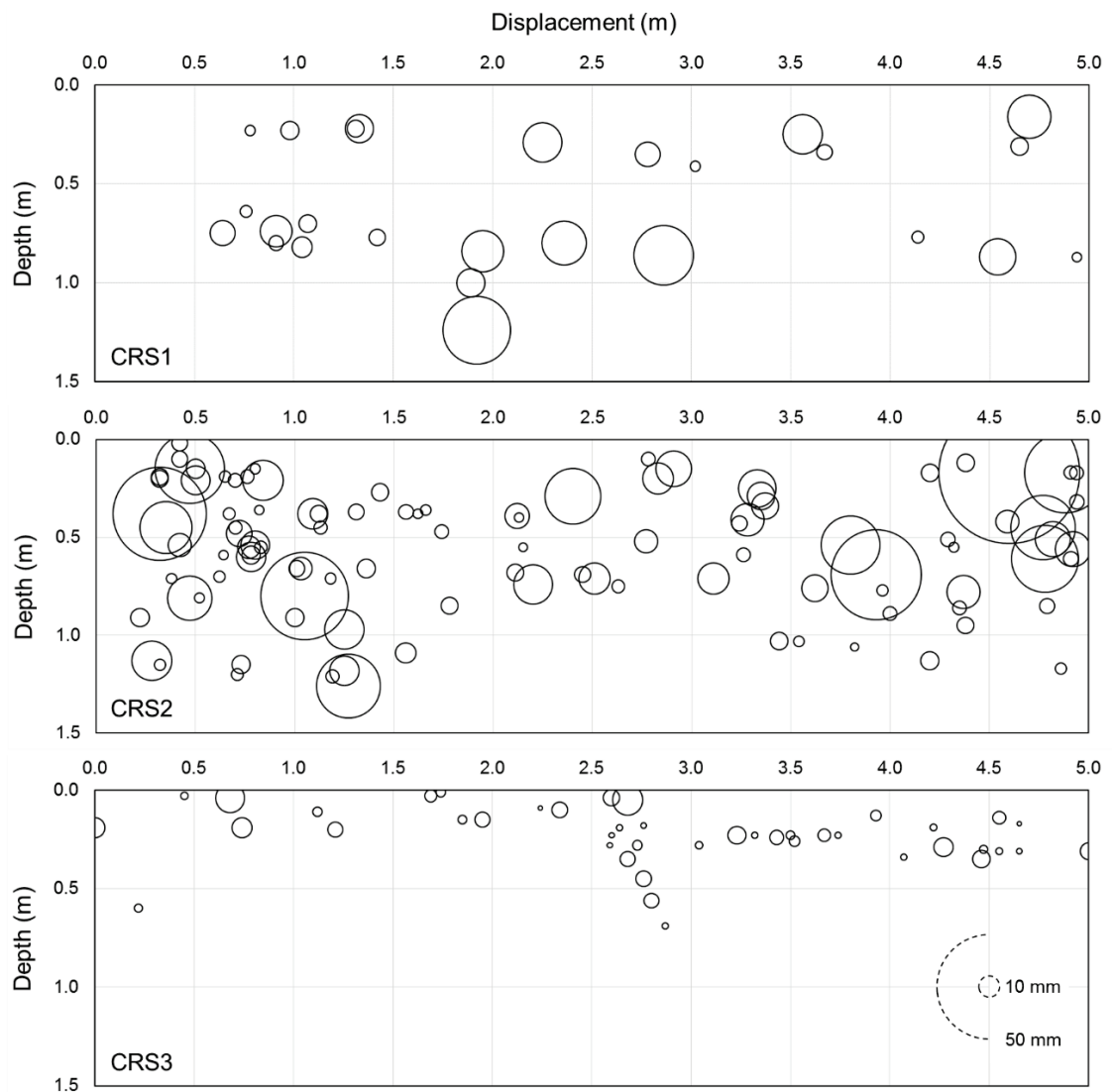


Figure 7.6 Distribution of coarse roots (> 1.5 mm Ø) in 5 m wide bank exposures at three sites on the Tagliamento. Width of circles represents root diameter.

It is suggested that further work should look more closely at relationships between coarse roots and the distribution of above-ground biomass and clonal patch dynamics. All woody plants within 5 m of the coarse root surveys were mapped and recorded, and so in the first instance, spatially explicit analysis of relationships with the root distributions plotted above may be undertaken with data that have already been collected. Furthermore, data from nineteen 10 x 10 m vegetation plots, collected to validate the similarity of plant communities near the original profile sites, may also be reanalysed to investigate broad relationships between root and stem density. Piercy and Wynn (2008) identified basal stem area to be a significant but relatively weak predictor of coarse root volume ratio in Appalachian headwater stream banks. However, it is suggested that more targeted and spatially explicit studies of poplar, with its peculiar suckering behaviour, may show stronger above- and below-ground linkages for roots in this size range. The small sample sizes of coarse roots

and trees due to the methods adopted may explain the relatively weak associations between these features identified by Piercy and Wynn (2008) and the present study (Section 5.3.1a).

Additional dendrochronological studies are required which focus specifically on the horizontal roots responsible for clonal expansion. Such investigations may, if supported by sufficient independent stratigraphic dating evidence, be able to determine whether most patch expansion occurs close to the surface, immediately after fine sediment deposition, and the extent to which these suckering roots exploit more deeply buried, perhaps isolated layers of fine sediments later in the life of the trees.

Another approach for studying clonal expansion in riparian poplar may be the intensive study of a small number of stem patches over a long time period, ideally beginning at the time of establishment, or alternatively using a space-for-time substitution. On the Tagliamento, a field surveying study may be integrated with the already large image dataset available from fixed oblique cameras monitoring the floodplain (see Bertoldi et al., 2013), increasingly high resolution aerial imagery available (e.g., Surian et al., 2015), and LiDAR datasets (Pizzuto et al., 2010, Picco et al., 2015). Noting the patchy distribution of the large ($\gg 0.5$ m DBH) poplars present at the morphologically static La Rupe site on the Noce river, a coring and tree mapping study was initiated in an attempt to discover the spatial and temporal relationships of the stems with each other (see Appendix E). This was complemented by a second survey of younger poplar stems on what appeared to be one of the few active landforms at 'Biotopo La Rupe': a point bar at the nature reserve's downstream limit. Analysis of this dataset of 59 trees from the Noce and the additional approx. 100 cores awaiting processing from the Tagliamento vegetation plots will, with extension of the surveys, begin to shed light on the rates, extent and controlling factors of riparian poplar clonal expansion in contrasting riparian environments.

7.4.4 Extending whole root system investigations

The large-scale excavation of entire coarse root systems in this project was particularly novel. However, added value can be extracted from the measurements and samples already collected, and there would also be great benefit in excavating and recording more examples of gross root systems. Regarding the latter, the case studies in the preceding chapter were all of a similar age – at around the end of the biogeomorphological and beginning of the ecological stages in terms of the biogeomorphic life cycle of Corenblit et al. (2014). It would therefore be interesting to uncover buried components of representatives of other important stages in the landform cycle, e.g., pioneer islands (i.e., deposited trees), recently established patches of seedlings or stems closer to ten years of age. Though requiring considerably more

effort, the complete excavation of a clonal patch of stems would also be profitable (as discussed above). In this case, the non-cohesive substrates of the Tagliamento make it an ideal system for such excavations.

With regard to existing data, the SfM models captured could also be subjected to more formal study of root architectural parameters (branching angles, inter-nodal distances, tapering rates, etc.) and quantitative analyses (e.g., volumetric and biomass estimates), though they would require significant manual point cloud editing. In total, 67 cores and 112 sections were taken from the root system exposures, and these could be analysed in far greater detail than the simple ring counting employed in the present study. Quantitative microscopic analysis of wood vessel size and density, as well as annual growth patterns in the periderm, could shed further light on events influencing the development of the root systems' peculiar forms.

7.5 REFERENCES

- BERTOLDI, W., GURNELL, A. M. & WELBER, M. 2013. Wood recruitment and retention: The fate of eroded trees on a braided river explored using a combination of field and remotely-sensed data sources. *Geomorphology*, 180-181, 146-155.
- COLLINS, B. D., MONTGOMERY, D. R., FETHERSTON, K. L. & ABBE, T. B. 2012. The floodplain large-wood cycle hypothesis: A mechanism for the physical and biotic structuring of temperate forested alluvial valleys in the North Pacific coastal ecoregion. *Geomorphology*, 139, 460-470.
- CORENBLIT, D., STEIGER, J., GONZÁLEZ, E., GURNELL, A. M., CHARRIER, G., DARROZES, J., DOUSSEAU, J., JULIEN, F., LAMBS, L., LARRUE, S., ROUSSEL, E., VAUTIER, F. & VOLDOIRE, O. 2014. The biogeomorphological life cycle of poplars during the fluvial biogeomorphological succession: a special focus on *Populus nigra* L. *Earth Surface Processes and Landforms*, 39, 546-563.
- DUMITRASCU, M., GRIGORESCU, I., DOROFTEI, M., KUCSICSA, G., MIERLA, M., DRAGOTA, C. S. & NASTASE, M. Assessing invasive terrestrial plant species *Amorpha fruticosa* in three wetland areas in Romania: Danube delta biosphere reserve, comana natural park and mures floodplain natural park. 13th International Multidisciplinary Scientific Geoconference and EXPO, SGEM 2013, 2013 Albena. 113-124.
- GENET, M., STOKES, A., SALIN, F., MICKOVSKI, S., FOURCAUD, T., DUMAIL, J. F. & VAN BEEK, R. 2005. The influence of cellulose content on tensile strength in tree roots. *Plant and Soil*, 278, 1-9.
- GRYTA, H., CARRICONDE, F., CHARCOSSET, J. Y., JARGEAT, P. & GARDES, M. 2006. Population dynamics of the ectomycorrhizal fungal species *Tricholoma populinum* and *Tricholoma scalpturatum* associated with black poplar under differing environmental conditions. *Environmental Microbiology*, 8, 773-786.
- GURNELL, A. 2014. Plants as river system engineers. *Earth Surface Processes and Landforms*, 39, 4-25.
- GURNELL, A. M., CORENBLIT, D., GARCÍA DE JALÓN, D., GONZÁLEZ DEL TÁNAGO, M., GRABOWSKI, R. C., O'HARE, M. T. & SZEWCZYK, M. 2015. A Conceptual Model of Vegetation-hydrogeomorphology Interactions Within River Corridors. *River Research and Applications*.
- GURNELL, A. M., PIÉGAY, H., SWANSON, F. J. & GREGORY, S. V. 2002. Large wood and fluvial processes. *Freshwater Biology*, 47, 601-619.
- HALES, T. C., COLE-HAWTHORNE, C., LOVELL, L. & EVANS, S. L. 2013. Assessing the accuracy of simple field based root strength measurements. *Plant and Soil*, 372, 553-565.
- HAO, X. M., CHEN, Y. N., GUO, B. & MA, J. X. 2013. Hydraulic redistribution of soil water in *Populus euphratica* Oliv. in a central Asian desert riparian forest. *Ecology*, 6, 974-983.
- HARNER, M. J., OPITZ, N., GELUSO, K., TOCKNER, K. & RILLIG, M. C. 2011. Arbuscular mycorrhizal fungi on developing islands within a dynamic river floodplain: An investigation across successional gradients and soil depth. *Aquatic Sciences*, 73, 35-42.

- HARNER, M. J. & STANFORD, J. A. 2003. Differences in cottonwood growth between a losing and a gaining reach of an alluvial floodplain. *Ecology*, 84, 1453–1458.
- HATHAWAY, R. L. & PENNY, D. 1975. Root Strength in Some Populus and Salix Clones. *New Zealand Journal of Botany*, 13, 333-344.
- IMADA, S., YAMANAKA, N. & TAMAI, S. 2008. Water table depth affects Populus alba fine root growth and whole plant biomass. *Functional Ecology*, 22, 1018-1026.
- JANSEN, C., VAN DE STEEG, H. M. & DE KROON, H. 2005. Investigating a trade-off in root morphological responses to a heterogeneous nutrient supply and to flooding. *Functional Ecology*, 19, 952-960.
- KIKVIDZE, Z., ARMAS, C., FUKUDA, K., MARTÍNEZ-GARCÍA, L. B., MIYATA, M., ODA-TANAKA, A., PUGNAIRE, F. I. & WU, B. 2015. The role of arbuscular mycorrhizae in primary succession: Differences and similarities across habitats. *Web Ecology*, 10, 50-57.
- KWAN, H. & SWANSON, S. 2014. Prediction of Annual Streambank Erosion for Sequoia National Forest, California. *Journal of the American Water Resources Association*, 50, 1439-1447.
- LEHMANN, A. & RILLIG, M. C. 2015. Understanding mechanisms of soil biota involvement in soil aggregation: A way forward with saprobic fungi? *Soil Biology and Biochemistry*, 88, 298-302.
- LODGE, D. J. 1989. The influence of soil moisture and flooding on formation of VA-endo- and ectomycorrhizae in Populus and Salix. *Plant and Soil*, 117, 243-253.
- LYONS, J., TRIMBLE, S. W. & PAINE, L. K. 2000. Grass versus trees: Managing riparian areas to benefit streams of central North America. *Journal of the American Water Resources Association*, 36, 919-930.
- MARDHIAH, U., CARUSO, T., GURNELL, A. & RILLIG, M. C. 2014. Just a matter of time: Fungi and roots significantly and rapidly aggregate soil over four decades along the Tagliamento River, NE Italy. *Soil Biology and Biochemistry*, 75, 133-142.
- NAKAI, A., YURUGI, Y. & KISANUKI, H. 2009. Growth responses of Salix gracilistyla cuttings to a range of substrate moisture and oxygen availability. *Ecological Research*, 24, 1057-1065.
- NEATROUR, M. A., JONES, R. H. & GOLLADAY, S. W. 2007. Response of three floodplain tree species to spatial heterogeneity in soil oxygen and nutrients. *Journal of Ecology*, 95, 1274-1283.
- OSTOJIĆ, A., ROSADO, J., MILIŠA, M., MORAIS, M. & TOCKNER, K. 2013. Release of nutrients and organic matter from river floodplain habitats: Simulating seasonal inundation dynamics. *Wetlands*, 33, 847-859.
- PASQUALE, N., PERONA, P., FRANCIS, R. & BURLANDO, P. 2012. Effects of streamflow variability on the vertical root density distribution of willow cutting experiments. *Ecological Engineering*, 40, 167-172.
- PICCO, L., TONON, A., RAVAZZOLO, D., RAINATO, R. & LENZI, M. A. 2015. Monitoring river island dynamics using aerial photographs and lidar data: the tagliamento river study case. *Applied Geomatics*, 7, 163-170.
- PIERCY, C. & WYNN, T. 2008. Predicting Root Density in Streambanks. *JAWRA Journal of the American Water Resources Association*, 44, 496-508.
- PIOTROWSKI, J. S., LEKBERG, Y., HARNER, M. J., RAMSEY, P. W. & RILLIG, M. C. 2008. Dynamics of mycorrhizae during development of riparian forests along an unregulated river. *Ecography*, 31, 245-253.
- PIZZUTO, J., O'NEAL, M. & STOTTS, S. 2010. On the retreat of forested, cohesive riverbanks. *Geomorphology*, 116, 341-352.
- POLLEN-BANKHEAD, N. & SIMON, A. 2010. Hydrologic and hydraulic effects of riparian root networks on streambank stability: Is mechanical root-reinforcement the whole story? *Geomorphology*, 116, 353-362.
- POLLEN, N. & SIMON, A. 2005. Estimating the mechanical effects of riparian vegetation on stream bank stability using a fiber bundle model. *Water Resources Research*, 41, 1-11.
- POLLEN, N., SIMON, A. & COLLISON, A. 2004. *Advances in assessing the mechanical and hydrologic effects of riparian vegetation on streambank stability*.
- PRIETO, I., ARMAS, C. & PUGNAIRE, F. I. 2012a. Hydraulic lift promotes selective root foraging in nutrient-rich soil patches. *Functional Plant Biology*, 39, 804-812.
- PRIETO, I., ARMAS, C. & PUGNAIRE, F. I. 2012b. Water release through plant roots: New insights into its consequences at the plant and ecosystem level. *New Phytologist*, 193, 830-841.
- RILLIG, M. C. & MUMMEY, D. L. 2006. Mycorrhizas and soil structure. *New Phytologist*, 171, 41-53.

- ROOD, S. B., BIGELOW, S. G., POLZIN, M. L., GILL, K. M. & COBURN, C. A. 2015. Biological bank protection: Trees are more effective than grasses at resisting erosion from major river floods. *Ecohydrology*, 8, 772-779.
- SINGER, M. B., SARGEANT, C. I., PIÉGAY, H., RIQUIER, J., WILSON, R. J. S. & EVANS, C. M. 2014. Floodplain ecohydrology: Climatic, anthropogenic, and local physical controls on partitioning of water sources to riparian trees. *Water Resources Research*, 50.
- SNYDER, K. A. & WILLIAMS, D. G. 2007. Root allocation and water uptake patterns in riparian tree saplings: Responses to irrigation and defoliation. *Forest Ecology and Management*, 246, 222-231.
- STEIGER, J. & GURNELL, A. M. 2003. Spatial hydrogeomorphological influences on sediment and nutrient deposition in riparian zones: observations from the Garonne River, France. *Geomorphology*, 49, 1-23.
- STETTLER, R. F., BRADSHAW, H. D., JR., HEILMAN, P. E. & HINCKLEY, T. M. (eds.) 1996. *Biology of Populus and its Implications for Management and Conservation*, Ottawa, Ontario, Canada: National Research Council of Canada Research Press.
- STOCKS, S. M. & THOMAS, C. R. 2001. Strength of mid-logarithmic and stationary phase *Saccharopolyspora erythraea* hyphae during a batch fermentation in defined nitrate-limited medium. *Biotechnology and Bioengineering*, 73, 370-378.
- STROMBERG, J. C. 2001. Influence of stream flow regime and temperature on growth rate of the riparian tree, *Platanus wrightii*, in Arizona. *Freshwater Biology*, 46, 227-239.
- SURIAN, N., BARBAN, M., ZILIANI, L., MONEGATO, G., BERTOLDI, W. & COMITI, F. 2015. Vegetation turnover in a braided river: Frequency and effectiveness of floods of different magnitude. *Earth Surface Processes and Landforms*, 40, 542-558.
- TAKAGI, K. & HIOKI, Y. 2013. Autecology, distributional expansion and negative effects of *Amorpha fruticosa* L. on a river ecosystem: A case study in the Sendaigawa River, Tottori Prefecture. *Landscape and Ecological Engineering*, 9, 175-188.
- THOMAS, C. R., ZHANG, Z. & COWEN, C. 2000. Micromanipulation measurements of biological materials. *Biotechnology Letters*, 22, 531-537.
- TISDALL, J. M. 1991. Fungal hyphae and structural stability of soil. *Australian Journal of Soil Research*, 29, 729-743.
- VAN DE WIEL, M. J. & DARBY, S. E. 2007. A new model to analyse the impact of woody riparian vegetation on the geotechnical stability of riverbanks. *Earth Surface Processes and Landforms*, 32, 2185-2198.
- YU, T., FENG, Q., SI, J., XI, H., LI, Z. & CHEN, A. 2013. Hydraulic redistribution of soil water by roots of two desert riparian phreatophytes in northwest China's extremely arid region. *Plant and Soil*, 372, 297-308.
- ZANONI, L., GURNELL, A., DRAKE, N. & SURIAN, N. 2008. Island dynamics in a braided river from analysis of historical maps and air photographs. *River Research and Applications*, 24, 1141-1159.
- ZHANG, C. B., CHEN, L. H. & JIANG, J. 2014. Why fine tree roots are stronger than thicker roots: The role of cellulose and lignin in relation to slope stability. *Geomorphology*, 206, 196-202.
- ZHAO, L., SCHAEFER, D., XU, H., MODI, S., LACOURSE, W. & MARTEN, M. Elastic properties of *aspergillus nidulans* studied with atomic force microscopy. In: LAUDON, M. & ROMANOWICZ, B., eds. 2005 NSTI Nanotechnology Conference and Trade Show - NSTI Nanotech 2005, 2005 Anaheim, CA. 243-245.

Appendix A

LASER PARTICLE SIZER SETTINGS

As described in Chapter 3, sediment particle size distribution for fine fractions (< 1 mm) was determined from analysis on a Beckman Coulter LS 13 320 Laser Diffraction Particle Size Analyzer, with Auto-Prep Station. Details of the standard operating procedure used are given below, in Table A.1.

Table A.1 Standard Operating Procedure for laser particle size analyzer

Fluid:	
Include PIDS:	Yes
Use Auto-Prep Station:	Yes
Run length:	100 seconds
Number of runs:	2
Pump speed:	65
Sonicate before first run:	10 seconds
Sonicate between runs:	No
Sonicate during run:	Yes
Sonicate Power:	8
Compute sizes:	Yes
Optical model:	sediment.rf780d PIDS included
Export size data:	Yes
Average All Runs:	Yes
Repeat Cycle:	Yes
Auto Rinse first:	No
Measure Offsets:	Yes
Align:	Yes
Measure Background:	Yes
Measure Loading:	Load sample using Auto-Prep Station
Start Run(s):	Yes
Auto Rinse Last:	Yes
Auto-Prep Station Settings:	
Sonicate for	10 seconds
Sonicate Power:	7
Empty tube for	12 seconds
Pulsed Flush for	5 seconds
Wait after emptying for	0 seconds
Auto-Dilute:	By Obscuration, 10%

Appendix B

COMPLETE CORRELATION TABLES

Only the strongest tree and sediment variable correlates of root diameter and area variables were presented in Chapter 5. The complete results of the Spearman correlation analyses are given below.

B.1 TREE VARIABLES

Table B.1 Spearman correlation coefficients of relationships between root (rows) and tree (columns) variables. Figures in bold are significantly different from zero at $\alpha = 0.05$

	Age of Nearest Tree	Length of Nearest Tree	Vertical Growth Rate of Nearest Tree	Radial Growth Rate of Nearest Tree	Horizontal Distance to Nearest Tree	Absolute Distance to Nearest Tree	Average Age of Nearest Trees	Average Length of Nearest Trees	Avg. Vertical Growth Rate of Nrst. Trees	Avg. Radial Growth Rate of Nrst. Trees
Root Density	0.069	0.084	0.160	0.086	-0.043	-0.215	-0.034	0.144	0.298	-0.015
Root Area Ratio	0.121	0.195	0.192	0.133	-0.100	-0.236	0.093	0.218	0.225	0.032
Median Diameter	-0.045	0.170	0.121	0.048	-0.009	0.000	0.204	0.119	-0.031	0.056
Mean Diameter	0.059	0.231	0.157	0.122	-0.072	-0.101	0.206	0.198	0.026	0.066
Maximum Diameter	0.057	0.153	0.177	0.132	-0.062	-0.171	0.056	0.167	0.198	0.016
Skewness of Diameter Distribution	-0.044	-0.070	0.036	-0.003	-0.010	-0.102	-0.165	-0.044	0.202	-0.092
Kurtosis of Diameter Distribution	-0.049	-0.075	0.030	-0.019	-0.014	-0.104	-0.167	-0.053	0.197	-0.100
Standard Deviation of Diameter Distribution	0.072	0.187	0.160	0.137	-0.090	-0.151	0.118	0.173	0.088	0.021
Coefficient of Variation of Diam. Distrib.	0.061	0.047	0.086	0.080	-0.072	-0.153	-0.051	0.065	0.155	-0.059
First Quartile of Diameter Distribution	-0.055	0.265	0.231	0.165	0.116	0.122	0.290	0.224	0.062	0.217
Third Quartile of Diameter Distribution	0.113	0.281	0.140	0.083	-0.094	-0.102	0.306	0.218	-0.057	0.075
Median Area	-0.045	0.171	0.121	0.046	-0.007	0.003	0.205	0.119	-0.032	0.056
Mean Area	0.063	0.202	0.166	0.139	-0.074	-0.133	0.145	0.188	0.082	0.051
Maximum Area	0.057	0.153	0.177	0.132	-0.062	-0.171	0.056	0.167	0.198	0.016

	Age of Nearest Tree	Length of Nearest Tree	Vertical Growth Rate of Nearest Tree	Radial Growth Rate of Nearest Tree	Horizontal Distance to Nearest Tree	Absolute Distance to Nearest Tree	Average Age of Nearest Trees	Average Length of Nearest Trees	Avg. Vertical Growth Rate of Nrst. Trees	Avg. Radial Growth Rate of Nrst. Trees
Skewness of Area Distribution	-0.029	-0.052	0.052	0.001	-0.036	-0.152	-0.145	-0.020	0.218	-0.103
Kurtosis of Area Distribution	-0.025	-0.051	0.050	-0.006	-0.040	-0.154	-0.142	-0.021	0.215	-0.105
Standard Deviation of Area Distribution	0.055	0.168	0.161	0.123	-0.081	-0.154	0.088	0.160	0.122	0.007
Coeff. of Variation of Area Distribution	0.017	0.011	0.097	0.055	-0.024	-0.135	-0.095	0.042	0.232	-0.059
First Quartile of Area Distribution	-0.055	0.262	0.226	0.162	0.111	0.118	0.287	0.219	0.057	0.213
Third Quartile of Area Distribution	0.114	0.278	0.136	0.082	-0.092	-0.098	0.305	0.214	-0.061	0.078
Fine Root Density	-0.024	-0.036	0.108	0.047	0.007	-0.155	-0.151	0.046	0.299	-0.073
Fine Root Area Ratio	-0.032	0.042	0.177	0.078	0.025	-0.136	-0.062	0.103	0.317	-0.024
Median Fine Root Diameter	-0.097	0.133	0.124	0.009	0.043	0.072	0.165	0.066	0.015	0.073
Mean Fine Root Diameter	-0.034	0.186	0.153	0.053	0.019	0.041	0.216	0.133	0.028	0.111
Skewness of Fine Root Diam. Distrib.	0.014	-0.132	-0.066	-0.023	-0.024	-0.107	-0.188	-0.047	0.137	-0.060
Kurtosis of Fine Root Diameter Distribution	-0.064	-0.214	-0.177	-0.123	-0.069	-0.127	-0.240	-0.165	0.003	-0.137
Std. Dvn. of Fine Root Diameter Distr.	0.127	0.199	0.199	0.146	0.042	-0.022	0.150	0.230	0.211	0.149
Coeff. Var. of Fine Root Diameter Distr.	0.108	-0.014	0.011	0.036	-0.030	-0.113	-0.071	0.055	0.134	-0.014
First Quartile of Fine Root Diameter Distr.	0.067	0.333	0.355	0.245	0.280	0.249	0.326	0.346	0.283	0.352
Third Quartile of Fine Root Diameter Distr.	0.092	0.320	0.334	0.207	0.177	0.120	0.295	0.324	0.262	0.250
Coarse Root Density	0.115	0.128	0.120	0.115	-0.114	-0.248	0.074	0.151	0.151	0.022
Coarse Root Area Ratio	0.091	0.126	0.125	0.159	-0.105	-0.187	0.040	0.137	0.131	0.054
Median Coarse Root Diameter	0.090	0.116	0.104	0.168	0.018	0.007	0.103	0.139	0.007	0.143
Mean Coarse Root Diameter	0.057	0.111	0.123	0.177	-0.024	-0.049	0.031	0.116	0.088	0.108
Maximum Coarse Root Diameter	0.065	0.100	0.110	0.142	-0.075	-0.143	0.014	0.101	0.118	0.055

B.2 SEDIMENT VARIABLES

Table B.2 Spearman correlation coefficients of relationships between root (rows) and sediment (columns) variables. Figures in bold are significantly different from zero at $\alpha = 0.05$

	% Gravel	% Sand	% Silt + Clay	% Organic Matter	Mean Particle Size (Φ)	d50 (Φ)	d90 (Φ)	Sorting (Φ)	% Water (in field)	Root Interval Midpoint Depth (m)
Root Density	-0.420	0.104	0.557	0.500	0.546	0.552	0.561	0.487	0.289	0.405
Root Area Ratio	-0.425	0.242	0.482	0.438	0.486	0.471	0.503	0.505	0.323	0.340
Median Diameter	-0.225	0.344	0.076	0.105	0.099	0.066	0.111	0.180	0.159	0.051
Mean Diameter	-0.278	0.346	0.184	0.185	0.212	0.176	0.226	0.300	0.228	0.100
Maximum Diameter	-0.393	0.264	0.403	0.360	0.415	0.395	0.423	0.428	0.291	0.243
Skewness of Diameter Distribution	-0.290	0.092	0.357	0.310	0.343	0.344	0.341	0.261	0.220	0.128
Kurtosis of Diameter Distribution	-0.307	0.107	0.366	0.320	0.352	0.351	0.345	0.260	0.222	0.134
Standard Deviation of Diameter Distribution	-0.314	0.281	0.280	0.259	0.302	0.273	0.313	0.355	0.237	0.150
Coefficient of Variation of Diam. Distrib.	-0.264	0.104	0.349	0.304	0.341	0.332	0.351	0.332	0.232	0.122
First Quartile of Diameter Distribution	-0.143	0.346	-0.062	-0.014	-0.022	-0.051	-0.027	0.077	0.044	0.036
Third Quartile of Diameter Distribution	-0.175	0.320	0.046	0.070	0.083	0.046	0.105	0.227	0.134	0.110
Median Area	-0.223	0.342	0.073	0.102	0.096	0.063	0.107	0.176	0.156	0.051
Mean Area	-0.321	0.314	0.270	0.253	0.292	0.259	0.303	0.356	0.247	0.144
Maximum Area	-0.393	0.264	0.403	0.360	0.415	0.395	0.423	0.428	0.291	0.243
Skewness of Area Distribution	-0.368	0.119	0.437	0.384	0.426	0.426	0.426	0.325	0.242	0.221
Kurtosis of Area Distribution	-0.371	0.114	0.442	0.388	0.430	0.432	0.426	0.323	0.238	0.227
Standard Deviation of Area Distribution	-0.349	0.291	0.318	0.293	0.340	0.311	0.347	0.374	0.257	0.172
Coeff. of Variation of Area Distribution	-0.333	0.116	0.419	0.369	0.409	0.409	0.414	0.350	0.245	0.200
First Quartile of Area Distribution	-0.143	0.347	-0.063	-0.013	-0.023	-0.052	-0.029	0.074	0.043	0.037
Third Quartile of Area Distribution	-0.163	0.311	0.034	0.059	0.071	0.034	0.094	0.217	0.125	0.103

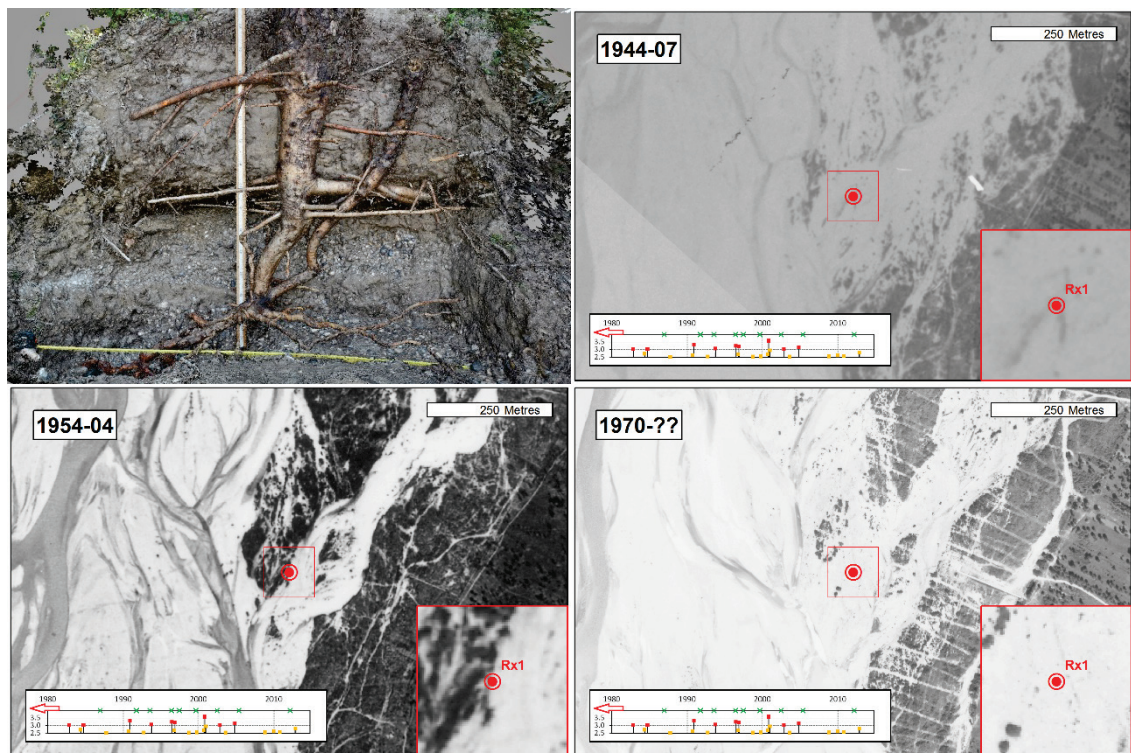
	% Gravel	% Sand	% Silt + Clay	% Organic Matter	Mean Particle Size (Φ)	d50 (Φ)	d90 (Φ)	Sorting (Φ)	% Water (in field)	Root Interval Midpoint Depth (m)
Fine Root Density	-0.398	0.054	0.533	0.463	0.522	0.531	0.518	0.391	0.253	0.337
Fine Root Area Ratio	-0.496	0.180	0.578	0.517	0.578	0.578	0.580	0.471	0.301	0.362
Median Fine Root Diameter	-0.157	0.311	-0.001	0.028	0.020	0.007	0.011	0.071	0.089	-0.003
Mean Fine Root Diameter	-0.205	0.312	0.079	0.097	0.100	0.083	0.104	0.172	0.088	0.034
Skewness of Fine Root Diam. Distrib.	-0.043	-0.131	0.167	0.132	0.146	0.157	0.139	0.071	0.002	0.125
Kurtosis of Fine Root Diameter Distribution	-0.060	-0.014	0.092	0.106	0.071	0.074	0.067	0.008	0.010	0.074
Std. Dvn. of Fine Root Diameter Distr.	-0.188	-0.010	0.307	0.236	0.300	0.299	0.314	0.288	0.110	0.197
Coeff. Var. of Fine Root Diameter Distr.	-0.125	-0.125	0.294	0.232	0.276	0.286	0.280	0.200	0.049	0.173
First Quartile of Fine Root Diameter Distr.	-0.078	0.108	0.042	0.020	0.059	0.037	0.064	0.170	0.021	0.093
Third Quartile of Fine Root Diameter Distr.	-0.227	0.146	0.240	0.191	0.248	0.230	0.259	0.312	0.140	0.168
Coarse Root Density	-0.343	0.062	0.403	0.339	0.418	0.404	0.447	0.386	0.158	0.409
Coarse Root Area Ratio	-0.252	0.090	0.283	0.226	0.297	0.280	0.311	0.304	0.143	0.248
Median Coarse Root Diameter	-0.063	0.034	0.095	0.064	0.090	0.084	0.087	0.133	0.043	0.067
Mean Coarse Root Diameter	-0.092	0.062	0.119	0.080	0.120	0.106	0.124	0.186	0.083	0.062
Maximum Coarse Root Diameter	-0.201	0.086	0.225	0.173	0.231	0.216	0.242	0.256	0.121	0.186
% Fine Roots by Density	0.229	-0.324	-0.115	-0.129	-0.142	-0.105	-0.162	-0.235	-0.186	-0.098
% Fine Roots by Area	0.276	-0.255	-0.237	-0.223	-0.255	-0.223	-0.270	-0.306	-0.222	-0.125

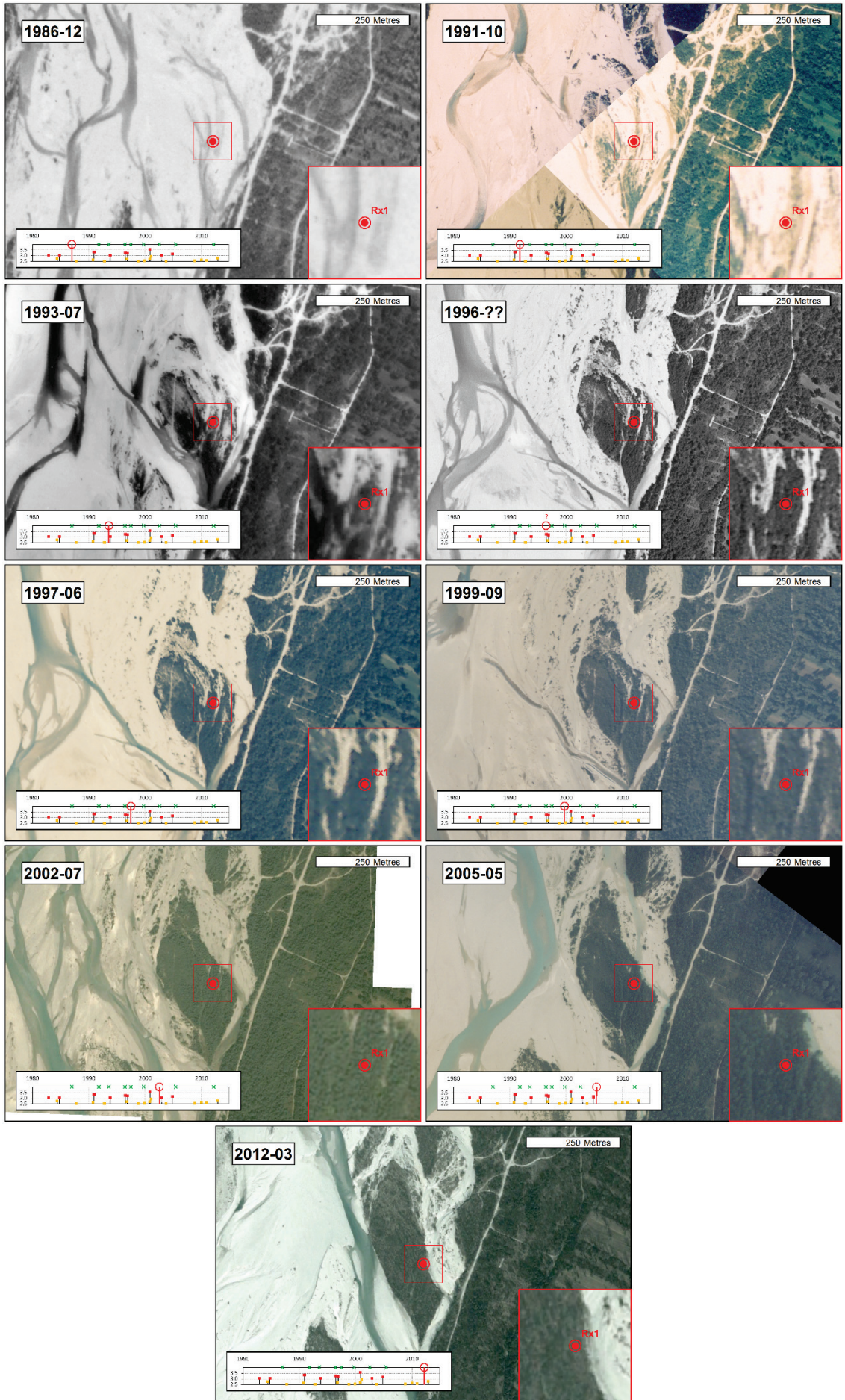
Appendix C

AERIAL IMAGE SEQUENCES

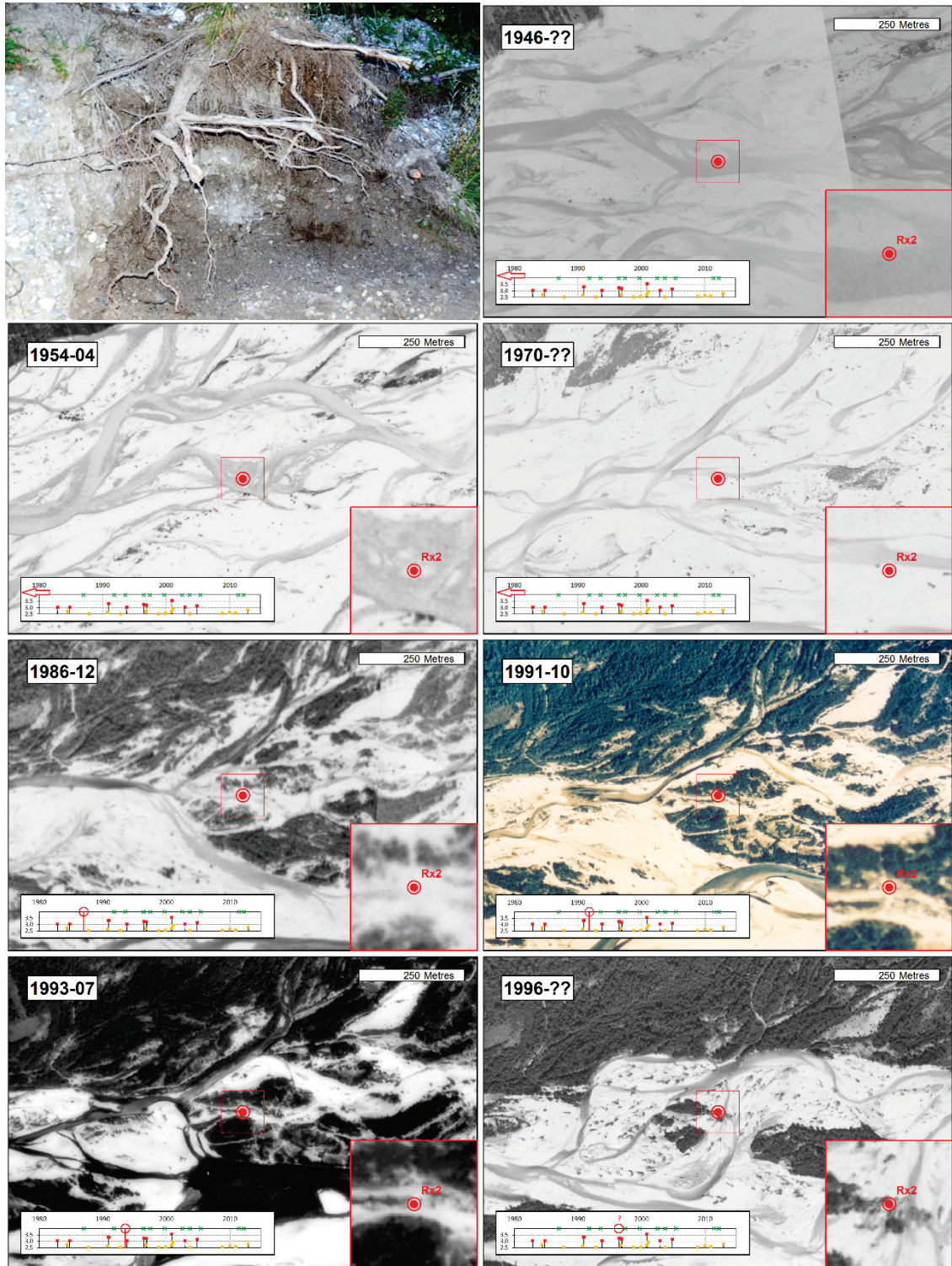
Section 6.3.2 presented aerial images showing only the most significant morphological changes in the vicinity of the case study trees. Presented below are the complete sequences of all available images. Please see Table 6.1 for image source information. Image excerpts are oriented with north at the top. Inset in each figure is an approximate date, scale bar, miniature cropped hydrograph indicating the timing of the image (red line and circle) with respect to major floods (> 3.0 m stage) and orange (> 2.5 m) square symbols), as well as a larger scale magnification, the extent of which is indicated by the outline on the main image. Note that the initial “Rx...” labels are used to identify the case study trees in the magnified frames.

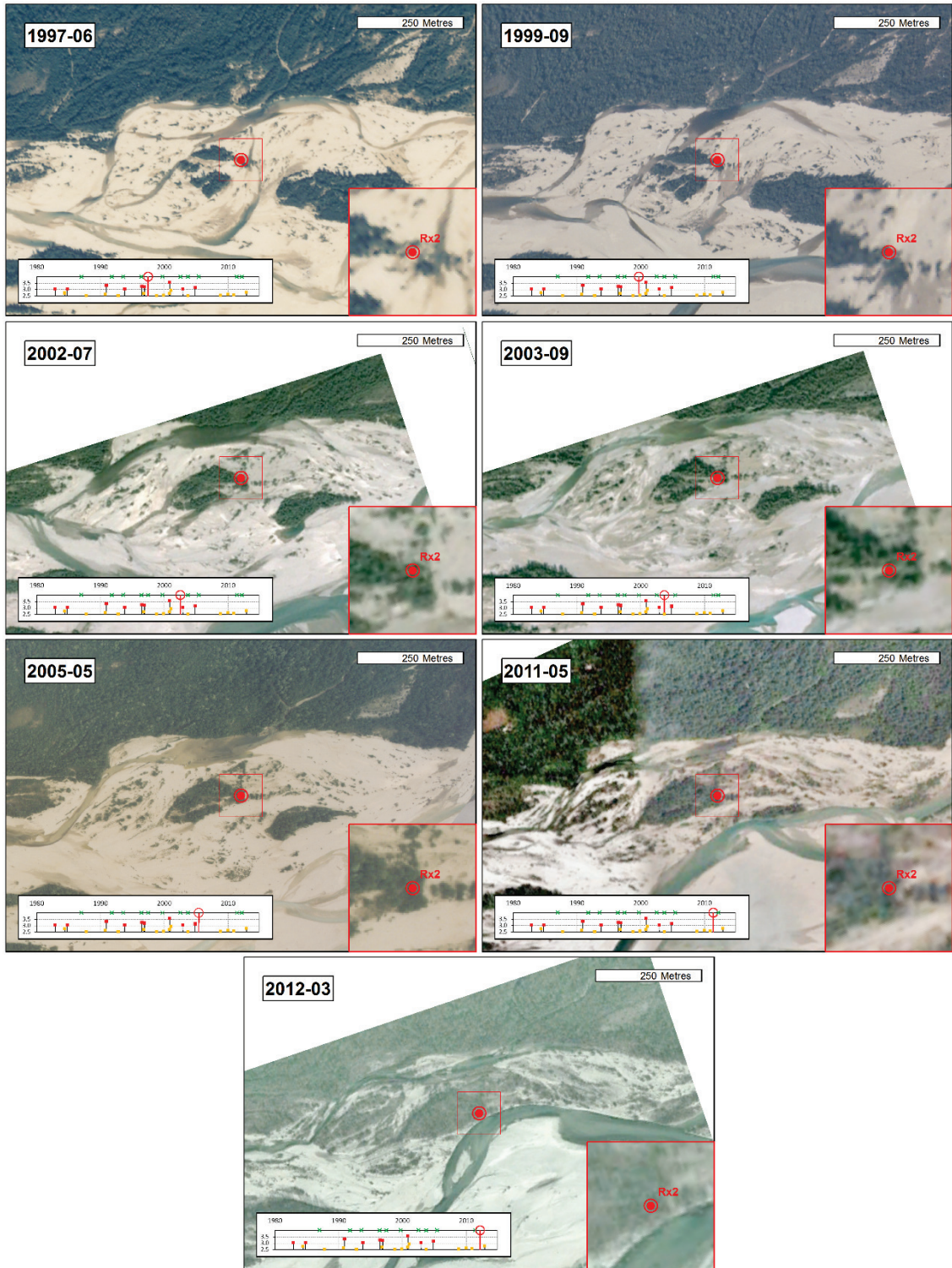
C.1 CASE STUDY “R1” (“RX1”)



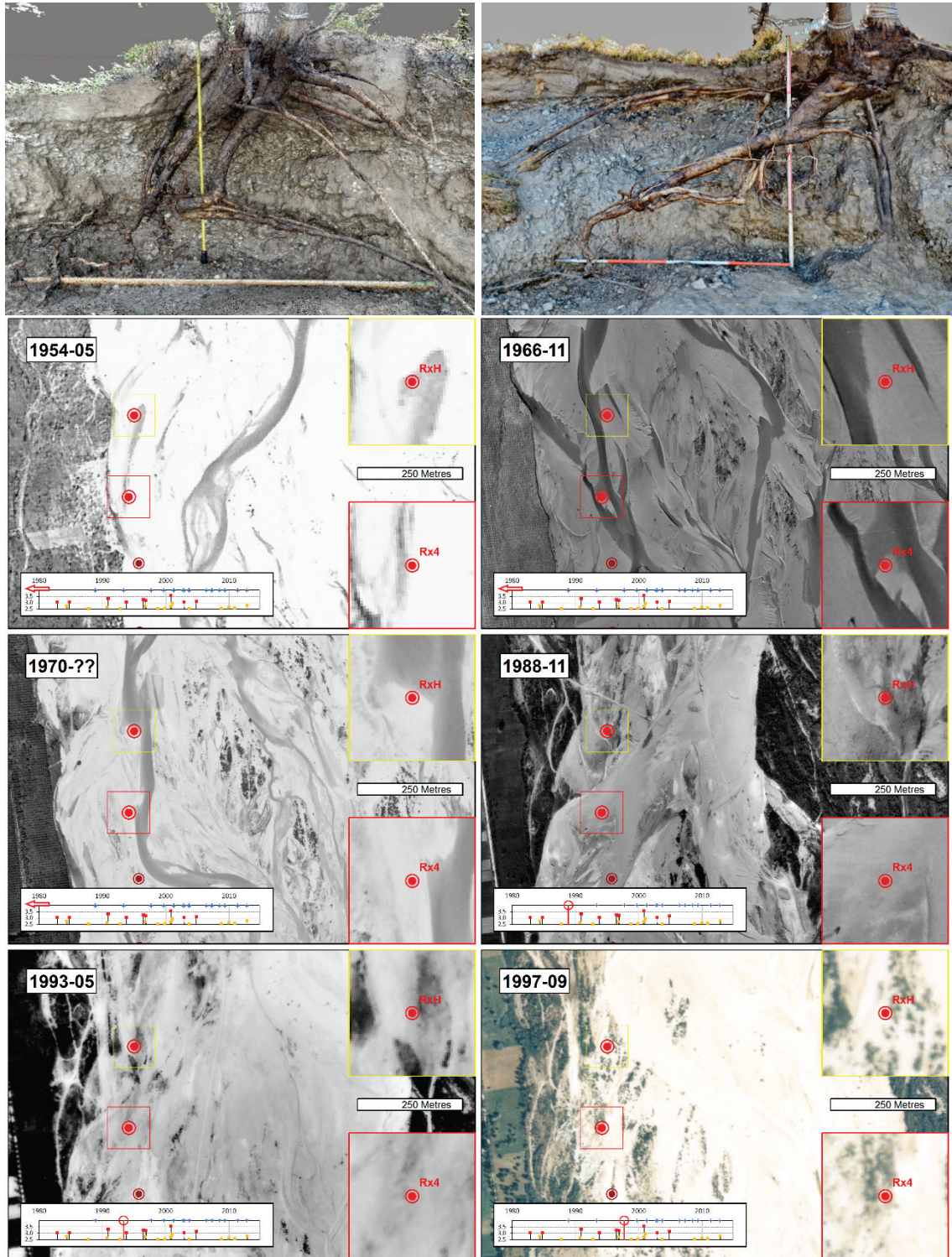


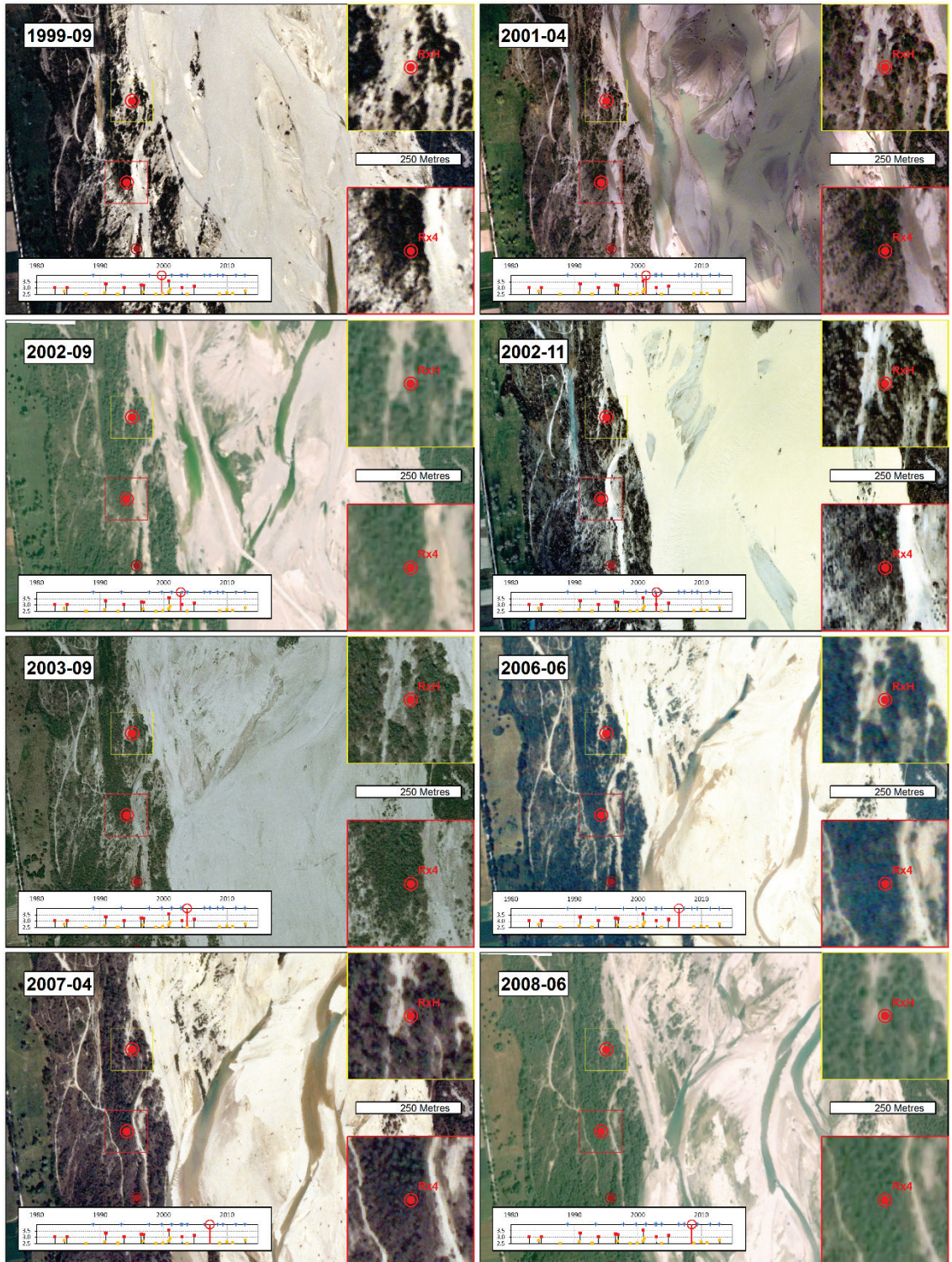
C.2 CASE STUDY “R2” (“RX2”)

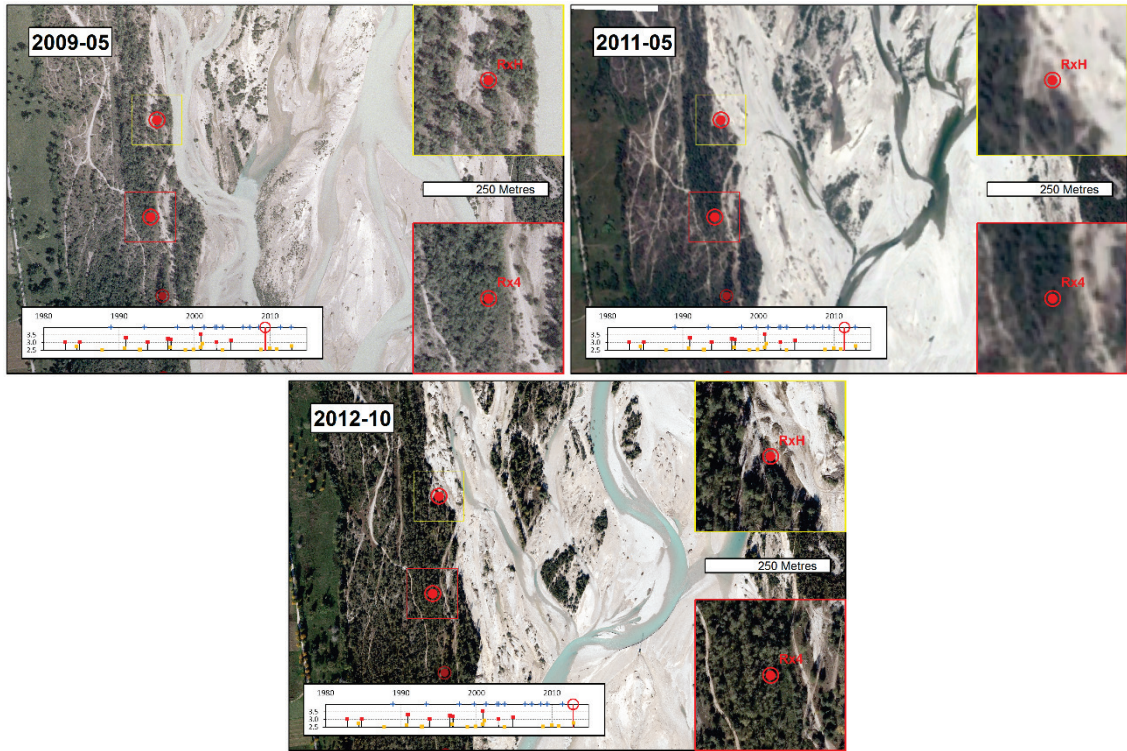




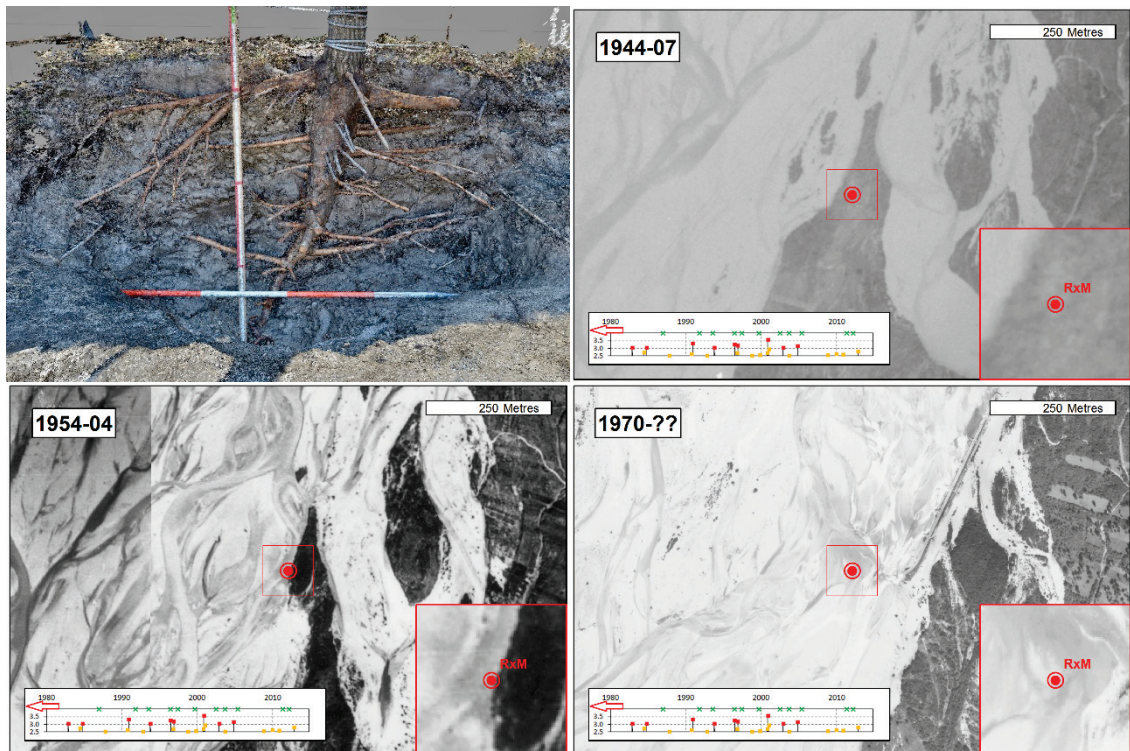
C.3 CASE STUDIES “R3” AND “RC” (“RX4” AND “RXH”)

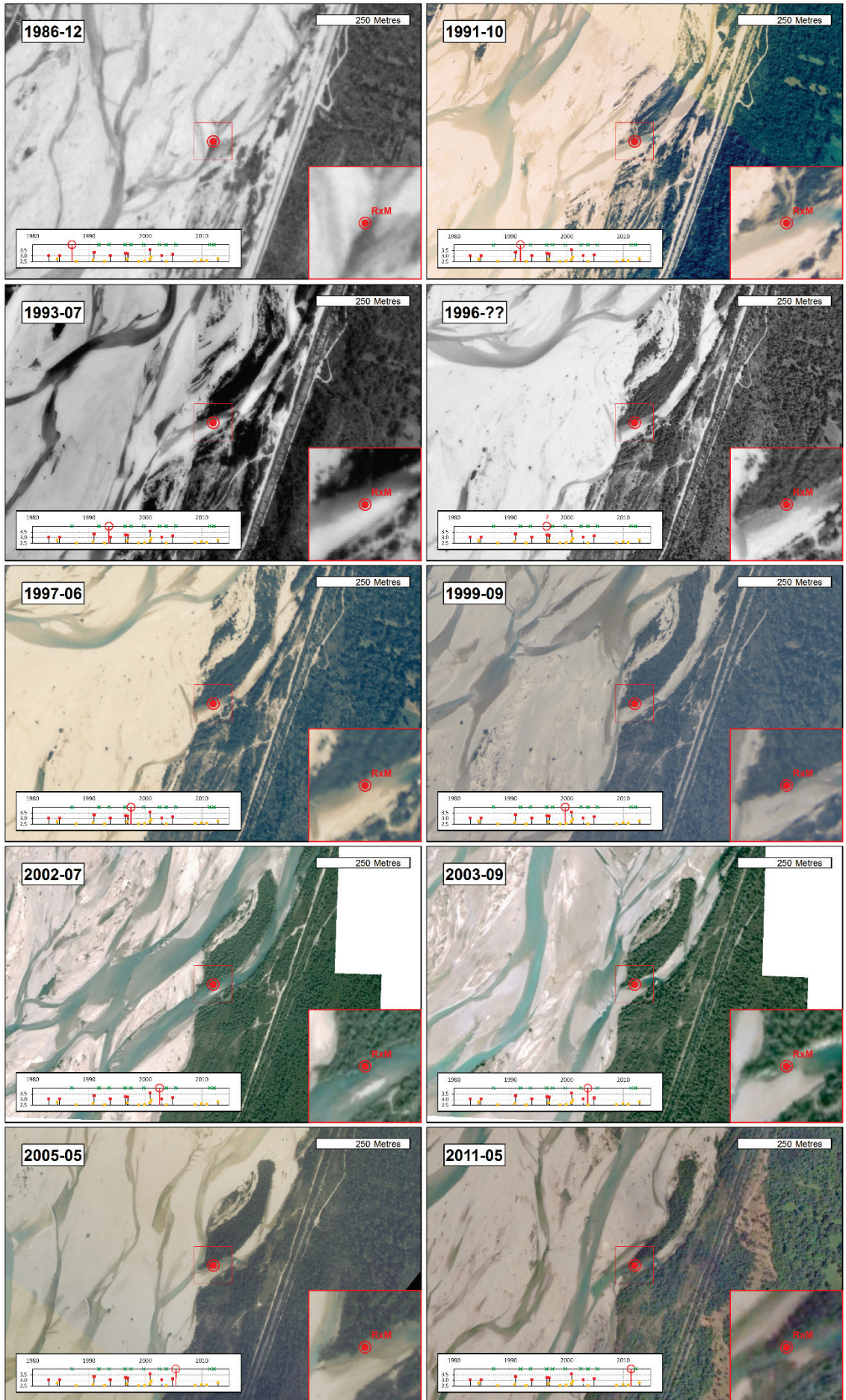


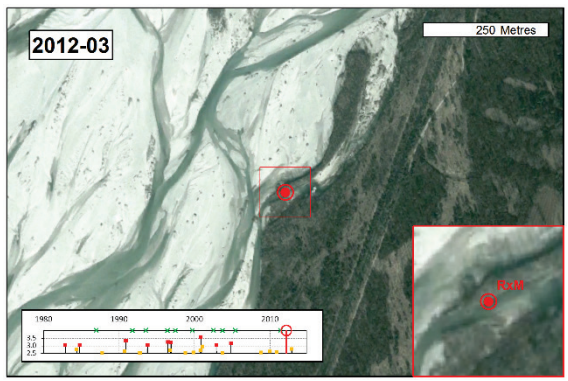




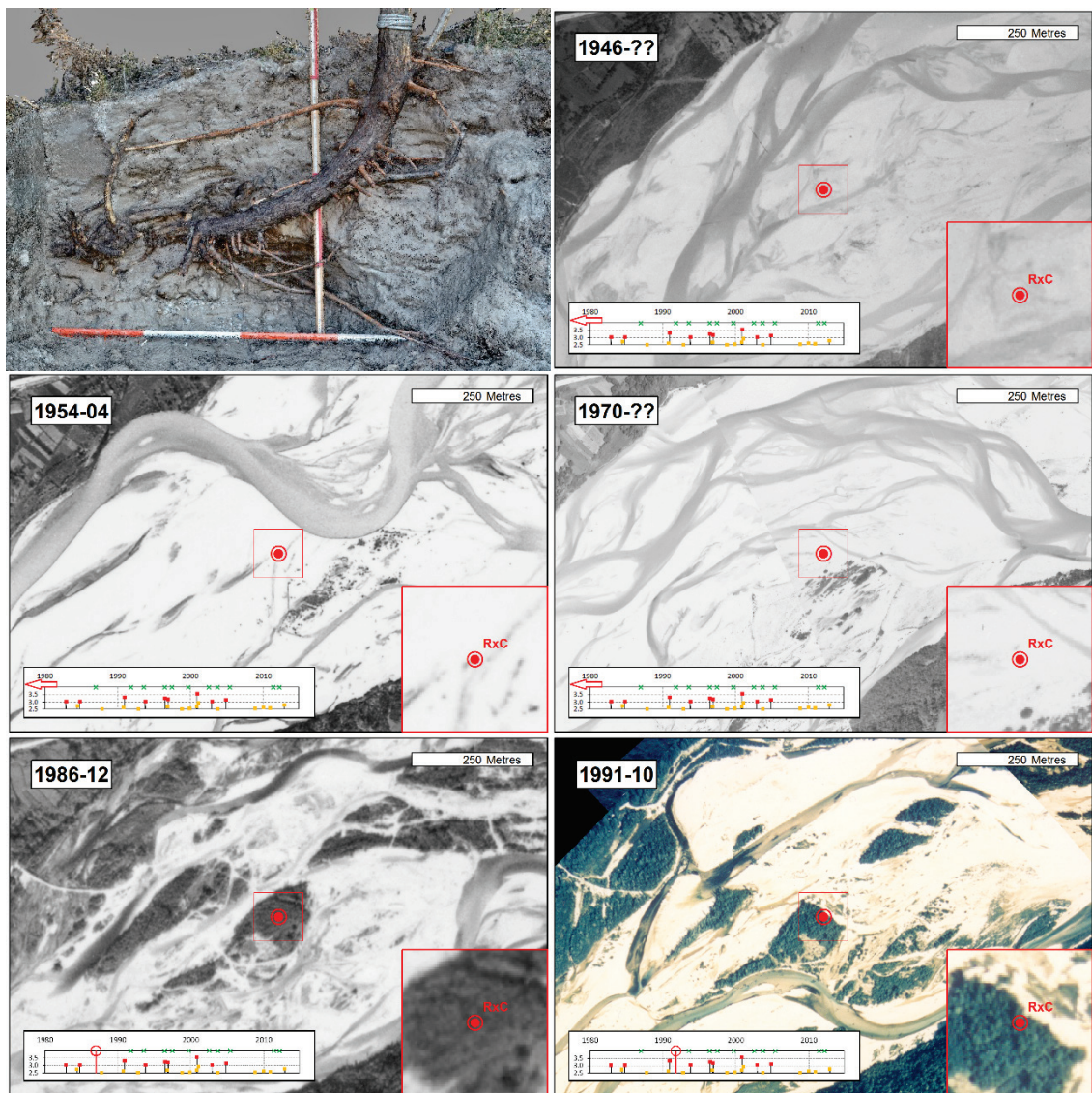
C.4 CASE STUDY “RA” (“RxM”)

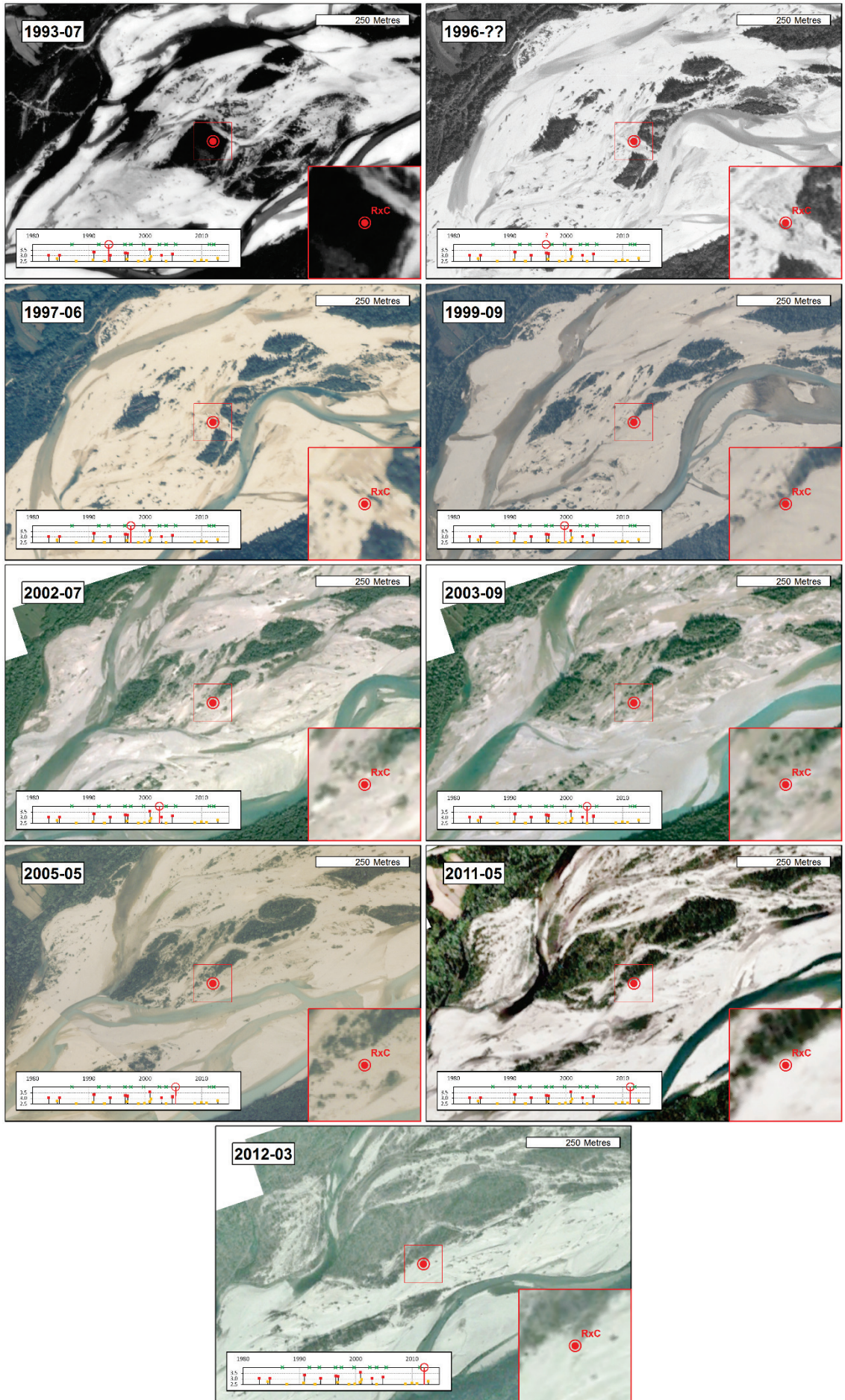




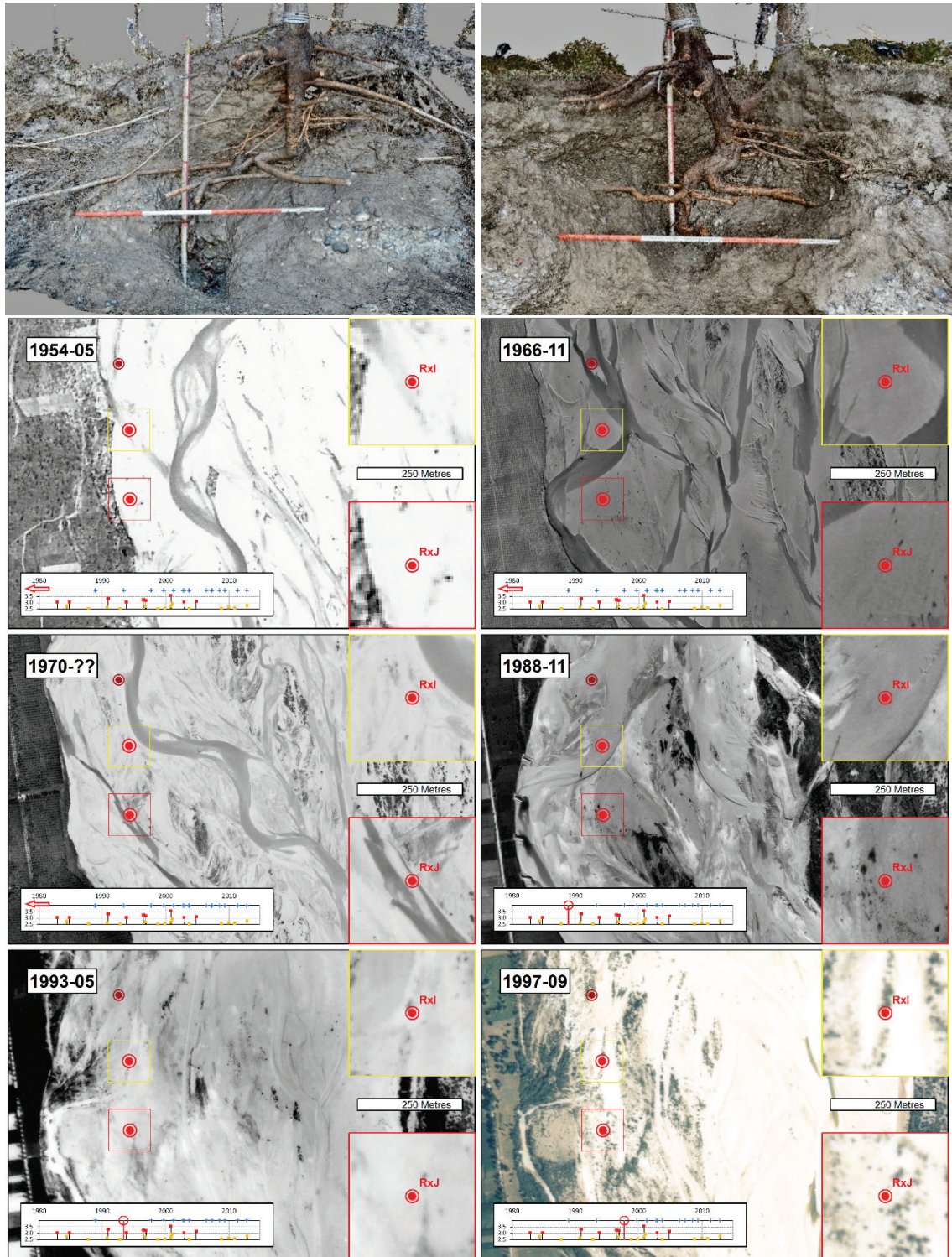


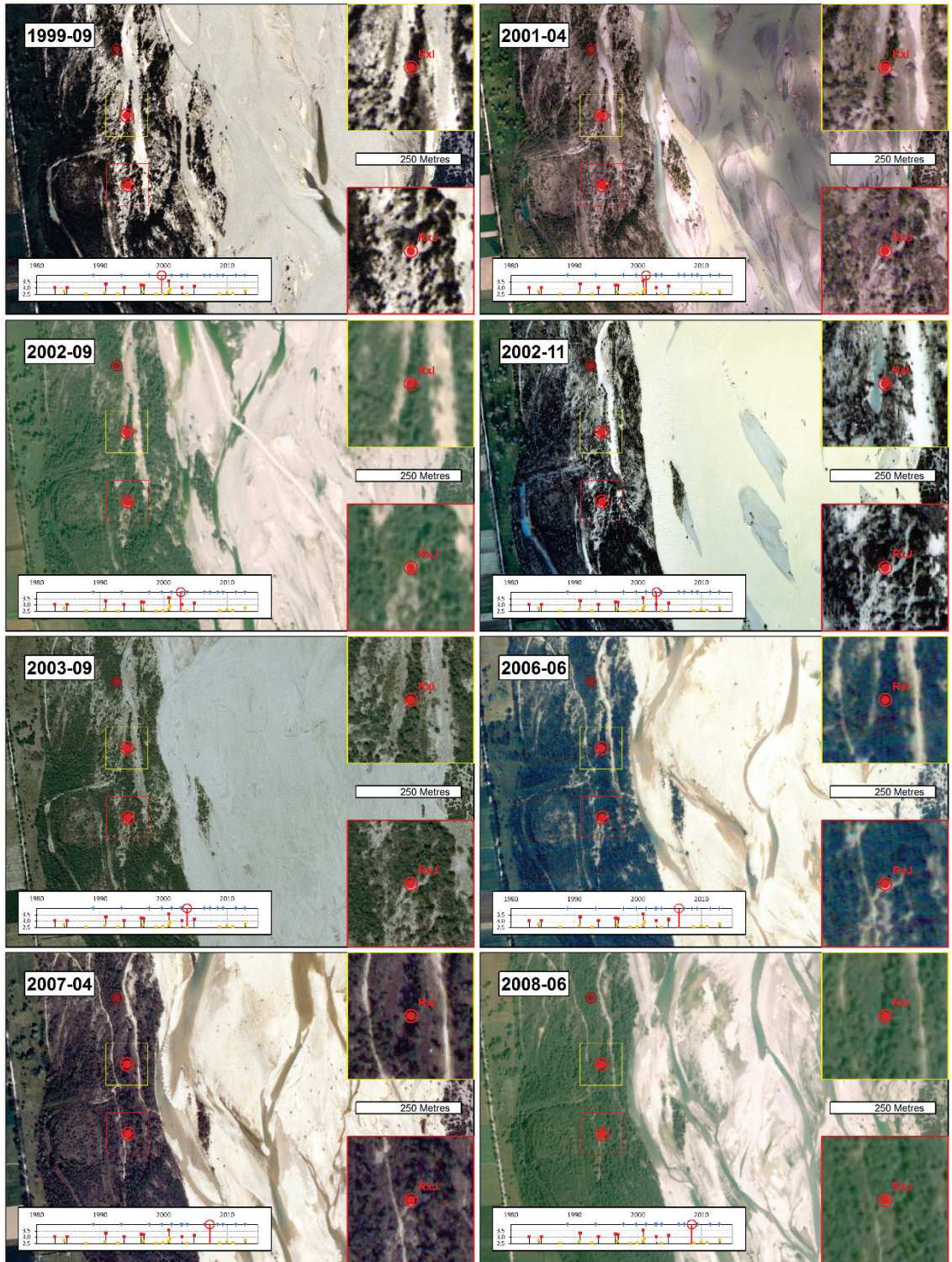
C.5 CASE STUDY “RB” (“RxC”)

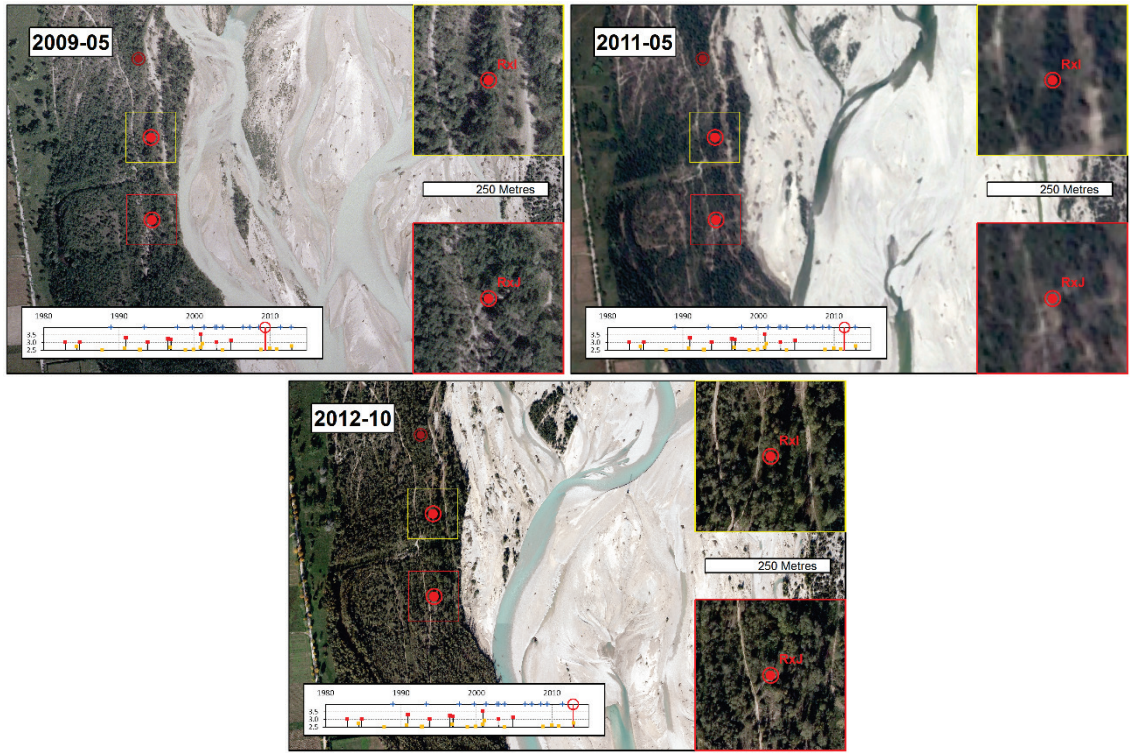




C.6 CASE STUDIES “RD” AND “RE” (“RXI” AND “RXJ”)







Appendix D

STRUCTURE FROM MOTION PHOTOGRAMMETRY

As described in Section 6.2.2, photogrammetric models of the roots were generated using the commercially available software Agisoft Photoscan 1.1.6, using a standard workflow (align photos > generate sparse point cloud > dense point cloud > triangulate mesh) using ‘high’ accuracy and quality presets. Figures relating to the level of detail of the models are presented in Table D.1. Further screen captures are presented in the figures below. The dense point cloud of each case study tree is shown first in oblique upstream, then downstream and top view.

Table D.1 Key statistics of the SfM models

Case study ID	Number of images	Number of points in point cloud			Polygonal mesh	
		Sparse	Dense	Total	Faces	Vertices
R1	228	423,201	30,342,002	30,765,203	2,022,788	1,018,572
R3	181	431,838	29,907,679	30,339,517	1,993,839	1,004,551
RA	200	21,853	35,453,984	35,475,837	7,090,761	3,554,772
RB	228	15,310	41,215,683	41,230,993	8,243,106	4,131,019
RC	272	15,368	51,502,350	51,517,718	10,300,442	5,160,477
RD	188	14,755	34,823,043	34,837,798	6,964,588	3,492,891
RE	225	19,783	44,896,487	44,916,270	8,979,274	4,501,326
<i>Averages</i>	<i>217</i>	<i>134,587</i>	<i>38,305,890</i>	<i>33,635,417</i>	<i>6,513,543</i>	<i>3,266,230</i>

D.1 CASE STUDY R1





D.2 CASE STUDY R3



D.3 CASE STUDY RA



D.4 CASE STUDY RB





D.5 CASE STUDY RC



D.6 CASE STUDY RD



D.7 CASE STUDY RE





Appendix E

SITE INFORMATION AND METHODS

FOR PRELIMINARY FURTHER DATA COLLECTION

E.1 SUPPLEMENTARY STUDY SITE: BIOTOPO LA RUPE

This protected riparian forest area on the Noce river, in a relatively low-gradient reach approximately 4.5 km upstream of its confluence with the Adige in Trentino, Italy, is dominated by mature *Populus nigra* and *Salix* spp. In spite of its island-braided form at this site, unlike the Tagliamento, the Noce has a strongly regulated flow regime, due to the existence of several hydropower dams. As a consequence of the rarity of large floods, the channel morphology is essentially stable and there is little fine sand in the bank profiles. It was hypothesised that the large daily stage fluctuations (Figure E.1) and lack of hydromorphologically-driven vegetation dynamics would have significant influences on the root system structure of the poplar-dominated sites at La Rupe, providing an informative comparison with the Tagliamento. The site originated when, in a large flood in 1926, the straightened and embanked engineered channel to the east (Figure E.2) burst its banks and the decision was made not to repair this channel. The braided form was essentially generated in and immediately after this single event.

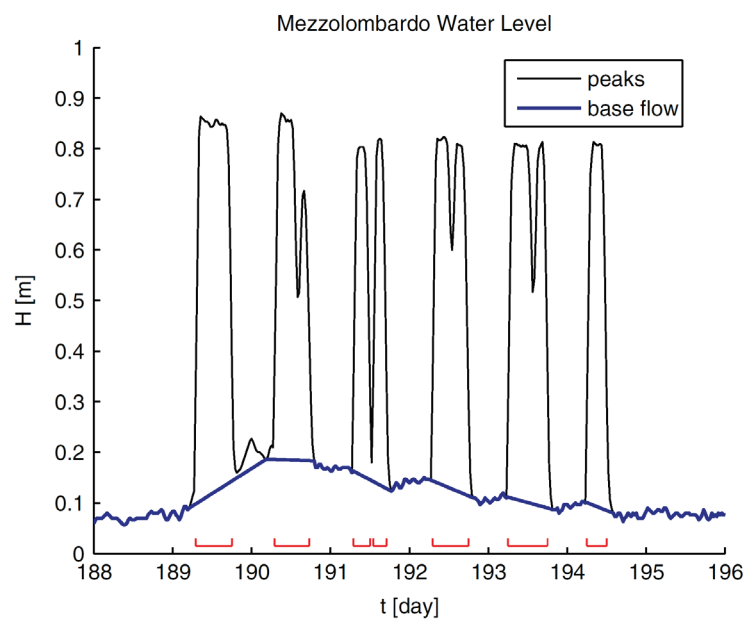


Figure E.1 Typical river stage fluctuation at the Mezzolombardo gauge on the Noce, approx. 400 m upstream of La Rupe, showing daily hydropeaking due to releases from the power station 3 km upstream. Period of record is July 8th – 15th 2007. Zolezzi et al. (2011)



Figure E.2 Annotated aerial image of Biotopo La Rupe, showing channel banks (red), position of old, straightened channel (blue) and sampling sites (green – symbols identify bank profiles and areas indicate tree surveys). Flow is from north (top) to south. Imagery: DigitalGlobe, accessed via ESRI

E.2 FUNGAL HYPHAL LENGTH DENSITY

The extent of hyphal colonisation in the sediment samples was assayed according to a modified version of the aqueous extraction protocol of Jakobsen et al. (1992) followed by intersect measurement after Tennant (1975). Where sediment samples were replicated in the field, subsamples were bulked for this analysis. Large root fragments (> 0.2 mm \varnothing and/or 5 mm length) were manually removed, washed and retained for subsequent analyses.

Aggregates in 5 g of sediment were dispersed by shaking end-over-end for 30 s in 100 ml of a 3.5 g L^{-1} sodium hexametaphosphate solution and then allowed to stand for at least 30 min. The subsamples were then gently washed on a 38 μ m sieve (using a manual spray pump) to remove clay particles, before being backwashed into identical Erlenmeyer flasks and made up to 200 ml with water. The samples were resuspended by vigorous swirling (by hand) for 5 s and after 1 min settling time, a 10 ml aliquot was removed using a measuring pipette inserted to a depth of 30 mm. This aliquot was transferred to a 0.45 μ m cellulose nitrate filter (25 mm \varnothing) and the water removed by vacuum. The extract was stained for 5 min with 0.4 % Trypan Blue before being washed and the filter transferred to a slide and fixed with

lactoglycerol (1:1:1 lactic acid, glycerol and water). Slides without an even coverage of the extract were rejected.

Each slide was inspected at 200x magnification under a compound microscope with a crosshair eyepiece, stopping 50 times to cover the entire area of the extract on the filter paper. The number hyphal intersections with the crosshair was recorded for each stop, and the total hyphal length (m) per gram of sieved sediment was estimated from the formula below (for a 200 ml suspension and units of mm, mm², g and ml).

$$\frac{\pi \times \text{Intersections} \times \text{Filter area}}{20 \times \text{Stops} \times \text{Field of view diameter} \times \text{Sample mass} \times \text{Aliquot volume}}$$

As hyphal length varied by 4 orders of magnitude across the samples and the extraction method was designed for surface soils, it was necessary to perform an initial optimisation step. Sediment subsample mass and aliquot volume were adjusted (between 2 and 25 g and 5 and 15 ml, respectively) to give up to approximately 10 intersections per stop. Only measurements from these optimised subsamples were used in subsequent analyses.

E.3 OPTICAL ANALYSIS OF ROOTS

Following sieving, all roots (besides any small fragments in subsamples for particle size analysis and hyphal length) were extracted from the fine fraction of fixed-volume samples collected in 2014, then scanned and analysed with WinRHIZO software (Regent Instruments Inc., Canada).

Root extraction was achieved by a modified flotation and sieving method after Miller et al. (1995) and Cook et al. (1988). Firstly, aggregates in the samples were dispersed in a 10 g L⁻¹ sodium hexametaphosphate solution. Where the dry volume of samples exceeded 300 ml, these were treated in smaller batches and analytical data later recombined. Each batch was agitated vigorously for 30 s in a 1 L beaker (swirling by hand, changing directions) in sufficient dispersant to immerse the solids to approx. 30 mm depth, and then allowed to stand for at least 30 min. The material was then transferred to a 5 L plastic jug, 500 ml of tap water added and then the sample was resuspended by hand vortexing again. After a 10 s settlement period, the supernatant, containing most of the roots, was transferred to a 1 L beaker on a magnetic stir plate, vortexed once more (600 rpm, 5 s), and after a second 10 s settlement period, this supernatant poured onto a 0.5 mm sieve. The two suspension and settlement steps were repeated until only non-root organic debris and/or root fragments < 2 mm long and < 0.5 mm diameter remained in the jug. Some samples from the 'La Rupe' site contained a vast number of these small root fragments and it was not possible to separate

them all from mineral sediment and other organic debris. Any small aggregates decanted with the roots were broken down on the sieve with a gentle manual water spray. Roots retained on the sieve were backwashed onto plastic weigh boats and dried overnight at 40 °C in a ventilated oven.

Owing to the wide range of root diameters (< 50 µm to 12 mm) and root conditions (principally, the problem of rough bark on larger roots) in the samples, it was not possible to optimise WinRHIZO analysis for the full sample set. Consequently, larger roots (> 4 mm Ø approx.) were analysed with a more aggressive smoothing filter in order to reduce the incidence of false lateral root detection. Diameter class width intervals were every 50 µm from 0 to 1.5 mm and every 250 µm for root segments > 1.5 mm Ø. Image capture was performed on a flatbed scanner (Epson Perfection V700 Photo) in clear acrylic trays and the smaller root diameter extracts were immersed in water.

E.4 ROOT BREAKING STRESS

At root profile excavation sites, a range of roots between approx. one and ten millimetres in diameter were selected for strength testing. A length of around 30 cm of each root was exposed and attached to a metal rigging thimble as described in Section 7.4.2. This was then attached in series to a force transducer (Transducer Techniques MLP Series) and mechanical winch, or pulling handle. Force was then gradually applied in the same axis as the root alignment until the root broke, and maximum tension measured on the transducer was recorded. The average diameter at the point of breaking was measured using digital calipers, and breaking stress calculated as the maximum tension per unit sectional area (as approximated by that of a circle of the root's average diameter). Tests where the root pulled out of the bank, or broke at or below the point of attachment to the thimble were disregarded. If the root appeared dead (determined by low density and elasticity), this was also noted.

E.5 COARSE ROOT SURVEYS

At three locations on the Tagliamento (Figure E.3), larger, five metre wide bank sections were excavated and prepared for measuring coarse root distributions. Site selection was based on the same criteria as described in Section 3.4.1. CRS1 was located on the same bank and just a few metres downstream from case study tree R3. CRS2 was located on the same bank and approximately ten metres downstream of tree R1. Only CRS3 was isolated from other profiles or case study trees, but the site is illustrated in Figure 6.51 C. Working in one

metre wide sections, the diameters of all roots > 1.5 mm were recorded and each mapped (depth and displacement from left hand edge) using a sliding measuring staff assembly.



Figure E.3 Position of coarse root surveys. Map data © 2015 Google

E.6 TREE MAPPING

At the La Rupe site, two apparently clonal patches of mature poplars (upstream areas in Figure E.2) and a large dense stand of younger poplars (50 – 500 mm DBH) on what appeared to be a slowly accreting point bar (downstream area in Figure E.2) were surveyed. Each tree greater than 50 mm DBH was labelled and then its height and diameter measured and recorded as described in Section 3.4.1. Locations were then mapped by measuring distance and bearing to at least two GPS-located datums. Trees were finally cored for dendrochronological samples as described in Section 3.4.1.

E.7 REFERENCES

- COOK, B. D., JASTROW, J. D. & MILLER, R. M. 1988. Root and mycorrhizal endophyte development in a chronosequence of restored tallgrass prairie. *New Phytologist*, 110, 355-362.
- JAKOBSEN, I., ABBOTT, L. K. & ROBSON, A. D. 1992. External hyphae of vesicular-arbuscular mycorrhizal fungi associated with *Trifolium subterraneum* L. *New Phytologist*, 120, 371-380.
- MILLER, R. M., REINHARDT, D. R. & JASTROW, J. D. 1995. External hyphal production of vesicular-arbuscular mycorrhizal fungi in pasture and tallgrass prairie communities. *Oecologia*, 103, 17-23.
- TENNANT, D. 1975. A Test of a Modified Line Intersect Method of Estimating Root Length. *Journal of Ecology*, 63, 995-1001.
- ZOLEZZI, G., SIVIGLIA, A., TOFFOLON, M. & MAIOLINI, B. 2011. Thermopeaking in alpine streams: Event characterization and time scales. *Ecohydrology*, 4, 564-576.